UNIVERSIDAD AUTÓNOMA DE MADRID

Facultad de Ciencias

Departamento de Biología Molecular

Role of oligomeric TCR complexes and TCR-interacting molecules in T cell development and activation

Doctoral Thesis

Rashmi Kumar

Madrid, May 2010

Tesis Doctoral

Role of oligomeric TCR complexes and TCR-interacting molecules in T cell development and activation.

Esta memoria ha sido presentada por la licenciada Rashmi Kumar para optar al grado de Doctor en Ciencias Biológicas:

Directores de la tesis

Dr. Hisse Martien van Santen
Científico Titular
Centro de Biología Molecular 'Severo Ochoa'
Universidad Autónoma de Madrid

Dr. Balbino Alarcón Sánchez
Profesor Investigador del Consejo Superior de Investigaciones Científicas
Centro de Biología Molecular 'Severo Ochoa'
Universidad Autónoma de Madrid

VºBº El Director

Este trabajo ha sido realizado en el Centro de Biología Molecular ‘Severo Ochoa’ bajo la dirección de los Drs. Hisse Martien van Santen y Balbino Alarcón, con financiación de los proyectos 2004 2 0E 105 del CSIC, BFU2006-04031 y BFU2009-08009 del Plan Nacional.

TO MY PARENTS

ACKNOWLEDGEMENTS

First of all, I want to thank my thesis advisors, Dr. Balbino Alarcón and Dr. Hisse Martien van Santen, for their enthusiastic support to both me and my work. Balbino encouraged me to aim high and strive for the best while Hisse has been instrumental in my professional development. Balbino has been an inspiration and model of dedication, humanity and his love for science that I am looking to emulate in my own career. I cannot thank Balbino in words for the support during my stay in Spain both personally and professionally. I am particularly grateful to Hisse, my first advisor, for imparting the scientific acumen needed, as well as the technical skills, the patience and perseverance needed for success. His patience and deliberate perfectionist approach to science and in guiding me made a lasting impression.

Science run on team-work and to keep these men running it is necessary for many things to come together. The Bal lab has been enjoyable and fun atmosphere for me because of the amazing people in it. I want to thank all present and past members of Bal's lab. In particular I want to thank (past members) Pilar and Ruth for their help and sharing their experience whenever I needed, Irene Z., Toni, Maite, Ramon, Lara, Lucia and Juanjo for their timely help and support. Of the present members, I thank Raquel for being a good friend who always listen to me and help me out, Richard, Maria, Enrique, Pilar, Nuria, and Irene for their friendliness and collaboration. I would like to thank Cristina, Tania, and Valentina for all the technical help, without them it is practically impossible to work in the lab. Apart from this, all of them are great co-workers who filled our lab space with enthusiasm and humour. I am deeply indebted to Esther and Aldo for being great colleagues, and great friends throughout my stay here. Words of thanks are not enough to thank Elena, who formatted and designed my thesis, Thanks a lot Elena, for the beautification of the thesis and all your help, all helped me. Thanks to my lab members for giving their valuable time in translating the thesis summary in Spanish.

I also thank all the CBMSO members, personal department and all central facilities, in particular I would like to thank Maite and Milagros from the Electron Microscopy facility and Berta and Silvia from FACS facility, they always helped me in learning the techniques. I would like to thank the members of Marisa's and Fresno's lab for their friendliness and their kindness to provide the reagents.

I am very thankful to Dr. Federico Mayor, Dr. Petronila Penela and Dr. Wolfgang Schamel for their sound advice and collaboration.

Last, and most of all, I would like to thank all my friends Shalini, Chanchal ,Deepa Harsh, Manish, Apul, Pawan, Jalaj and Sandrea. They made my stay easier and more fun over the last five years.

Most importantly, I would like to thank my family members for all their help and support. In particular I would like to thank my mother-in-law who came all the way to Madrid for helping me with the home stuff during my pregnancy and thesis writing period. I cannot thank enough to my parents who thoroughly dedicated themselves for their children and taught me to love learning and always encouraged and

supported me unconditionally. I would also thank my siblings Manisha and Vineet for giving me all kind of support and love, mere talking to them on weekends give me energy for coming week. I am grateful to God for creating ‘Tishya’ my angel for me, she gives me immense happiness and her smile gives me courage to cope with all difficulties. Finally, most of all I thank my husband for his boundless support at all phases of my life, Amit without you this thesis and this wonderful life is not imaginable.

SUMMARY

Summary

Two of the most intriguing properties of the TCR complex are its low affinity but high sensitivity to antigen stimulation and its ability to activate different signaling pathways in function of the strength of interaction with its peptide-MHC (pMHC) ligands. During T cell development, correct discrimination between weak and strong pMHC interactions and subsequent differential activation of signaling pathways and genetic programs is the basis for positive and negative selection which ensures that only self-MHC restricted, but tolerant T cells mature. After successful completion of differentiation in the thymus, T cells enter the peripheral lymphoid organs as naive T cells. Upon encounter with their specific antigen naive T cells differentiates into effector cells which are able to coordinate the immune response. Part of the effector cells becomes memory T cell which remains dormant until the next antigen encounter. Memory T cells respond more vigorously upon reencounter with antigen and are more sensitive to low doses of antigen than naive T cells. These properties are the basis of immunity. The mechanisms underlying the ability of the TCR to differentiate between high affinity and low affinity ligands and to translate this into activation of differential signaling cascades, as well as the mechanism providing memory T cells with increased sensitivity are largely unknown.

It has previously been shown that the TCR is expressed on the surface of resting T cells as a combination of oligomers of different sizes and that the larger oligomers are preferentially activated in response to low doses of antigen. We hypothesized that enrichment for more and larger oligomeric TCR complexes would provide memory T cells with higher antigen sensitivity. In this study, we show by quantitative electron microscopy analysis, that previously activated and memory T cells indeed have more and larger TCR oligomers at the cell surface than their naive counterparts. We also show that a mutation in the transmembrane of CD3ζ impairs oligomeric TCR complex formation and that loss of oligomeric TCR complexes causes decreased antigen sensitivity of T cell lines and antigen experienced T cells. This provides direct evidence for larger TCR oligomers as directly responsible for increased sensitivity of antigen-experienced T cells.

In the second part of this work we describe a search and initial analysis of proteins that associate differentially with the TCR complex during positive and negative selection, hypothesizing that such differentially associating proteins provide thymocytes with a mechanism to differentially activate downstream signaling pathways. We developed a mouse model of T cell differentiation that allowed us to isolate a large number of thymocytes undergoing positive or negative selection in a synchronized fashion. Using this model we performed a biochemical screen for differentially associating proteins and phosphoproteins. We found that the G protein coupled receptor kinase 2 (GRK2) associates with the TCR complex during positive selection and dissociates upon induction of negative selection. Analysis of T cell differentiation in mice that lack one copy of the GRK2 gene indicates that the efficiency of positive selection is reduced. Furthermore, reduction in GRK2 expression affects the sensitivity of DP thymocytes towards antigen, suggesting a direct role of GRK2 in TCR-dependent signaling and affects migration of DP and SP thymocytes towards the chemokine SDF-1α. The observation that this migration is inhibited by stimulation via the TCR indicates a functional link between CXCR4 mediated migration and TCR signaling in these thymocytes.

INDEX

INDEX

ABBREVIATIONS

ABBREVIATION

+/-	Heterozygous
-/-	Homozygous deficient
+/+	Wild Type
Ab	Antibody
APC	Antigen presenting cell
BCR	B cell Antigen receptor
BN-PAGE	Blue native PAGE
bp	Base pair (s)
BSA	Bovine serum albumin
CD	Cluster of differentiation
Co-IP	Co-immunoprecipitation
CTL	Cytotoxic T lymphocytes
DAG	Diacylglycerol
Dig	Digitonin
DN	Double negative stage in T cell development, $CD4^-CD8^-$
dNTPs	Deoxynucleosidetriphosphate
DP	Double positive stage of T cell development, $CD4^+CD8^+$
EM	Electron Microscopy
ERK	Extracellular signal-regulated kinase
FACS	Fluorescence activated cell sorting
FCS	Fetal calf serum
FITC	Fluorescein isothiocynate
Gads	Grb2 like adaptor protein
GFP	Green fluorescent protein
Grb2	Growth factor receptor bound protein2
GRK2	G protein coupled receptor kinase 2
GPCR	G protein coupled receptor
IB	Immunoblot
Ig	Immunoglobulin
IL	Interleukin
IP	Immunoprecipitation
IP3	Inositol-1,4,5 triphosphate
ITAM	Immunoreceptor tyrosine-based activation motif
Kb	Kilobase pairs
Kd	Kilodalton
LAT	Linker for activation of T cells
MAPK	Mitogen-activated protein kinase
MFI	Mean fluorescence intensity
MHC	Major histocompatibility complex
NF-κB	Nuclear transcription factor κ B
NFAT	Nuclear factor for activated T cells
P	Probability
PAGE	Polyacrylamide gel electrophoresis
PBS	Phosphate buffered saline
PE	Phycoerythrin
pMHC	MHC presenting antigenic peptides
RT	Room temperature
SD	Standard deviation
SP	Single positive, CD4 or CD8
SDS	Sodium dodecyl sulfate
Self-pMHC	MHC presenting self peptides
SLP76	SH2 domain-containing leukocyte phosphoprotein of 76 kD
Src	Sarcoma protein kinase
Syk	Spleen tyrosine kinase

TCR	T cell antigen receptor
tet	Tetracycline
T_H cell	Helper T cell
TM	Transmembrane
WT	Wild Type
WB	Western blot
ZAP70	Zeta-associated protein of 70 kD

INTRODUCTION

INTRODUCTION

The adaptive immune system exhibits pathogen specificity and antigenic memory. It consists of two major cell types: B lymphocytes comprise the humoral branch of the immune system and recognize soluble antigens via their B cell receptor (BCR), while T lymphocytes are part of cell mediated branch and recognize pathogen derived peptides bound to the MHC molecules of antigen presenting cells (APCs) via their T cell receptors (TCRs). T cells expressing a αβ TCR are the predominant T cell population and play a central role in coordinating the responses of the innate and adaptive immune system and in providing antigenic memory. The haematopoetic precursors of the T cells differentiate in the thymus and upon successful completion of this process the now mature, naive T cell migrate to the peripheral lymphoid tissues (spleen, lymph node and Peyer's patches). Naive T cells migrate from one lymphoid organ to another via blood and lymph in search of a potential threat to the immune system. Once a naive T cell encounters an antigen presented by professional antigen presenting cells (APCs), it gets activated leading to the initiation of a cascade of intracellular biochemical signals that results in effector cell generation. Effector T cells have a lower activation threshold and high capacity of cytokine production. After pathogen clearance most of the effector cells die while a small fraction persists as a memory T cells (Chandok and Farber, 2004). Antigenic memory allows a faster and stronger response to a reencounter with specific pathogens. At the population level, this is due to an increased T cell frequency (Askonas et al., 1982) and preferential outgrowth of higher affinity T cell clones that will form the memory T cell pool (Busch and Pamer, 1999; Malherbe et al., 2004; Zehn et al., 2009). At the cellular level, memory T cells are more sensitive to antigen stimulation, converts more rapidly into effector T cells and produce larger amounts of effector molecules (Bachmann et al., 1999; Bruno et al., 1995; Cho et al., 1999; Veiga-Fernandes et al., 2000; Zimmermann et al., 1999).

1. The αβ T cell receptor complex

The TCR complex is the defining cell surface structure of the T lymphocyte and is crucial for its differentiation and function. The TCR complex is composed of an antigen-recognizing clonotypic TCRαβ heterodimer and a signal-transducing unit containing the invariant CD3γε, CD3δε and CD3ζζ dimers (Figure 1). The TCR α and β chains are glycoproteins of 45KD, consisting of one variable and one constant Ig domain linked by a disulfide bridge. The gene segments encoding the variable domains are generated via a random somatic gene rearrangement process (Garman et al., 1986b) to give rise to high diversity of antigen specificities needed to be able to respond to the rapidly changing pathogens. The Ig like domains are followed by a stalk region (19 residues in the TCRα chain, 15 residues in the TCRβ chain), a 22 amino acid long transmembrane (TM) domain and a short 4-10 amino acid long intracellular region. The CD3 subunits (CD3ε ,CD3γ, and CD3δ) each have an Ig like ectodomain, a 10 residue long connecting peptide , TM region and a long cytoplasmic (45-110 residue) domain containing one immunoreceptor tyrosine-based activation motif (ITAM)(Reth, 1989). The cytoplasmic domain of CD3ε contains in addition two more recently identified regions,

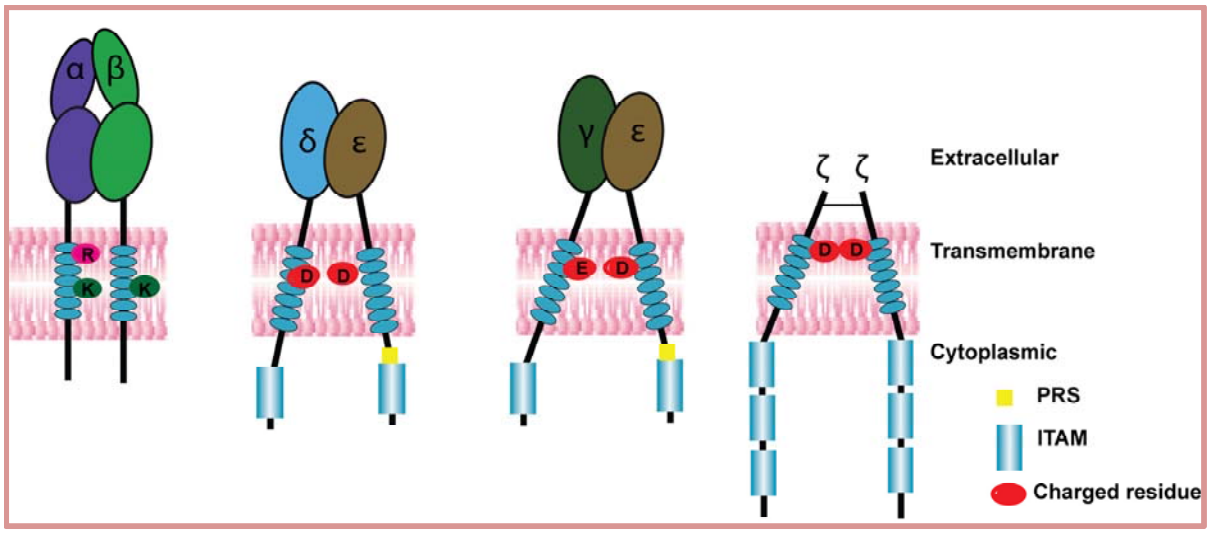

Figure 1: TCR components. The TCR consists of a ligand binding αβ heterodimer, the CD3 heterodimers, CD3δε, CD3γε, and the TCRζζ homodimer. Three basic residues are located in the TM domains of the TCR heterodimer and a pair of acidic residues is located in each of the three signaling dimers.

the proline-rich sequence (PRS) and the basic-rich sequence (BRS) whose function in T cell signaling is only beginning to be understood (Brodeur et al., 2009a; Brodeur et al., 2009b). CD3ε binds noncovalently with CD3δ and CD3γ in a mutually exclusive manner yielding CD3δε and CD3γε heterodimers (Alarcon et al., 1991; Arnett et al., 2004; Sun et al., 2004). CD3ζ forms a disulfide linked homodimer (Koning et al., 1990) and contains a very small extracellular region of 9 amino acid, a TM domain and a cytoplasmic tail containing three ITAM motifs. Via their ITAM motifs and PRS and BRS sequences, the CD3 chains allow the TCR complex to connect to the downstream signaling pathways.

All TCR and CD3 subunits are cotranslationally translocated into the ER and a strict quality control mechanism assures that only fully assembled TCR complexes reach the cell surface (Delgado and Alarcon, 2005; Mallabiabarrena et al., 1992; Minami et al., 1987). During assembly, CD3ε first dimerizes with either CD3γ or CD3δ and the resulting εγ and εδ dimers associate with the TCRα and TCRβ subunits (Alarcon et al., 1988; Koning et al., 1990; San Jose et al., 1998). Incorporation of CD3ζζ is the last step of the assembly and only after this step is the TCR transported to the plasma membrane (Manolios et al., 1991; Minami et al., 1987; Sancho et al., 1989) . ER-retention motifs in the cytoplasmic tails of the CD3 subunits prevent transport of incompletely assembled TCR complexes from the ER to the cell surface and it has been suggested that progressive masking of the retention motifs by the subsequently incorporated CD3 subunits enables cell surface expression of only the completely assembled receptor complex (Delgado and Alarcon, 2005).

1.1. Stoichiometry and valency of the αβ T cell antigen receptor

The stoichiometry (molar ratio of the different subunits within a TCR complex) and the valency (the number of ligand binding TCRαβ heterodimers per complex) of the TCR complex on the resting T cells are central issues in understanding the mechanism of the T cell activation, especially in view of the need

for multivalent peptide-MHC (pMHC) ligands to achieve this activation (Boniface et al., 1998; Cochran et al., 2000). Early on, it was observed that the initially proposed composition of a single TCRαβ dimer associated with one dimer each of CD3γε, CD3δε and CD3ζζ met with an imbalance in charged residues in the transmembrane regions of these components (Figure 2A). Charged TM residues are known to be important for the stability of the complex, and they were proposed to drive the association between TCR and CD3 components by forming pairwise ionic interactions (Cosson et al., 1991; Manolios et al., 1990) (Figure 1). TCRα has two basic amino acids, TCRβ has one basic amino acid (3 basic amino acids in total), and the CD3 dimers each have one acidic amino acid in their trans-membrane regions (6 acidic amino acid in total) (Clevers et al., 1988; Klausner et al., 1990). It was proposed that a structure containing two TCRαβ subunits for each of the CD3 dimers (an αβ:δε:γε:ζζ stoichiometry of 2:1:1:1) would equilibrate this charge imbalance (Figure 2B). Indeed, size determination of solubilised complexes (Exley et al., 1995) and co-immunoprecipitation and FRET assay on T cells from mice co-expressing two different TCRαβ complexes (Fernandez-Miguel et al., 1999) suggested that the TCR complex contained at least two TCRαβ subunits. Importantly, evidence was provided that these were cell surface expressed TCR complexes, excluding the possibility that these were aberrantly assembled complexes that had been retained intracellularly. However, other studies did not find evidence for co-immunoprecipitation of the two different TCRs (Hou et al., 1994; Punt et al., 1994). In these studies different detergents were used to solubilize the TCR complexes (the relatively mild detergent Brij 96 vs the harsher detergent digitonin) and this could explain the differences in the observations: it has been shown that the type of detergent determines whether TCR subunits can be co-immunoprecipitated or not (Alarcon et al., 2006).

More recently, an alternative explanation has been provided to solve the apparent charge imbalance between the transmembrane domains of the TCR subunits, suggesting once more the classical stoichiometry of one TCRαβ dimer and one each of the three CD3 dimers (Call et al., 2002). Combination of wild type TCR and CD3 chains and TCR and CD3 chains mutated in the charged transmembrane residues were translated *in-vitro* in the presence of plasmacytoma derived microsomes, followed by sequential non-denaturing immunoprecipitation and analysis of association between the different subunits. This study provided evidence that selective association of TCRα with CD3δε and TCRβ with CD3γε was dependent on the simultaneous presence of the basic amino acid of the particular TCR chain and the two acidic amino acid residues in the associating CD3 dimer. Similarly, association of CD3ζζ with the other subunits was dependent on the simultaneous presence of the remaining basic amino acid in TCRα and two acidic amino acids in the CD3ζζ dimer (Figure 2). This has led to the proposition that three triangular interactions between one basic and two acidic amino acids form the basis of TCR complex assembly, giving rise to a αβ:δε:γε.ζζ stoichiometry of 1:1:1:1. However, these data do not necessarily reflect the stoichiometry of the TCR complex at the cell surface, as glycosylation or other post

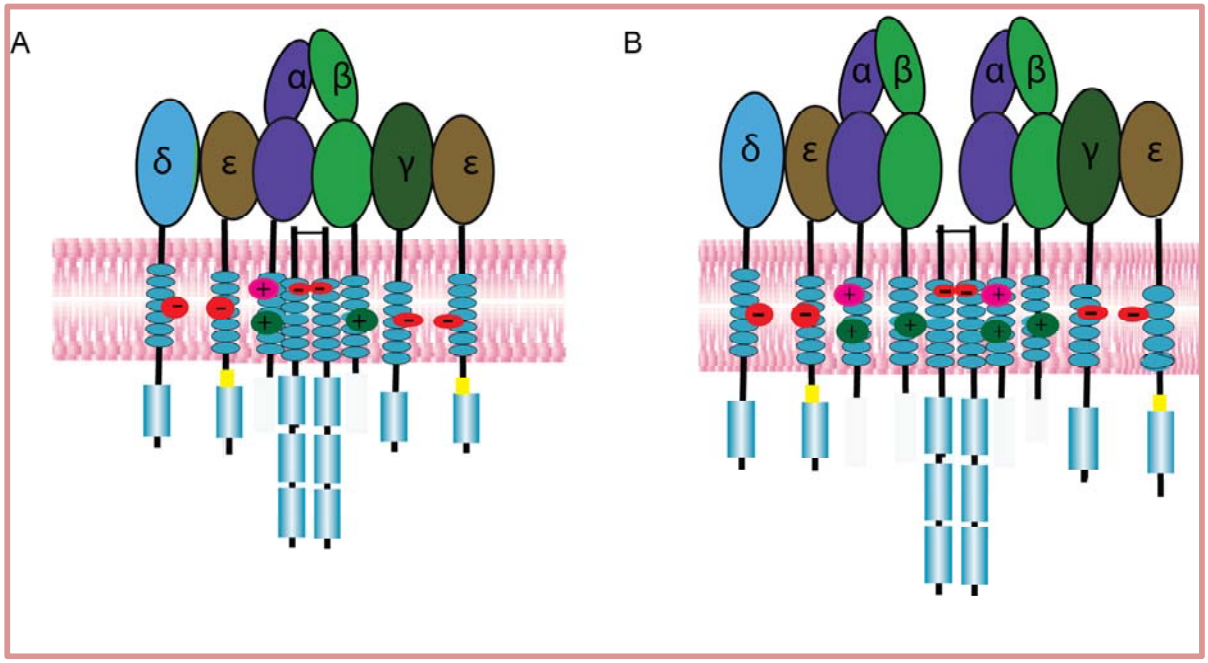

Figure 2: TCR stoichiometry. (A) The monovalent model contains only one ligand binding TCRαβ domain. **(B)** The bivalent model consists of a TCR with two ligand binding αβ domain with one of each CD3δε, CD3γε and TCRζζ subunits.

translational modification may affect the assembly of the surface complex. In addition, ζ might only assemble with the other subunits in the Golgi apparatus *in-vivo* (Dietrich et al., 1999). Finally, the choice of detergent (digitonin) used to solubilize the TCR complex in order to perform the immunoprecipitations may have conditioned the results.

1.2 TCR oligomers in resting T cells

Determination of the composition of the TCR complex via blue native polyacrylamide gel electrophoresis (BN-PAGE) has shown that TCR complexes at the cell surface of resting T cells co-exist as monovalent and oligomeric TCR complexes (Schamel et al., 2005), adding an extra layer of complexity to the stoichiometry and valency of this complex. BN-PAGE is a native protein complex separation technique that determines the relative abundance and number of different complexes formed by a certain protein. Since proteins are not denatured, they are separated based on their complex size and shape on a polyacrylamide gel (Schagger and von Jagow, 1991; Schamel and Reth, 2000). Solubilization of membranes from resting primary T cells and T cell lines in digitonin, followed by size separation by BN-PAGE and immunoblotting for TCR results in detection of only one size of complexes (Figure 3A) (Hellwig et al., 2005; Schamel et al., 2005; Zapata et al., 2004). Gel shift assays have provided evidence that these digitonin-extracted complexes contain only one TCRαβ dimer and two CD3ε containing dimers (Schamel et al., 2005). When the membranes are solubilised in Brij96 instead of digitonin, a combination of the digitonin-sized complex and larger complexes are detected via BN-PAGE and immunoblotting (Schamel et al., 2005), showing the co-existence of monomeric and oligomeric TCR complexes. The co-existence of TCR complexes of different sizes is supported by the analysis via electron microscopy of the cell surface replicas of resting primary T cells and T cell lines labelled

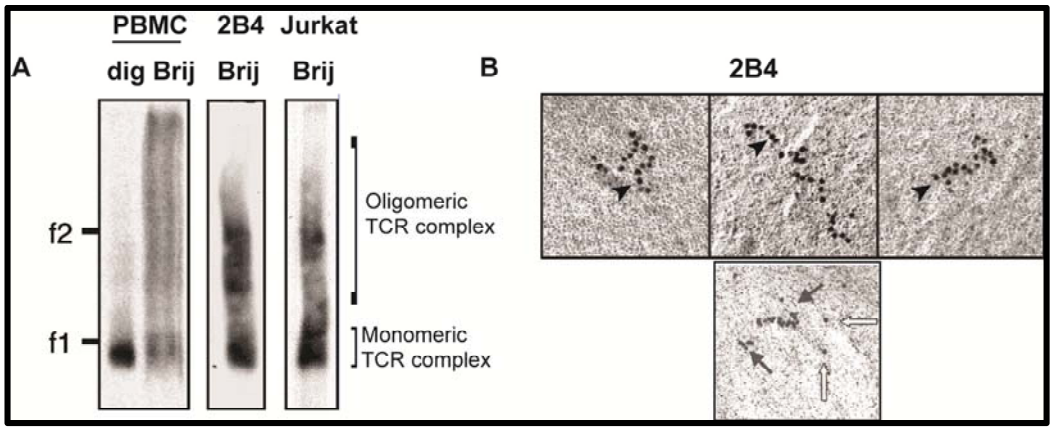

Figure 3: Existence of monomeric and oligomeric TCR complexes on the T cell surface. A) BN-PAGE. **B)** Electron microscopic analysis of cell surface. Figure reproduced from (Schamel et al., 2005)

with anti-TCR- or anti-CD3-specific antibodies and protein A conjugated gold: single gold particles and clusters with a size of up to twenty particles can be detected on the cell surface of the same resting T cell (Figure 3B) (Schamel et al., 2005).

The oligomeric TCR complexes are disrupted by treatment of cells with methyl-β-cyclodextrin, a cholesterol-sequestering agent, suggesting that the oligomeric TCRs reside within the lipid rafts (Schamel et al., 2005). This explains why these complexes can only be detected in detergents, such as Brij 96, that do not extract cholesterol from the membrane. On the other hand, this partitioning into the cholesterol-rich rafts has allowed selective extraction of oligomeric TCR complexes from the cell membrane with saponin. The ratio between the TCRαβ dimers, the CD3ε-containing dimers and CD3ζζ dimers is not significantly different between saponin, Brij96 and digitonin-extracted TCR complexes, suggesting that the oligomeric complexes are formed by multimers of the digitonin-solubilized monovalent complex (unpublished data, Schamel's lab).

It has been shown that the oligomeric TCR complexes are phosphorylated at lower concentrations of antigen than the monomeric complexes (Schamel et al., 2005). This has led to the hypothesis that the oligomeric TCR complexes are responsible for the high sensitivity of T cells in spite of the low affinity of the TCRαβ dimers for their pMHC ligands.

2. T cell receptor signaling

Upon binding to its antigenic peptide-MHC (pMHC), the TCR complex activates various intracellular signaling pathways that are necessary both during T cell development and triggering of an adaptive immune response. While affinity of the TCR for antigenic pMHC is low [(1-50μM (Davis et al., 1998)], the T cell is very sensitive to these peptides and can be activated by a few antigenic peptide molecules on the APC (Irvine et al., 2002; Purbhoo et al., 2004). In spite of a 10^3 to 10^4 fold higher concentration of self pMHC than the antigenic pMHC on the membrane of the APCs and only a tenfold difference in affinity, the TCR is very specific for the antigenic pMHC. There are

various models which explain these complex phenomena of TCR-triggering.

The clustering or aggregation model emphasizes the need of pMHC clustering in order to activate a TCR complex, which allows clustering of TCR complexes and signal spreading through efficient phosphorylation of neighbouring TCR complexes. Support for this model has come from the observation that soluble class I and class II pMHC ligands are only able to stimulate T cells when they are in multivalent form (Boniface et al., 1998; Cochran et al., 2001). Furthermore, it has been shown that MHC class II and also MHC class I complexes can be found in clusters on the surface of APCs (Fooksman et al., 2006; Vogt et al., 2002).

The conformational change model describes how a structural change, associated with TCR ligation is transmitted to the cytoplasmic tails of CD3 complexes. It has been shown that a proline rich region in CD3ε is exposed upon TCR stimulation, which leads to the binding of the adaptor protein Nck (Gil et al., 2002). Neither kinases nor co-receptors are required for the induction of conformational change, suggesting that the conformational change is a direct consequence of ligand binding. More recent evidence indicates that both the conformational change and clustering are necessary for full T cell activation (Minguet et al., 2007).

The kinetic segregation model is based on the hypothesis that a dynamic equilibrium exists between phosphatases and kinase activities in the cell, which results in low steady-state phosphorylation (Davis and van der Merwe, 2006). T cells form multiple zones of close contacts upon binding their pMHC ligands, on the APCs. Due to spatial restrictions membrane-bound inhibitory phosphatases like CD45 and CD148 are excluded from these close membrane junctions. As a consequence, the equilibrium shifts towards kinases in these small areas, which in turn lead to the phosphorylation of TCR and signaling (Choudhuri and van der Merwe, 2007). Many studies showing segregation of CD45 and CD148 from areas of TCR triggering supported this model (Irles et al., 2003; Lin and Weiss, 2003; Varma et al., 2006). However, the ability of soluble antibodies and soluble pMHC oligomers to activate T cells without apparently inducing spatial segregation cannot be explained by this model.

2.1. Signaling through the TCR complex

Signaling through the TCR occurs upon binding to its pMHC ligands. The earliest step after ligand binding is the phosphorylation of ITAMs of the CD3 chains by Src protein tyrosine kinase Lck (Danielian et al., 1989).The co-receptors CD4 and CD8 can bind to Lck and play a role in delivering active Lck to the pMHC-engaged TCR (Mallaun et al., 2008; Veillette et al., 1988). The extent of ITAM phosphorylation correlates with the half life of TCR-pMHC binding and the availability of activated Lck (phosphorylated at Tyr 394) (Kersh et al., 1998). The Syk family kinase ZAP-70 (ζ-chain associated protein of 70kD) then binds to the phosphorylated ITAMs via its tandem SH2 (Src homology 2) domain, and is activated. ZAP70 binding to phosphorylated ITAMs prolongs the transient TCR-pMHC interaction, thereby generating a more sustained intracellular signal. ZAP70 phosphorylates LAT (linker for activation of T cells), a raft associated adaptor protein, which upon phosphorylation functions as a scaffold for various other signaling molecules including

the adaptor protein Grb2, Gads and phospholipase Cγ1(PLCγ1).

Recruitment of Grb2 to phosphorylated LAT leads to the activation of PI3K (phosphatidyl inositol 3-kinase), which catalyses the conversion of PIP_2 (phosphatidyl inositol 4, 5-bisphosphate) to PIP_3 (phosphatidylinositol 3, 4 5-triphosphate). In the membrane, PIP3 serve as a docking site for PH (pleckstrin homology) domain containing proteins, like PLCγ1, Itk and Vav. SLP-76 and LAT together bind PLCγ1, which catalyses the cleavage of phosphatidyl inositol 4,5-bisphosphate (PIP2) into inositol 1,4,5 triphosphate (IP3) and diacyl glycerol (DAG) (Samelson, 2002). IP3 stimulates calcium release for subsequent Ca^{2+} dependent NFAT activation. DAG activates Ras GRP, protein kinase C θ (PKCθ), the three MAPK pathways (ERK, JNK, p38) and Akt. Activation of MAPK results in the activation of the transcription factor AP1. PKCθ switches on the CARMA/Bcl10/IκB kinase (IKK) pathway leading to the activation of NFκB transcription factor. Propagation of Stimuli from the TCR eventually leads to the nuclear localization of NFAT, NFκB and AP1, which in turn leads to activation of the genetic programs underlying T cell activation (Figure 4).

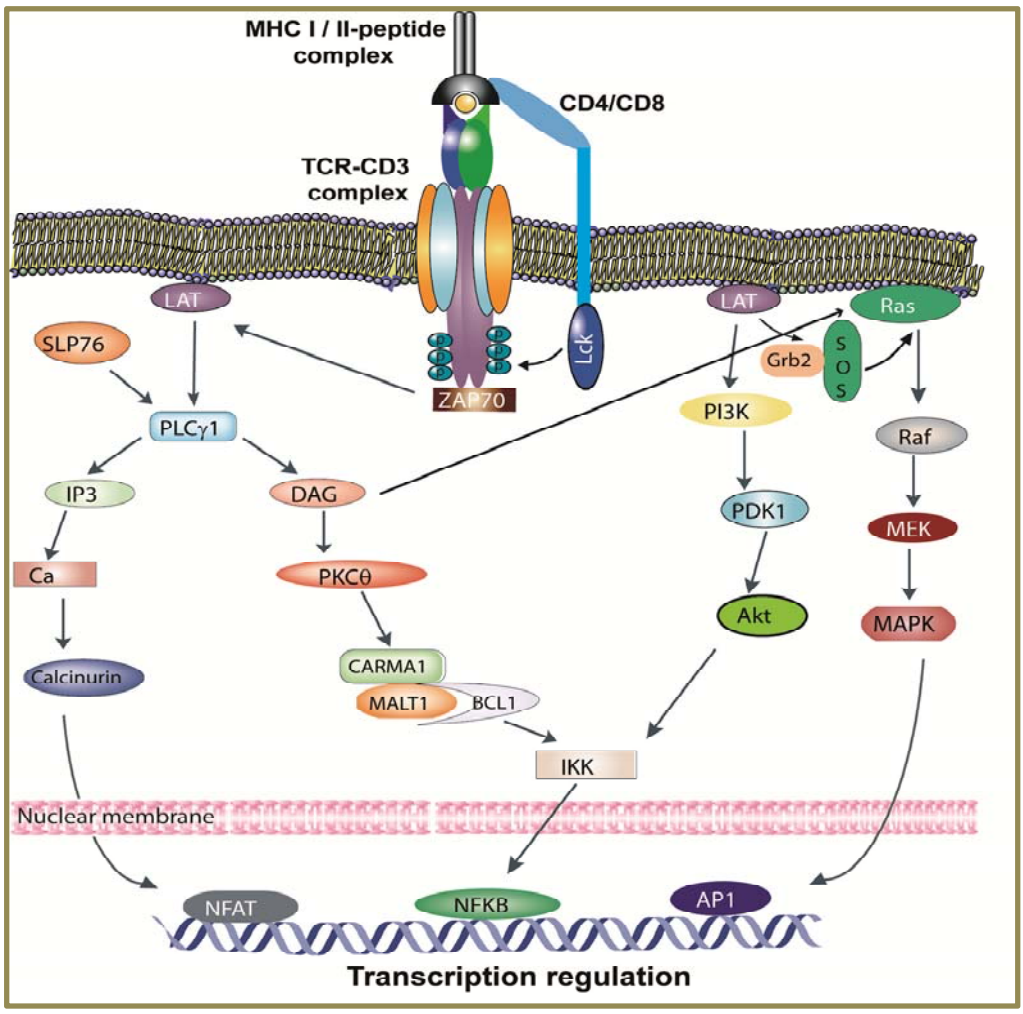

Figure 4: TCR proximal signaling. A simplified schematic representation of the TCR proximal signaling upon MHCp binding.

3. αβ T cell differentiation

T cells arise from haematopoietic stem cell derived T- lymphoid progenitor cells in the bone marrow that migrate to the thymus (Le Douarin and Jotereau, 1975). Within the thymus the distinct stages of differentiation can be distinguished by expression of stage specific cell surface proteins, including the TCR complex, CD4, CD8, CD44 (hyaluronic acid binding adhesion molecule) and CD25 (the α-chain of the IL2 receptor) (Figure 5). The most immature hematopoietic cells lack the expression of CD4 and CD8 and are called double negative (DN) thymocytes. At the DN stage, thymocytes undergo a differentiation program from the DN1 ($CD44^+CD25^-$) through the c-Kit^+ (stem cell factor receptor) $CD44^+CD25^+$ DN2 stage to become the C-Kit^- $CD44^-CD25^+$ DN3 stage. During progression through these stages, the precursors become progressively restricted in their lineage potential (von Boehmer, 2000). At the DN3 stage, V (D) J rearrangement at the T*crb* (TCRβ), T*crg* (TCRγ) and T*crd* (TCRδ) loci occurs (Garman et al., 1986a; Habu et al., 1987). Notch signaling and the rearrangement status of these loci determine whether the cells develop into αβ T cells or γδ T cells. This process is not yet clearly defined, although the strength of the TCR signal may influence this process (Garbe et al., 2006). Upon productive rearrangement of the T*crb* locus, the resulting TCRβ chain associates with the pre-Tα, and the CD3 molecules to form the pre-TCR complex. Expression of the pre-TCR complex rescues thymocytes from cell death and induces proliferation and progression through the $CD25^-$ $CD44^-$ DN4 stage to the $CD4^+CD8^+$ double positive (DP) stage (von Boehmer et al., 1989). At the DP stage, thymocytes rearrange the T*cra* locus leading to the expression of the αβ TCR complex (Kreslavsky et al., 2008; Shinkai et al., 1993), at which stage the thymocytes undergo the processes of positive and negative selection

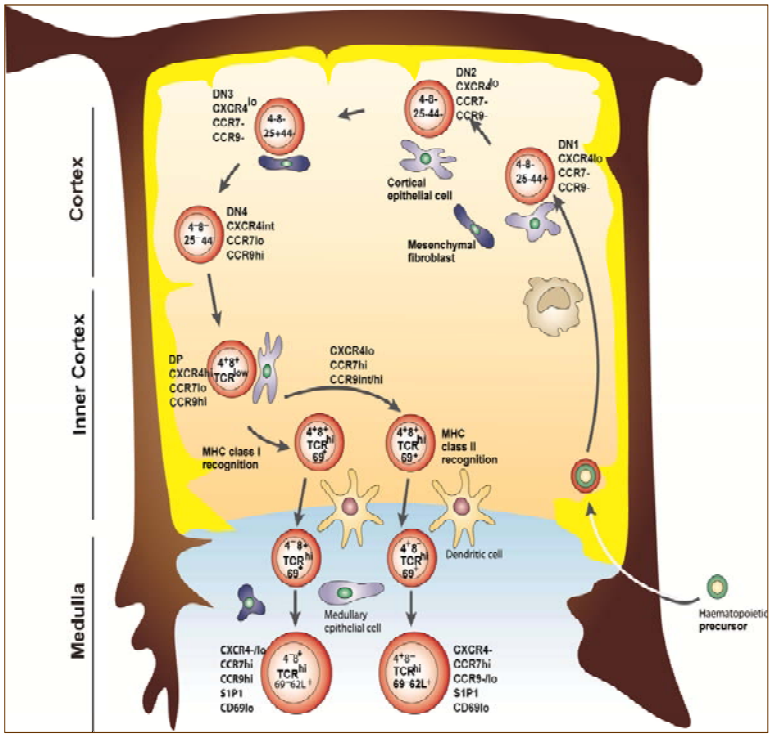

Figure 5: Schematic representation of T-cell development in the Thymus.
The thymic microenvironment is divided into discrete cortical and medullary areas, characterized by the presence of particular stromal cell types. Lymphoid progenitors enter the thymus through blood vessels at the cortico-medullary junction and then migrate in a highly defined pattern through the thymus, correlating with distinct stages of their development. Migration of the cells is regulated by stage specific expression of the appropriate chemokine receptors. The earliest precursors lack expression of the TCR and the coreceptors CD4 and CD8 (DN thymocytes), and can be subdivided into distinct stages based on the expression pattern of CD25 and CD44. Rearrangement of the TCRβ chain occurs at the CD25+CD44- DN3 stage in the outer cortex. Upon formation of the pre-TCR complex, cells progress to CD4+CD8+ DP stage while moving to the inner cortex. Upon rearrangement of the TCRα chain cells undergo positive selection. Negative selection is predominantly mediated by dendritic cells in the medulla. Cells that have successfully passed both selective processes finally mature into the appropriate CD4 or CD8 SP lineage via the process of lineage commitment and leave the thymus.

Knock-out mice for each of the TCR and CD3 chains have confirmed the essential role of these components in thymic development. Thymocytes of mice lacking the rearrangement associated genes (RAG) 1 or 2 are unable to rearrange the TCR loci and are blocked at the DN3 stage (Mombaerts et al., 1992). Thymocytes of mice with a null mutation in the T*crb* locus or the CD3ε gene are also completely arrested at this stage (DeJarnette et al., 1998; Malissen et al., 1995). These components are therefore absolutely critical for transition to DN4 to DP stage. However in mice with inactivated CD3γ or pre-Tα genes a low number of thymocytes reaches the DP (Haks et al., 1998), while thymocytes lacking expression of CD3δ or CD3ζ reach the DP stage in appreciable numbers (Love et al., 1993; Malissen and Schmitt-Verhulst, 1993). These differences in phenotype may reflect differences in the extent to which each of these chains is critical for expression at the cell surface of the pre-TCR and TCR itself, but also suggest unique contributions of these chains or their domains to the signaling events necessary for each of the differentiation steps. In line with this latter possibility, progressive deletion of the cytoplasmic domains of CD3ε shows that the PRS is absolutely required for pre-TCR driven cell expansion while the BRS is necessary for DN to DP transition (Brodeur et al., 2009b).

3.1. Thymic migration and egress

Each of the thymic differentiation steps takes place at a specialized anatomical location in the thymus and differentiating thymocytes migrate through the thymus in a spatially and timely coordinated pattern to reach these locations (Figure 5) (Lind EF, 2001; Petrie., 2003). Chemotaxis is one of the main mechanisms underlying this migration. Chemokine receptors, a subfamily of the G-protein coupled receptors (GPCRs) are expressed in a stage specific manner by thymocytes and the corresponding chemokines are expressed in defined thymic locations (Campbell JJ, 1999; Misslitz A, 2006). This provides a mechanism of stage-dependent migration.

Bone marrow derived precursors enter into the thymus at the cortico-medullary junction via high endothelial venules and migrate towards the outer cortex. CXCR4 is highly expressed on thymocytes from the DN2 to the DP stage and signaling by CXCR4 upon interaction with its ligand CXCL12 (SDF1α) is required for proper migration of early progenitors to the cortex (Ara et al., 2003; Plotkin et al., 2003; Plotkin J, 2003). A complete block in thymocyte development observed upon conditional deletion of CXCR4 in DN1 cells (Plotkin et al., 2003), indicates that transition to the next differentiation stage and migration to the appropriate location are tightly linked. CXCR4 mediated PI3K signaling along with signaling via Notch and pre-TCR has also been shown to promote differentiation from the DN3 stage to the DP stage (Janas et al.,2010). CXCR4 is downregulated on DP thymocytes upon receiving signals that lead to positive selection (Suzuki et al., 1998). This downmodulation is thought to facilitate migration of DP thymocytes from the cortex to the medulla. Positively selected DP thymocytes also increase expression of CCR7. Its ligands CCL19 and CCL21 are produced by mTEC in the thymus (Nitta et al., 2009; Ueno et al., 2004). In medulla CCR7-mediated migration contributes to the negative selection of tissue-restricted antigens (TRA)-reactive CD4 or CD8 thymocytes (Nitta et al., 2009). Chemokine receptor CCR7 contributes to the chemokinesis

of SP cells and is necessary for attracting them towards the medulla (Ehrlich et al., 2009).

CCR9 is expressed at all stages of thymocytes differentiation, but with maximum expression at DP stage (Carramolino et al., 2001; Poznansky et al., 2002). CCR9 is down regulated in mature thymocytes and loss of response to its ligand CCL25 occurs just before thymocytes emigration, which shows that CCL25/CCR9 interaction acts as a retention factor for thymocytes in thymus.

After T cell development mature thymocytes exit from the thymus and reach the peripheral lymphoid organs. Sphingosine-1-phosphate (S1P) and S1P receptor1 (S1P1) regulate the T cell exit. S1P is more highly expressed in blood than in tissues including the thymus (Schwab et al., 2005). Its receptor S1P1 is highly expressed by mature thymocytes and last stage of thymocytes development upregulate its expression (Allende et al., 2004; Kurobe et al., 2006; Matloubian et al., 2004). S1P1 deficiency results in retention of T cells in both thymus and peripheral lymph nodes (Matloubian et al., 2004). CD69 has been shown to have a role in thymic egress. Downregulation of CD69 is necessary for thymocytes exit as mice that constitutively express high level of CD69 on mature T cell fail to exit and they accumulate in medulla (Feng et al., 2002).(Figure 5).

4. Positive and negative selection of thymocytes

Upon expression of αβ TCR DP thymocytes undergo one of the three fates: death by neglect, resulting in death of 90-95% of DP thymocytes due to the failure of the αβ TCR to bind to the self pMHC and thereby not providing survival signals to the cell; positive selection, promoting survival and development of self tolerant T cells and negative selection which ensures removal of autoreactive cells. Thus the processes of thymic selection establish a diverse T cell repertoire that is self MHC restricted and self tolerant (referred as central tolerance) (Hogquist et al., 2005) (Figure 6)

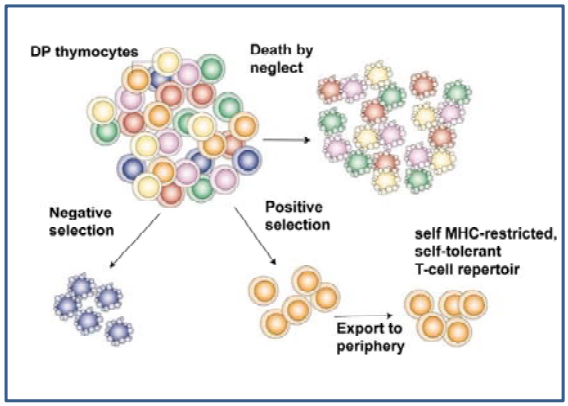

Figure 6: Thymic selection process. DP thymocytes that expresses TCRs that do not recognizes self-peptide-MHC ligand undergo apptosis termed as death by neglect, thymocytes having TCRs which interact with self peptide-MHC ligands with high affinity undergoes apoptosis (negative selection), whereas DP thymocytes that expresses TCRs with low affinity for self peptide-MHC ligands differentiate into SP thymocytes (positive selection). SP thymocytes then exported from the thymus to populate peripheral lymphoid organs [reproduced from (Palmer, 2003)]

Positive and negative selections are both dependent on interaction of the TCR complex with the self pMHC molecules of the thymic stroma. Two hypotheses have been put forward to understand how the interaction between the same receptor-ligand pair can lead to such opposite outcomes. The Avidity model predicts that the sum of affinities provided by the TCR-pMHC interactions determine whether a thymocyte is positively or negatively selected. This model is supported by experiments in which it was shown that agonist peptides promoted positive selection in FTOC at very low concentration, but induced negative selection at high concentrations (Ashton-Rickardt et al., 1994; Sebzda et al., 1994). The Affinity model emphasises the quality of the individual TCR-pMHC interaction, where low

affinity pMHC ligands induces positive selection and high affinity pMHC ligands induce negative selection (Hogquist et al., 1994). Recent work has shown that a very narrow affinity threshold exists that discriminates between positive or negative selection for a given TCR specificity (Naeher et al., 2007).

Determination of the characteristics of the interaction of the TCR and positively and negatively selecting ligands by plasmon resonance has shown a correlation among ligand affinity, half life and selection outcome (Alam et al., 1999). Agonist peptides were shown to have longest half life of binding and lowest K_D value and this coincided with negative selection. Antagonist peptides had very fast dissociation rate and the highest K_D value, coinciding with positive selection. This suggested that the half life of the interaction between the TCR and pMHC was responsible for the activation of the different signaling pathways discriminating between positive and negative selection. Later the role of co-receptors in the thymic selection process was investigated, leading to the concept of apparent affinity (Naeher et al., 2007).

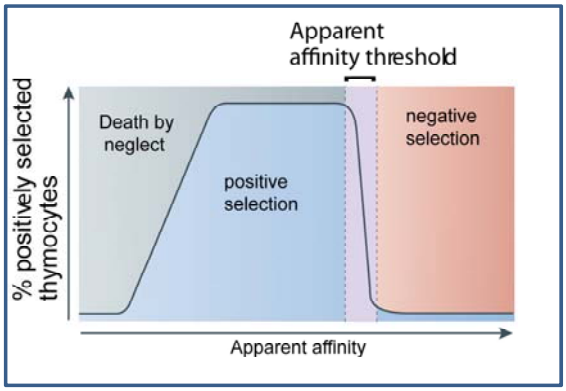

Figure 7: Affinity threshold. Thymic selection depends on the apparent affinity of peptide-MHC complexes for the TCR-co-receptor pair. Apparent affinity threshold of the interaction of the TCR-co-receptor with a self peptide-MHC complex (with a dissociation constant of ~ 6μM; indicated in purple) defines whether a self antigen will induce positive or negative selection

This describes the trimeric interaction between the pMHC complex and the TCR-co-receptor pair. With the use of pMHC tetramer representing positively selecting, negatively selecting and boundary ligands for three different MHC class I restricted TCRs the apparent affinity threshold and half life of binding were calculated: small increases or decreases around a K_D of 6μM and half life of 1-3 seconds led to negative and positive selection (Daniels et al., 2006; Naeher et al., 2007) (Figure 7).

5. Differential signaling through TCR-CD3 complex leading to alternate fates of DP thymocytes

In DP thymocytes engagement of TCR with self-pMHC complexes triggers signaling through the TCR that leads to positive selection or negative selection. There is evidence that distinct TCR-linked signaling pathways lead to these alternate fates.

5.1. Bcl-2 family member proteins

The Bcl-2 family consists of the pro-apoptotic members Bax, Bak, Bim and Bid and anti-apoptotic members such as Bcl-2 and Bcl-X_L. Overexpression of either Bcl-2 or Bcl-X_L protects DP thymocytes from dying, and deletion of Bim leads to delayed apoptosis of thymocytes (Bouillet et al., 1999). Deletion of both Bax and Bak results in the prolonged survival of thymocytes in culture (Rathmell et al., 2002). Apart from the role of Bcl-2 family members in death by neglect they have also shown to be involved in negative selection of thymocytes. Pro-apoptotic Bim defiency makes thymocytes resistant to apoptosis induced by anti-CD3 antibodies or antigen in OT-I and HY TCR^{tg} mice (Bouillet et al., 2002).

5.2. Ras

Ras is a member of the large superfamily of small GTPases. Conversion of its inactive form (GDP bound) to active form (GTP bound) leads to the engagement of many downstream signaling pathways. Guanine nucleotide exchange factors (GEFs) are involved in this GDP to GTP exchange. Ras is required for thymocytes development, T-cell proliferation and IL2 production (Cantrell, 2002). Positive selection is specifically blocked in mice expressing a dominant negative form of Ras while negative selection remains unaffected (Swan et al., 1995).

5.3. MAPK

Differential MAPK activation in positive and negative selection is widely accepted as a mechanism underlying the discrimination between these two events. Activation of MAPK pathway involves sequential phosphorylation and activation of a three kinase cascade: MEKK, MEK, MAPK (Sohn et al., 2003). In T cells MAP kinase, ERK1/2, p38 and JNK are activated in response to TCR crosslinking (Dong et al., 2002). Targeted disruption of the *erk* gene or expression of dominant negative Ras, specifically blocks positive selection (Pages et al., 1999; Swan et al., 1995) while inhibition of p38 with inhibitors or disruption of the *jnk* gene and expression of dominant negative JNK results in block in negative selection (Sabapathy et al., 2001; Sugawara et al., 1998). Differences in the kinetics of ERK activation is considered to be the basis of positive and negative selection, as positively selecting ligands induces a slow and sustained ERK activity, where as negatively selecting ligand provoke a strong and robust but transient ERK activity. In comparison both positively and negatively selecting ligands induce p38 and JNK with similar kinetics (McNeil et al., 2005; Werlen et al., 2000).

The MAPK pathway is regulated by Ras. The adaptor protein Grb2 which is constitutively associated with Sos (son of sevenless) through its SH3 domain, connects Ras to TCR induced signaling pathways. Sos is a GEF with dual activity for Ras and Rac, and can therefore activate both the ERK and JNK/p38 pathway. Thymocytes heterozygous for Grb2, show inefficient JNK/p38 activation but normal ERK activation and as a consequence show impaired negative selection but normal positive selection (Gong et al., 2001)

RasGRP (Ras Guanine nucleotide releasing protein1), another GEF for Ras, has been shown to be required for TCR mediated Ras-Erk activation, and hence shown to be critical for positive but not negative selection (Dower et al., 2000). Moreover there is no Ras activity in PLCγ1 deficient T cells as PLCγ1 produces the secondary messenger DAG that directly binds to RasGRP1 and activates it. However, Ras can be activated at the plasma membrane by Grb2/Sos in response to in strong but not to weak stimuli (Parez de castro et.al., 2004). From these observations, positive selection signals were thought to induce RasGRP/Ras/ERK pathway, and negative selection signals were thought to induce Grb2-Sos/Rac/JNK p38 pathway.

Recently, it was shown that positive selection inducing signals resulted in subcellular compartmentalization of RasGRP/Ras/Erk to the Golgi membrane, where as negative selection inducing signals led to localization of Grb2-Sos/Ras/Erk to the plasma membrane. (Daniels et al., 2006).

Positive selector induced activation of ERK has been shown to last longer in Golgi than in the plasma membrane. In contrast, JNK remains distributed throughout the cell independent of the type of TCR input. Therefore the retention of ERK in the plasma membrane upon signaling leading to negative selection may thus releave competition between ERK and JNK and enable phosphorylated JNK and other effector molecules to initiate negative selection successfully. Thus, subcellular compartmentalization of Ras-GEF and Ras upon TCR stimulation is now widely accepted to be the branch point of positive and negative selection (Yasuda and Kurosaki, 2008).

5.4. MINK-Nck

MINK (misshapen-Nck-interacting kinase (NIK)-related kinase) has a preferential role in negative selection (McCarty et al., 2005). TCR stimulation with a negatively selecting peptide induces association of MINK to Nck. This association in turn leads to JNK activation and upregulation of Bim and BimEL proapoptotic proteins that have a role in negative selection (Bouillet et al., 2002). The Nck-MINK interaction potentially links MINK to the TCR complex. Nck binds to the TCR complex of mature T cells upon induction of a conformational change by strong TCR ligands. The conformational change exposes a polyproline rich sequence in CD3ε, which can be detected in a pull down assay with the N terminal SH3.1 domain of Nck (Gil et al., 2002). In the thymus, both positively and negatively selecting ligands induce the conformational change, as detected in the Nck SH3.1 pull down assay (Gil et al., 2005), making it difficult to draw a direct correlation between Nck binding and negative selection. However, an alternative method to detect the exposure of the proline-rich sequence of CD3ε, i.e. labelling with the APA1/1 antibody, only occurs in thymocytes upon stimulation with negative selection inducing antibodies (Risueno et al., 2005), showing a strong correlation. The reason for this apparent discrepancy has not yet been resolved.

6 G protein-coupled Receptor Kinase 2

The G protein-coupled receptor kinases (GRKs) family consists of seven serine/threonine protein kinases that have been divided into three subfamilies based on a sequence homology: the visual GRKs GRK1 (rhodopsin kinase) and GRK7 (cone opsin kinase); the β-adrenergic receptor kinases, GRK2 (β-ARK1) and GRK3 (β-ARK2); and the GRK4 subfamily consisting of GRK4, GRK5 and GRK6. The main role of GRKs is to specifically recognize and phosphorylate agonist activated G-protein coupled receptors (GPCRs). In addition to this GRKs phosphorylates many non-receptor substrates such as tubulin, synucleins or phosducins (Ruiz-Gomez et al., 2000). GRKs have also been implicated in desensitization of several GPCRs independent of phosphorylation leading to attenuation of signal transduction of GPCR, showing secondary role of their kinase activity (Pao and Benovic, 2002,Carman et al., 1999) and suggesting a scaffold role for this family of proteins. GRKs interact with variety of proteins implicated in signaling and trafficking involved in essential biological pathways assigning novel roles for GRKs in physiology and diseases.

6.1 Structure and substrate specificity

GRKs share a common structural architecture: they contain a central catalytic domain varying between 263-266 amino acids

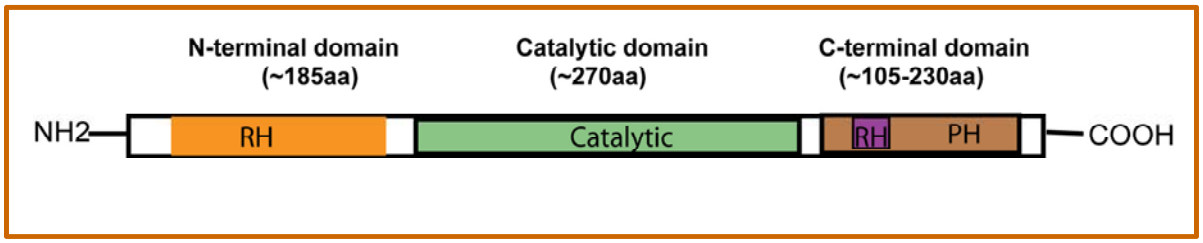

Figure 8: Domain structure of GRK2. GRK2 contains three primary domains: The NH2-terminal domain involved in GPCR binding followed by a central catalytic domain that involved in serine-threonine phosphorylation of targeted proteins, and a variable COOH-terminal domain that regulates phospholipid association.

that mediates substrate phoshphorylation, about 185 amino acid long NH2 terminal domain that is important for receptor binding, and a variable COOH-terminal domain that is involved in phospholipid association.The N-terminal region of GRKs consists of a RH domain of 120 aa, which in case of GRK2 and 3 provide a potential mechanism of phosphorylation independent regulation of GPCR signaling and a Gαq/11 binding site (Carman et al., 1999). A Gβγ-binding site has been described in the N-terminal domain of GRK2 that helps in membrane targeting of GRK2 (Willets et al., 2003). The C-terminal domain of GRKs is important for their subcellular localization and agonist dependent translocation to the membranes. GRK2 and 3 contain a plekstrin homology domain (PH) which facilitates its interaction with membrane phospholipid PIP2 and free Gβγ subunits (Ribas et al., 2007).

6.2 Roles of GRK2

Out of the seven members of the GRK family, GRK2 is the most thoroughly characterized member, it not only binds and phosphorylates a large number of GPCRs, but its substrates also include large number of cytosolic proteins which are not GPCRs. Apart from its kinase activity, GRK2 has the capacity to modulate the activity of various signaling proteins by scaffolding signaling complexes and transporting them to receptors, in an agonist dependent manner.

Phosphorylation of GPCRs: classical role

Upon ligand binding, GRK2 associates with agonist coupled GPCRs and phosphorylate serine-threonine residues within the intracellular loops and C-terminal domain of these receptors. In an agonist unbound state G-protein coupled receptors (GPCR) remain in an inactive conformation, but upon agonist binding this receptor undergoes a conformational change to expose a surface that acts as a guanine nucleotide exchange factor for the heterotrimeric G-proteins. After activation GDP is released from the G-protein which in turn facilitates binding of GTP. The GTP-bound G-protein undergoes a conformational change that causes its release from the receptor and dissociation into activated α and βγ subunits, which leads to the activation of downstream signaling pathway. GRK2 also recognises the activated form of the receptor and becomes catalytically active.

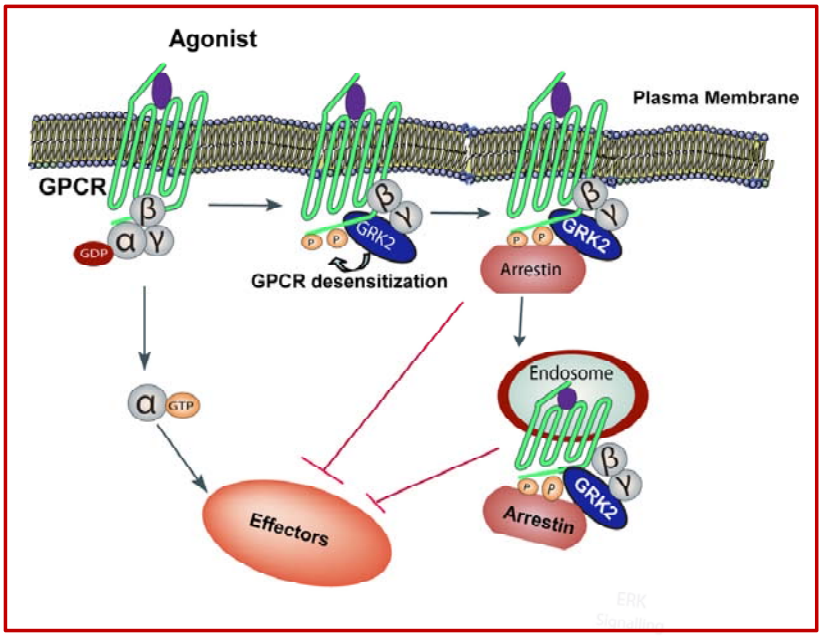

Figure9. Schemetic representation of GRK2 mediated desensitization of GPCRs. In the absence of receptor stimulation, the Gα subunit is GDP bound and remain associated with Gβγ subunits. Upon ligand binding GTP is exchanged for Gα bound GDP, which leads to the conformational change in Gα subunit and its dissociation from Gβγ subunits. The dissociated Gα and Gβγ subunits activate several downstream intracellular signaling pathways. Subsequently GRK2 is recruited to agonist occupied GPCRs and phosphorylates threonine-serine residues within the intracellular domains of the GPCRs, which results in subsequent recruitment of β-arrestins. β-arrestins target GPCRs to clathrin-mediated internalization which resulta in further inhibition of GPCR signaling.

Activated GRKs then phosphorylate intracellular domain of the receptor and are then released. As a result of GRK2 mediated phosphorylation of the receptor, recruitment of β-arrestin occurs. Later, β-arrestin initiate clathrin dependent internalization of GPCRs resulting in receptor degradation or resensitization inside endosomal compartments (Figure9).

6.3 GRK2 Interactions

GRK2 has been shown to interact with a variety of proteins and these interactions are both phosphorylation-dependent and independent (Table 1). It was shown that GRK2 binds to several proteins involved in intracellular signaling and receptor trafficking such as PI3kinase, Akt, caveolin, G protein subunits, clathrin and MAPKs. Many of these proteins are predominantly required for TCR signaling and hence, GRK2 interaction with them may be of particular importance in T cells.

Recently it has been shown that p38MAPK associates with endogenous GRK2 and is phosphorylated by GRK2 (Peregrin et al., 2006). Phosphorylation of p38 by GRK2 attenuates binding and activation of p38 by its upstream activator MKK6 which results in the inhibition of activation of downstream substrates of p38. GRK2 directly phosphorylates p38 at Thr123 which is located at the entrance of the docking groove and is highly conserved. Activation of p38 by MKK6 is dependent on the expression of GRK2, and is reduced or enhanced when GRK2 expression is increased or decreased respectively. Moreover altered GRK2 expression modifies p38-mediated cellular processes such as LPS induced TNFα production in macrophages. Recently, association of GRK2 with MEK and ERK has been found which seems to control the chemokine induction of MAPK activation (Jimenez-Sainz et al., 2006). The GRK2-MEK1/2 interaction reduces CCL2 induced ERK1/2 activation in HEK293 cells overexpressing GRK2, while a decreased level of GRK2 promote a more robust ERK activation upon agonist treatment. Moreover, GRK2 mediated inhibition of CCL2 induced ERK activation did not require kinase activity of GRK2 nor its interction with G-protein subunits.

Table 1. GRK2 interacting proteins [adapted from (Hansen et al., 2004; Ribas et al., 2007)]

GRK2 interacting protein	Functinal consequences
GPCR	GPCR desensitization
Gβγ	Activated Gβγ subunits increases GRK2 kinase activity by binding and recuting it to plasma membrane
Gα	GRK2 inhibits Gαq/11-mediated signaling via a phosphorylation independent mechanism.
Caveolin	Caveolin inhibits GRK2 activity
Calmodulin	Calmodulin inhibits GRK2 activity
Clathrin	GPCR internalization
Tubulin	GRK2 phosphorylates tubulin,which may affects its interaction with microtuble associated proteins
Actin	Inhibition of GRK2 activity
Synucleins	GRK2 phosphorylates synucleins
c-Src	c-Src phosphorylates GRK2 and increases its kinase activity
MEK1	GRK2-MEK1/2 interaction inhibits chemokine mediated ERK1/2 activity.
ERK1/2	ERK1/2 Phosphorylate GRK2 and decreases GRK2 mediated receptor phosphorylation, and inhances GRK2 degradation
p38 MAPK	GRK2 phosphorylates p38 MAPK and impairs its activation
PI3K	GRK2 mediated recruitment of PI3K increases receptor endocytosis
PKA	PKA phosphorylates GRK2 and promotes its binding to Gβγ
PKC	PKC phosphorylates GRK2 and reverts the inhibition of GRK2 by Calmodulin and there by increases the GRK2 activity
Akt	GRK2 inhibits Akt kinase activity
GIT1	GRK2 translocate GIT1 to the membrane

GRK2 binding to PI3Kγ promotes its plasma membrane recruitment after agonist stimulation, which results in increased receptor endocytosis in HEK293T cells overexpressing GRK2 (Naga Prasad et al., 2001). The 197aa PIK domain of PI3K is important for this interaction, and overexpression of PIK domains inhibits PI3K-GRK2 interaction attenuating β2-adrenoreceptor endocytosis (Naga Prasad et al., 2002; Perrino et al., 2005). Furthermore, GRK2 interacts with the serine threonine kinase Akt directly through its C-terminus, leading to agonist dependent inhibition of Akt via a so far unknown mechanism, (Liu et al., 2005). Grk2 also interacts with GIT and act as anchoring proteins for this protein. (Premont et al., 1998).

6.4. Subcellular localization and regulation of GRK2 activity

Most GRK2 proteins are located in the cytosol and translocate to the plasma membrane upon GPCR stimulation. Specific interaction of the PH domain of GRK2 directly with the phospholipid PIP2 leads to its translocation to the plasma membrane (DebBurman et al., 1995). In addition, binding of PH domain to Gβγ subunit liberated after receptor mediated G protein activation also leads to its membrane targeting. GRK2 binding to Gβγ subunit is promoted by agonist induced phosphorylation of GRK2 at Ser685 by PKA (Cong et al., 2001b). As described previously, GRKs play a key role in GPCR signaling and

activity of GPCR is strongly dependent on the cellular complement and functionality of GRK proteins. It has been shown that several pathological conditions are associated with altered expression of GRK2 and has been associated with impaired GPCR signaling. Hence, GRK2 activity and subcellular distribution are tightly regulated (Figure 10).

GPCR activation leads to production of intracellular messengers, which can regulate the GRK2 activity. Calmodulin, a universal mediator of Ca^{2+} signal can regulate the GRK2 activity. Calmodulin interact with GRK2 at both the amino and carboxyl terminal and directly inhibits its activity (Krasel et al., 2001). Receptor phosphorylation by GRK2 is also modulated by the action of several protein kinases that directly phosphorylate GRK2. Activation of β2AR lead to a rapid and transient increase in c-Src mediated phosphorylation of GRK2 at tyrosine residues of the N-terminus (Y13, Y86 and Y92), resulting in an upregulation of GRK2 kinase activity (Sarnago et al., 1999). cSrc-mediated phosphorylation of GRK2 also enhances its interaction with Gαq, and promotes its degradation by the proteasome pathway (Mariggio et al., 2006). P42/p44 MAPK is also shown to regulate the GRK2 activity. ERK1/2 phosphorylate GRK2 at serine670 leading to inhibition of receptor phosphorylation by GRK2. MAPK phosphorylation at Ser 670 impairs the association of Gβγ subunit with GRK2 resulting in inhibition of its catalytic activity towards receptors substrate and also leads to impairment of its translocation to the membrane (Elorza et al., 2000). Both c-Src and ERK1/2 mediated phosphorylation of GRK2 leads to its degradation via proteasome mediated pathway (Elorza et al., 2003; Penela et al., 2001).

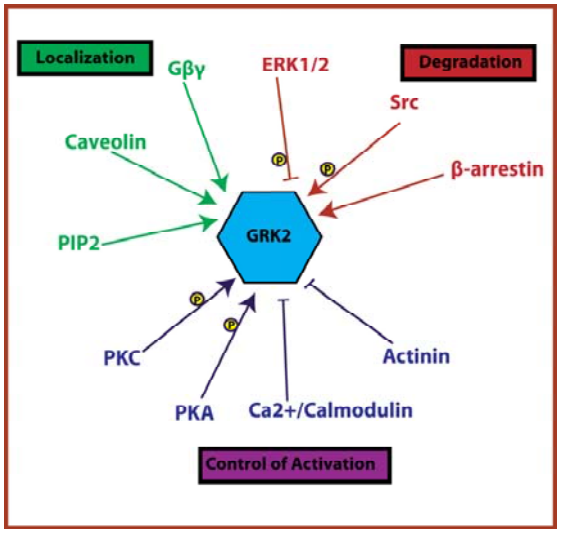

Figure 10: Regulators of GRK2 activity. Schematic representation of the mechanism involved in regulation of subcellular level, localization and degradation of GRK2. [adapted from (Ribas et al., 2007)]

In addition PKC can also modulate GRK2 activity. PKC phosphorylates GRK2 at Ser 29, which prevent GRK2 inhibition by calmoduluin and enhances membrane targeting of GRK2 (Krasel et al., 2001; Winstel et al., 1996). In addition PKA activated through G-coupled receptors directly phosphorylate GRK2 at Ser 685, leading to its membrane targeting and enhanced activity towards GPCRs (Cong et al., 2001a).

6.5. Roles for GRK2 in Immune response and lymphocyte migration

Cells of the immune system express high levels of GRK2 (Chuang et al., 1992; De Blasi et al., 1995), and its levels in immune cells are dynamically regulated, suggesting an important role in regulation of immune activity. Moreover, altered expression of GRK2 correlates with many disease phenotypes; for example rheumatoid arthritis (RA) or multiple sclerosis (MS) show significant down-regulation of GRK2 and GRK6 expression (Lombardi et al., 1999; Vroon et al., 2005) in lymphocytes. However, hypertension in

humans is associated with increased expression of GRK2 in lymphocytes (Gros et al., 1999). In inflammatory diseases, disease pathologies need the activation and recruitment of T cells, monocytes and neutrophils. Migration of these cell types is enhanced and chemokine receptor signaling is also increased. GRK2 has been shown to have a prominent role in regulation of GPCRs signaling, desensitization and internalization. Further research has revealed a complex GRK2 interactome and show a role for GRK2 kinase activity in inhibiting chemokine-induced immune cell migration.

Studies using murine GRK2$^{+/-}$ T lymphocytes have shown its effect on cell migration. It has been shown that around 50% reduction of GRK2 levels in T cells isolated from these mice correlates with a significant increase in the *in-vitro* chemotactic response of these cells as well as their signaling. Low GRK2 activity significantly enhances CCR5 agonist-induced calcium mobilization, signaling to protein kinase B (PKB) and ERK1/2 as well as directed migration of these cells to CCR5 (Vroon et al., 2004) and CXCR4 (Jimenez-Sainz et al., 2006) agonists gradients in vitro. In contrast, Penela et al has shown that GRK2 positively regulates the integrin dependent motility in epithelial cell types and fibroblasts, GRK2 appears to function as a positive regulator of both S1P receptor activation of the ERK cascade and the migration machinery (Penela et al., 2008a). Moreover it was shown that this activity was dependent on phosphorylation dependent association of GRK2 with GIT1, a scaffold protein involved in cell migration processes. It has been reported that GRK2 phosphorylate and activates ezrin in the transformed epithelial cell lines (Cant and Pitcher, 2005). This could play a role in dynamics of actin cytoskeleton which is linked to motility of certain cell types. Furthermore, GRK2 could also contribute to migration by specifically phosphorylating tubulin (Yoshida et al., 2003).

OBJECTIVES

AIMS OF THE STUDY

Previously activated and memory T cells (antigen experienced T cells) have a lower activation threshold in comparison to naive T cells. Their activation is less dependent on co-stimulatory signals and is initiated with lower amounts of antigen. However, the precise mechanisms underlying this increased sensitivity are not clear. Recently it has been shown through biochemical and electron microscopy techniques that both monomeric and oligomeric TCR complexes co-exist on the cell surface of resting T cells. Moreover, it has been shown that the oligomeric complexes become preferentially activated at low doses of antigen, suggesting that they provide T cells with their high antigen sensitivity. We therefore hypothesized that the increased sensitivity to antigen experienced T cells is caused by an increase in the number and size of oligomeric TCR complexes. To address this hypothesis, the principal objectives of the first part of my thesis work were:

1) To compare the number and size of oligomeric TCR complexes on naive and antigen experienced T cells.

2) To design and generate mutants of the TCR complex that specifically impairs oligomeric TCR formation.

3) To investigate the role of oligomeric complexes in T cell differentiation and T cell activation.

The second part of my thesis work was aimed at finding new molecular mechanisms via which the TCR complex is able to transmit the appropriate signal for positive and negative selection of DP thymocytes. Several signaling pathways downstream of the TCR complex have been shown to be involved in positive and negative selection in a quantitatively or qualitatively different manner, but the molecular mechanism that allow TCR to differentially activate one or the other of these signaling cascades are largely unknown. We hypothesised that differential signaling during thymic selection is dependent on the differential association of intracellular factors to the TCR complex depending on the strength of interaction of the TCR complex with pMHC ligands expressed by the thymic stroma. To address the validity of this hypothesis the principal objectives of the second part of my thesis work were:

1) To standardized a mouse model to obtain large number of double positive thymocytes undergoing positive and negative selection *in-vivo.*

2) To perform a biochemical screen using this model to search for proteins associating differentially with the TCR complex during either positive or negative selection.

3) To investigate the role of such differentially associating proteins in T cell selection.

MATERIALS & METHODS

MATERIALS

1. Cell lines

COS: The COS-7 cell line was obtained by immortalizing a CV-1 cell line derived from kidney cells of the African green monkey with a version of the SV40 genome that can produce large T antigen but has a defect in genomic replication (Gluzman, 1981).

293T: Human Embryonic Kidney 293 cells, often referred to as HEK 293 were generated by transformation of cultures of normal human embryonic kidney cells with sheared adenovirus 5 DNA (Graham et al., 1977).

2B4: The 2B4 cell line is a murine T cell hybridoma which has been obtained by immunization of a B10A mouse with pigeon cytochrome C (Samelson et al., 1983).It recognizes the minimal pigeon and moth cytochrome C derived epitope (ANERADLIAYLKQATK) bound to I-E^k.

MA5.8: MA5.8 cell line is a derivative of 2B4 cell line which lacks CD3 ζ chain (Sussman et al., 1988).

DCEK: The DCEK fibroblast cell line stably transfected with plasmids encoding I-E^k and CD80 used as a antigen presenting cells for 2B4 and AND T cells.(R. Germain National Institutes of Health, Bethesda, MD).

T2K^b: T2K^b is a H2-Kb transfected derivative of the human cell T2, a fusion between a T-lymphoid blastoid cell line (LCL) and B-LCL (Alexander et al., 1989)

2. Animal models

C57BL/6: C57BL/6 and CD45.1-congenic C57BL/6 mice (kindly provided by Dr. C. Ardavin, Centro Nacional de Biotecnología, Madrid) were used as recipient animals for bone marrow reconstitution experimemts.

OT-I: OT-1 is a MHC class I restricted TCR transgenic line. This TCR recognizes the octameric peptide SIINFEKL (derived from OVA) in the context of H2K^b molecule (Hogquist et al., 1994). All T cells in these animal expresses Vα2 and Vβ5 molecule. CD3ζ-deficient mice (Love et al., 1993), acquired from the Jackson Laboratories were crossed to OT-1 TCR^{tg} mice and used as a bone marrow donors.

AND: AND is MHC class II restricted TCR transgenic animal which expresses AND TCR (Vα11.1 Vβ3) which recognises MCC88-103 and PCC88-104 in context of I-E^k molecule (Kaye et al., 1983).

TANDRAG: The TANDRAG triple-transgenic mice express the AND TCR together with a TIM construct containing the I-E^k-restricted MCC epitope under regulation of a tetracycline-responsive promoter (Tet-off) TA; (van Santen et al., 2004). These mice were bred onto a RAG1-deficient H-2^k-positive background.

GRK2: GRK2$^{+/-}$ mice (Jaber et al., 1996) on a C57BL6 background were a gift from Dr. Fedrico Mayor Jr. This line was crossed to OT-1 and AND TCR transgenic lines.

All animals were bred and maintained under SPF conditions in the animal facility of the 'Centro de Biología Molecular Severo Ochoa' in accordance with applicable national and European guidelines. All animal procedures were approved by the ethical committee of the 'Consejo Superior de Investigaciones Científicas'.

3 Reagents

3.1 Culture medium

COS and 293T cell lines were maintained in DMEM (Gibco) supplemented with 2 mM L-Glutamine, 100 U/ml penicillin, 100 U/ml streptomycin and 10% FCS.

Bone marrow derived cells were maintained in Iscove's medium (IMDM, sigma) supplemented with 10%FBS, 25ng/ml IL7, 25ng/ml IL6, 50 ng/ml SCF and 50ng/ml Flt3-ligand (all cytokines from Preprotech). Cell lines MA5.8 and 2B4 were cultivated in RPMI1640 (sigma) supplemented with 2 mM L-Glutamine, 100 U/ml penicillin, 100 U/ml streptomycin and 5% FCS. Primary T cells and Blast cells were maintained in RPMI1640 (sigma) supplemented with 2 mM L-Glutamine, 100 U/ml penicillin, 100 U/ml streptomycin ,10µM β-mercaptoethanol, 1 mM Na-pyruvate and 10% FCS.

3.2 Peptides

Table 2 : List of peptides

Peptide	Sequence
MCCp	ANERADLIALKQATK
OVAp	SIINFKEL

3.3 Primary Antibodies

Table 3: List of antibodies

Antibody	Clone	Isotype	Species	Generated by
CD3ζ	448	Polyclonal	Rabbit	San Jose et al,1998
CD3ε	APA1/1	IgG1	Mouse	Alarcon et al,1991
h,Mcd3ε	M20	Polyclonal	Goat	Santa Cruz Biotechnology
mCD3εγ	145-2C11	IgG1	Hamster	ATCC
mCD3εδ				
GRK2	C5/1.1	IgG2a	Mouse	Upstate
GRK2	Polyclonal	IgG	Rabbit	Santacruz
Actin	DM1A	IgG1	Mouse	Sigma
GFP	7.1 and 13.1	IgG1κ	Mouse	Roche
4G10biot	4G10	IgG2b	Mouse	Upstate
448bio	448	Polyclonal	Rabbit	San Jose et al,1998
Phospho-tyrosine	4G10	IgG2b	Mouse	Upstate

3.4. Secondary Antobodies

Table 4: List of secondary antibodies

Antibody	Specificity	Source
Anti-mouse IgG-HRPO	Murine HC and LC	GE Healthcare UK limited
Anti-rabbit IgG-HRPO	Rabbit F(ab')2 fragment	GE Healthcare UK limited
Anti-goat IgG HRPO	Goat IgG (H+L)	Thermo Scientific

3.5 Fluorescent Antibodies

Table 5. List of fluorescent antibodies

Antibody	Source
CD4-FITC/PE/ /Biotin	ImmunoTools/ BD pharmingen
CD8-perCP/Biotin	BD pharmingen
2C11-PE/biotin	BD pharmingen
H57-biotin	eBioscience
αβTCR-FITC	ImmunoTools
Vα11-biotin	BD pharmingen
Vα2-PE/biotin	BD pharmingen
T370-biotin	eBioscience
CD5-biotin	eBioscience
CD69-FITC/PE/biotin	BD pharmingen
CD44-FITC/biotin	ImmunoTools/ BD pharmingen
CD25-biotin/APC	BD pharmingen
CD62L-FITC	BD pharmingen
CD90-biotin	BD pharmingen
CD19-PE/Biotin	eBioscience/ BD pharmingen
CD3PE/biotin	BD pharmingen
B220-FITC/biotin	BD pharmingen
IFN-γAPC	MACS Milteny biotech
CD4-perCP	BD pharmingen
CD8-FITC	ImmunoTools
HSA-FITC/CD24biotin	BD pharmingen
CD3(17A2)-FITC/PE	BD pharmingen
VB14-FITC	BD pharmingen
VB3 -PE/biotin	BD pharmingen
CD16/32	BD pharmingen
CD8-VIO BLUE	MACS Milteny biotech
CD45.2-APC	BD pharmingen
$H2^{kb}$- biotin	BD pharmingen
CD44-PE	BD pharmingen
CD90.2-PE	BD pharmingen
CD8-PE	BD pharmingen
$H2^{Kb}$-PE	BD pharmingen

3.6. Lysis buffer

Thymocytes and transformed cells were lysed in Brij 96 lysis buffer (0.33% v/v Brij 96, Fluka), 150mM NaCl, 20mM Tris HCl, pH7.8.

Phosphatase and protease inhibitors

Sodium orthovanadate (100x) - 50mM solution in dH_2O

Sodium fluoride (100x)-1M solution in dH_2O

Aprotinin (1000x) - 10mg/ml solution in dH_2O

Leupeptin (1000x) – 10mg/ml solution in dH_2O

PMSF (100x) – 100mM solution in ethanol.

METHODS

1. Molecular Biology

1.1. Kits Gel extraction- QIAquick gel extraction kit (Qiagen) and Mutagenesis-QuikChange™ Site directed mutagenesis kit (Stratagene) were used according to manufacturer's instruction.

1.2.Oligonucleotides

The oligonucleotides used were HPLC grade and were purchased from Invitrogen. All sequences are shown in the 5' to 3' direction with mutated residues stain in red.

Table 6: List of primers used for site directed mutagenesis

Name	Sequence	Use
Bal448(5')	GCTACTTGCTAGATGGAATCGCC TTCATCTACGGAGTCATC	L9A
Bal449(3')	GATGACTCCGTAGATGAAGGCG ATTCCATCTAGCAAGTAGC	
Bal450(5')	CGGAGTCATCATCACAGCCGCG TACCTGAGAGCAAAATTCAGC	L19A
Bal451(3')	GCTGAATTTTGCTCTCAGGTACG CGGCTGTGATGGATGACTCCG	

Table 7: Primers used for cloning

Name	Sequence	Use
Bal197	CCCCTCGAGAAGCAGAAG ATGAAGTGG	addition 5'Xho site in murine zeta chain costruct
Bal466	GGCTCGAGTGGCTGTTAG CGAGGGGC	addition 3' Xho1 site in murine zeta chain construct
Bal556	CCCAGATCTACCATGAAGT GGAAAGTGTCTGTT	addition 5' BglII site in murine zeta chain construct
Bal557	GGGGCGGCCGCTTAGCGA GGGGCCAGGGTGAC	addition 3'NotI site in murine zeta chain construct
Bal 630	GGGGCGGCCGCTTTATTG CTACAGCTCGTC	addition 3'NOT-1 site in EGFP of pLEGP-N1

Table 8: Primers used for sequencing

Name	Sequence	Use
Sp6	GAT TTA GGT GAC ACT ATA	Reverse sequencing primer
T7	AAT ACG ACT CAC TAT GG	Forward sequencing primer for pGEM3
pSRα	CCTTTGTCCGGCGCTCCC TTGG	Forward sequencing primer
pLEGFP-N1	CGTCCCGCCGTCCAGCTC GACCAG	Forward sequencing primer
pCR2.1	CTGGCCGTCGTTTTAC	Forward sequencing primer

1.3. Site directed mutagenesis:-

Plasmids were diluted to 5ng/µl. A 1x PCR mix containing the following components was prepared. Stratagene reaction buffer, 10ng plasmid, 125 ng each primer, 1µl dNTPs mix, 2.5U/µl Pfu Turbo polymerase (Stratgene), sterile dd H2O to a final volume of 50µl. The PCR program was as followos:

95ºC: 0:30

95ºC: 0:30

55 ºC: 1:00

68 ºC: 2 min/kb plasmid length

Go to 2 16 cycles

4 ºC:<< forever

End

After PCR, reactions were placed on ice for 2 minutes. 10U DpnI were added to the PCR reaction and incubated for 1 hour at 37 ºC to digest parental supercoiled methylated dsDNA. DNA was then transformed into competent bacteria.

1.4. Cloning procedure:

Construct 1

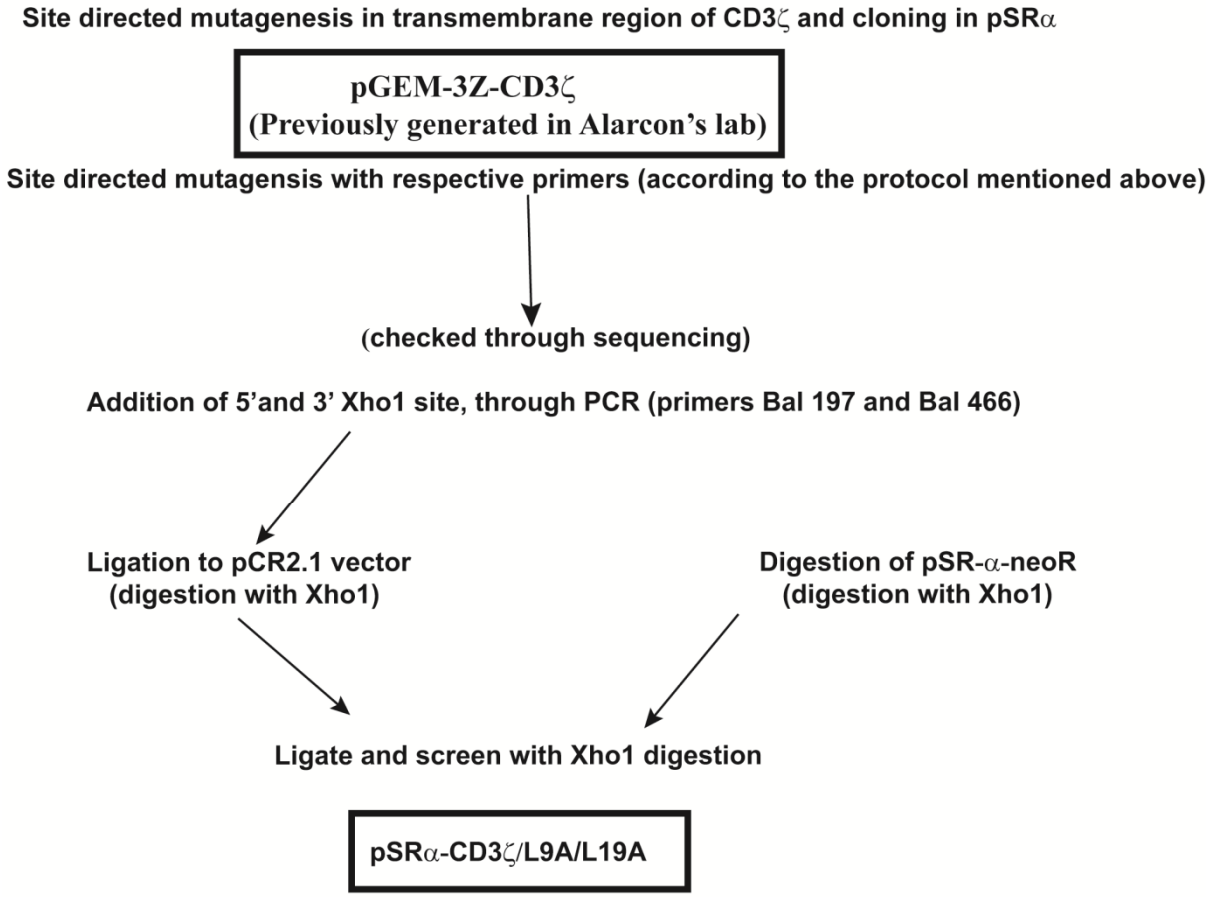

Construct 2

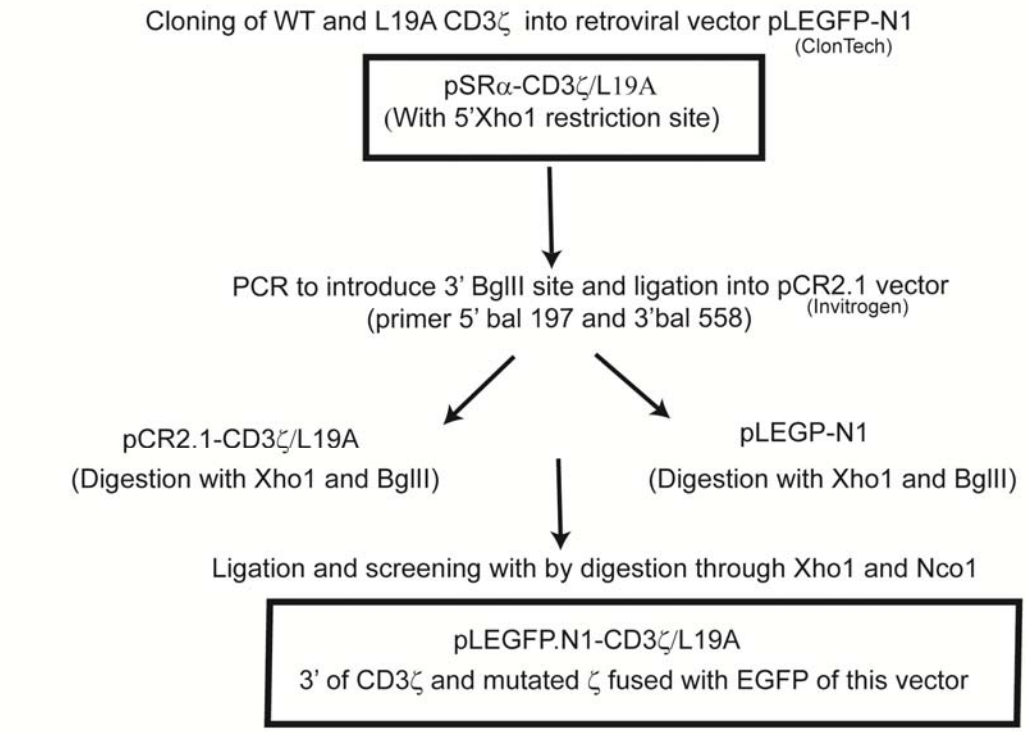

Construct 3

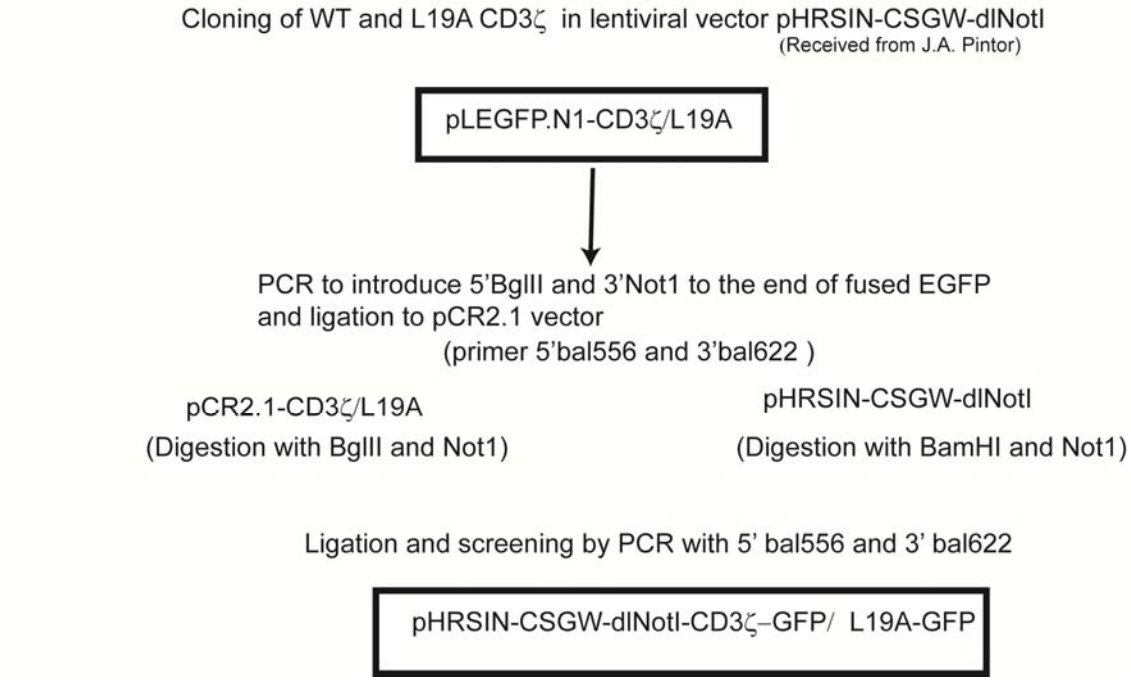

1.5. Transfection:

I.Transient transfection through electroporation: 5x10^6.COS7 cells, cells were suspended in 200µl DMEM supplemented with 10% FBS and 20 mM HEPES pH7.4. COS cells were incubated in the cuvette of transfection with 20 µg salmon sperm DNA, 5 µg of the plasmid of interest and 37.5 µM NaCl (150mM). The cells were pulsed at 200 mV and 960 µF. After transfection cells were mixed gently and resuspended in 10 ml DMEM supplemented with 10% FBS in 100 mm falcon plate. Expression of the plasmid was checked 24-48 hrs post transfection.

5-10x10^6 MA5.8 cells, were used were resuspended in 500 µl of RPMI with 20%FCS and 10mM HEPES. Cells were incubated in the cuvette of electropration with 40 µg of plasmid of interest for 10 min at room temperature. The cells were pulsed at 240mV and 500 mF approximately for 22 ms. After the pulse cells were resuspended in 10 ml complete RPMI with 5%FCS. Expression of plasmid was checked 24 or 48 hrs after transfection.

II. Stable Transfection: For generation of stable transfectants, electroporated cells were plated after 48 hrs in 96 well flat bottom plate at 20,000 cells/well, in 100 µl complete RPMI with 10% FCS and selection of Geniticin (G418,1mg/ml). After another 2 days, 100 µl of fresh medium was added. 100 µl of medium was then replaced every 4 days, until single clones could be seen in the plates. The selected clones were transferred to 24 well plates and analysed by FACS or western blotting, to check for the expression of plasmid.

III. Lentiviral Transfection and transduction:

Day 1:293T packaging cell lines were plated at 250,000 cells/well of a p6 plate in 2 ml of DMEM complete medium with 10% FCS.

Day 2:293T cells were transfected by JetPEI method. For each p6 well 1.5µg of the relevent lentiviral vector construct,.1 µg of pCMV8.9 (gag-pol) and 0.5 µg of pMDG (VSVg envelope) plasmids were mixed together in 100 µl of 150mM NaCl. Then 6 µl of JetPEI reagent was mixed in 100 µl of 150 mM NaCl and added to the DNA mixture, vortexed and centrifuged. The mixture was incubated for 20 min at RT before addition to the 293T cells..
and then cells were grown for 2 days.

Day 3: MA5.8 or 2B4 cell were thawed.and put in culture.

Day 4: supernatant of harvested 293T cell culture was filtered through a 0.45 micron filter (millipore), polybrene(sigma) was added to the filterd supernatant at 8 µg/ml. 2B4 or MA5.8 cells were plated in p24 well plate at 1x10^5 cells per well, and 1 ml filtered supernatant containing viral particles was added. Plates were centrifuged for 90 minutes at 975g at 32°C. After centrifugation plates were incubated at overnight 37°C.

Fresh medium was added to the transfected 293T cells in order to obtain a second batch of viral particles containing supernatants for a second round of transduction.

Day 5: Medium from the transduced cell cultures was carefully removed without disturbing the live cells settled to the bottom. Then the cells were transduced with the second batch of viral supernatant in presence of polybrene at the same condition as of 1st round. After 6hrs cells were diluted in fresh RPMI+5%FCS and after 48 hrs of transduction cells were checked for the expression of

relevent proteins through FACS and western blotting.

IV. Bone marrow transduction (BMT):

For bone marrow transduction, the protocol for transfection and transduction was similar as above with the following modifications.

Day1: CD3ζ -/- OT-1^{tg} donor animals were injected intraperitonially with 5 Flurouracil (150mg/kg).

Day2: 293T cells were harvested as described above.

Day3: Donor mice were sacrificed and bone marrow cells were obtained by flushing the femurs with PBS+2%FCS. After removal of RBCs via hypotonic lysis the remaining cells were resuspended in Iscove's medium supplemented with 10% FCS, IL-7 (25ng/ml), IL-6 (25ng/ml), SCF (50ng/ml) and Flt3-ligand (50ng/ml; all cytokines were obtained from Preprotech).Cells were cultured overnight at 37°C in p24 well.plates at 1x10^6 per well.

Medium from the transfected 293T cells was changed for fresh complete IMDM medium.

Day4: Bone marrow cells were transduced with supernatant of the 293T cultures as described above. Recpient mice were sub-lethally irradiated 6Gy.

Day 5: Transduced bone marrow cells were harvested from the p24 plates, washed, counted and 3-5x10^6 cells were injected in the plexus of each recipient C57BL/6 or C57BL/6 CD45.1-congenic mouse.

Mice were maintained at our animal house facility, and kept on drinking water supplemented with 200 µg/ml tetracycline (Sigma). Animals were sacrificed 6-8 weeks after reconstitution and analysed.

.

2 Cell biological Methods

2.1. Isolation of murine lymphoid cells

Spleen, lymph nodes (LN) and thymus were isolated placed in PBS, and single cell suspensions were prepared by gently crushing the organs between glass slides. Cells were transferred to the falcon tubes, centrifuged, washed and resuspended in PBS or culture medium. Cells from the spleen were centrifuged and resuspended in 4ml of erythrocyte lysing buffer (150mM NH4Cl,10mM KHCO3, 0.1mM EDTA) for 5 minutes at RT. PBS was added to fill up the tube and then cells were centrifuged at 1200rpm for 5 minutes. Pelleted lymphocytes were resuspended in PBS or culture medium.

2.2. Preparation of T cell blasts

OT-1 blasts were generated by stimulating whole spleen cell suspensions of OT-1 mice with 10 pM of OVAp (SIINFEKL, synthesized in the proteomic facility of the Centro de Biología Molecular via f-moc chemistry) and 0,5 µg/ml anti-CD28 in RPMI-10% FCS, supplemented with 2mM glutamine, 1 mM sodium pyruvate and 1x10^{-5} M β-mercapto-ethanol. After 2 days, cultures were centrifuged, resuspended in fresh medium supplemented with saturating amounts of recombinant human IL-2 and expanded for 6-12 more days.

2.3. Cell stimulation

i. Antigen stimulation: MA5.8 cells were stimulated at 1x10^5 cells per well in flat bottom 96 well plates containing a monolayer of 5x10^4 I-E^k and CD80 transfected DCEK fibroblasts (a kind gift of Dr. R. Germain, National Institutes

of Health, Bethesda, MD) loaded with the indicated amounts of the MCCp (ANERADLIAYLKQATK, synthesized in our center via f-moc chemistry). T cells were cultured for the indicated times before measurement of expression of TCR downmodulation,CD25 and CD69 induction .

ii. Tetramer stimulation: Biotinylated K^bOVAp tetramers (Daniels and Jameson, 2000), generated by incubation of pre-folded c-terminally biotinylated soluble K^bOVAp complexes (generously provided by Dr. E. Palmer) with unlabeled streptavidin, were added at the indicated concentrations to T cells at the start of culture in R10 medium in round bottom 96 well plates. T cell blasts were cultured for 24hrs in presence of tetramer and then stained intracellulary for measurement of IFNγ.

iii. T cell stimulation: Primary macrophages or T2Kb cells were used as antigen presenting cells for OT-1 mice, while irradiated spleen cells from micen of the H-2^k haplotype or DCEK cells were used as antigen presenting cells for AND TCR^{tg} animals.

Primary macrophages were obtained via peritoneal lavage of C57BL/6 mice that had been injected (i.p.) three days before with thioglycolate solution (30% thioglycolate-1ml/mouse). Macrophages were plated at $0.7x10^4$ cells per well of flat bottom 96 well plates the day before the stimulation assay in RPMI-10% FCS supplemented with 1mM Na-Pyruvate and $1x10^{-5}$ M βME (complete medium). The macrophages were loaded with the required amounts of peptide for 7 to 10 hours followed by washing with PBS before addition of T cells (100,000 cells/well) in complete medium.

Cells from one spleen were obtained as described before, resuspended in RPMI+0.5%FCS or in PBS. and γ-irradiated at 1500 rads. Cells were then washed and plated at $1x10^6$ cells per well of p96 U bottom plates. Splenocytes were then loaded with the indicated amounts of peptide and incubated overnight

DCEK cells and T2Kb cells were plated at 50,000 and 100,000 cells per well of p96 flat bottom plate, respectively, and incubated with the indicated amounts of peptide.

2.4. Flow cytometry

Cells were stained on ice in PBS, 1% BSA, 0,02% NaN_3 with saturating amounts of either directly labelled antibodies or with labelled primary antibodies and then appropriate fluorescently-labelled secondary antibodies. Cells were acquired on a FACScalibur flow cytometer (Becton-Dickinson, Franklin Lakes, NJ). Data were analyzed with FlowJo software (TreeStar, Ashland, OR).

Functional assay:

i. Induction of CD69 and CD25 expression: To check for the cell surface expression of CD69, cells were stimulated as stated above. After 24 hrs of incubation, cells were harvested and stained with anti CD69 antibody along with either anti CD8 or anti CD4 antibody for OT-1^{tg} and AND^{tg} T cells respectively. CD25 expression was measured after 48 hrs of stimulation.

ii. TCR downmodulation: Cells were stimulated with peptide loaded APCs or anti CD3 antibody for 3 hrs. Cells were harvested

and stained with anti-TCR antibodies. The. percentage of TCR downmodulation was calculated by dividing the corresponding MFI value of the TCR staining of the stimulated cells by the MFI value of non-stimulated cells and multiplying by 100.

iii. IFNγ expression: For detection of intracellular IFNγ, cells were treated with 2.5 µg/ml BFA during the last 4hrs of culture. Cells were then surface-stained before fixation and permeabilization with a commercially available kit (BD Pharmingen), followed by staining with saturating amounts of an APC-coupled anti-murine IFNγ mAb (Miltenyi).

2.5. T cell migration assay

Thymocytes were obtained by disaggregation of thymus and resuspended at $10x10^6$cells/ml in RPMI medium without FCS, and starved for one hour at 37ºC before start of the experiment. 100 µl of thymocytes suspension was then added to the top chamber of a 5 µM pore polycarbonate transwell chamber (coaster, corning,NY). Which was then placed in the bottom chamber containing 0.4µg/ml SDF1-α (Preproptech) After 3hrs of incubation at 37ºC, cells were harvested from the upper and lower wells and counted. In case of stimulation, 5µg/ml anti CD3ε antibody was added to the top chamber at the start of at the start of migration. Migration was expressed as the % of cell input.

3. Protein Biochemistry

3.I. Whole lysate and immunoprecipitation

Whole thymus was lysed directly in 0.33% v/v Brij96 lysis buffer (150mM NaCl ,20mM Tris HCl pH7.8, 20mMNaF, 1mM Na3VO4, leupeptin, aprotinin and PMSF) using a dounce homogenizer. and incubated on ice for 45 minutes. The cell lysate was centrifuged at maximum speed at 4°C for 15 minutes in a microfuge and the supernatant was transferred to a clean tube. 2B4 cells and MA5.8 cells were lysed by addition of Brij 96 lysis buffer to the cell pellet.

Protein concentration in whole lysates was determined using a BCA kit (Thermo scientific) according to the manufacturer's instruction. For SDS-PAGE analysis of whole lysates, the required amount of lysate was mixed with the appropriate volume of concentrated sample buffer and boiled. Alternatively whole lysates were mixed with an equal volume of cold acetone and incubated for 20 minutes on ice. and centrifuged for 20 minutes at 4°C. The supernatant was discarded and the pellet was resuspended in sample buffer. Samples were boiled for 5 minutes at 95°C, and then stored at -20°C, or loaded directly on SDS-PAGE.

For imunoprecipitacion lysates were cleared through preincubation with the sepharose beads for 1 hr. Then 2 µg of specific antibody was added to the lysates which were incubated for overnight at 4°C on the rotating wheel. 30 µl sepharose A/G beads were added and incubated for 1 hr on a rotating wheel at 4°C. IPs was washed 3 times with cold lysis buffer. After the final wash, beads were resuspended in either reducing or non reducing sample buffer. Samples were

boiled for 5 minutes at 95°C, and then stored at -20°C, or loaded directly on SDS-PAGE.

3.2. SDS-PAGE and western blotting (WB)

Protein samples were separated by SDS-PAGE. Samples were prepared with reducing or non-reducing sample buffer, boiled for 10 min at 95ºC and run on 10% or 12% gels, depending on the experiment and the size of the protein (s) of interest. Gel system from BIO-RAD was used for electrophoresis. Subsequently, proteins were transferred by wet blotting to nitrocellulose (Bio Rad) or PVDF membranes (Millipore). membranes were incubated in 10% skimmed milk in PBS/Tween for 1 hour at RT. For detection of specific proteins, membranes were then incubated in an antibody dilution (normally in 5% skimmed milk) overnight at 4°C. Membranes were washed with wash buffer (PBS/Tween) and then incubated with the appropriate HRPO coupled secondary antibody dilution for 1 hr at RT. Membranes were washed 3x15 minutes in wash buffer followed by detection by enhanced chemiluminescence detection system (ECL, BIO RAD).

3.3. Antibody array

Detergent extracts were prepared by lysing thymuses in brij-lysis buffer containing protease and phosphatase inhibitors. Signal transduction antibody array (Hypromatrix) were blocked for 1 hour at RT in 5% skimmed milk in TBST (150 mM NaCl, 25mM Tris, 0.05%Tween-20, pH7.5) and then incubated with whole lysates for 2hrs at RT on shaker. Arrays were washed 3x15 minutes with TBST and incubated with the appropriate biotinylated antibodies for 2 hrs at RT. After washing, the arrays were incubated with HRPO-conjugated streptavidin and developed through ECL system.

3.4. Cell separation through magnetic beads

Single cell suspensions of thymocytes were prepared in PBS+0.1%BSA and stained with anti-CD8 antibody. Stained cells were then incubated with anti-rat IgG-conjugated magnetic beads (Dynal, Invitrogen) according to the manufactrer's instruction for 45 min. at 4ºC. Bead bound and unbound cells were separated by a magnetic field and separately lysed in Brij 96 lysis buffer. Efficiency of purification was established by staining an aliquot of the cells just after labeling with the biotynylated anti-CD8 antibody and aliquot of the unbound cells with fluorescently labelled anti-CD4 antibody and strepatvidin and analysed by flow cytometer.

4. Microscopy

4.1. Immunohistochemistry

Thymuses were isolated from mice and fixed in 4% paraformaldehyde (in PBS) at RT for 2hrs. They were then incubated in 30% sucrose at 4°C for 16hrs. They embeded in OCT (Tissue-Tek, Sakura) and frozen at -70ºC Cryostat sections of 10µm were obtained by using a 2800 Frigocut cryostat (Leica) and adhered on glass slides previously treated with gelatine solution. The sections were then stored at -20°C until they were used for staining.

For staining, glass slide containing thymic sections were allowed to thaw for 30 minutes at RT. The sections were fixed again

with 4% paraformaldehyde for 10 min at RT, and quenched with 20mM NH4Cl .They were then blocked for 1hour with TNB (100mM Tris-HCl, pH7.4, 300mM NaCl, 0.25% triton-x100, 10% FBS) and incubated with primary antibody at a dilution of 4µg/ml in TNB for 16h at 4°C or 2hrs at room temperature in a humid chamber. They were incubated with fluorescently conjugated secondary antibodies in TNB for 1 hr at RT. Nucleus were stained with topro dye. Sections were mounted in DAKO mounting medium.

4.2. Confocal microscopy

Samples were visualized on a confocal LSM510 Meta laser scanning microscope (Zeiss) at 40x magnification, with the pinhole adjusted to a 1.5-µm section. Detectors were set to obtain the optimal signals below saturation. Images were analyzed with the LSM 5 Image Browser and imageJ software.

4.3. Electron Microscopy

Immunogold labeling, replica preparation and EM analysis:

Immunogold labeling and cell surface replica preparations were performed as previously described (Pinto da Silva and Kan, 1984; Schamel et al., 2005). In brief, T cell preparations were washed in PBS and fixed in 1% paraformaldehyde, followed by labeling with the anti-human CD3 mAb OKT3 or the anti-murine CD3ε mAb 145-2C11 (both purified from hybridoma supernatants in the laboratory) and 10nm gold-conjugated protein A (Sigma-Aldrich, St. Louis, MO). Labeled cells were adhered to poly-L-lysine-coated mica strips and post-fixed with 0.1% glutaraldehyde. Samples were covered with another strip of mica and frozen in liquid propane via plunge freezing. Frozen sandwiches were split in liquid nitrogen and up to four of the original mica strips were mounted at the same time on the sample table of a Balzers BAF400 freeze fracture apparatus submerged in liquid nitrogen (for a detailed description of this apparatus and relevant protocols see Severs, 2007 (Severs, 2007)). Samples were rapidly transferred to the liquid nitrogen-cooled BAF400 apparatus, followed by freeze etching under vacuum conditions to remove excess of water. Samples were shaded with platinum and coated with carbon according to experimentally optimized conditions (175 Hz of Pt, 350 Hz of C), followed by warming to room temperature. Samples were removed from the BAF400 apparatus, and floated on domestic bleach solution. After overnight digestion of organic material in the bleach solution, replicas were extensively washed in distilled water and mounted on Ni/Cu grids. Replicas were analyzed via transmission electron microscopy on a JEOL 1010 microscope operated at 80kV.

RESULTS

RESULTS

1. Section 1

We have previously shown that the TCR complexes in resting human peripheral blood T cells and human and murine T cell lines is expressed on the cell surface as a combination of monomeric TCRs and TCR oligomers of different sizes (Schamel et al., 2005). The oligomeric TCR complexes are preferentially activated upon stimulation with small amounts of antigen, suggesting that they provide T cells with their high sensitivity. Since antigen experienced T cells are characteristically more sensitive to antigen, we therefore analyzed whether previously stimulated and memory T cells, were enriched for oligomeric TCR complexes at the cell surface. We furthermore generated a mutant in CD3ζ that impaired oligomeric TCR formation in order to provide direct evidence that oligomeric TCR complexes provide T cells with greater sensitivity.

1.1. Increase in the percentage and size of oligomeric TCR complexes on previously stimulated and memory T cells

We prepared cell surface replicas from anti-CD3 labelled fresh human peripheral blood T lymphocytes and peripheral blood lymphoblast. Lymphoblasts were generated after stimulation for 2 days with PHA and expansion for three more days in fresh medium containing IL-2. Analysis by electron microscopy of replicas of individual cells showed the co-existence of single gold particles and clusters of gold particles on the surface of both freshly isolated and PHA activated peripheral blood lymphocytes (Figure 11 A).

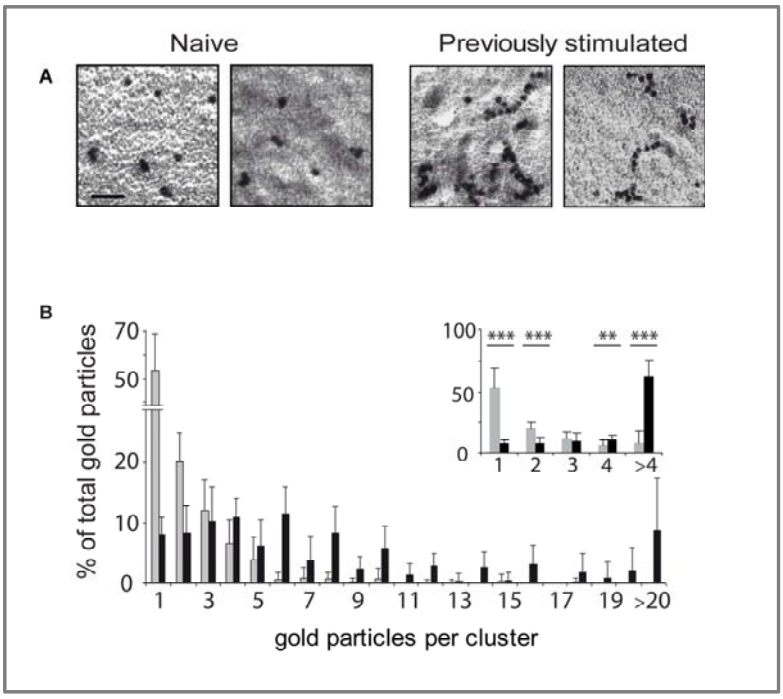

Figure 11: Distribution of TCRs on PHA-stimulated and freshly isolated human peripheral blood T cells.
A) High magnification images (100.000x) of replicas showing distribution of gold particles on the cell surface (scale bar: 50 nm).
B) Quantification (mean +/- SD) of distribution of gold particles between clusters of the indicated sizes for freshly isolated (grey bars) and PHA-stimulated (black bars) human T cells. Inset shows the distribution of gold between clusters of 1, 2, 3, 4, or more particles and statistical analysis (Student's T test: * $p<0.05$; ** $p<0.01$; *** $p<0.001$). Replicas of 19 PHA-activated T cells (9414 particles) and 9 freshly isolated T cells (2707 particles) were counted.

However, quantitative analysis showed that the previously stimulated cells had an increased percentage of larger TCR oligomers as compared to the freshly isolated cells (Figure 11B), indicating that the T cell stimulation leads to a change in distribution of the TCR complexes that lasted for days after the stimulating agent had been removed.

We also isolated naïve and memory $CD4^+$ T cells from spleen and lymph nodes of C57BL/6 mice based on their reciprocal CD62L and CD44 expression pattern (Budd et al., 1987; Lee and Vitetta, 1991) via a depletion strategy in which only $CD4^+CD44^{lo}CD62L^{hi}$ (mostly naïve) or $CD4^+CD44^{hi}CD62L^{lo}$ (mostly memory) T cells were spared (Figure 12A, left and middle panel respectively). The $CD4^+CD44^{hi}CD62^{lo}$ T cells were resting T cells, as indicated by the observation that their size was similar to the size of the $CD4^+CD44^{lo}CD62^{hi}$ T cells (Figure 12A, right panel).

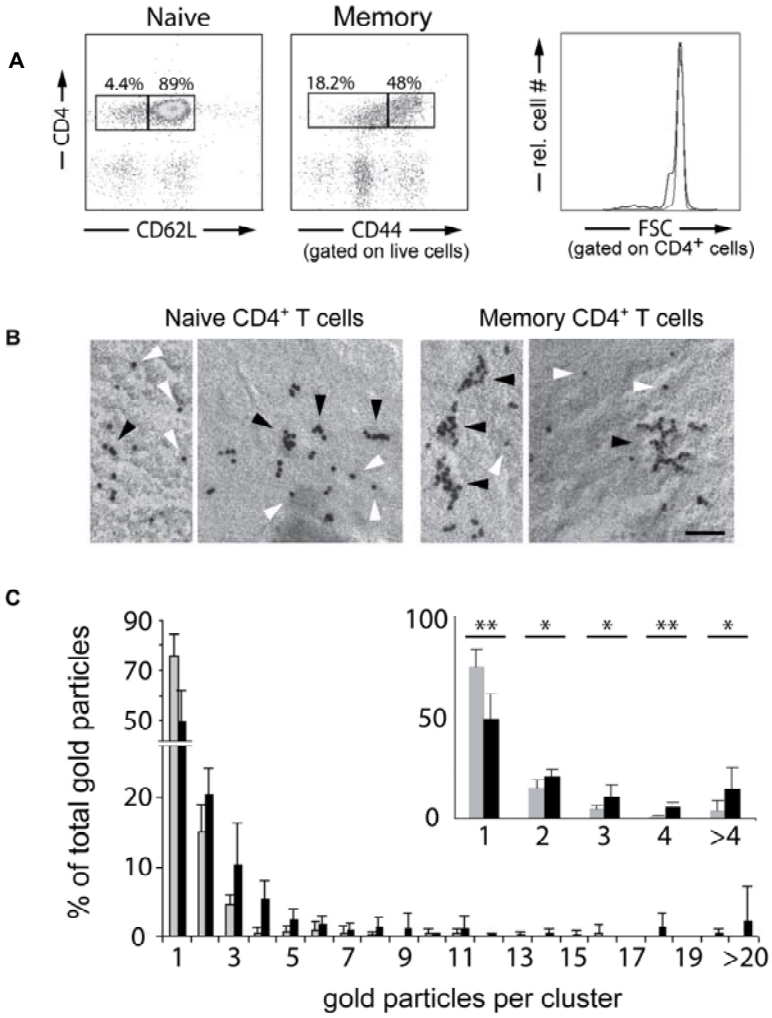

Figure 12: Distribution of oligomeric TCR complexes on murine $CD62L^{hi}CD44^{lo}$ and $CD44^{hi}CD62L^{lo}$ $CD4^+$ T cells.
A) Enrichment of $CD62L^{hi}$ and $CD44^{hi}$ $CD4^+$ T cell populations. The overlay plot shows the FSC profiles of the $CD62L^{hi}$ and $CD44^{hi}$ $CD4^+$ T cells.
B) High magnification images (100.000x) of replicas of the cell surface of $CD62L^{hi}$ and $CD44^{hi}$ $CD4^+$ T cells (scale bar: 100 nm).
C) Quantitative (mean +/- SD) analysis of distribution of gold particles between clusters of the indicated sizes for $CD62L^{hi}$ (grey bars) and $CD44^{hi}$ (black bars) $CD4^+$ T cells. The inset shows the distribution between clusters of 1, 2, 3, 4, or more particles and statistical analysis (* $p<0.05$; ** $p<0.01$; *** $p<0.001$). Quantification of 5 replicas of $CD62L^{hi}$ cells (2718 particles) and 5 $CD44^{hi}$ cells (3198 particles) is represented.

This suggested that these were true memory cells and not recently activated CD44^{hi} T cells. Both T cell populations were fixed and labeled with the anti-CD3 mAb 145-2C11, followed by labeling with gold-conjugated protein A and preparation of cell surface replicas. Quantitative analysis of the replicas showed an increased percentage of gold particles forming part of large oligomeric clusters on the population enriched for memory T cells, as compared to the naïve population (Figure 12B and C). Thus, polyclonal CD4^{+} memory T cells, that were activated under completely physiological conditions, i.e. not by experimentally administered antigens, had more and larger TCR oligomers on the cell surface than naïve CD4^{+} T cells.

1.2. Design and generation of mutations in the TCR complex to impair TCR oligomer formation

In order to establish a causal relationship between TCR oligomers and sensitivity to antigen, we wished to design mutants of the TCR or the CD3 chains that could impair oligomer formation. CD3ζ appeared to be a promising candidate based on a biophysical study in which it was shown that peptides representing the transmembrane region of this molecule could form both dimers and tetramers (Torres et al., 2002). Importantly, the same study defined amino acid residues within the transmembrane region that selectively showed high interaction energy within the tetramers (Figure 13A).

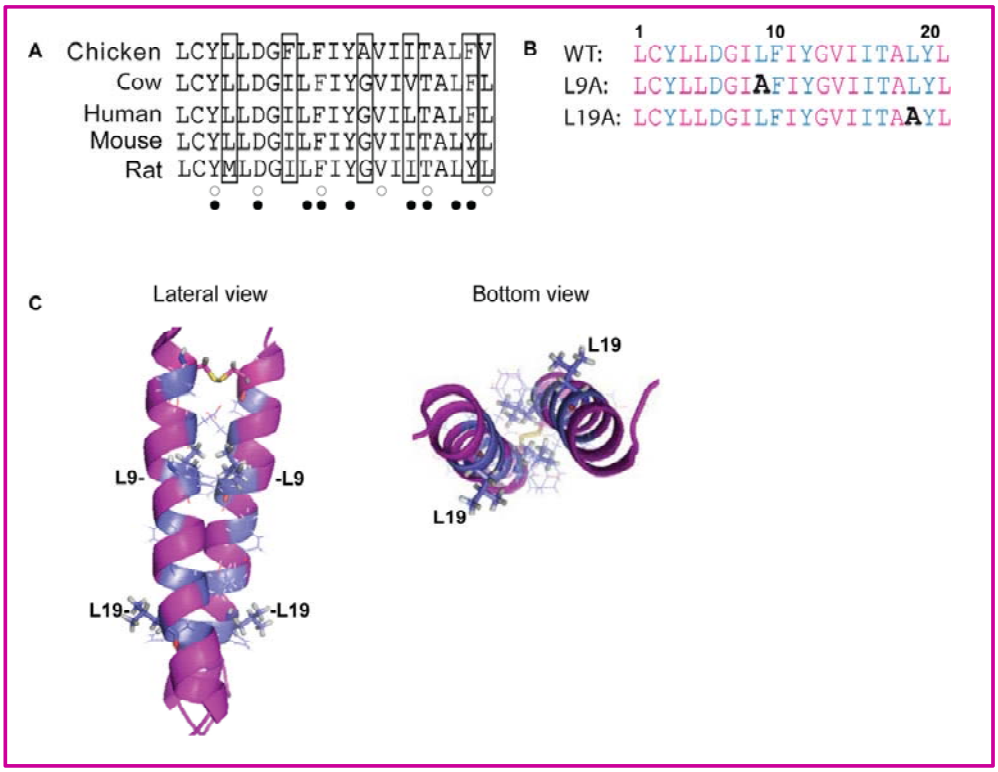

Figure 13: Transmembrane region of CD3ζ. A) Comparison between the transmembrane sequences of CD3ζ in different species. Non-conserved residues are inside boxes and residues with high interaction energy in dimer and tetramer are represented by open and filled circles, respectively (Torres et al., 2002)
B) Representation of the transmembrane sequences of WT, L9A, and L19A CD3ζ. The alanine substitution are shown in bold, while residues implicated in tetramer formation are shown in blue. **C)** Representation of the transmembrane region of the CD3ζ dimer, as determined via NMR. (Call et al., 2006). The alpha-helix forming backbone of the amino acids is shown as a ribbon diagram with all amino acids implicated in tetramer formation represented in blue and with side chain residues as lines.. The L9 and L19 residues are indicated and their side chains are represented as stick.

Out of these residues we chose to mutate two leucines in position 9 and 19 of the transmembrane region into alanines (L9A and L19A mutants, (Figure 13B), as these leucine residues (i) had high interaction energy only in the tetramer structure, (ii) appeared to be in small islets of residues with high interaction energy in the tetramer (2 out of 3 surrounding residues for the leucine in position 9 [L9] and 3 out of 4 surrounding residues for the leucine in position 19 [L19]), (iii) were conserved among species and (iv) had long amino acid side chains that should have a higher probability of interacting with neighboring molecules.

In the course of the generation of L9A and L19A mutant CD3ζ chains, the structure of the transmembrane domain of the CD3ζ dimer was published (Figure 13C). This structure indicated that the CD3ζ dimer formed a perfectly symmetrical unit, with most of the residues implicated in tetramer formation forming an interface outwards of the dimer (Figure 13C bottom view, blue coloured amino acid residues). These residues were thus potentially in a position to interact with a neighbouring CD3ζ dimer or with other molecules. The L19 residue was one of these residues pointing out, in a position favourable to form contacts with other proteins. However, the L9 residue appeared to be involved in hydrophobic interactions between the two transmembrane regions of the CD3ζ dimer.

1.3. Reconstitution of a CD3ζ deficient cell line with the L9A and L19A CD3ζ chains.

Wild type (WT), L9A or L19A CD3ζ chains were transfected into the CD3ζ-deficient MA5.8 cell line, which is derived from the murine T hybridoma 2B4, specific for a moth cytochrome c (MCC)-derived peptide (Sussman et al., 1988). Pools of transfectants, expressing these CD3ζ chains, were analyzed for their ability to express the TCR complex at the cell surface (Figure 14A). Transfectants expressing the L19A CD3ζ chains reconstituted expression of the TCR complex at the cell surface to a level similar to transfectants expressing wild type CD3ζ and to the parental 2B4 line. However, the L9A CD3ζ mutant only partially reconstituted cell surface expression of the TCR complex which coincided with the effect of this mutation in dimer formation (Call et al., 2006).

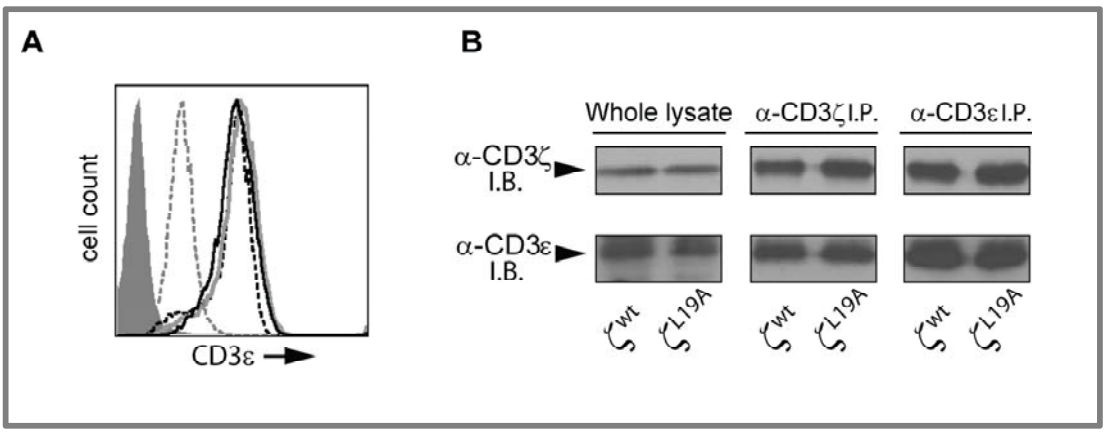

Figure 14: Analysis of CD3ζ mutant. A) Flow cytometric measurement of CD3ε expression by MA5.8 cells (filled grey histogram), 2B4 cells (dashed black line), and MA5.8 cells transfected with wild type CD3ζ (grey line), L9A CD3ζ (dashed grey line) and L19A CD3ζ (black line).
B) Association between wild type or L19A CD3ζ chains and CD3ε complexes. Whole lysates or immunoprecipates of the indicated antibodies were run on non-reducing SDS gels, followed by immunoblotting with the indicated antibodies.

As the amount of TCR expressed at the cell surface could influence the distribution of the TCR and the sensitivity of T cells to antigenic stimuli, thereby complicating interpretation of the results, we excluded this mutant from further analysis and focused our attention on the L19A mutant.

To check whether L19A CD3ζ formed homodimers and assembled correctly with the other components of the TCR complex, we performed immunoprecipitation and immunoblot experiments. Transfectants expressing the WT or L19A CD3ζ chain were lysed in the mild detergent Brij96 and whole lysates and immunoprecipitates with antibodies specific for the CD3ε and CD3ζ chains were separated by non-reducing SDS-PAGE and transferred to nitrocellulose membranes. The membranes were sequentially probed with antibodies specific for CD3ζ and CD3ε (Figure 14B). WT and L19A CD3ζ transfectants expressed equal amounts of the respective CD3ζ chains, formed homodimers and were capable of associating with the other CD3 components to a similar extent.

1.4. The L19A CD3ζ chain impairs oligomeric TCR formation

WT and L19A CD3ζ transfectants were then immuno-labelled with an anti CD3ε antibody and with 10 nm gold-conjugated protein-A.

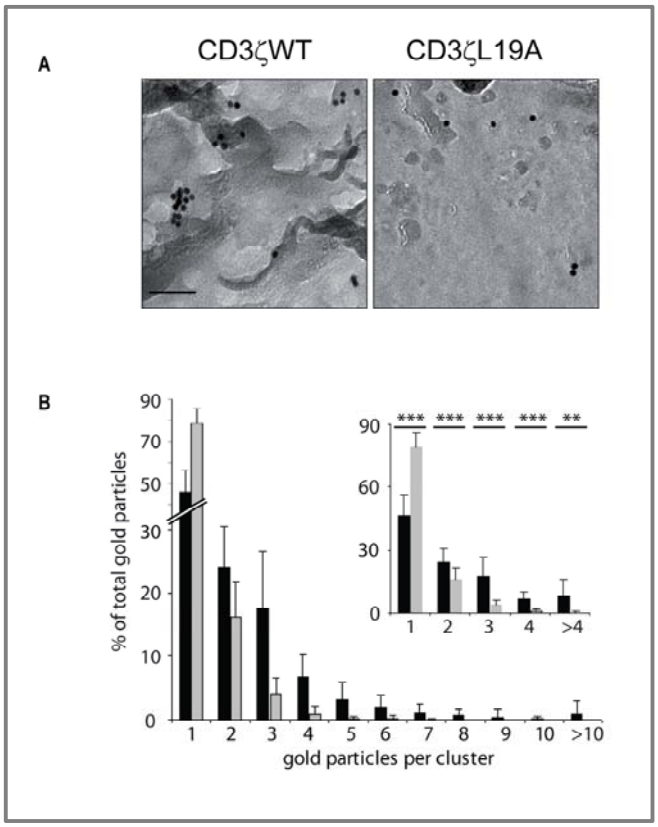

Figure 15: A mutation in the transmembrane region of CD3ζ impairs oligomeric TCR formation.
A) High magnification images (100.000x) of cell surface replicas of MA5.8 cells transfected with wt ζ and mutated L19A ζ (scale bar: 100 nm) showing distribution of gold particles.
B) Quantification (mean +/- SD) of distribution of TCR complexes in oligomeric clusters in MA5.8 cells reconstituted with wild type (black bars) or L19A CD3ζ (grey bars). Inset shows distribution of gold particles between clusters of 1, 2, 3, 4 or more particles and statistical analysis (* $p<0.05$; ** $p<0.01$; *** $p<0.001$). Quantification of replicas of 15 WT CD3ζ reconstituted cells (12041 particles) and 21 L19A CD3ζ reconstituted cells (8348 particles) is shown.

Analysis of cell surface replicas by electron microscopy showed that over 50% of the gold particles in WT CD3ζ transfectants were detected as clusters, and about 15% were in clusters larger than 3 particles reaching a size of up to 17 gold particles (Figure 15A and B). In sharp contrast, in L19A CD3ζ transfectants barely any gold cluster bigger than 3 particles were observed (~1%), with the largest clusters reaching only 6 particles. Hence the L19A CD3ζ chain impaired the organization of the TCR into oligomeric complexes without affecting the TCR expression level at the cell surface or its association with the other CD3 chains.

1.5. L19A CD3ζ transfectants have reduced antigen sensitivity

WT and L19A CD3ζ transfectants were stimulated with graded amounts of MCCp presented by the DCEK cell line. After 24 hrs the transfectants were analyzed for expression of CD69 and after 48hrs they were stained intracellularly to determine IFNγ production. L19A CD3ζ transfectants were able to respond to the stimulus showing that the mutation did not affect signaling per se, but they needed much higher amounts of the antigen than WT transfectants to reach a similar level of IFNγ production and did not reach the level of CD69 expression by WT transfectants at the amounts of antigen tested (Figure 16).

Thus, a mutation in CD3ζ that diminished the formation of TCR oligomers, without affecting the level of expression of the TCR at the cell surface, reduced sensitivity of T cells to antigen stimulation. This showed that oligomeric TCR complexes endow T cells with high sensitivity to antigen.

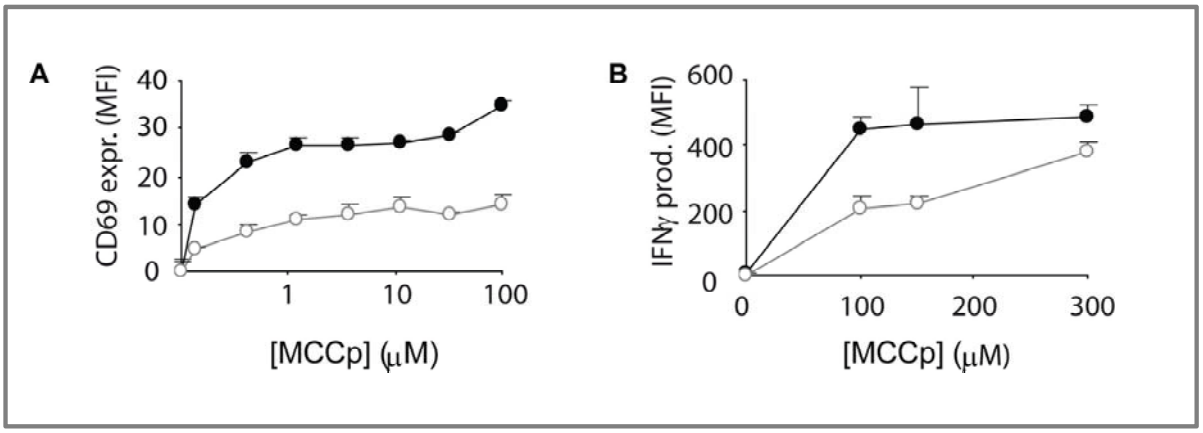

Figure 16: Impairment of oligomeric TCR complex formation reduces sensitivity to antigenic stimulation. MA5.8 cells reconstituted with WT (black circles) or L19A (open circle) CD3ζ were stimulated with the indicated amounts of MCCppresented by DCEK and A) CD69 induction and B) IFNγ production were measured at 24 and 48hrs, respectively.

1.6 Analysis of oligomeric TCR complexes *in vivo.*

We wished to determine the potential role of oligomeric TCR complexes during T cell differentiation and activation *in-vivo*. We chose to transduce bone marrow precursors from CD3ζ deficient mice (Love et al., 1993) with lentiviral vectors coding for the WT and L19A CD3ζ chain and to use these transduced bone marrow cells to reconstitute irradiated recipient mice. To facilitate this analysis we also decided to use CD3ζ-deficient bone marrow precursors that were also transgenic for the OT-1 TCR (OT-1^{tg}), specific for an ovalbumin derived peptide (OVAp) presented by the H2K^{b} molecule (Hogquist et al., 1994). Finally, we decided to generate fusion proteins of WT and L19A CD3ζ with GFP, in order to be able to unequivocally detect cells transduced with the WT or L19A CD3ζ chains in the reconstituted animals.

Verification of CD3ζ-GFP fusion proteins:

MA5.8 cells were transduced with lentiviral vectors coding for the WT or L19A CD3ζ-GFP chains.The GFP fusion proteins were tested for their ability to restore cell surface expression of the TCR and for their capacity to associate with the other TCR components (Figure 17A and B).Both WT and L19A CD3ζ-GFP chains reconstituted cell surface expression of the TCR to a similar extent and were capable of associating with the other TCR components.

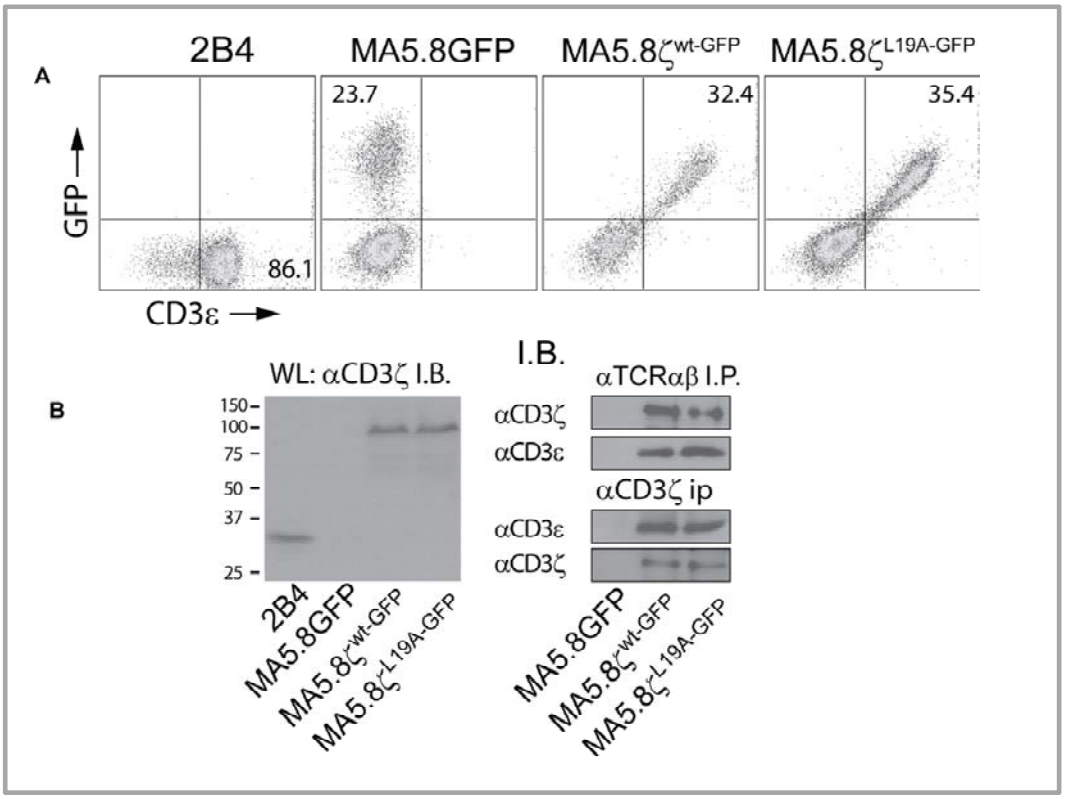

Figure 17: Generation of GFP-linked wild type and L19A CD3ζ chains. A) Cell surface expression of the TCR complex in MA5.8 cells transduced with wild type and L19A CD3ζ-GFP chains. 2B4 cells and MA5.8 cells reconstituted with GFP only are included as controls. Cells were surface-stained with a mAb against CD3ε and signals for both this staining and GFP were measured by flow cytometry. Note that both constructs are able to rescue TCR cell surface expression to a similar extent and that they quantitatively associate with CD3ε.
B) Biochemical analysis of homodimer formation by wild type and L19A GFP-linked CD3ζ and their capacity of interaction with TCRαβ and CD3ε. Whole lysates (WL) and immunoprecipitates of the anti-TCRβ mAb H57.597 or the anti-CD3ζ serum of Brij96-solubilized cells were separated by non-reducing SDS-PAGE and immunoblotted with the indicated antibodies.

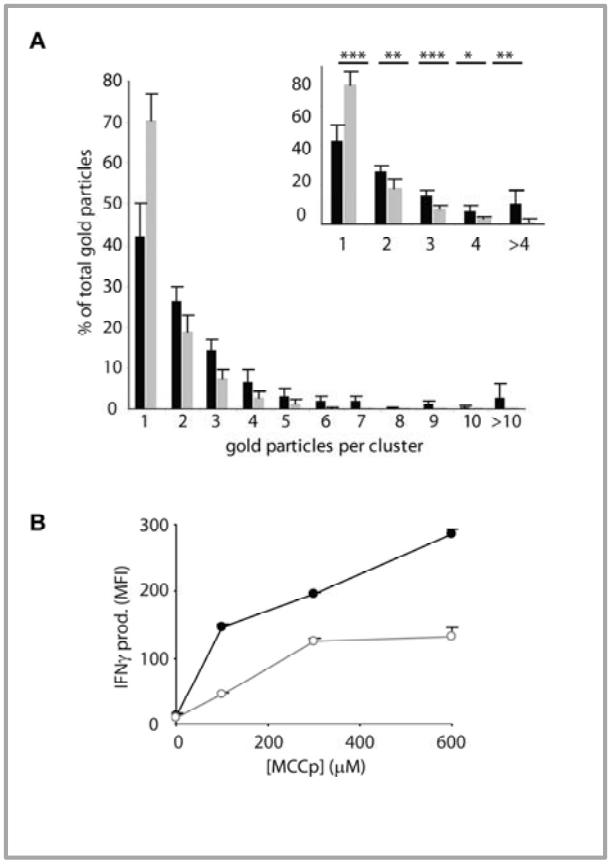

Figure 18: Reduced oligomeric TCR formation and reduced antigen sensitivity of GFP linked L19A CD3ζ reconstituted MA5.8 cells. A) Quantification (mean +/- SD) of the distribution of TCR complexes on the cell surface of MA5.8 T cells reconstituted with wild type or L19A GFP-linked CD3ζ chains. The inset shows the distribution of gold particles between clusters of 1,2,3,4 or more gold particles and the statistical analysis (* $p<0.05$; ** $p<0.01$; *** $p<0.001$). Quantification of 6 WT CD3 ζ-GFP reconstituted cells (5375 particles) and 6 L19A CD3 ζ-GFP reconstituted cells (6462 particles) is shown.
B) Production of interferon-γ by reconstituted MA5.8 cells upon stimulation by DCEK cells loaded with the indicated amounts of the MCCp (black circles: wild type GFP-linked CD3ζ; open circles L19A GFP-linked CD3ζ).

However, as observed for the L19A CD3ζ transfected cells, L19A CD3ζ-GFP expressing cells were less sensitive to antigenic stimulation and had fewer and smaller oligomeric complexes at the cell surface than WT CD3ζ-GFP expressing cells (Figure 18A and B). The L19A GFP-fusion protein could therefore be used to study the role of oligomeric TCR complexes *in-vivo*.

4.1.7. T cell differentiation in L19A CD3ζ-GFP reconstituted mice

Bone marrow cells isolated from OT-1^{tg}, CD3ζ-deficient mice were transduced with lentiviral vectors encoding for WT or L19A mutant CD3 ζ-GFP chains, or GFP alone and inoculated into sub-lethally irradiated B6 recipients. Four to six weeks after reconstitution, the ability of WT and L19A mutant CD3ζ-GFP expressing bone marrow precursors to reconstitute both thymic and peripheral T cell populations was compared.

Wild type and L19A CD3ζ-GFP expressing thymocytes differentiated similarly into CD8 SP thymocytes, while GFP expressing thymocytes did not differentiate beyond the DP stage (Figure 19A). This showed that differentiation beyond the DP stage was dependent on expression of the WT or L19A CD3ζ-GFP chains, and that the L19A CD3ζ-GFP protein permitted the TCR signaling necessary for positive selection. Consistent with normal thymic differentiation, both WT and L19A CD3ζ-GFP expressing $CD8^+$ OT-1^{tg} T cells were found in peripheral lymphoid organs (Figure 19B). These cells had similar amounts of the TCR at the cell surface, and their expression of CD69, CD25, CD28, LFA-1, CD44 and CD62L was very similar to that observed on control OT-1^{tg} T cells,

indicating that they were naïve, resting T cells. Thus, the L19A CD3ζ chain permitted normal differentiation of OT-1^{tg} T cell precursors into naïve CD8^{+} T cells, suggesting that oligomeric TCR complexes did not play an essential role in OT-1^{tg} T cell differentiation or that such complexes were not present on these T cell precursors.

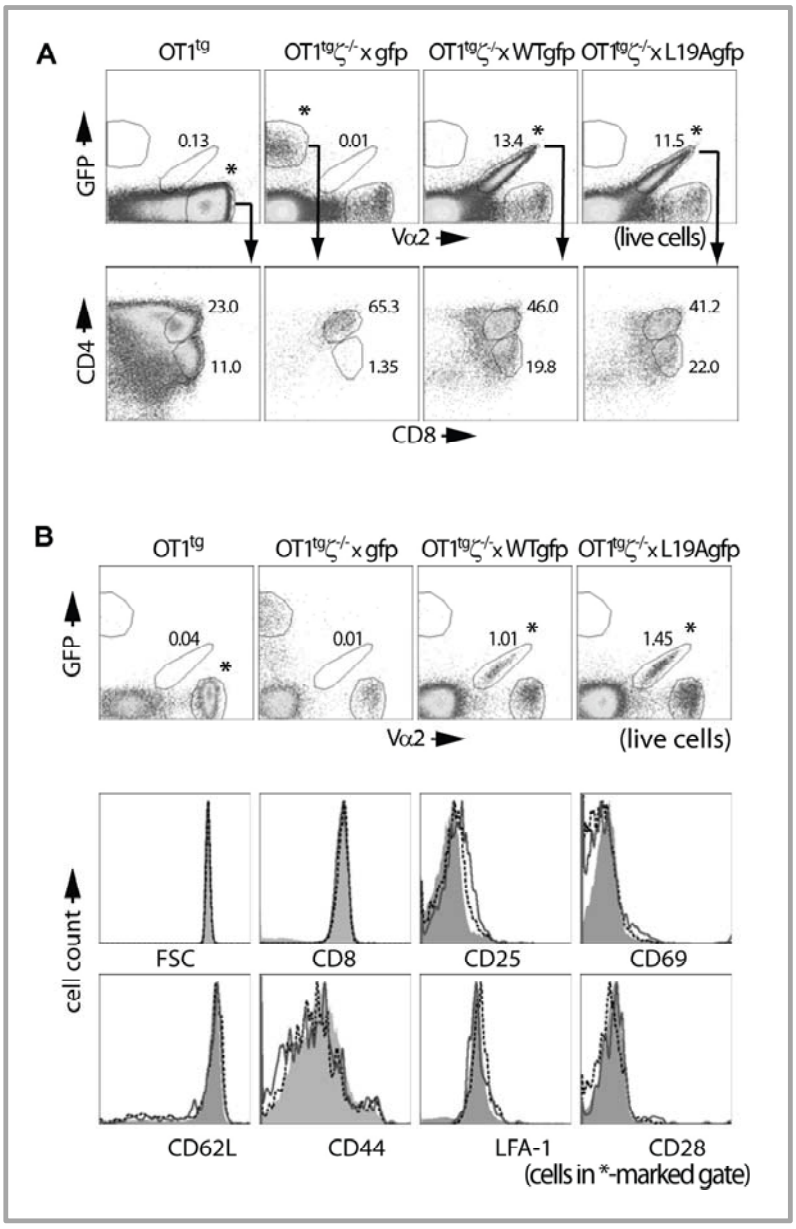

Figure 19: The role of oligomeric TCR complexes in thymic development. A) Differentiation capacity of thymocytes from CD3ζ-deficient, OT-1^{tg} bone marrow precursors transduced with the indicated constructs.
B) Expression of the L19A CD3ζ-GFP chain allows generation of naive OT-1^{tg} CD8+ T cells. Overlay plots show expression of the indicated molecules on Vα2+ cells of OT-1^{tg} mice (shaded histogram) and Vα2+GFP+ cells from wild type (dashed black line) and L19A (grey line) CD3ζ-GFP reconstituted animals.

1.8. L19A CD3ζ reconstituted OT-1^{tg} T cells show a weaker response upon restimulation than WT CD3ζ reconstituted cells

WT and L19A CD3ζ-GFP expressing naïve OT-1^{tg} T cells were stimulated overnight with OVAp-loaded macrophages to test their sensitivity to antigen. These cells showed equal OVAp dependent up-regulation of CD69 (Figure 20), indicating that they were equally sensitive to TCR stimulation.

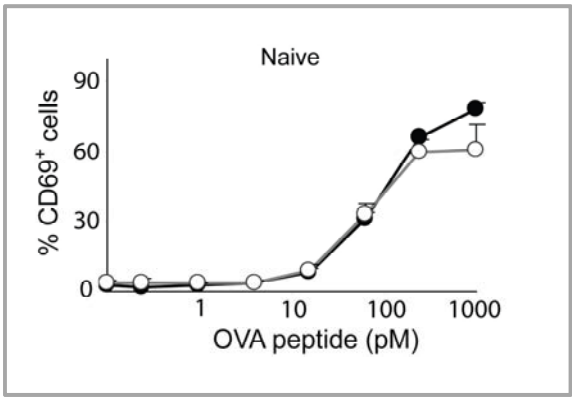

Figure 20: Activation of naive wild type and L19A CD3ζ.GFP reconstituted T cells. WT (black circles) or L19A (open circles) CD3ζ.GFP -expressing peripheral T cells (naïve).Cells were stimulated overnight with OVAp-loaded macrophages and CD69 expression was measured via flow cytometry.

We also stimulated these cells for 2 days with OVAp and expanded them for five more days in fresh medium supplemented with. IL2. At this point both cultures consisted almost exclusively of GFP^{+}CD8^{+} T cells that expressed similar amounts of the TCR at the cell surface (Figure 21A). However, when we compared the response of these *in-vitro* activated and expanded WT and L19A CD3ζ-GFP expressing OT-1^{tg} T cells, we observed a clear difference in response to antigen stimulation. L19A CD3ζ-GFP expressing cells responded worse in terms of CD69 expression and IFNγ production than their WT CD3ζ-GFP expressing counterparts (Figure 21B and C). This suggested that impairement of oligomeric TCR complex formation reduced the sensitivity of previously activated T cells.

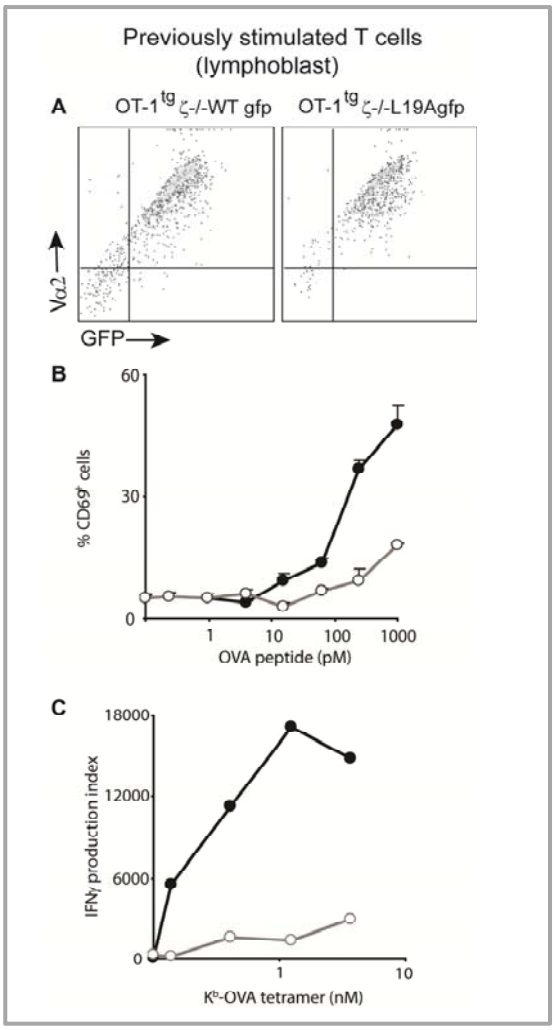

Figure 21: A) TCR expression of lymphoblast generated from transduced T cells.
Antigen sensitivity of previously activated WT and L19A CD3ζ-GFP reconstituted T cells B&C: Previously stimulated WT (black circle) and L19A (open circle) CD3ζ-GFP reconstituted OT-1^{tg} T cells were restimulated *in-vitro* with **B)** OVAp loaded macrophages or **C)** k^{b}-OVA tetramers and expression of CD69**(B)** and production of IFNγ **(C)** was measured 24hrs later by flow cytometry.

1.9. Expression of the L19A CD3ζ-GFP chain disrupts oligomeric TCR complex formation in previously stimulated OT-1^{tg} T cells.

To establish whether the difference in sensitivity of the previously stimulated L19A CD3ζ-GFP expressing OT-1 T cells was

indeed due to a difference in the number and size of oligomeric TCR complexes, we labeled part of these cells with CD3-specific antibodies and 10nm gold-conjugated protein A and prepared cell surface replicas. Analysis of the cell surface replicas of the previously stimulated WT and L19A CD3ζ-GFP expressing OT-1^{tg} T cells showed a significant reduction in the number and size of the oligomeric TCR complexes in the L19A CD3ζ-GFP expressing cells (Figure 22).This showed that the reduced sensitivity of the previously stimulated L19A CD3ζ-GFP reconstituted T cells indeed correlated with reduction in the number and size of oligomeric TCR complexes.

Together these data indicated that the role of oligomeric TCR complexes *in-vivo* was most pronounced in cells that had received previous antigenic stimulation; in line with the observation that these complexes are enriched in previously stimulated and memory T cells.

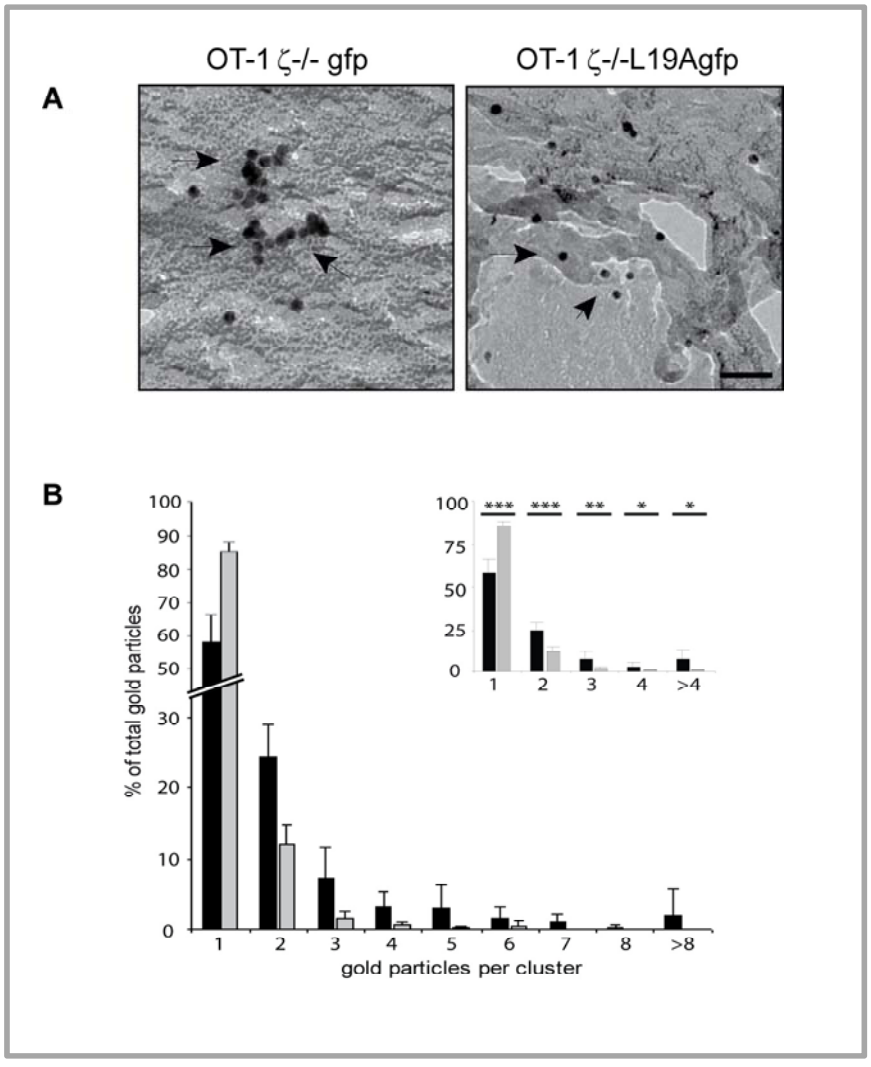

Figure 22: Distribution of TCR complexes on previously activated WT and L19A CD3ζ-GFP expressing T cells.
A) High magnification images (100.000x) of cell surface replicas of transduced T cell blasts showing distribution of gold particles on the cell surface. (Scale bar-100nm)
B) Quantification (mean +/- sem) of distribution of TCR complexes on the cell surface of T cell blasts expressing WT (black bars) or L19A (grey bars) CD3ζ-GFP chains. Inset shows distribution of gold particles between clusters of 1, 2, 3, 4 or more particles and statistical analysis (* p<0.05; ** p<0.01; *** p<0.001).Quantification of 7 WT CD3-ζ GFP reconstituted cells (3137 particles) and 7 L19A CD3-ζ GFP reconstituted cells (4257 particles) is shown.

2.Section 2

We hypothesized that the capacity of the TCR-CD3 complex on thymocytes to differentially activate downstream signaling pathways in function of the strength of interactions with its pMHC ligands depended on the differential association with other proteins involved in signal production. We decided to perform a biochemical screen for such proteins, and therefore developed a dynamically controlled murine model of T cell differentiation that would allows us to obtain a large number of DP thymocytes undergoing positive or negative selection *in-vivo*. This model system should enable us to perform the biochemical screen for such differentially associating proteins, without the need of extensive purification of this population *ex-vivo*. One of the major advantage of such a model should be the better conservation of protein-protein associations or signaling-induced protein modifications in T cells, which have been shown to be dependent on continued contact of the TCR with the pMHC molecules (Germain et al., 2002). Moreover, the ability to enrich for the populations actively undergoing positive or negative selection should facilitate the detection of differential TCR signaling during these events.

2.1. Development of a dynamic *in-vivo* model of synchronous T cell differentiation

The basis of our model is a double transgenic mouse line in which expression of a recombinant reporter gene encoding for a strong T cell agonist can be regulated by a tetracycline (tet) sensitive transactivator expressed under control of a tissue specific promoter (Kistner et al., 1996; van Santen et al., 2004). The reporter gene, TIM codes for a MHC class II associated invariant chain (Ii) in which the CLIP region is replaced by the minimal moth cytochrome c (MCC) derived T cell epitope (ANERADLIALKQATK) under control of a minimal CMV promoter and 7 TetO sequences (Figure 23A) (van Santen et al., 2004). Ii associates with MHC class II molecules upon cotranslational translocation into the ER and the CLIP region embeds itself in the peptide binding groove of the MHC class II molecule, thereby preventing that the MHC class II molecule bind peptides in the ER. Ii directs the MHC class II molecules to the endocytic route, where Ii is degraded by the resident proteases. Removal of the CLIP region from the peptide binding groove is catalysed by the the DM complex, allowing the MHC class II molecule to bind peptides generated in the endocytic route and to present these peptides at the cell surface to $CD4^+$ T cells (Pieters, 2000). Removal of the CLIP by the DM complex is not complete and upto 10% of the MHC class II molecules at the cell surface present CLIP (Eastman et al., 1996). It has been shown previously that by changing CLIP for the desired MHC class II binding peptide one can efficiently obtain MHC class II molecules presenting these peptides at the cell surface (Nakano et al., 1997). The TIM construct therefore permits efficient presentation of the MCC peptide by the MHC class II complexes. Expression of the TIM gene is controlled by the TA gene, consisting of the tet sensitive transactivator ('tet-off') under control of a MHC class II promoter (Figure 23A). In the TA transgenic line used in these studies, expression of the transactivator is restricted to stromal cells of the thymus (van Santen et al., 2004; Witherden et al., 2000). Binding of the transactivator to the regulatory

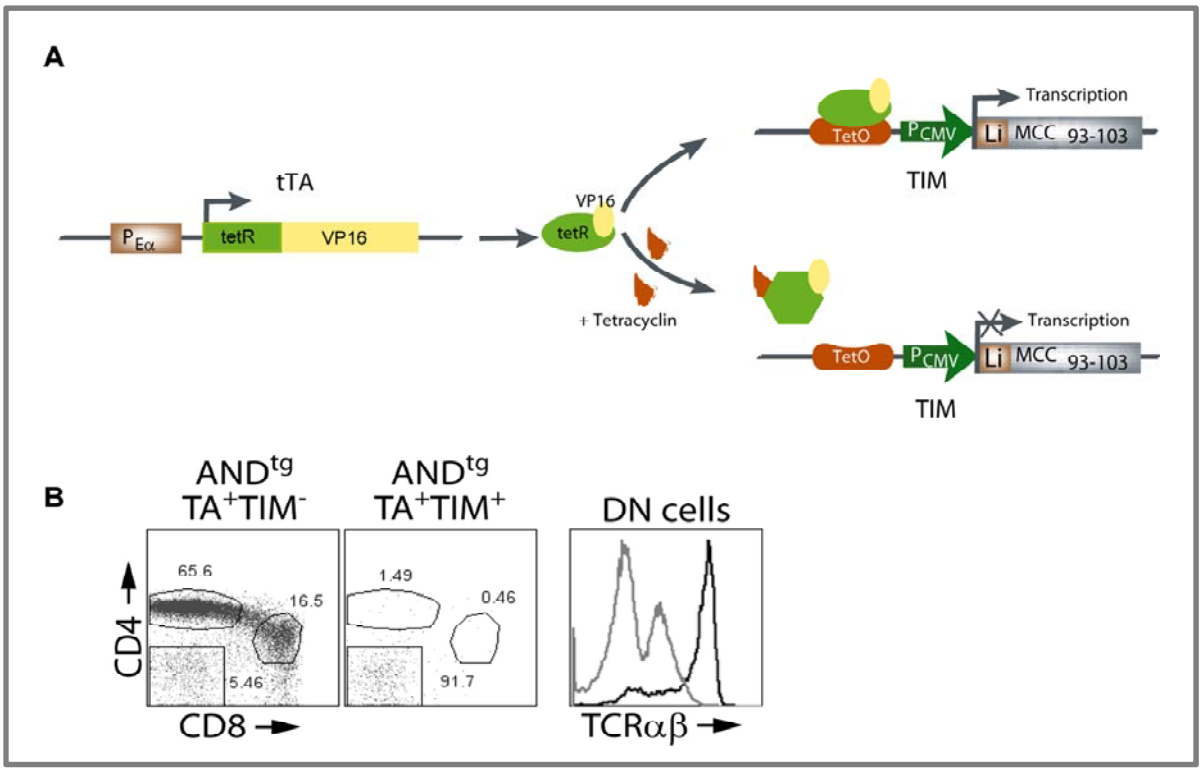

Figure 23: Animal model: A) The TANDRAG line consists of a negative selection-inducing pMHC ligand (TIM) whose expression can be controlled in vivo via a tetracycline (tet)-regulated gene expression system (TA) (van Santen et al., 2004)). **B)** This ligand is specifically recognized by AND TCR-transgenic thymocytes and T cells. As in almost all other TCR-transgenic models, the AND TCR is already expressed at the CD4-CD8- double-negative (DN) pre-selection stage, and differentiation is blocked at this stage due to premature induction of apoptosis (compare CD4 vs. CD8 profiles of TIM- (left plot) and TIM+ (right plot) animals, and the overlay showing TCR expression on the DN populations in these mice).

sequences upstream of the reporter gene allows transcription of the reporter gene. When tetracycline binds to the transactivator, it induces a conformational change in the transactivator that inhibits its binding to the regulatory sequences of the reporter gene and thereby abrogates its expression (Figure 23A). We crossed these double transgenic mice with mice transgenic for the AND (AND^{tg}) TCR, recognizing the MCC epitope bound to the MHC class II I-E^{k} molecules (Kaye et al., 1989). We brought the resulting line onto a RAG1 deficient background (Mombaerts et al., 1992), thereby assuring that the T cells could only express the AND^{tg} TCR. Thymocytes in such mice (reffered to as TANDRAG) did not differentiate beyond the DN stage (Figure 23 B).This is due to recognition of the MCC epitope by the prematurely expressed AND^{tg} αβ TCR complexes on this population (Figure 23B).

I. Optimization of the model to obtain DP thymocytes undergoing positive selection:

Treatment of TANDRAG mice with tet in the drinking water allowed the DN thymocytes to differentiate over the next 4-6 days into DP thymocytes and during the following 4 days into fully mature CD4 SP thymocytes that expressed a high level of the AND^{tg} TCR and downmodulated CD24 (Figure 24, top row and bottom row). This showed that the model recapitulated the expected

differentiation pattern from DN thymocytes via DP into CD4 SP thymocytes. DP thymocytes at day 6 of tet treatment were clearly in the process of increasing expression of the TCR complex and CD5 at the cell surface, indicative of a successfully undergoing positive selection process (Figure 24,bottom row) (Huesmann et al., 1991). At this point few CD4 SP thymocytes were present, avoiding excessive contribution of this population to our planned screen. We therefore chose as a source of DP thymocytes undergoing positive selection TANDRAG animals treated for 6 days with tet.

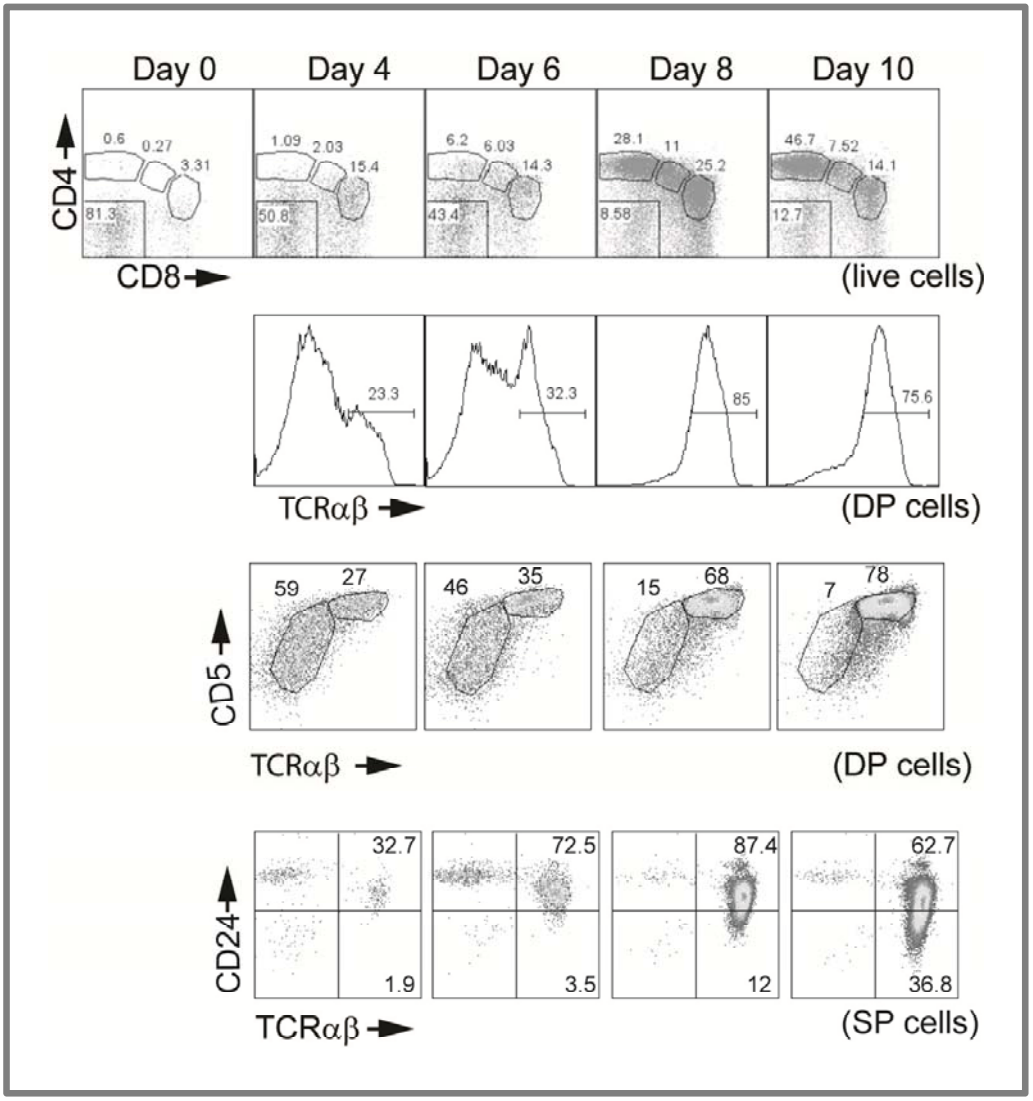

Figure 24: System optimization: positive selection. When mice transgenic for the AND TCR and the components of the tet-regulated pMHC ligand (referred to as TANDRAG mice) receive tet (administered via their drinking water), expression of the high affinity pMHC ligand is abrogated and the thymocytes differentiate over the course of the next 10 days, first into $CD4^+CD8^+$ double-positive (DP) thymocytes, and then into $CD4^+$ single-positive (SP) thymocytes. The transition through these stages is accompanied by the typical changes in expression of other cell surface proteins, such as upregulation of the TCR complex and CD5 at the DP stage (middle panels, 6 day Tet) and downregulation of CD24 at SP stage.

II Optimization of the model to obtain DP thymocytes undergoing signaling events leading to negative selection:

We first established whether reappearance of the MCC epitope led to physical deletion of DP thymocytes, the proof of successful negative selection. TANDRAG mice were treated for 6 days with tet-containing drinking water to induce the maturation of DN precursors into DP thymocytes and were subsequently given normal drinking water for a period of 24, 36 or 48 hrs. The mice were then sacrificed and thymuses were isolated. Thymocytes were analysed by flow cytometry to determine the effect of reappearance of the MCC epitope. In parallel a part of the thymus was analysed by quantitative PCR for the expression of TIM RNA. Withdrawal of tet resulted indeed in disappearance of DP thymocytes, starting at 36 hrs after withdrawing tet (Figure 25A).

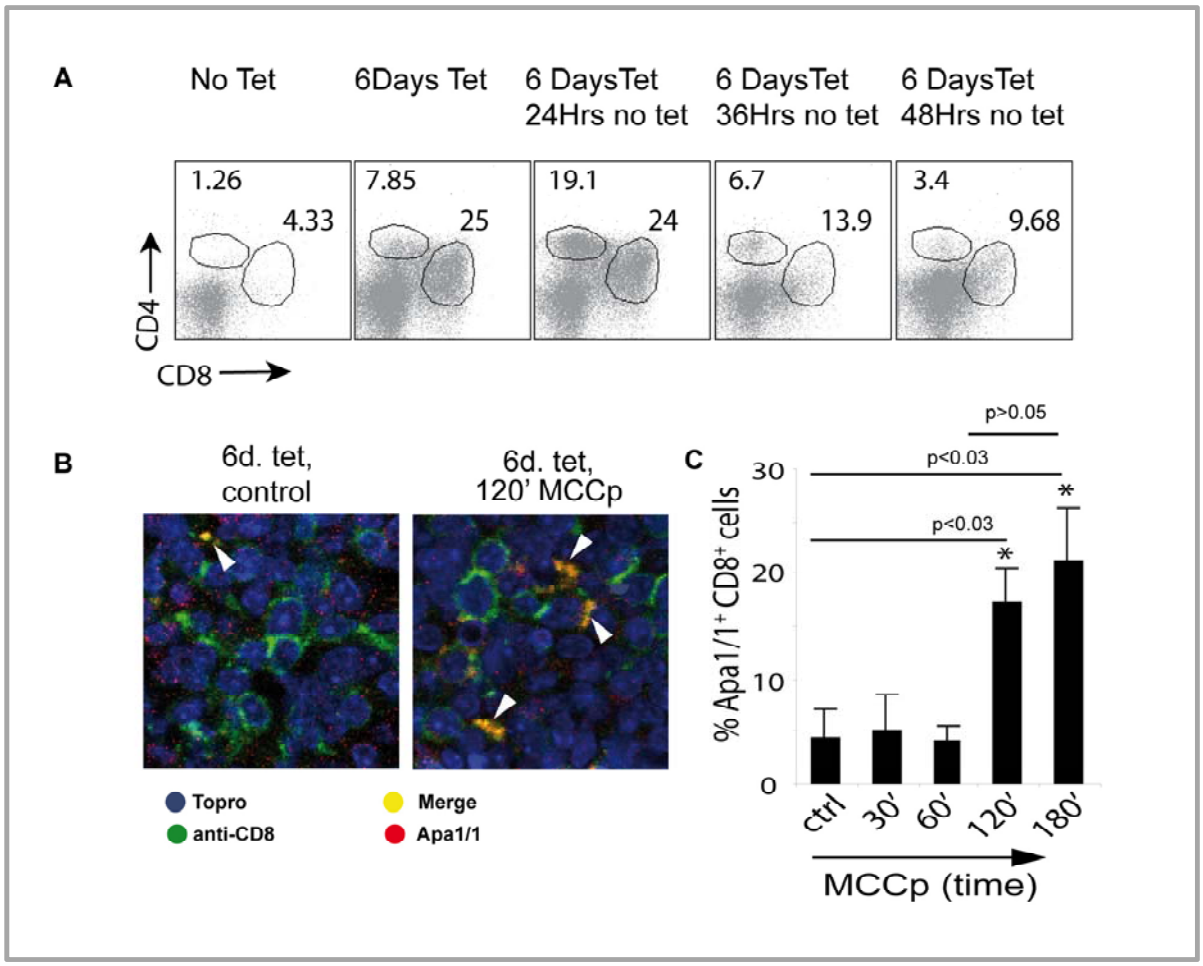

Figure 25: System optimization: negative selection A) Disappearance of double positive thymocytes after removal of tetracycline for different time periods.
B) To obtain thymocytes receiving signals leading to negative selection, 6 day-treated mice were inoculated intravenously with a moth cytochrome c-derived peptide (MCCp) recognized by the AND TCR transgenic thymocytes. This allows rapid and homogenous formation of the pMHC ligands, in contrast to waiting until levels of Tet in the mice have lowered sufficiently to allow transcription of the tet controlled ligand and achieving a sufficient number of ligands at the cell surface to induce negative selection. TCR-CD3 interactions with pMHC complexes that lead to negative selection coincide with the appearance of a conformational change in the TCR-associated CD3ε chain, which can be detected by a conformation-dependent mAb Apa1/1 (yellow dots) (Risueno et al., 2006).
C) Analysis of histological sections of 6 day-treated thymi at various time points after peptide injection show that within two hours after peptide injection there is a strong increase in the number of DP cells positive for the conformational change (immuno-histological sections and graph).

For the purpose of our interactomic screen we needed to know when DP thymocytes were receiving TCR-mediated signals inducing negative selection, not when they were dying. We therefore decided to determine how much time after exposure to the MCC epitope the CD3ε chains of AND^{tg} DP thymocytes underwent a conformational change. This conformational change correlates with induction of negative selection, is one of the earliest indicators of the signaling leading to negative selection, and can be detected by immunohistochemistry with the conformation dependent mAb Apa1/1 (Risueno et al., 2006). We also decided not to use tet withdrawal as a means to re-introduce expression of the MCC epitope and provide the DP thymocytes with stimuli leading to negative selection. Instead, we chose to inoculate mice intravenously with synthetic MCCp. We reasoned that this would result in a rapid and homogenous formation of the pMHC ligands that induce the signals leading to negative selection, thereby creating a homogenous population of DP thymocytes receiving signals leading to negative selection at the same time. We feared that removal of tet from the drinking water of the mice would lead to a less homogenous and slower formation of these pMHC complexes, given that this strategy depended on a decrease of the concentration of tet in the mouse to a level that permitted re-expression of the TIM RNA.

TANDRAG mice were treated for 6 days with tet and were then inoculated with MCCp (100µg) through the tail vein. At various time points after inoculation, mice were sacrificed and their thymuses were isolated and processed for immunohistological analysis. Cryosections were labelled with an anti-CD8 antibody to identify the DP population, the nuclear marker topro to distinguish individual cells and the Apa1/1 antibody to detect the conformational change. Labelled sections were analysed by confocal microscopy (Figure 25B) and then quantified for Apa1/1 staining (Figure 25C). An abrupt and significant increase in the percentage of CD8$^+$ thymocytes that were labelled by the Apa1/1 antibody was apparent at two hours after MCCp administration. This percentage did not change significantly over the next hour, and we therefore decided to use thymuses from TANDRAG mice that had been treated for 6 days with tet and had received MCCp 2 hours before sacrifice as a source of DP thymocytes receiving signals leading to negative selection.

2.2. A screen for proteins associating differentially with the TCR complex or showing differential tyrosine phosphorylation during positive and negative selection

TANDRAG mice were treated for six days with tet and were sacrificed two hours after intravenous inoculation with PBS or MCCp to obtain thymuses enriched for DP thymocytes undergoing positive or negative selection, respectively. Thymuses were isolated and the complete organs were directly extracted with the detergent Brij96 by Dounce homogenization. The Brij96 detergent is relatively mild and therefore more apt to conserve weak protein-protein interactions. Furthermore, it does not extract cholesterol from the membranes, thereby conserving the lipid rafts that have an important role as organizing platforms of intracellular signaling (Moran and Miceli, 1998; Viola et al., 1999).

We used antibody arrays that permit probing for interaction with 400 proteins implicated in signal transduction (Figure 26) to search for proteins that interact differentially with the TCR complex during positive and negative selection.

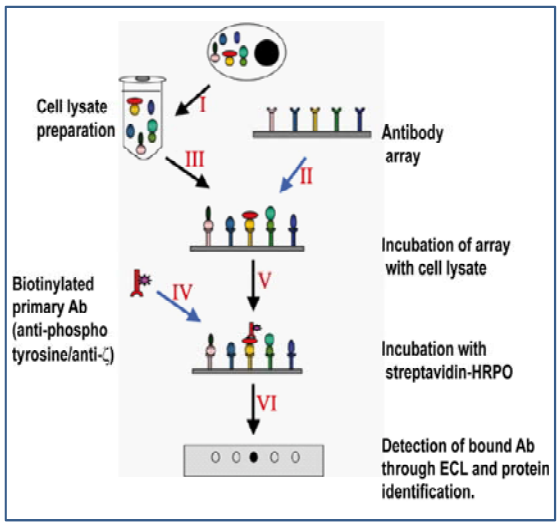

Figure 26: Antibody array: Schematic representation of the Ab-array system to identify new proteins in that are differentially phosphorylated or associated differentially with the TCR complex as a consequence of signals leading to positive or negative selection. (Adapted from Hypromatrix Antibody Array Instruction manual)

In order to obtain the maximal amount of information from these experiments we decided not only to screen these arrays for differentially interacting proteins but also for proteins that were differentially phosphorylated on tyrosine residues during positive and negative selection. The antibody arrays were incubated in parallel with half of the detergent extract prepared from thymuses in condition of positive and negative selection, followed by incubation with a phosphotyrosine specific antibody (Figure 27B). We performed a specificity control by incubating another set of arrays with the remaining half of detergent extract and labelling with the anti-phosphotyrosine antibody in the presence of phenyl phosphate, which competes with phosphorylated tyrosine residues for binding to the antibody (Figure 27A). The arrays incubated with the anti-phosphotyrosine antibody in presence of phenyl phosphate were sequentially probed with an antiserum specific for CD3ζ (Figure 27C). Taking into account the results from the control for non-specific interactions, we found various candidate proteins that showed differential tyrosine phosphorylation or association with the TCR complex under these conditions. Out of these candidates we selected a group of proteins for independent confirmation of their differential association or phosphorylation, based on the criteria of the novelty of their implication in T cell differentiation and/or the differential implication in positive and negative selection, as well as the availability of antibodies different from the ones spotted on the arrays (Table 9). In the first series of independent confirmation experiments of the selected candidates, the differential association of GRK2 with the TCR was clearly confirmed (see below).

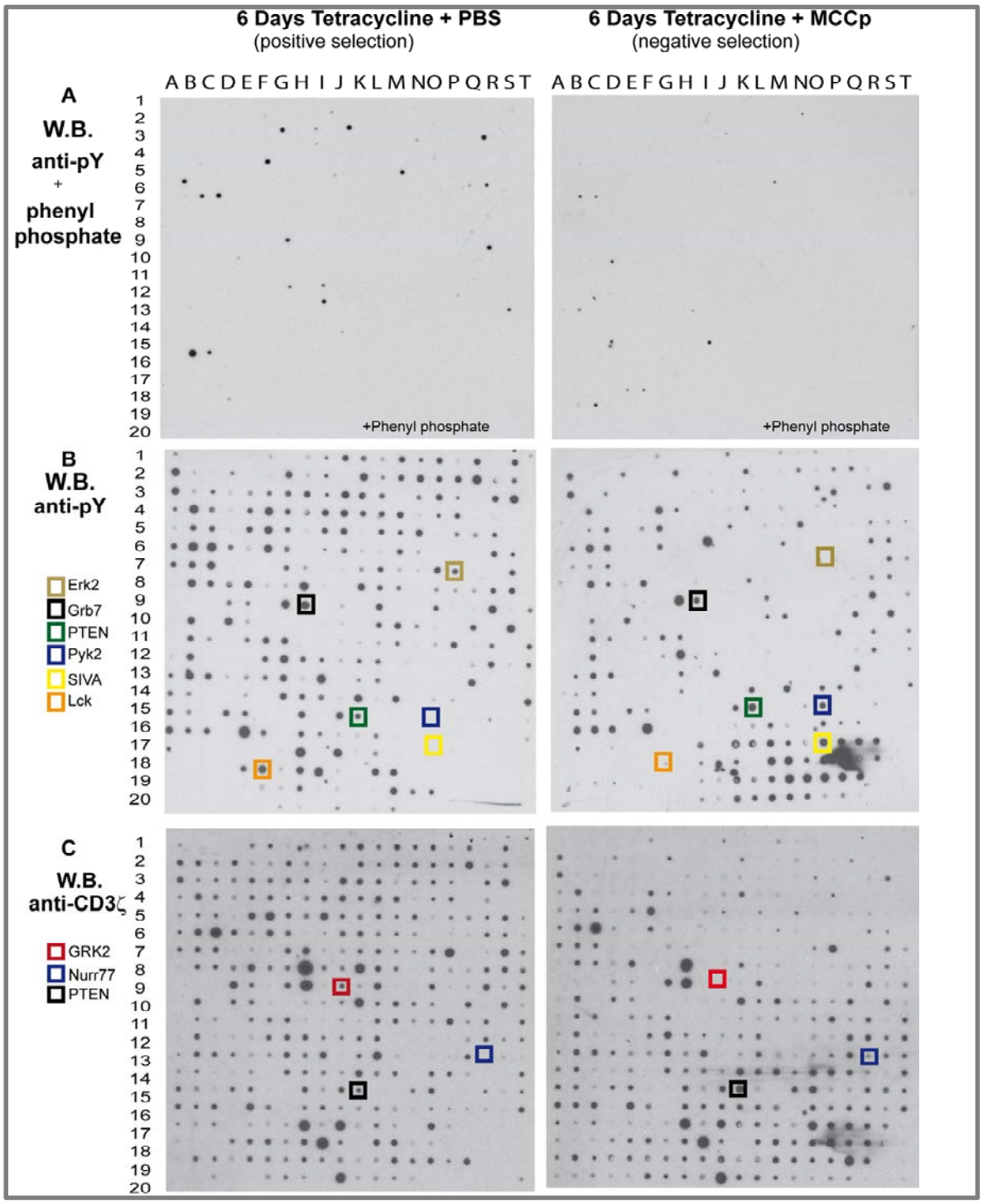

Figure 27: Identification of proteins associating differentially during positive and negative selection. Two groups of TANDRAG animals were treated with tet for 6 days and then animals were inoculated with PBS (positive selection) or MCCp (negative selection) through the tail vein (negative selection condition), 2Hrs prior to the assay. Thymic detergent extracts were hybridized,.in parallel with the antibody arrays, followed by incubation of the arrays with a biotinylated phospho tyrosine specific Ab in presence **(A)** or abscence **(B)** of phenylphosphate or with **(C)** a biotinylated CD3ζ-specific antibody. Bound antibody was detected with SA-HRPO and ECL.The position of the spot on the array allows identification of the proteins in volved in differential association or phosphorylation.

Table 9: List of proteins identified through antibody array. Antibody array was quantified through gel quantification system and optical density for spot was calculated. Value written here is the division of value obtained in positive selection condition divided by value obtained in negative selection condition. Value 1 is control, less than 1 is positive for negative selection condition while value more than 1 is positive for positive selection condition. Proteins of interest which were further studied are depicted in red.

Identified protein	Detection	Positive/Negative (value)
BRCA1	Tyrosine phosphorylated	1.08
HSP70	Tyrosine phosphorylated	1.08
PYK2	Tyrosine phosphorylated	0.06
Grb7	Tyrosine phosphorylated	2.69
PTEN	Tyrosine phosphorylated	0.48
SIVA	Tyrosine phosphorylated	0.02
ERK2	Tyrosine phosphorylated	8
Bcl6	Tyrosine phosphorylated	8
BclxL	Tyrosine phosphorylated	5
Bim	Tyrosine phosphorylated	13
Lck	Tyrosine phosphorylated	15
c-Src	Tyrosine phosphorylated	17
BRCA1	TCR-Associated	1.08
β-Catenin	TCR-Associated	1.13
PAR4	TCR-Associated	0.25
PARP	TCR-Associated	0.06
PTEN	TCR-Associated	0.2
Cyclin E	TCR-Associated	3.4
Rab11	TCR-Associated	0.2
Rab5	TCR-Associated	0.21
Apaf1	TCR-Associated	8.5
Erk1	TCR-Associated	18
GRK2	TCR-Associated	9

We decided to focus our attention on GRK2, as it had so far not been shown to be involved in T cell differentiation. Furthermore, its classically defined role in regulation of G-protein coupled receptors, such as chemokine receptors appaerd interesting in view of the importance of thymocytes migration during T cell development.

2.3. Confirmation of differential GRK2-TCR interaction by immunoprecipitation and immunoblot assay.

The antibody array showed a clear decrease in the signal for TCR-associated GRK2 during negative selection (Figure 28A). We confirmed this differential association via direct immunoprecipitation assays. We prepared detergent extracts from thymuses of two groups of mice that had been treated as describe above in order to obtain DP populations undergoing positive selection or negative selection. We immunoprecipitated GRK2 from these extracts with a GRK2-specific antibody that was different from the one spotted on the array and upon separation of the immunoprecipitate by SDS-PAGE and immunoblotting, labelled the membrane with anti CD3ζ antibody to check the association between GRK2 and CD3ζ (Figure 28B). This confirmed that CD3ζ associated with GRK2 only under conditions of positive selection.

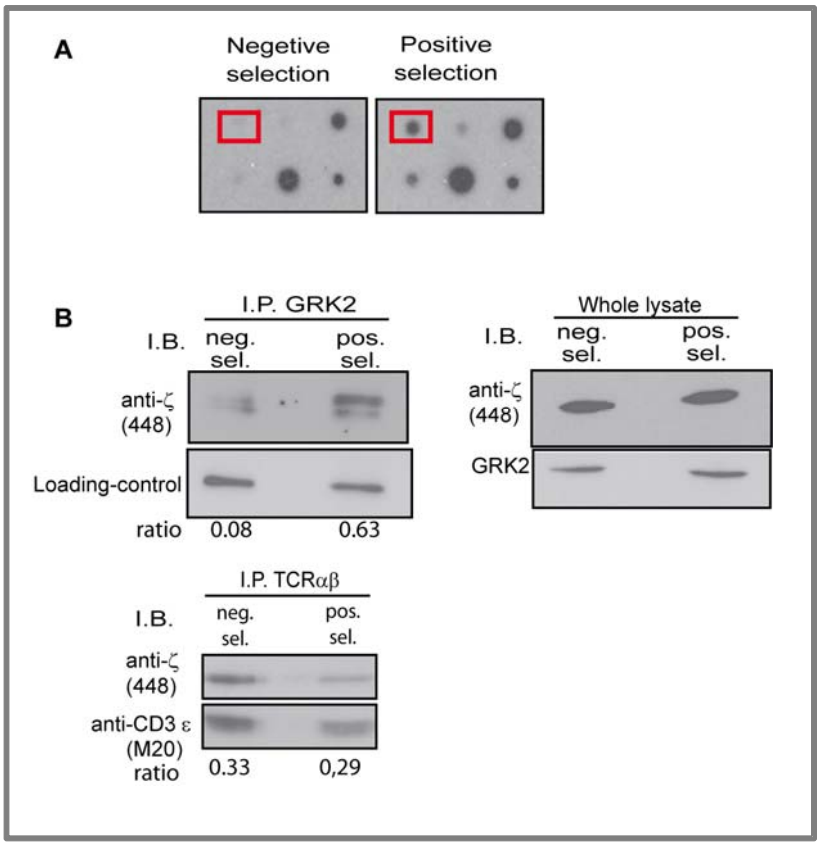

Figure 28: Association between GRK2 and the TCR complex during positive selection.
A) A portion of Ab-array showing association of GRK2 with positive selection condition while it is absent in negative selection condition. **B)** Direct confirmation of the differential GRK2 association with the TCR complex during positive selection by immuno-precipitation and immuno-blot analysis of thymic extracts obtained from TANDRAG mice treated for 6 days with tet and subsequently inoculated with PBS or MCCp

As we did not know through which subunits GRK2 is associated with the TCR complex, we verified that the apparent dissociation of GRK2 from the TCR complex under conditions of negative selection was not an artefact caused by dissociation of CD3ζ from the other components of the TCR complex. We performed immunoblotting experiments, immunoprecipitating the TCR complex from detergent of positively and negatively selecting thymuses with a TCRαβ specific antibody and blotted with CD3ε and CD3ζ (Figure 28B, lower panel). Quantitative analyses of these blots showed that the ratio between CD3ε and CD3ζ did not change under these conditions.

2.4. Identification of the cell populations in which the GRK2-TCR association occurs

As at day 6 of tet treatment both DN and DP populations are present in the thymus of TANDRAG mice (Figure 24), we needed to formally prove that the association of GRK2 with the TCR-CD3 complex occurred in DP thymocytes by purifying this population. We treated TANDRAG mice for 6 days with tet to obtain thymuses containing DN and DP (Figure 29A, input 6 days) thymocytes, we furthermore treated a group of animals for 9 days with tet to obtain thymuses containing DP and SP thymocytes, allowing us to determine whether association also occurred in 4SP thymocytes (Figure 29A, input 9 days).Upon isolation of the thymuses of these mice we prepared single cell suspensions and separated the DP from DN or 4SP populations by staining the thymocytes with an anti-CD8 antibody (which labelled the DP population) and then isolating the labelled population by the use of magnetic beads (Figure 29A).

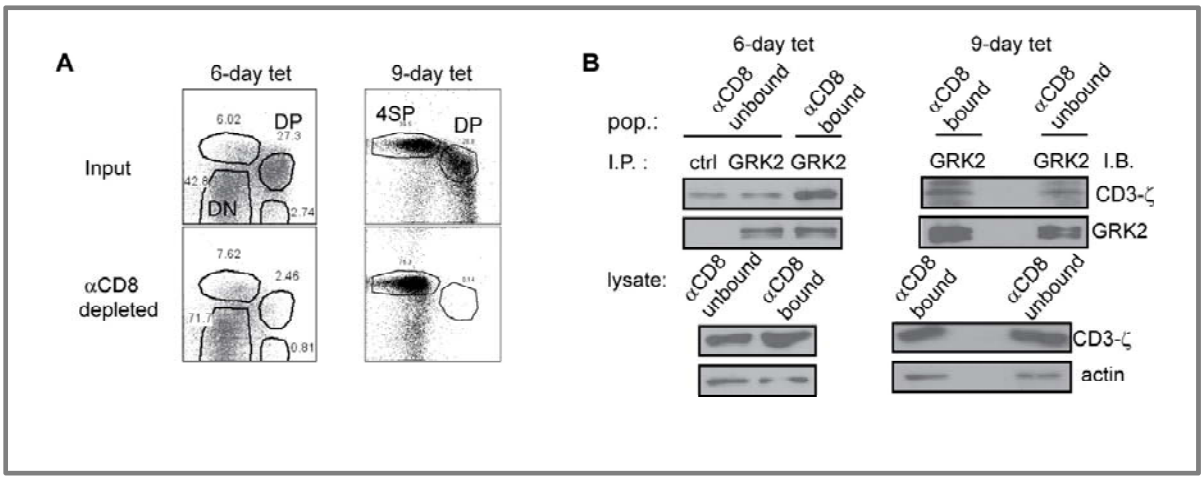

Figure 29: Biochemical analysis of the interaction between GRK2 and the TCR complex. Association of GRK2 with the TCR complex at DP and SP stage. Cell suspensions, prepared from thymuses isolated from TANDRAG animals treated for 6 and 9 days with tet, were enriched for DN and DP or DP and SP population respectively, using anti CD8α antibodies and magnetic beads.
A) FACS profile showing thymic populations before and after separation through magnetic beads.
B) Detergent extracts made from these separated populations were analyzed via immuno-precipitation and immuno-blotting for association between GRK2 and the TCR complex. An anti-human CD3 antibody (OKT3) was used as an isotypic negative control for the anti-GRK2 antibody used for immuno-precipitation.

Bead-bound, enriched for DP cells, and unbound cells, enriched for either DN or 4SP cells, were separately lysed in Brij96 detergent and lysates were immunoprecipitated with the GRK2-specific antibody and analyzed via immunoblotting for its association with CD3ζ (Figure 29B). These experiments showed that the interaction between GRK2 and the TCR complex was above background in the DP and 4SP enriched thymocyte and indicated that the interaction started at the DP stage.

Finally we wished to determine whether association of GRK2 with the TCR was lost upon stimulation of the 4SP population. We treated TANDRAG mice for 9 days with tet, resulting in the appearance of both DP and 4SP thymocytes, and inoculated them with MCCp or PBS 2 hours before sacrifice and isolation of the thymus. Analysis of GRK2 immunoprecipitation via western blot showed a decrease in the amount of associated CD3ζ, upon MCCp injection (Figure 30). This partial reduction of association suggested that CD3ζ and the TCR dissociated not only in the DP but also in the 4SP population upon stimulation with MCCp.

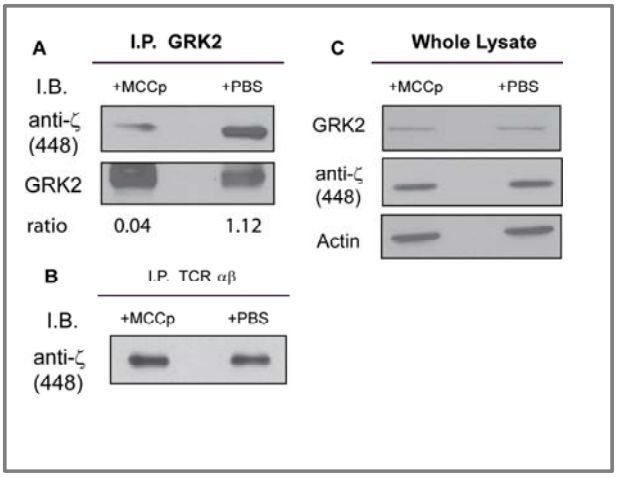

Figure 30: Interaction between GRK2 and TCR complex at day 9. TANDRAG were treated for 9 days with tet, and then they were injected with MCCp or PBS. GRK2 dissociates from TCR upon stimulation (upper left panel) while equal amount of CD3ζ remained associated with the TCR under both conditions (lower left panel). Left panel shows equal amount of zeta and GRK2 in whole lysate.

2.5. Analysis of T cell differentiation in GRK2$^{+/-}$ mice

In order to determine whether GRK2 played a role in T cell differentiation, we analyzed mice that lacked one functional copy of the GRK2 gene (GRK2$^{+/-}$ mice) (Jaber et al., 1996). Homozygous knock-out (GRK2$^{+/-}$) animals of the original colony die around gestational day 15 (E15) (Jaber et al., 1996) prohibiting a direct analysis of the thymic phenotype of such animals. We tried to obtain fetal liver from GRK2$^{-/-}$ embryos at E10-E11, as at that stage of embryonic differentiation the haematopoietic stem cells reside in this organ (Cumano et.al.2007). These cells could in principle be used to reconstitute the haematopoietic system of lethally irradiated recepients and to test their potential for differentiation into the T cell lineage. However, when analyzing the genotype of E10-E11 embryos of our colony, we found that out of the 24 embryos analysed only 3 were GRK2$^{-/-}$ and they were already in the process of resorption (data not shown). This prevented us from studying the role of GRK2 in thymocytes differentiation via this strategy.

GRK2$^{+/-}$ mice express 50-60% less GRK2 than wild type animals in various tissues and it has been demonstrated that such reduction affects GRK2 dependent signaling (Kleibeuker et al., 2008; Peregrin et al., 2006) and migration (Penela et al., 2008b; Vroon et al., 2004). We therefore crossed GRK2$^{+/-}$ animals with AND^{tg} mice and with OT-1^{tg} mice (Hogquist et al., 1994), which express a MHC class I-restricted TCR that recognizes an ovalbumin-derived epitope, reasoning that such TCR-transgenic animals should allow a much clearer detection of any perturbation in TCR-dependent processes during T cell selection.

I. Phenotypic analysis of AND^{tg} GRK2$^{+/+}$ and GRK2$^{+/-}$ animals:

We first analyzed the expression level of GRK2 in thymocytes of AND^{tg} GRK$^{+/+}$ and GRK$^{+/-}$ mice, and found that AND^{tg}GRK2$^{+/-}$ thymocytes expressed about 60% less GRK2 than AND^{tg}GRK2$^{+/+}$ thymocytes (Figure 31A). Phenotypic analysis of thymus showed no major block in thymocyte differentiation as a consequence of reduced GRK2 expression. The distribution of GRK2$^{+/+}$ and GRK2$^{+/-}$ AND^{tg} thymocytes between the major subsets was almost identical (Figure 31B). Total cell numbers were neither significantally different, although there was a tendency to fewer cells in the GRK2$^{+/-}$ animals.

However a more detailed comparison of the thymus of these mice showed two very consistent and statistically significant differences. At the DP stage there was a clear reduction in the percentage of GRK2$^{+/-}$ AND^{tg} thymocytes expressing a higher level of TCR at the cell surface as compared to GRK2$^{+/+}$ AND^{tg} thymocytes. (Figure 31C).This reduction in TCR expression was specific for the DP stage, as 4SP thymocytes of both types of animals expressed an equal number of TCR complexes at the cell surface. This excluded the possibility that GRK2 was involved in general mechanisms of regulation of the level of TCR expression. Increase in TCR expression in the DP stage is a key event during positive selection and is dependent on interaction with selecting MHC ligands and signaling via the TCR complex (Watanabe et al., 2000). Our data therefore indicated that the efficiency of positive selection in AND^{tg}GRK2$^{+/-}$

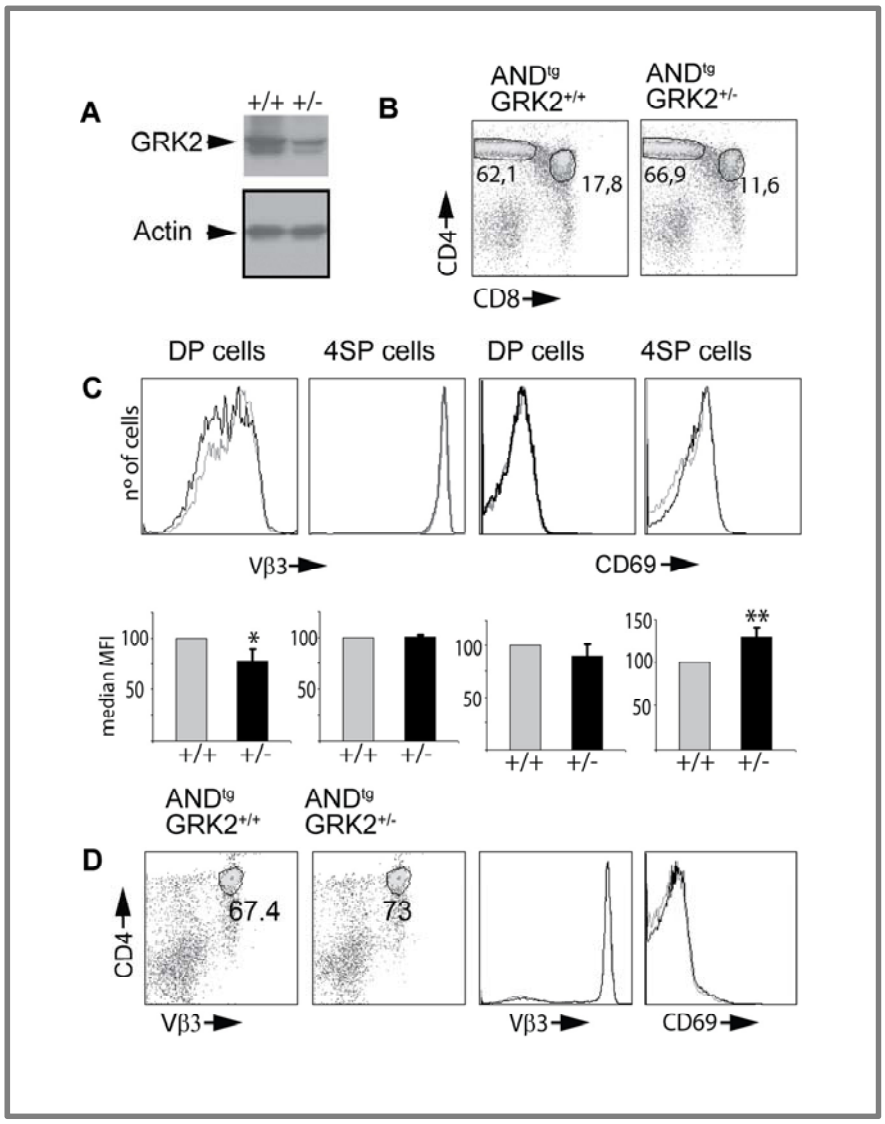

Figure 31: Phenotypic analysis of GRK2+/- AND^{tg} mice.
A) Immuno-blot of whole lysates of GRK2$^{+/+}$ and GRK2$^{+/-}$ AND^{tg} total thymocytes showing a 60% reduction in expression of GRK2 in the heterozygous thymocytes.
B) CD4 vs. CD8 profile of GRK2$^{+/+}$ and GRK2$^{+/-}$ AND^{tg} thymocytes on an H-2^{kb} background.
C) Overlays of TCR expression (left panels) and CD69 expression (right panels) on DP and 4SP GRK2$^{+/+}$ (gray lines) and GRK2$^{+/-}$ (black lines) AND^{tg} thymocytes. Quantification of expression levels and statistical analysis are shown in the bar graphs below each overlay for three independent experiments with one or two mice per group (gray bars: GRK2$^{+/+}$ thymocytes; black bars: GRK2$^{+/-}$ thymocytes; * p<0.043 and ** p<0.026, student t-test).
D) Phenotypic analysis of lymphocytes from peripheral lymph node (left panel), overlay plots of TCR and CD69 profiles in GRK2$^{+/+}$ (gray lines) and GRK2$^{+/-}$ (black lines) AND^{tg} lymphocytes.

mice was reduced as compared to their wild type counterparts, thereby implying a limiting role for GRK2 during this process. The other phenotype we observed was a statistically significant decrease in the downmodulation of CD69 at the cell surface of mature CD4 single positive thymocytes in GRK2$^{+/-}$ as compared to GRK2$^{+/+}$ mice. (Figure 31C). Downmodulation of CD69 has been shown to be essential for exit of mature thymocytes to the periphery (Feng et al., 2002). Expression of CD69 on AND^{tg}GRK2$^{+/+}$ and GRK2$^{+/-}$ DP thymocytes was not significantly different, indicating that this phenotype was also stage specific.

Peripheral AND^{tg}GRK2$^{+/-}$ CD4^{+} T cells were present in normal numbers and the expression level of the TCR and CD69 on these cells was indistinguishable from wild type AND^{tg} T cells (Figure 31D). This indicated that, at steady state conditions, the role of GRK2 in AND^{tg} T

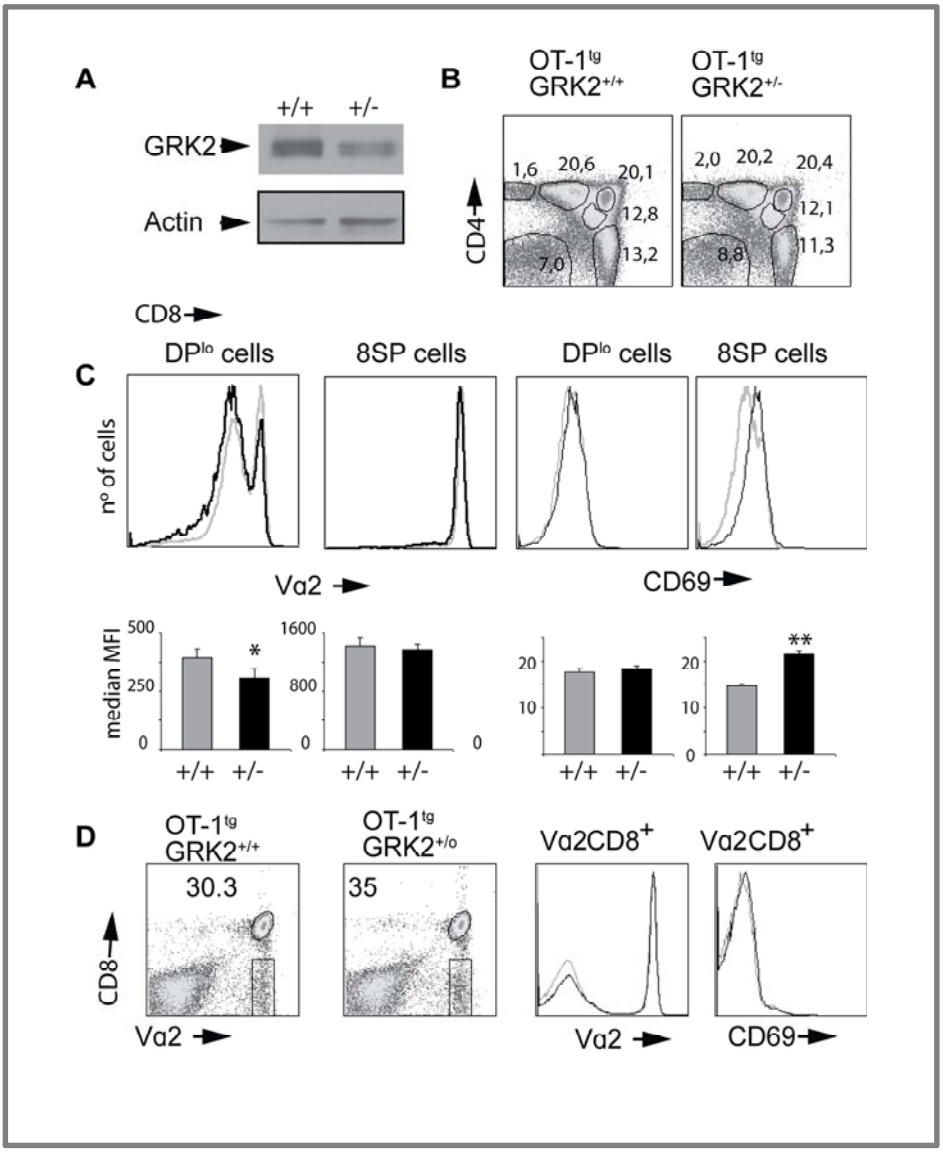

Figure 32: Phenotype of GRK2+/- OT-1tg mice.
A) Immuno-blot of whole lysates of GRK2$^{+/+}$ and GRK2$^{+/-}$ OT-1^{tg} total thymocytes showing a reduction in expression of GRK2 in the heterozygous thymocytes.
B) CD4 vs. CD8 profile of GRK2$^{+/+}$ and GRK2$^{+/-}$ OT-1^{tg} thymocytes
C) Overlays of TCR expression (left top panels) and CD69 expression (right top panels) on DP and 4SP GRK2$^{+/+}$ (gray lines) and GRK2$^{+/-}$ (black lines) OT-1^{tg} thymocytes. Quantification of expression levels and statistical analysis are shown in the bar graphs below each overlay for one out of two experiments, with four to five mice per group (gray bars: GRK2$^{+/+}$ thymocytes; black bars: GRK2$^{+/-}$ thymocytes; * $p<0.01$ and ** $p<0.000001$, Student's t test).
D) Phenotypic analysis of lymphocytes from peripheral lymph node (left panel),overlay plots of TCR and CD69 profiles in GRK2$^{+/+}$ (gray lines) and GRK2$^{+/-}$ (black lines) OT^{tg} lymphocytes.

cells is most limiting during the process of thymic differentiation.

II. Phenotypic comparison of OT-1^{tg} GRK2$^{+/+}$ and GRK2$^{+/-}$ animals:-

We also compared OT-1^{tg} animals on a GRK2$^{+/+}$ and GRK2$^{+/-}$ background, permitting us to determine whether the phenotype observed in AND^{tg} animals was restricted to this particular clone and/or to MHC class II-restricted T cells. The thymic phenotype of OT-1^{tg}GRK2$^{+/-}$ mice showed confirmed the phenotype observed in AND^{tg}GRK2$^{+/-}$ mice: reduction in expression of GRK2 (Figure 31), reduced TCR up-regulation at the DP stage and reduced CD69 downmodulation at the SP stage. (Figure 32). Again peripheral GRK2$^{+/+}$ and GRK2$^{+/-}$ OT-1^{tg} T cells were indistinguishable for TCR and CD69 expression (Figure 32D).

Together these data suggested that GRK2 played limiting roles during positive selection at the DP stage and the egress of mature thymocytes from the thymus in both MHC class I and MHC class II restricted T cells.

2.6. Induction of apoptosis in GRK2+/+ and GRK2+/- thymocytes

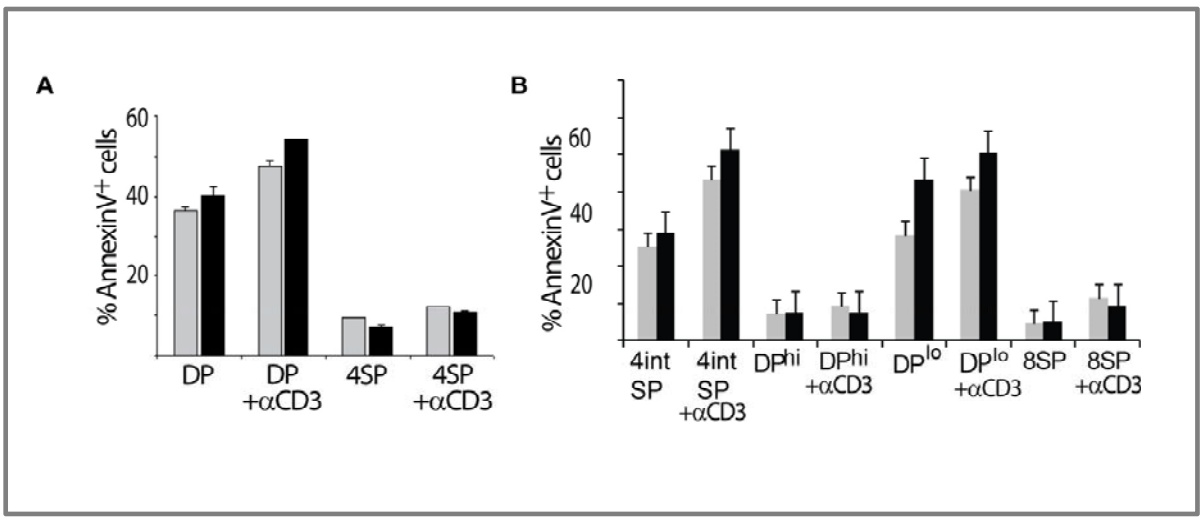

Figure 33: Induction of apoptosis.Percentage of AnnexinV positive cells in the indicated thymic subpopulation of GRK2$^{+/+}$ (gray bars) and GRK2$^{+/-}$ (black bars) of AND^{tg} thymocytes **(A)** OT-1^{tg} thymocytes **(B)** upon 4 hours of culture in absence or presence of 5 µg/ml of a soluble stimulatory anti-CD3ε antibody.

We cultured AND^{tg} GRK2$^{+/+}$ and GRK2$^{+/-}$ thymocytes *in-vitro* in presence or absence of a stimulatory anti-CD3ε antibody, in order to determine whether apoptosis caused by lack of TCR-mediated stimuli or induced by strong TCR stimuli was altered in GRK2$^{+/-}$ thymocytes. As compared to GRK2$^{+/+}$ thymocytes, the DP subpopulation of AND^{tg} GRK2$^{+/-}$ thymocytes showed slightly increased levels of AnnexinV staining upon 4 hrs of culture in absence of stimuli (Figure 33A). This indicated that these thymocytes were slightly more prone to apoptosis, and could explain the observed phenotype of reduced efficiency of positive selection (taking into account that positive selection rescues DP thymocytes from programmed cell death). GRK2$^{+/-}$ 4SP thymocytes were, if anything, slightly less sensitive to apoptosis. Upon stimulation with the anti-CD3ε antibody, there was a clear increase in Annexin V^{+} DP AND^{tg} GRK2$^{+/+}$ and GRK2$^{+/-}$ thymocytes. Interestingly, the increase in the percentage of Annexin V^{+} cells was very similar in both cases (about 1.3 fold), suggesting that TCR-induced apoptosis was not majorly affected by a reduction in GRK2 levels.

Similarly, OT-1^{tg} GRK2$^{+/-}$ thymocytes cultured for 4 hours in vitro showed slightly increased percentages of AnnexinV^{+} thymocytes in the more immature DP^{hi}, DP^{lo} and 4^{int} populations, as compared to the corresponding GRK2$^{+/+}$ populations (Figure 33 B). Again, stimulation with the stimulatory anti-CD3ε antibody increased the percentage of Annexin V^{+} cells in the immature GRK2$^{+/+}$ and GRK2$^{+/-}$ populations to a similar extent.

Thus, while apoptosis *in-vitro* caused by lack of stimuli was slightly increased in GRK2$^{+/-}$ DP thymocytes, TCR induced apoptosis, reflective of negative selection, was not affected. This suggested that the phenotype observed in the GRK2$^{+/-}$ animals was mostly due to impaired positive selection and not to exacerbated negative selection.

2.7 Reduced sensitivity of AND^{tg} GRK2$^{+/-}$ thymocytes to TCR mediated stimuli

Given that positive selection is strictly dependent on TCR-CD3 mediated signaling and in view of the observation that GRK2 is associated with the TCR of DP thymocytes during positive selection, we sought to determine whether a reduction in the amount of GRK2 directly affected TCR dependent activation events. In vitro stimulation of AND^{tg} GRK2$^{+/+}$ and GRK2$^{+/-}$ thymocytes with graded amounts of the MCC peptide showed a marked reduction in TCR down-modulation and CD69 up-regulation in GRK2$^{+/-}$ DP thymocytes as compared to GRK2$^{+/+}$ DP thymocytes (Figure 34). This difference in response was not observed in CD4^{+} SP thymocytes nor in CD4^{+} lymphocytes from lymph nodes (Figure 35), indicating that the reduction in GRK2 does not cause a general deffect in internalization of the TCR complex or expression of the CD69 molecule at the cell surface. These data suggested that GRK2 plays a direct role in signaling via the TCR complex and also suggested that the reduction in efficiency in positive selection of AND^{tg} GRK2$^{+/-}$ DP thymocytes was at least partly due to a reduction in GRK2-dependent TCR-CD3 mediated signaling processes.

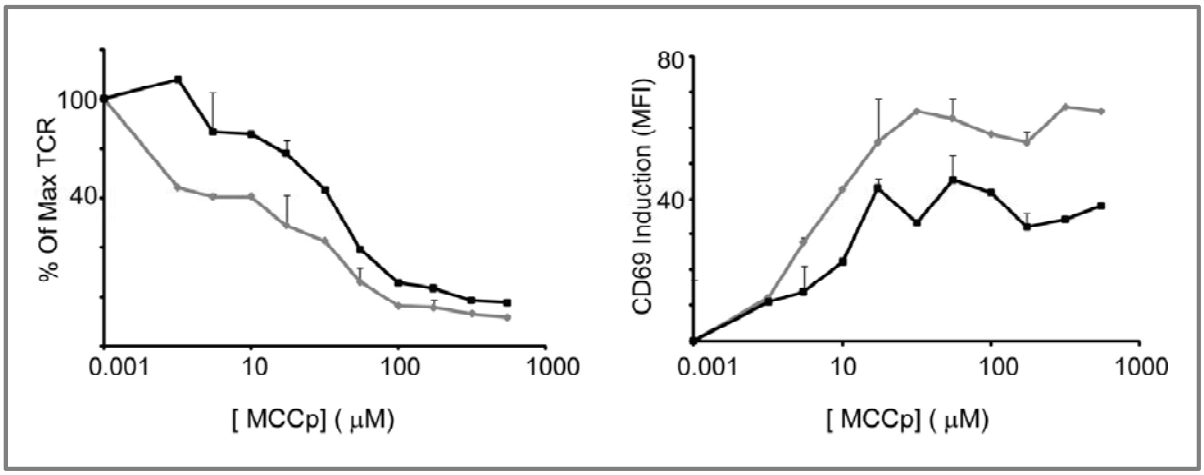

Figure 34: Functional analysis of DP T cells of GRK2$^{+/+}$ and GRK2$^{+/-}$ AND^{tg} mice. *In vitro* stimulation assays of AND^{tg} GRK2$^{+/+}$ (gray lines) and GRK2$^{+/-}$ (black lines) DP T cells, measuring up-regulation of **A)** TCR downmodulation and **B)** CD69 upregulation upon stimulation with graded amounts of the MCC peptide presented by DCEK cells.

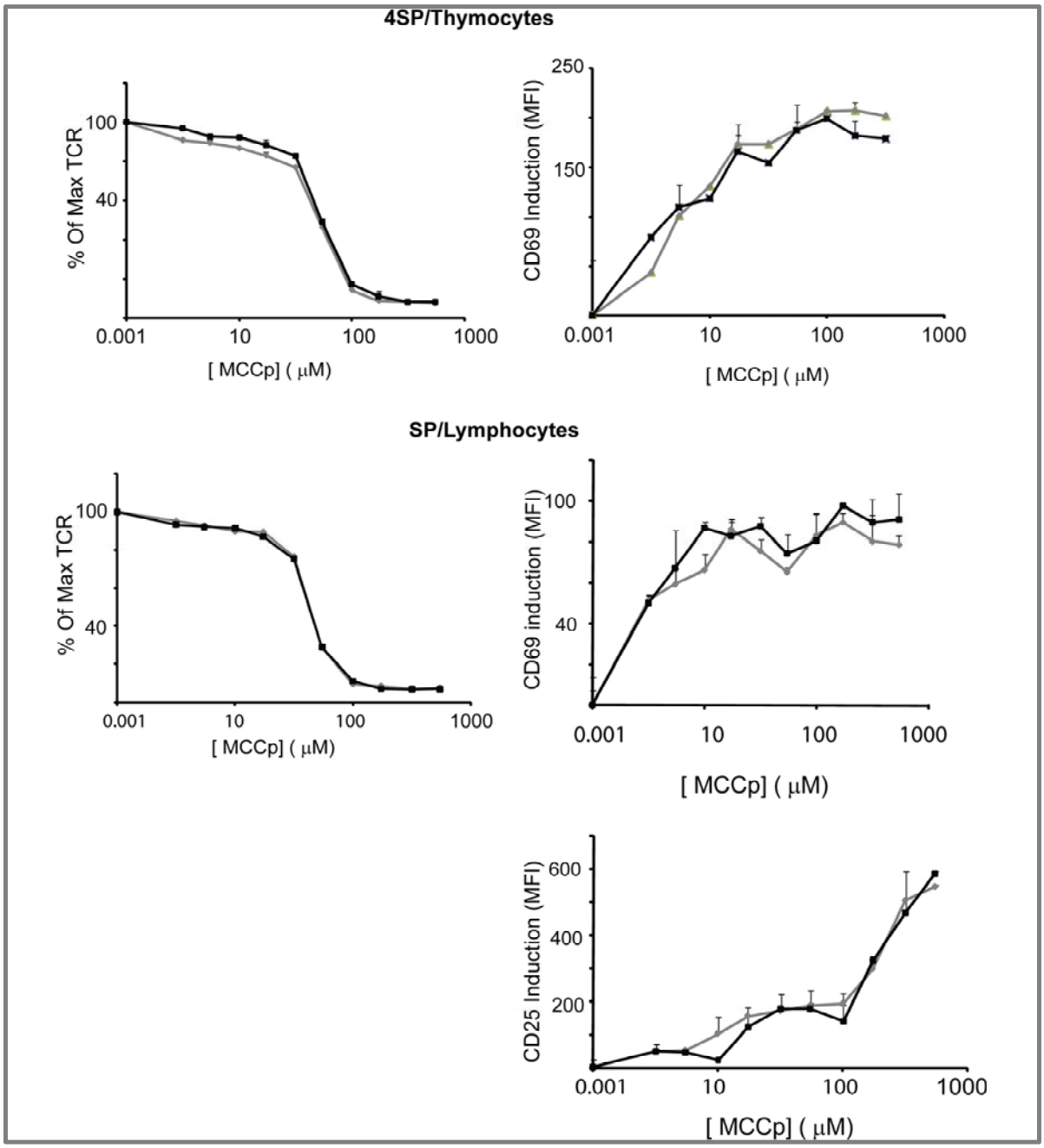

Figure 35: Functional analysis of 4SP (thymocytes) and mature lymphocytes from GRK2$^{+/+}$ and GRK2$^{+/-}$ AND^{tg} mice. *In vitro* stimulation assays of AND^{tg} GRK2$^{+/+}$ (gray lines) and GRK2$^{+/-}$ (black lines) T cells, measuring downmodulation of TCR and up-regulation of CD69 and CD25 upon stimulation with graded amounts of the MCC peptide presented by DCEK cells.

2.8. Reduction in cell number and appearance of $CD4^{lo}CD8^{lo}$ $GRK2^{+/-}$ AND^{tg} thymocytes in presence of weaker positively selecting ligands.

AND^{tg} thymocytes can not only be positively selected by the $I\text{-}E^{k}$ allele but also by the $I\text{-}A^{b}$ allele (Kaye et al., 1992). The interaction between the AND^{tg} TCR and the $I\text{-}A^{b}$ allele is of weaker strength than its interaction with $I\text{-}E^{k}$ (Kaye et al., 1992). If positive selection was indeed diminished in $GRK2^{+/-}$ animals, and if this depended at least partially on reduced signaling capacity of the TCR complex in $GRK2^{+/-}$ animals, a weaker interaction via the $I\text{-}A^{b}$ allele should exacerbate the reduction in positive selection observed in the AND^{tg} $GRK2^{+/-}$ mice in presence of the $I\text{-}E^{k}$ allele (Figure 31A).

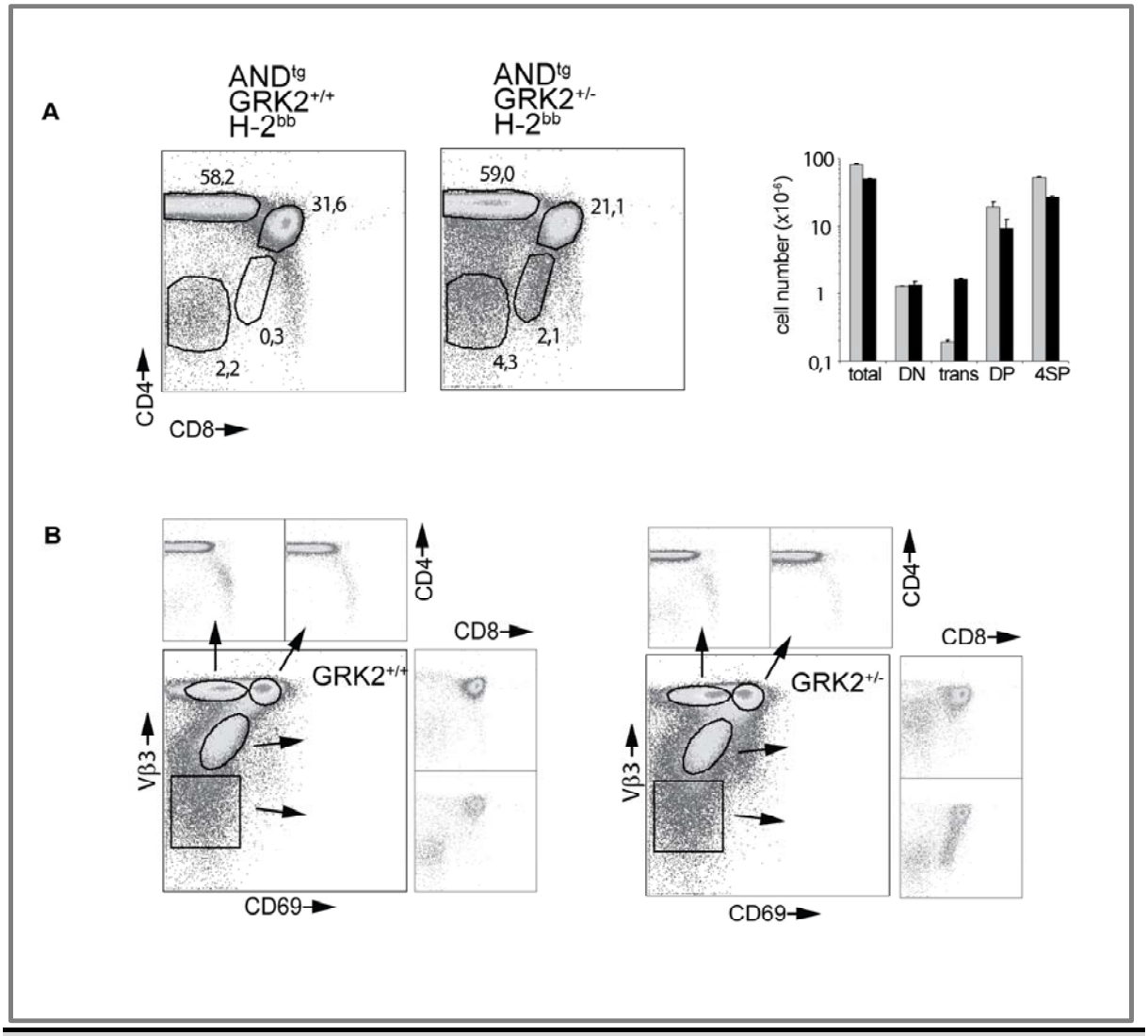

Figure 36: Reduced DN to DP transition of $GRK2^{+/-}$ $ANDt^{g}$ thymocytes in presence of weaker positively selecting TCR ligands. A) CD4 vs. CD8 profiles and quantification of the indicated thymocyte subsets in $GRK2^{+/+}$ and $GRK2^{+/-}$ AND^{tg} mice in a $H\text{-}2^{bb}$ background (gray bars: $GRK2^{+/+}$ thymocytes; black bars $GRK2^{+/-}$ thymocytes).
B) Quadruple staining of thymocytes with CD4, CD8, CD69 and the transgenic Vβ3 TCR segment shows that the $CD4^{lo}CD8^{lo}$ thymocytes observed in $GRK2^{+/-}$ mice are $CD69^{lo}TCR^{lo}$ thymocytes.

The outcome was slightly different from the one expected. The total number of thymocytes in AND^{tg} GRK2$^{+/-}$ H-2^{bb} mice was reduced by 40% as compared to their wild type counterparts and manifested itself as of the DP population (Figure 36A). Thus the tentative reduction in cell number observed in the I-E^{k} background became much more pronounced in presence of only the weaker I-A^{b} allele. This suggested that positive selection was quantitatively affected.

However, there was a second phenotype: the GRK2$^{+/-}$ animals contained a CD4^{lo}CD8^{lo} population that was not detected in GRK2$^{+/+}$ animals (Figure 36B). Four colour labelling of thymocytes with antibodies specific for TCRβ, -CD69, -CD4 and -CD8 showed that these cells were contained within the most immature TCR^{lo}CD69^{lo} subset (Figure 36B). This indicated that these were pre-selection thymocytes and not DP thymocytes down-modulating CD4 and CD8 upon receiving signals inducing negative selection, as such thymocytes express CD69 (Kishimoto et al., 1995). It therefore appeared that these were thymocytes transitioning from the DN to the DP stage. This transition is mediated by the pre-TCR complex in mice with a polyclonal T cell repertoire, but is usually mediated by the TCRαβ complex in TCR^{tg} mice (Croxford et al., 2008). The reduction in DP and 4SP thymocytes could therefore have been the consequence of reduced efficiency of DN to DP transition. But the observation that appearance of this intermediate population in AND^{tg} GRK2$^{+/-}$ mice was allele-dependent indicated a role for TCR-mediated signaling in this transition and implied a role for GRK2 in this signaling process.

2.9. Stage dependent alterations in thymocyte migration upon reduction in GRK2 expression.

Reduction in GRK2 levels leads to increased migration of mature T lymphocytes (Vroon et al., 2004), most likely caused by less efficient GRK2-dependent desensitization of activated chemokine receptors. The distinct stages of thymocyte differentiation occur at strictly defined location within the thymus and depend on proper migration of the thymocytes to these sites (Petrie., 2003). It was therefore of interest to assess whether reduction in GRK2 expression changed the migratory capacity of thymocytes. CXCR4 is expressed predominantly by DN and DP thymocytes and is downregulated after positive selection (Suzuki et al., 1998). We therefore tested the *in-vitro* migratory response of AND^{tg} GRK2$^{+/+}$ and GRK2$^{+/-}$ thymocytes to the CXCR4 ligand SDF-1α (CXCL12). DN and 4SP GRK2$^{+/-}$ thymocytes migrated more to SDF-1α than the GRK2$^{+/+}$ DN and 4SP thymocytes, but DP GRK2$^{+/-}$ thymocytes migrated consistently less than DP GRK2$^{+/+}$ thymocytes in response to this cytokine (Figure 37 & Table 10). As observed before for mature T cells co-stimulation via the TCR reduced migratory capacity in both GRK2$^{+/+}$ and GRK2$^{+/-}$ thymocytes. (Peacock and Jirik, 1999; Schneider et al., 2009). Together these data showed that a reduction in GRK2 altered the migration capacity of AND^{tg} thymocytes and suggested that GRK2 regulated migration of DP vs DN and 4SP thymocytes in a different manner.

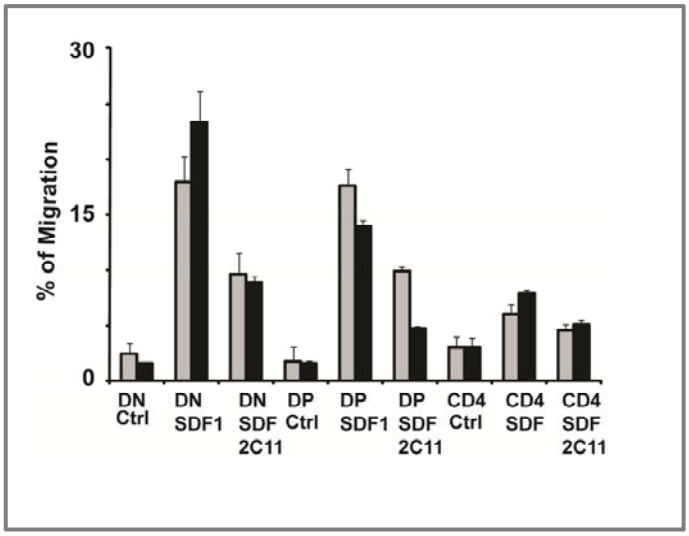

Figure 37: Migration of GRK2+/+ and GRK2+/- AND^{tg} thymocytes in response to SDF-1α. Unfractionated thymocytes suspensions were added to the upper chamber of a transwell plate in presence or absence of the anti-CD3 Ab 2C11. These chambers were then placed in the lower chambers of the transwell plate containing medium with or without SDF-1α. After 3 Hrs, thymocytes of the lower chamber were collected, counted and labelled with anti-CD4 and anti-CD8 antibodies and analysed by flow cytometry. The percentage migration was determined by dividing the absolute number of cells of each population of the lower chamber by the absolute number of these cells in the input population.

Table 10: Migration of GRK2$^{+/+}$ and GRK2$^{+/-}$ thymocytes .Quantification and statistical analysis of relative migration of GRK2$^{+/-}$ thymocytes of each thymocytes subpopulation for each treatment.

Cell population	Conditions	GRK2+/- MIGRATION (Relative to WT)	SD	p Value
DN	Control	80.540	20.140	0.265
	SDF1α	108.470	34.030	0.661
	SDF1α+2C11	74.640	20.850	0.197
DP	Control	91.890	19.750	0.772
	SDF1α	79.800	3.110	**0.018**
	SDF1α+2C11	48.130	16.040	**0.004**
4SP	Control	88.740	45.950	0.673
	SDF1α	146.100	22.830	**0.021**
	SDF1α+2C11	110.000	40.590	0.663

DISCUSSION

DISCUSSION

Section 1

The number and size of oligomeric complexes increases in previously stimulated and memory T cells and provides these cells with increased antigen sensitivity.

The acquired immune system provides its host with “antigenic memory”, permitting a faster and stronger response when reencountering specific pathogens and thereby providing immunity. The capacity to respond stronger and faster upon reencounter is in part the consequence of both an increase in the size of T cell precursor population (Askonas et al., 1982) and a preferential growth of higher affinity T cell clones that will form the memory T cell pool (Busch and Pamer, 1999; Malherbe et al., 2004; Zehn et al., 2009). Memory T cells also convert more rapidly into effector T cells and produce larger amounts of effector molecules (Bachmann et al., 1999; Bruno et al., 1995; Cho et al., 1999; Veiga-Fernandes et al., 2000; Zimmermann et al., 1999). Finally, previously stimulated and memory T cells (‘antigen-experienced’ T cells) are more sensitive to stimulation via their TCR than naive T cells. This has been directly shown by the reduction in the amount of antigen these cells need to give rise to T cell activation (Ericsson et al., 1996; Kimachi et al., 1997; London et al., 2000; Pihlgren et al., 1996; Rogers et al., 2000; Slifka and Whitton, 2001).

The molecular mechanisms underlying the increase in sensitivity of antigen-experienced T cells have not been well defined. The TCR does not undergo somatic hypermutation, thereby excluding affinity maturation as a mechanism. Instead, other molecular changes must be at play. Based on previous observations made in our group we decided to study whether oligomeric TCR complexes might play a role in the increased sensitivity of antigen-experienced T cells. Biochemical and EM analysis of resting T cells and non-stimulated T cell lines had shown that TCR complexes co-exist as monomeric and oligomeric complexes and that the larger oligomeric TCR complexes were preferentially activated upon stimulation of the T cell with low amounts of antigen (Schamel et al., 2005).

We hypothesized that, if oligomeric TCR complexes provided T cells with increased antigen sensitivity, an increase in the number and size of oligomeric complexes should provide higher antigen sensitivity. In a direct comparison of resting with pre-activated and expanded human peripheral blood T lymphocytes and of murine naïve with memory $CD4^+$ T cells, we have shown here that the previously stimulated, antigen experienced T cells indeed have more oligomeric complexes at the cell surface. Similar comparison of naïve and antigen-experienced murine monoclonal ovalbumin-specific T cells has shown an identical change in distribution, correlating with increased antigen-sensitivity of the antigen-experienced T cells (María Férez, Balbino Alarcón and Hisse-Martien van Santen, see accompanying manuscript).

It was previuoly described that soluble bivalent MHC ligands bind better to previously activated mouse $2C^{tg}$ $CD8^+$ T cells than to their naive counterparts (Fahmy et al., 2001). It was suggested that the distribution of TCR changes after stimulation. Our data provide direct evidence that such changes occur in previously stimulated T cells and make it likely that the increase in size of oligomeric

complexes upon stimulation is the mechanism underlying the increase avidity of bivalent pMHC ligands for the TCR complex of these previously stimulated T cells.

Normal differentiation of L19A CD3ζ-expressing OT-1^{tg} T cells.

Oligomeric TCR complexes could play an important role in positive and negative selection, either because of a need of amplification of the signals generated by positively selecting ligands, or by amplifying the signals generated by few negative selection-inducing self-peptides. They might thus either serve as an essential component to make positive selection possible or to provide extra safety in assuring that negative selection and hence generation of a self-tolerant T cell repertoire, is as efficient as possible. In the conditions under which we have studied the OT-1^{tg} model it is a positive selection model. We found no evidence that positive selection is affected by the L19A CD3ζ chain, suggesting that oligomeric T cell complexes play no major role during this process in OT-1^{tg} T cells. Using other positively selecting TCR^{tg} models should permit us to assess whether this is generally true or not, and negative selection models such as the HY model (Kisielow et al., 1988) should allow us to address whether negative selection is compromised by the L19A mutation. Unfortunately we do not know yet whether thymocytes express oligomeric complexes at any stage of their differentiation. The relatively low expression of the TCR on thymocytes and the moderate efficiency of the EM immuno-labeling technique have so far not permitted us to obtain reliable data.

Within the peripheral OT-1^{tg} T cell pool, the role of oligomeric TCR complexes only becomes detectable in the transition from naïve to antigen-experienced T cells, where L19A CD3ζ expressing OT-1^{tg} T cells show less sensitivity towards stimulus than WT CD3ζ expressing cells. This defect in sensitivity coincides with a strong reduction in oligomeric complexes in the cell surface replicas of the L19A CD3ζ expressing cells. Thus oligomeric TCR formation and function could be restricted to antigen experienced T cells.

Mechanisms of oligomeric TCR complex formation

The integrity of oligomeric TCR complexes is strictly dependent on the presence of cholesterol in the cell membrane (Schamel et al., 2005) indicating a key role for the lipid environment. However, protein-protein contacts between adjacent TCR complexes could play a role as well. As previously observed (Schamel et al., 2005) the size of the gold particles used to detect the TCR clusters (10 nm) is in the order of the estimated diameter of the extracellular domains of the TCR and CD3 chains together (~16 nm) (Sun et al., 2004). The spacing between gold particles in the clusters we observed on the cell surface replicas is small enough to be compatible with direct contact between individual TCR complexes.

If protein-protein contacts are indeed necessary for oligomeric TCR complex formation, CD3ζ should be one of the subunits that are directly involved the formation of these complexes. CD3ζ ('A face') could either form heterotypic, L19 dependent interactions with a yet unknown B face or an alternation of homotypic, L19 dependent A-A interactions and B-B interactions (Figure 38) The A-A interaction would reflect the observed ability of the CD3ζ transmembrane domains to form tetramers (Torres et al., 2002). The B face

could be formed primarily by the Cα domain, according to recent findings that the C and F strands of Cα play an important role in the dimerization of TCRαβ heterodimers (Kuhns et al.2010).

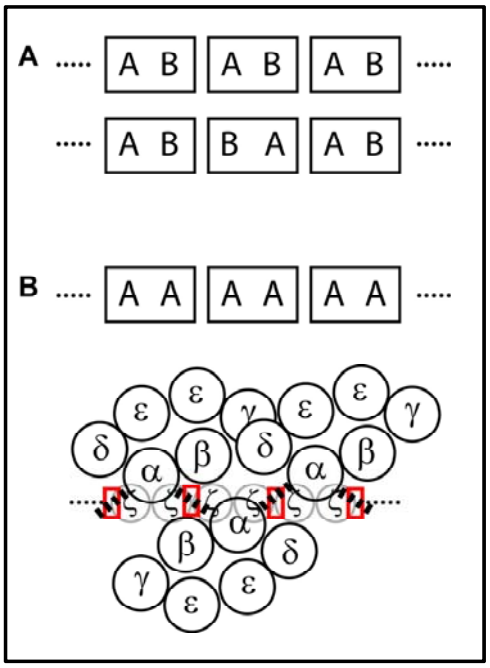

Figure 38: models of CD3ζ-dependent TCR oligomerization A) Oligomerization via a mechanism in which interactions between individual TCR complexes (boxes) are dependent on a heterotypic, L19-dependent interaction between CD3ζ dimers (A-face) and another, not yet defined TCR component (B-face) (top line) or on alternation of homotypic, L19-dependent interactions between CD3ζ dimers and homotypic interactions between the other TCR components (bottom line).
(B). TCR oligomerization mediated by concatenation of homotypic L19-dependent interactions between CD3ζ dimers. This model assumes that due to its symmetry, the CD3ζ dimer can interact on both sides with adjacent CD3ζ dimers. This model is compatible with that of Davis and colleagues (Kuhns et al., 2010), since the A-face could consist of both the Cα ectodomain and the transmembrane domain of CD3ζ. The lower part of the figure provides a hypothetical ordering of the transmembrane regions (circles) of the TCR components indicated, taking into account the proposed orientation of these segments in digitonin-solubilized ER microsomes (Call et al., 2002) and making it compatible withthe data of Davis and colleagues (Kuhns et al., 2010). The red squares indicate theinteraction between the CD3ζ dimers and the dashed lines the interaction face between the ectodomains of Cα

Taking into account the perfect symmetry of the CD3ζ transmembrane domain observed in NMR studies (Call et al., 2006), an oligomeric TCR complex could also be formed by a repetition of L19-dependent symmetrical interactions between CD3ζ dimers, i.e. based exclusively on homotypic interactions. This could even occur in combination with the previously mentioned Cα domain interactions. These interactions must however somehow also depend on cholesterol

Given the importance of cholesterol in oligomeric TCR complex formation, a higher cholesterol and GM gangliosides content in antigen-experienced T cells could thus be an important factor for larger TCR oligomers formation as compared to naïve T cells. Such increases do occur after overnight stimulation of mature $CD4^+$ T cells with anti-TCR antibodies and are stably acquired by in vivo generated memory T cells (Brumeanu et al., 2007; Kersh et al., 2003). Gene expression profiling of naïve, effector and memory cells show up-regulation of some cholesterol transporters and biosynthesis genes (Hashimoto et al., 2003; Holmes et al., 2005). Up-regulation of these genes in response to T cell activation leads to increased cholesterol content in plasma membrane, which could allow formation of more oligomeric TCR complexes.

Oligomeric TCR complexes may increase the avidity of the TCR-MHC interaction and allow signal spreading.

Oligomeric TCRs could provide T cells with increased sensitivity by permitting multivalent TCR-MHC interactions. A number of *in vitro* studies using well-defined soluble monovalent and multivalent MHC/peptide ligands have shown that T cell activation is dependent on interaction with multivalent MHC/peptide ligands (Boniface et al., 1998; Cochran et al., 2000). At the same time, the MHC molecules on the cell surface of APCs have been shown to be able to form clusters,

which may even be enriched for particular antigenic peptides (Anderson et al., 2000; Kropshofer et al., 2002). Stimulation by adjacent MHC molecules presenting identical antigenic peptides does not appear to be an absolute requirement for T cell activation, as soluble bivalent MHC complexes presenting one antigenic peptide in combination with another unrelated peptide can stimulate T cells (Krogsgaard et al., 2005). However, the TCR of the interacting T cell could trigger activation of this T cell, either because the extra strength of interaction provided by the adjacent MHC/peptide complexes allows a sufficiently long time of interaction needed for T cell activation, and/or because concomitant binding of agonistic and non-agonistic pMHC complexes allows spreading of TCR activation from the agonistic pMHC interacting TCR to the adjacent ones. A mechanism for signal spreading could be just be the lateral ITAM phosphorylation within the TCR oligomer by agonist pMHC-dependent Lck recruitment (Schamel et al., 2006). The lateral ITAM phosphorylation would thus be a "passive" mechanism of signal spreading facilitated within TCR oligomers. However, the existence of conformational changes as a mechanism to transmit information on ligand binding to the cytoplasmic tails of the CD3 signaling subunits (Gil et al., 2002) led us to propose that TCR oligomers could allow the existence of an "active" mechanism of signal spreading by permitting the transmission of the active conformation from pMHC-contacted to non-contacted TCRs within the same oligomer (Schamel et al., 2006). Such a cooperativity effect has been recently demonstrated by expressing a conformational inactive mutant of CD3ε in T cells that carry an excess of endogenous wild type CD3ε (Martinez-Martin et al., 2009). Expression of the conformational inactive mutant prevents the adoption of the active conformation by the TCRs containing wild type CD3ε. Therefore, in addition to higher avidity for antigen, derived from the multivalency of TCR oligomers, these provide the possibility of extensive cooperativity between pMHC-engaged and non-engaged TCRs. Accordingly, it would be plausible that previously activated and memory T cells would have increased antigen sensitivity as compared to naïve T cells because more and larger TCR oligomers both increase the chance of a multivalent TCR-MHC interaction and allow for more extensive signal spreading. Thus while antigen-experienced T cells cannot increase their sensitivity via affinity maturation, they achieve this by an avidity maturation mechanism.

Section 2

Search for proteins differentially involved in positive and negative selection using a kinetically controlled model of T cell selection.

Numerous studies have shown the importance of differential signaling via the TCR complex in positive and negative selection, highlighting the role of the MAPK pathways and pro or-anti apoptotic pathways (Bouillet et al., 1999; Bouillet et al., 2002; Dong et al., 2002; McNeil et al., 2005; Sugawara et al., 1998). However we still lack understanding of the molecular mechanism which allows the TCR complex to connect specifically to one or the other of these signaling cascades. Here we set out to discover new proteins implicated in these pathways, by performing a biochemical screen for TCR-associated or differentially

phosphorylated proteins during positive and negative selection, assuming that such differential association or phosphorylation underlies the ability of the TCR to connect to the differential signaling pathways.

The Model

The model we have developed has permitted us to perform a biochemical screen for proteins that interact differentially with the TCR complex or are differentially phosphorylated during positive and negative selection. We reasoned that a biochemical screen should provide complementary information to RNA-based screens for proteins involved in these processes as the RNA screen would not be expected to identify proteins whose expression level does not change during positive and negative selection nor detect proteins that undergo post-translational modifications. Indeed, the expression level of the candidate protein GRK2, whose role in T cell selection we investigated in more detail, did not change under the conditions used in our screen.

The model faithfully reproduces typical phenotypical changes associated with maturation of an MHC class II-restricted T cell clone: progression from DN stage to the DP stage, where the thymocytes upregulate TCR and CD5, and maturation into CD4 single positive thymocytes. An important advantage of the model is that positive selection occurs via the physiological self-MHC complexes. Other models in which T cell differentiation can be halted, such as the OT-1^{tg}x$TAP1^{-/-}$ model (Daniels et al., 2006), generate artificial positively selecting pMHC ligands that may not necessarily represents all the features of the physiological positively selecting pMHC ligands. It shares the advantage with the OT-1^{tg}x$TAP1^{-/-}$ model that peptide-induced negative selection occurs in a mouse in which no peripheral mature T cells are present. The 'bystander' activation of these mature T cells and the concomitant production of cytokines and glucocorticoids have been shown to have profound side effects on the thymocytes, resulting in non-physiological cell death (Martin and Bevan, 1998).

This work shows that the model allows sufficient enrichment for DP thymocytes undergoing positive or negative selection to detect relevant differentially implicated proteins without extensive purification of the DP cells. This permit to maintain the interactions of the thymocytes with the thymic stroma are maintained up to the moment of detergent extraction, which should better preserve any signaling intermediates. For mature T cells it has been shown that this continued contact strongly improves the posterior biochemical detection of signaling intermediates in these cells (Germain et al., 2002). During the optimization of our model we indeed observed better preservation of phosphorylation of p38 and Vav in detergent extracts directly prepared from whole thymus as compared to extracts made after first preparing single cell suspensions (data not shown).

Thus, this new model can generate a large and enriched population of DP thymocytes going synchronously through positive or negative selection under physiological conditions, thereby facilitating biochemical analyses of these processes. It may in principle also serve to study crosstalk between thymocytes and stroma during positive and negative selection.

The candidates

Out of the proteins that showed the clearest changes in TCR association or tyrosine phosphorylation in the array during positive and negative selection, we focused our initial attention on those proteins with no documented role in T cell selection (e.g. GRK2, Pyk2 and Grb7) or proteins known to be implicated in T cell selection but whose mechanism of action in this context was unknown (e.g. PTEN). PTEN is a negative regulator of PI3K and Akt pathway and has been shown to have a role in T cell survival and TCR signaling (Hagenbeek et al., 2004; Wang et al., 2000). A conditional knockout of PTEN shows impaired negative selection (Suzuki et. al. 2001) but the mechanisms of regulation of PTEN activity during positive and negative selection are unknown. The observation that PTEN could be found associated with the TCR and appeared tyrosine phosphorylated during negative selection therefore appeared of interest. The tyrosine kinase PYK2 has been shown to regulate adhesion and motility of various neuronal, epithelial and hematopoietic cell types and has been shown to be phosphorylated by TCR ligation (Collins et al.; Ostergaard and Lysechko, 2005). A role of PYK2 in T cell activation has been reported (Katagiri et al., 2000) and it has been found to translocate to the T cell-APC contact area upon stimulation (Sancho et.al 2002). Grb7 is an adaptor molecule that mediates signal transduction to downstream pathways through various cell surface receptors and has a role in cell migration during tumour progression (Shen and Guan, 2004). However, role of these proteins in context of T cell selection has not been addressed. It should be mentioned that interactions or phosphorylation events detected in the array do not necessarily indicate direct interaction of the candidate molecule with the TCR complex or direct phosphorylation of these proteins, but could reflect the presence of other associating molecules in the immune complexes detected via the array.

We performed an initial series of independent confirmation experiments with the limited panel of candidate protein-specific antibodies available to us. In these pilot experiments the differential association of GRK2 with the TCR complex was most readily confirmed. Apart from this technical reason we thought GRK2 was an interesting candidate to study, given the novelty of its potential implication in T cell selection. Furthermore, while the classical GPCR targets of GRK2, especially the chemokine receptors, play an important roles in thymocyte migration and thus affect T cell differentiation, its more recently described broader roles in interacting with and regulating a variety of proteins such as cSrc, ZAP70, ERK, MEK, p38, GIT and Akt, suggested that it could be intricately linked with a number of other signaling pathways relevant for T cell differentiation.

GRK2-TCR interaction

Our data show that the interaction between GRK2 and the TCR complex occurs in DP and CD4 SP AND^{tg} thymocytes but not in DN thymocytes, even though they express both GRK2 and the AND^{tg} TCR. This suggests that other stage-dependent factors play a role in this association. The pre-TCR could be one such factor, which in this case would prevent interaction. However, the fact that DN thymocytes in AND^{tg} and many other TCR-transgenc mice express αβ TCR already at the

DN stage and effectively displace the pre-TCR, make the pre-TCR an unlikely candidate. We could clearly show that the GRK2 and the TCR dissociate in DP thymocytes upon interaction with negative selection inducing pMHC ligands, and upon stimulation in CD4 SP thymocytes.

After we initiated our studies on GRK2, another group reported that GRK2 interacts with the TCR complex of thymocytes of C57BL/6 mice (DeFord-Watts et al., 2007). In a series of *in-vitro* assays with recombinants proteins the authors clearly showed that GRK2 interacts directly with the intracellular basic rich sequence (BRS) of CD3ε, located between the transmembrane region and the proline-rich sequence (PRS), and not with CD3γ,CD3δ, or CD3ζ. Our ability to visualize the GRK2-TCR association via CD3ζ is therefore most likely due to the interaction of CD3ζ and CD3ε within the TCR complex and does probably not indicate a direct interaction of CD3ζ with GRK2. It is not yet known which domain of GRK2 interacts with the CD3ε BRS.

The same study did not provide evidence in favor or against a differential association of GRK2 with the TCR complex. Immuno-precipitation of detergent extracts prepared from thymocytes suspensions with a stimulatory anti-CD3ε antibody and immunoblotting with GRK2 showed a very weak association (in comparison to the total amount of GRK2), but no direct comparison was shown of the extent of association in non-stimulated and stimulated thymocytes. It is therefore not clear whether the association observed upon treatment with the stimulatory anti-CD3ε antibody is indicative of a constitutive TCR-GRK2 interaction, contrasting with our findings, or whether it represents a small amount of GRK2 that has not dissociated upon antibody binding.

The fact that the GRK2-interacting BRS of CD3ε is directly adjacent to the PRS is interesting in view of possible mechanisms that cause dissociation of GRK2 from the TCR complex. The PRS undergoes a conformational change upon binding of the TCR to agonist and negatively selecting pMHC ligands or anti-TCR antibodies (Gil et al., 2002; Risueno et al., 2005), permitting binding of Nck to the CD3ε chain. Either the conformational change itself or the binding of Nck to the PRS could cause the observed dissociation of GRK2 from the BRS. The recently described mutants of the extracellular stalk region of CD3ε that have been shown to be defective in undergoing the conformational change (Martinez-Martin et al., 2009) should be extremely useful tools to address this potential mechanism of association and dissociation.

GRK2 and thymocyte selection

Given that association between GRK2 and the TCR complex at the DP stage only occurred under conditions of positive selection, we hypothesized that GRK2 may play a more important role in positive selection and less so during negative selection. As a first approach we used $GRK2^{+/-}$ mice (Jaber et al., 1996), in which GRK2 expression is reduced by about 60% and crossed these mice with OT-1 and AND TCR-transgenic mice. It should be mentioned that within this model one would not exclusively measure the role of the interaction between GRK2 and TCR complex but possibly also the role of GRK2 in TCR-independent processes. Indeed, our results show that

GRK2 plays a limiting role in both TCR dependent and independent processes.

In agreement with our hypothesis, in both mouse model studied the DP population of GRK2$^{+/-}$ cells showed reduced upregulation of the TCR which is a known marker of positive selection (Huesmann et al., 1991). In addition, in the AND^{tg} model on the alternative H2^{bb} background, representing weaker ligands for the AND^{tg} TCR (Kaye et al., 1992) a strong decrease in the number of DP and 4SP thymocytes was observed. The increase apoptotic response to *in-vitro* stimulation with CD3-specific antibody was not significantly different from GRK2$^{+/+}$ DP thymocytes in both models, indicating that negative selection was not affected. This indicates that reduction in GRK2 expression has a limiting role in positive selection, while negative selection appears unaffected.

The CD4^{lo}CD8^{lo} population that we observed in AND^{tg} GRK2$^{+/-}$ animals may very well reflect the importance of a GRK2-TCR interaction in the DN to DP transition. We do not yet have formal proof that this population indeed represents a transitional population, which will require purification and adoptive transfer into a recipient mouse. It is however unlikely to represent a population of thymocytes that is downmodulating the CD4 and CD8 receptors upon induction of negative selection: the cells express low amounts of CD69 and are only detected in mice that express generally weaker MHC ligands for the AND TCR. While in our analysis of TCR-GRK2 association in total DN thymocytes we could not detect any association, it is possible that it occurs in fraction of thymocytes that quickly differentiates into DP thymocytes. It has recently been shown by reconstituting CD3ε-deficient mice with CD3ε constructs lacking various intracellular domains that the BRS is crucial for the DN to DP transition (Brodeur et al.,2009b). Our data would indicate that interaction between GRK2 and the TCR via the BRS would be critical for this transition. The fact that the occurrence of this population is MHC haplotype dependent indicates the implication of TCR-mediated signaling and would point out to a direct, quantitative effect of GRK2 on the TCR-dependent signaling pathways. This would coincide with the observed reduction in antigen sensitivity of the AND^{tg} DP thymocytes in vitro.

While positive selection is a TCR-signaling dependent process, suggesting that GRK2 is directly implicated in TCR-mediated signaling, we also checked the response of GRK2$^{+/-}$ thymocytes in the TCR mediated processes of TCR downmodulation (Bachmann et al., 1997; Hemmer et al., 1998; Valitutti et al., 1995) and CD69 upregulation (Testi et al., 1994). We observed a marked reduction in both TCR downmodulation and CD69 upregulation in GRK2$^{+/-}$ thymocytes compared to GRK2$^{+/+}$, again indicating that GRK2 is a limiting factor in these TCR-signaling dependent processes. The reduction was specifically observed in DP thymocytes, while CD4 SP thymocytes and CD4^{+} T cells of both genotypes responded equally. The reasons for this stage specific reduction have not yet been clarified. It could be caused by the lower expression level of the TCR at the DP stage as compared to the 4SP and CD4^{+} stage, making the signaling via the TCR more sensitive to small changes in downstream pathways or it could reflect differences in the wiring of the TCR complex at these stages. Detailed biochemical analysis of the role of GRK2 in TCR mediated signaling may resolve

this issue. Comparison of our kinetically controllable TANDRAG model on $GRK2^{+/+}$ and $GRK2^{+/-}$ background should facilitate such biochemical analysis. In addition analysis of TCR-mediated signaling in T cell lines in which GRK2 is knocked-down by interfering RNA construct should be a powerful complementary approach.

Thymocyte migration, an integral part of thymocyte differentiation, was also affected in $GRK2^{+/-}$ mice. Previous reports described that mature $GRK2^{+/-}$ T cells migrated more than $GRK2^{+/+}$ T cells towards CCL4, probably due to a reduced GRK2-mediated phosphorylation of the activated CCR5 chemokine receptor (Vroon et al., 2004). *In-vitro* assay of SDF-1α induced migration showed the same effect in $AND^{tg}GRK2^{+/-}$ thymocytes. However, in DP thymocytes we observed the opposite effect: $GRK2^{+/-}$ thymocytes migrated less. One possible explanation for this apparent contradiction may come from the recent observation that CXCR4, the predominant receptor for SDF-1α uses TCR-associated signaling molecules for SDF-1α induced signaling and migration in mature T cells (Kumar et al., 2006; Schneider et al., 2009) and DN thymocytes (Janas et al.;2010 Trampont et al.,2010). We hypothesize that in DP thymocytes GRK2 is implicated in the convergence of the CXCR4 and TCR signaling pathways, which seems reasonable given the observed association between GRK2 and the TCR reported here and in the literature (DeFord-Watts et al., 2007) (Figure 28). This GRK2-dependent convergence of the two signaling pathways would cause a mutual amplification of the signals transmitted via the CXCR4- and TCR-dependent pathways. Under conditions of positive selection, a reduction in the amount of GRK2, as occurs in the $GRK2^{+/-}$ mice, would reduce signaling capacity of both the TCR complex and the CXCR4 receptor. Given the relatively weak activation of the signaling pathways downstream of the TCR by positively selecting ligands, positive selection would be quite dependent on input by the CXCR4 receptor pathway and a reduction in this input in $GRK2^{+/-}$ mice would cause less efficient positive selection. Vice versa, migration would be reduced as well, by the reduced efficiency of GRK2-dependent coupling of the CXCR4-signaling pathway to the TCR signaling pathway. In case of stimulation by negatively selecting ligands, GRK2 dissociates from the TCR complex and would thereby inactivate the CXCR4-dependent pro-migratory signals and would cause the thymocytes to stop. This would be useful to allow the thymocytes to halt long enough next to the stromal cells presenting the negatively selecting ligands and to allow sufficient time of interaction to fully activate the negative selection program. Under these conditions the role of GRK2 in promoting CXCR4- and TCR-dependent signaling has been lost due to its dissociation from the TCR. TCR-mediated signaling events are strong enough to independently induce negative selection. A reduction in the amount of GRK2 would therefore have no effect on negative selection or migration. Interestingly, signaling via CXCR4 has also been implicated in transmission of survival signals via the pre-TCR complex (Hernandez-Lopez et al., 2002; Trampont et al.). While such a role has not been established for CXCR4- mediated signaling in DP thymocytes, it is striking that we observe a slight increase in spontaneous apoptosis in $GRK2^{+/-}$ AND^{tg} thymocytes as compared to $GRK2^{+/+}$ thymocytes.

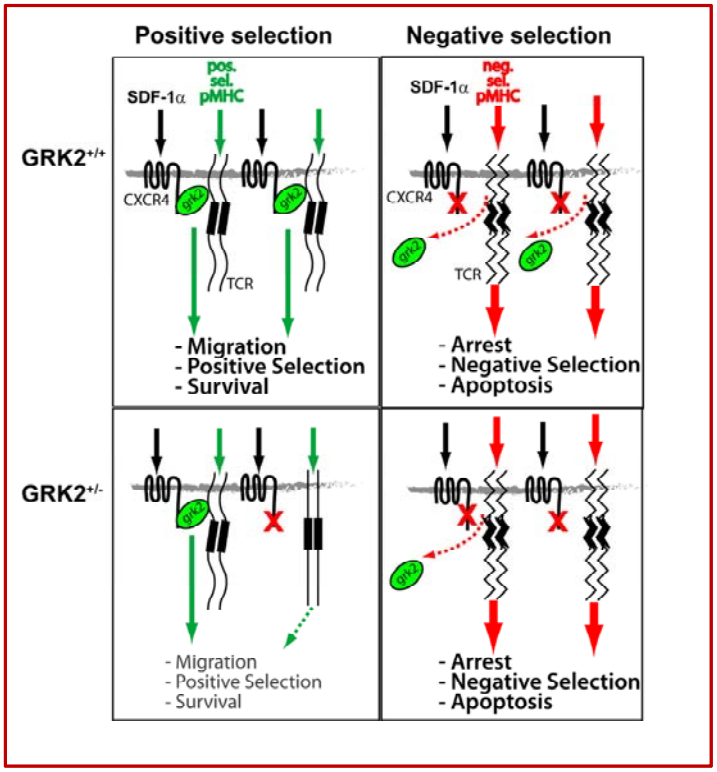

Figure 39: GRK2-dependent integration of the CXCR4 and TCR signaling pathways in DP thymocytes. The model assumes that GRK2-mediated integration of the TCR and CXCR4 signaling pathways is a limiting factor in the generation of signals necessary for positive selection, migration and survival. Given its dissociation from the TCR during negative selection, such an integrating role for GRK2 does not exist under these conditions. See main text for details.

Thus, part of the role of GRK2 could be to provide DP thymocytes with survival signals (Figure 39) and less efficient generation of these signals could be one of the underlying causes for the reduced efficiency of positive selection we observed in GRK2$^{+/-}$ animals.

The model is not directly applicable to 4SP thymocytes, as we observe the opposite effects of GRK2 reduction on migration and no effect on antigen sensitivity. We do not know what causes this difference, but the observation itself suggests that the interaction of GRK2 with the TCR and CXCR4 signaling machinery is quantitatively or qualitatively different in DP and 4SP thymocytes.

Finally GRK2$^{+/-}$ thymocytes show less efficient CD69 downregulation at the SP stage. Downregulation of CD69 is a prerequisite for thymic egress (Feng et al., 2002) and is mediated in conjunction with the S1P1 receptor (Alfonso et al., 2006). The S1P1 receptor is a direct target for GRK2 (Watterson et al., 2002) and the CD69 phenotype we observe is probably a reflection of the CD69-S1P1 receptor interaction. As far as known, TCR signaling is not involved in this maturation step and we speculate that the phenotype observed would be independent of GRK2-TCR interaction.

Together, the data show that a reduction in GRK2 affects the TCR-signaling dependent processes of upregulation of the TCR at the DP stage during positive selection. CD69 induction and TCR downmodulation in DP thymocytes as well as migration in DP and 4SP thymocytes affected as well. Whether this indicates a direct effect of GRK2 on TCR dependent signaling or whether it reflects an indirect effect via the apparent interwinement between chemokine recptor mediated signaling pathways and the TCR-mediated signaling pathways remains to be established.

CONCLUSIONS

CONCLUSIONS

1) Antigen experienced T cells express more and larger oligomeric TCR complexes on the cell surface than naive T cells.

2) A mutation of alanine to leucine at 19th position of the CD3ζ transmembrane domain impairs formation of oligomeric TCR complexes in a T hybridoma, without affecting assembly of the TCR complex or its level of expression at the cell surface.

3) Impairment in formation of oligomeric TCR complexes in the T hybridoma expressing the mutant CD3ζ chain results in decreased sensitivity towards antigen, showing that oligomeric TCR complexes provide increased antigen sensitivity.

4) Bone marrow precursors expressing the mutant CD3ζ chain permit normal T cell differentiation and naive T cell generation of a TCR-transgenic clone *in-vivo*, suggesting a minor or non-existent contribution of oligomeric complexes in these processes.

5) Primary TCR-transgenic T cells expressing the mutant CD3ζ chain show a normal primary T cell response, but respond worse than their wild type CD3ζ expressing counterparts to secondary stimulation. This coincides with a reduction in the size and number of oligomeric TCR complexes on these cells, showing that oligomeric TCR complexes are also responsible for increased antigen sensitivity in antigen experienced primary T cells.

6) GRK2 associates with the TCR complex in DP thymocytes only under conditions of positive selection.

7) OT-1^{tg} and AND^{tg} thymocytes with reduced GRK2 expression show less efficient upregulation of the TCR at the DP stage, suggesting that positive selection is less efficient and that GRK2 plays a role in this differentiation step.

8) AND^{tg} $GRK2^{+/-}$ DP thymocytes have decreased antigen sensitivity *in-vitro*, implicating a role for GRK2 in TCR-mediated signaling.

9) A $CD4^{lo}CD8^{lo}TCR^{lo}CD69^{lo}$ thymocyte population is present in AND^{tg} mice with reduced GRK2 expression and weaker positively selecting MHC ligands. This suggests that GRK2 plays a role in the transition of AND^{tg} thymocytes from the DN to DP stage

10) Reduction of GRK2 expression has opposite effects on the migration capacity of AND^{tg} DP and 4SP thymocytes towards SDF-1α, indicating differences in GRK2-dependent regulation of this process in both populations. TCR co-stimulation reduces migration in both populations, showing that the TCR signaling pathway interacts in both populations with the SDF-1α induced signaling pathway.

BIBLIOGRAPHY

BIBLIOGRAPHY

Alam, S.M., Davies, G.M., Lin, C.M., Zal, T., Nasholds, W., Jameson, S.C., Hogquist, K.A., Gascoigne, N.R., and Travers, P.J. (1999). Qualitative and quantitative differences in T cell receptor binding of agonist and antagonist ligands. Immunity *10*, 227-237.

Alarcon, B., Berkhout, B., Breitmeyer, J., and Terhorst, C. (1988). Assembly of the human T cell receptor-CD3 complex takes place in the endoplasmic reticulum and involves intermediary complexes between the CD3-gamma.delta.epsilon core and single T cell receptor alpha or beta chains. J Biol Chem *263*, 2953-2961.

Alarcon, B., Ley, S.C., Sanchez-Madrid, F., Blumberg, R.S., Ju, S.T., Fresno, M., and Terhorst, C. (1991). The CD3-gamma and CD3-delta subunits of the T cell antigen receptor can be expressed within distinct functional TCR/CD3 complexes. Embo J *10*, 903-912.

Alarcon, B., Swamy, M., van Santen, H.M., and Schamel, W.W. (2006). T-cell antigen-receptor stoichiometry: pre-clustering for sensitivity. EMBO Rep *7*, 490-495.

Alexander, J., Payne, J.A., Murray, R., Frelinger, J.A., and Cresswell, P. (1989). Differential transport requirements of HLA and H-2 class I glycoproteins. Immunogenetics *29*, 380-388.

Alfonso, C., McHeyzer-Williams, M.G., and Rosen, H. (2006). CD69 down-modulation and inhibition of thymic egress by short- and long-term selective chemical agonism of sphingosine 1-phosphate receptors. Eur J Immunol *36*, 149-159.

Allende, M.L., Dreier, J.L., Mandala, S., and Proia, R.L. (2004). Expression of the sphingosine 1-phosphate receptor, S1P1, on T-cells controls thymic emigration. J Biol Chem *279*, 15396-15401.

Anderson, H.A., Hiltbold, E.M., and Roche, P.A. (2000). Concentration of MHC class II molecules in lipid rafts facilitates antigen presentation. Nat Immunol *1*, 156-162.

Ara, T., Itoi, M., Kawabata, K., Egawa, T., Tokoyoda, K., Sugiyama, T., Fujii, N., Amagai, T., and Nagasawa, T. (2003). A role of CXC chemokine ligand 12/stromal cell-derived factor-1/pre-B cell growth stimulating factor and its receptor CXCR4 in fetal and adult T cell development in vivo. J Immunol *170*, 4649-4655.

Arnett, K.L., Harrison, S.C., and Wiley, D.C. (2004). Crystal structure of a human CD3-epsilon/delta dimer in complex with a UCHT1 single-chain antibody fragment. Proc Natl Acad Sci U S A *101*, 16268-16273.

Ashton-Rickardt, P.G., Bandeira, A., Delaney, J.R., Van Kaer, L., Pircher, H.P., Zinkernagel, R.M., and Tonegawa, S. (1994). Evidence for a differential avidity model of T cell selection in the thymus. Cell *76*, 651-663.

Askonas, B.A., Mullbacher, A., and Ashman, R.B. (1982). Cytotoxic T-memory cells in virus infection and the specificity of helper T cells. Immunology *45*, 79-84.

Bachmann, M.F., Barner, M., Viola, A., and Kopf, M. (1999). Distinct kinetics of cytokine production and cytolysis in effector and memory T cells after viral infection. Eur J Immunol *29*, 291-299.

Bachmann, M.F., Oxenius, A., Speiser, D.E., Mariathasan, S., Hengartner, H., Zinkernagel, R.M., and Ohashi, P.S. (1997). Peptide-induced T cell receptor down-regulation on naive T cells predicts agonist/partial agonist properties and strictly correlates with T cell activation. Eur J Immunol *27*, 2195-2203.

Boniface, J.J., Rabinowitz, J.D., Wulfing, C., Hampl, J., Reich, Z., Altman, J.D., Kantor, R.M., Beeson, C., McConnell, H.M., and Davis, M.M. (1998). Initiation of signal transduction through the T

cell receptor requires the multivalent engagement of peptide/MHC ligands [corrected]. Immunity *9*, 459-466.

Bouillet, P., Metcalf, D., Huang, D.C., Tarlinton, D.M., Kay, T.W., Kontgen, F., Adams, J.M., and Strasser, A. (1999). Proapoptotic Bcl-2 relative Bim required for certain apoptotic responses, leukocyte homeostasis, and to preclude autoimmunity. Science *286*, 1735-1738.

Bouillet, P., Purton, J.F., Godfrey, D.I., Zhang, L.C., Coultas, L., Puthalakath, H., Pellegrini, M., Cory, S., Adams, J.M., and Strasser, A. (2002). BH3-only Bcl-2 family member Bim is required for apoptosis of autoreactive thymocytes. Nature *415*, 922-926.

Brodeur, J.F., Li, S., Damlaj, O., and Dave, V.P. (2009a). Expression of fully assembled TCR-CD3 complex on double positive thymocytes: synergistic role for the PRS and ER retention motifs in the intra-cytoplasmic tail of CD3epsilon. Int Immunol *21*, 1317-1327.

B**rodeur, J.F., Li, S., Martins Mda, S., Larose, L., and Dave, V.P. (2009b).** Critical and multiple roles for the CD3epsilon intracytoplasmic tail in double negative to double positive thymocyte differentiation. J Immunol *182*, 4844-4853.

Brumeanu, T.D., Preda-Pais, A., Stoica, C., Bona, C., and Casares, S. (2007). Differential partitioning and trafficking of GM gangliosides and cholesterol-rich lipid rafts in thymic and splenic CD4 T cells. Mol Immunol *44*, 530-540.

Bruno, L., Kirberg, J., and von Boehmer, H. (1995). On the cellular basis of immunological T cell memory. Immunity *2*, 37-43.

Budd, R.C., Cerottini, J.C., Horvath, C., Bron, C., Pedrazzini, T., Howe, R.C., and MacDonald, H.R. (1987). Distinction of virgin and memory T lymphocytes. Stable acquisition of the Pgp-1 glycoprotein concomitant with antigenic stimulation. J Immunol *138*, 3120-3129.

Busch, D.H., and Pamer, E.G. (1999). T cell affinity maturation by selective expansion during infection. J Exp Med *189*, 701-710.

Call, M.E., Pyrdol, J., Wiedmann, M., and Wucherpfennig, K.W. (2002). The organizing principle in the formation of the T cell receptor-CD3 complex. Cell *111*, 967-979.

Call, M.E., Schnell, J.R., Xu, C., Lutz, R.A., Chou, J.J., and Wucherpfennig, K.W. (2006). The structure of the zetazeta transmembrane dimer reveals features essential for its assembly with the T cell receptor. Cell *127*, 355-368.

Campbell JJ, P.J., Butcher EC. (1999). Cutting edge: Developmental switches in chemokine responses during T cell maturation. JImmunol *163*, 2353-2357.

Cant, S.H., and Pitcher, J.A. (2005). G protein-coupled receptor kinase 2-mediated phosphorylation of ezrin is required for G protein-coupled receptor-dependent reorganization of the actin cytoskeleton. Mol Biol Cell *16*, 3088-3099.

Cantrell, D.A. (2002). Transgenic analysis of thymocyte signal transduction. Nat Rev Immunol *2*, 20-27.

Carman, C.V., Parent, J.L., Day, P.W., Pronin, A.N., Sternweis, P.M., Wedegaertner, P.B., Gilman, A.G., Benovic, J.L., and Kozasa, T. (1999). Selective regulation of Galpha(q/11) by an RGS domain in the G protein-coupled receptor kinase, GRK2. J Biol Chem *274*, 34483-34492
.

Carramolino, L., Zaballos, A., Kremer, L., Villares, R., Martin, P., Ardavin, C., Martinez, A.C., and Marquez, G. (2001). Expression of CCR9 beta-chemokine receptor is modulated in thymocyte differentiation and is selectively maintained in CD8(+) T cells from secondary lymphoid organs. Blood *97*, 850-857.

Chandok, M.R., and Farber, D.L. (2004). Signaling control of memory T cell generation and function. Semin Immunol *16*, 285-293.

Cho, B.K., Wang, C., Sugawa, S., Eisen, H.N., and Chen, J. (1999). Functional differences between memory and naive CD8 T cells. Proc Natl Acad Sci U S A *96*, 2976-2981.
Choudhuri, K., and van der Merwe, P.A. (2007). Molecular mechanisms involved in T cell receptor triggering. Semin Immunol *19*, 255-261.

Chuang, T.T., Sallese, M., Ambrosini, G., Parruti, G., and De Blasi, A. (1992). High expression of beta-adrenergic receptor kinase in human peripheral blood leukocytes. Isoproterenol and platelet activating factor can induce kinase translocation. J Biol Chem *267*, 6886-6892.

Clevers, H., Alarcon, B., Wileman, T., and Terhorst, C. (1988). The T cell receptor/CD3 complex: a dynamic protein ensemble. Annu Rev Immunol *6*, 629-662.

Cochran, J.R., Aivazian, D., Cameron, T.O., and Stern, L.J. (2001). Receptor clustering and transmembrane signaling in T cells. Trends Biochem Sci *26*, 304-310.

Cochran, J.R., Cameron, T.O., and Stern, L.J. (2000). The relationship of MHC-peptide binding and T cell activation probed using chemically defined MHC class II oligomers. Immunity *12*, 241-250.

Collins, M., Tremblay, M., Chapman, N., Curtiss, M., Rothman, P.B., and Houtman, J.C. The T cell receptor-mediated phosphorylation of Pyk2 tyrosines 402 and 580 occurs via a distinct mechanism than other receptor systems. J Leukoc Biol *87*, 691-701.

Cong, M., Perry, S.J., Hu, L.A., Hanson, P.I., Claing, A., and Lefkowitz, R.J. (2001a). Binding of the beta2 adrenergic receptor to N-ethylmaleimide-sensitive factor regulates receptor recycling. J Biol Chem *276*, 45145-45152.

Cong, M., Perry, S.J., Lin, F.T., Fraser, I.D., Hu, L.A., Chen, W., Pitcher, J.A., Scott, J.D., and Lefkowitz, R.J. (2001b). Regulation of membrane targeting of the G protein-coupled receptor kinase 2 by protein kinase A and its anchoring protein AKAP79. J Biol Chem *276*, 15192-15199.

Cosson, P., Lankford, S.P., Bonifacino, J.S., and Klausner, R.D. (1991). Membrane protein association by potential intramembrane charge pairs. Nature *351*, 414-416.

Croxford, A.L., Akilli-Ozturk, O., Rieux-Laucat, F., Forster, I., Waisman, A., and Buch, T. (2008). MHC-restricted T cell receptor signaling is required for alpha beta TCR replacement of the pre T cell receptor. Eur J Immunol *38*, 391-399.

Cumano A, Godin I. (2007) Ontogeny of the hematopoietic system. Annu Rev Immunol.;25:745-85.

Danielian, S., Fagard, R., Alcover, A., Acuto, O., and Fischer, S. (1989). The lymphocyte-specific protein tyrosine kinase p56lck is hyperphosphorylated on serine and tyrosine residues within minutes after activation via T cell receptor or CD2. Eur J Immunol *19*, 2183-2189.

Daniels, M.A., and Jameson, S.C. (2000). Critical role for CD8 in T cell receptor binding and activation by peptide/major histocompatibility complex multimers. J Exp Med *191*, 335-346.

Daniels, M.A., Teixeiro, E., Gill, J., Hausmann, B., Roubaty, D., Holmberg, K., Werlen, G., Hollander, G.A., Gascoigne, N.R., and Palmer, E. (2006). Thymic selection threshold defined by compartmentalization of Ras/MAPK signaling. Nature *444*, 724-729.

Davis, M.M., Boniface, J.J., Reich, Z., Lyons, D., Hampl, J., Arden, B., and Chien, Y. (1998). Ligand recognition by alpha beta T cell receptors. Annu Rev Immunol *16*, 523-544.

Davis, S.J., and van der Merwe, P.A. (2006). The kinetic-segregation model: TCR triggering and beyond. Nat Immunol *7*, 803-809.

De Blasi, A., Parruti, G., and Sallese, M. (1995). Regulation of G protein-coupled receptor kinase subtypes in activated T lymphocytes. Selective increase of beta-adrenergic receptor kinase 1 and 2. J Clin Invest *95*, 203-210.

DebBurman, S.K., Ptasienski, J., Boetticher, E., Lomasney, J.W., Benovic, J.L., and Hosey, M.M. (1995). Lipid-mediated regulation of G protein-coupled receptor kinases 2 and 3. J Biol Chem *270*, 5742-5747.

DeFord-Watts, L.M., Young, J.A., Pitcher, L.A., and van Oers, N.S. (2007). The membrane-proximal portion of CD3 epsilon associates with the serine/threonine kinase GRK2. J Biol Chem *282*, 16126-16134.

DeJarnette, J.B., Sommers, C.L., Huang, K., Woodside, K.J., Emmons, R., Katz, K., Shores, E.W., and Love, P.E. (1998). Specific requirement for CD3epsilon in T cell development. Proc Natl Acad Sci U S A *95*, 14909-14914.

Delgado, P., and Alarcon, B. (2005). An orderly inactivation of intracellular retention signals controls surface expression of the T cell antigen receptor. J Exp Med *201*, 555-566.

Dietrich, J., Kastrup, J., Lauritsen, J.P., Menne, C., von Bulow, F., and Geisler, C. (1999). TCRzeta is transported to and retained in the Golgi apparatus independently of other TCR chains: implications for TCR assembly. Eur J Immunol *29*, 1719-1728.

Dong, C., Davis, R.J., and Flavell, R.A. (2002). MAP kinases in the immune response. Annu Rev Immunol *20*, 55-72.

Dower, N.A., Stang, S.L., Bottorff, D.A., Ebinu, J.O., Dickie, P., Ostergaard, H.L., and Stone, J.C. (2000). RasGRP is essential for mouse thymocyte differentiation and TCR signaling. Nat Immunol *1*, 317-321.

Eastman, S., Deftos, M., DeRoos, P.C., Hsu, D.H., Teyton, L., Braunstein, N.S., Hackett, C.J., and Rudensky, A. (1996). A study of complexes of class II invariant chain peptide: major histocompatibility complex class II molecules using a new complex-specific monoclonal antibody. Eur J Immunol *26*, 385-393.

Ehrlich, L.I., Oh, D.Y., Weissman, I.L., and Lewis, R.S. (2009). Differential contribution of chemotaxis and substrate restriction to segregation of immature and mature thymocytes. Immunity *31*, 986-998.

Elorza, A., Penela, P., Sarnago, S., and Mayor, F., Jr. (2003). MAPK-dependent degradation of G protein-coupled receptor kinase 2. J Biol Chem *278*, 29164-29173.

Elorza, A., Sarnago, S., and Mayor, F., Jr. (2000). Agonist-dependent modulation of G protein-coupled receptor kinase 2 by mitogen-activated protein kinases. Mol Pharmacol *57*, 778-783.

Ericsson, P.O., Orchansky, P.L., Carlow, D.A., and Teh, H.S. (1996). Differential activation of phospholipase C-gamma 1 and mitogen-activated protein kinase in naive and antigen-primed CD4 T cells by the peptide/MHC ligand. J Immunol *156*, 2045-2053.

Exley, M., Wileman, T., Mueller, B., and Terhorst, C. (1995). Evidence for multivalent structure of T-cell antigen receptor complex. Mol Immunol *32*, 829-839.

Fahmy, T.M., Bieler, J.G., Edidin, M., and Schneck, J.P. (2001). Increased TCR avidity after T cell activation: a mechanism for sensing low-density antigen. Immunity *14*, 135-143.

Feng, C., Woodside, K.J., Vance, B.A., El-Khoury, D., Canelles, M., Lee, J., Gress, R., Fowlkes, B.J., Shores, E.W., and Love, P.E. (2002). A potential role for CD69 in thymocyte emigration. Int Immunol *14*, 535-544.

Fernandez-Miguel, G., Alarcon, B., Iglesias, A., Bluethmann, H., Alvarez-Mon, M., Sanz, E., and de la Hera, A. (1999). Multivalent structure of an alphabetaT cell receptor. Proc Natl Acad Sci U S A *96*, 1547-1552.

Fooksman, D.R., Gronvall, G.K., Tang, Q., and Edidin, M. (2006). Clustering class I MHC modulates sensitivity of T cell recognition. J Immunol *176*, 6673-6680.

Garbe, A.I., Krueger, A., Gounari, F., Zuniga-Pflucker, J.C., and von Boehmer, H. (2006). Differential synergy of Notch and T cell receptor signaling determines alphabeta versus gammadelta lineage fate. J Exp Med *203*, 1579-1590.

Garman, R.D., Doherty, P.J., and Raulet, D.H. (1986a). Diversity, rearrangement, and expression of murine T cell gamma genes. Cell *45*, 733-742.

Garman, R.D., Ko, J.L., Vulpe, C.D., and Raulet, D.H. (1986b). T-cell receptor variable region gene usage in T-cell populations. Proc Natl Acad Sci U S A *83*, 3987-3991.
Germain, R.N., Stefanova, I., and Dorfman, J. (2002). Self-recognition and the regulation of CD4+ T cell survival. Adv Exp Med Biol *512*, 97-105.

Gil, D., Schamel, W.W., Montoya, M., Sanchez-Madrid, F., and Alarcon, B. (2002). Recruitment of Nck by CD3 epsilon reveals a ligand-induced conformational change essential for T cell receptor signaling and synapse formation. Cell *109*, 901-912.

Gil, D., Schrum, A.G., Alarcon, B., and Palmer, E. (2005). T cell receptor engagement by peptide-MHC ligands induces a conformational change in the CD3 complex of thymocytes. J Exp Med *201*, 517-522.

Gluzman, Y. (1981). SV40-transformed simian cells support the replication of early SV40 mutants. Cell *23*, 175-182.

Gong, Q., Cheng, A.M., Akk, A.M., Alberola-Ila, J., Gong, G., Pawson, T., and Chan, A.C. (2001). Disruption of T cell signaling networks and development by Grb2 haploid insufficiency. Nat Immunol *2*, 29-36.

Graham, F.L., Smiley, J., Russell, W.C., and Nairn, R. (1977). Characteristics of a human cell line transformed by DNA from human adenovirus type 5. J Gen Virol *36*, 59-74.

Gros, R., Tan, C.M., Chorazyczewski, J., Kelvin, D.J., Benovic, J.L., and Feldman, R.D. (1999). G-protein-coupled receptor kinase expression in hypertension. Clin Pharmacol Ther *65*, 545-551.

Habu, S., Kimura, M., Katsuki, M., Hioki, K., and Nomura, T. (1987). Correlation of T cell receptor gene rearrangements to T cell surface antigen expression and to serum immunoglobulin level in scid mice. Eur J Immunol *17*, 1467-1471.

Hagenbeek, T.J., Naspetti, M., Malergue, F., Garcon, F., Nunes, J.A., Cleutjens, K.B., Trapman, J., Krimpenfort, P., and Spits, H. (2004). The loss of PTEN allows TCR alphabeta lineage thymocytes to bypass IL-7 and Pre-TCR-mediated signaling. J Exp Med *200*, 883-894.

Haks, M.C., Krimpenfort, P., Borst, J., and Kruisbeek, A.M. (1998). The CD3gamma chain is essential for development of both the TCRalphabeta and TCRgammadelta lineages. Embo J *17*, 1871-1882.

Hansen, J.L., Theilade, J., Haunso, S., and Sheikh, S.P. (2004). Oligomerization of wild type and nonfunctional mutant angiotensin II type I receptors inhibits galphaq protein signaling but not ERK activation. J Biol Chem *279*, 24108-24115.

Hashimoto, S., Nagai, S., Sese, J., Suzuki, T., Obata, A., Sato, T., Toyoda, N., Dong, H.Y., Kurachi, M., Nagahata, T., *et al.* (2003). Gene expression profile in human leukocytes. Blood *101*, 3509-3513.

Hellwig, S., Schamel, W.W., Pflugfelder, U., Gerlich, B., and Weltzien, H.U. (2005). Differences in pairing and cluster formation of T cell receptor alpha- and beta-chains in T cell clones and fusion hybridomas. Immunobiology *210*, 685-694.

Hemmer, B., Stefanova, I., Vergelli, M., Germain, R.N., and Martin, R. (1998). Relationships among TCR ligand potency, thresholds for effector function elicitation, and the quality of early signaling events in human T cells. J Immunol *160*, 5807-5814.

Hernandez-Lopez, C., Varas, A., Sacedon, R., Jimenez, E., Munoz, J.J., Zapata, A.G., and Vicente, A. (2002). Stromal cell-derived factor 1/CXCR4 signaling is critical for early human T-cell development. Blood *99*, 546-554.

Hogquist, K.A., Baldwin, T.A., and Jameson, S.C. (2005). Central tolerance: learning self-control in the thymus. Nat Rev Immunol *5*, 772-782.

Hogquist, K.A., Jameson, S.C., Heath, W.R., Howard, J.L., Bevan, M.J., and Carbone, F.R. (1994). T cell receptor antagonist peptides induce positive selection. Cell *76*, 17-27.

Holmes, S., He, M., Xu, T., and Lee, P.P. (2005). Memory T cells have gene expression patterns intermediate between naive and effector. Proc Natl Acad Sci U S A *102*, 5519-5523.
Hou, X., Dietrich, J., Kuhlmann, J., Wegener, A.M., and Geisler, C. (1994). Structure of the T cell receptor in a Ti alpha V beta 2, alpha V beta 8- positive T cell line. Eur J Immunol *24*, 1228-1233.

Huesmann, M., Scott, B., Kisielow, P., and von Boehmer, H. (1991). Kinetics and efficacy of positive selection in the thymus of normal and T cell receptor transgenic mice. Cell *66*, 533-540.

Irles, C., Symons, A., Michel, F., Bakker, T.R., van der Merwe, P.A., and Acuto, O. (2003). CD45 ectodomain controls interaction with GEMs and Lck activity for optimal TCR signaling. Nat Immunol *4*, 189-197.

Irvine, D.J., Purbhoo, M.A., Krogsgaard, M., and Davis, M.M. (2002). Direct observation of ligand recognition by T cells. Nature *419*, 845-849.

Jaber, M., Koch, W.J., Rockman, H., Smith, B., Bond, R.A., Sulik, K.K., Ross, J., Jr., Lefkowitz, R.J., Caron, M.G., and Giros, B. (1996). Essential role of beta-adrenergic receptor kinase 1 in cardiac development and function. Proc Natl Acad Sci U S A *93*, 12974-12979.

Janas, M.L., Varano, G., Gudmundsson, K., Noda, M., Nagasawa, T., and Turner, M.(2010) Thymic development beyond beta-selection requires phosphatidylinositol 3-kinase activation by CXCR4. J Exp Med *207*, 247-261, S241-242.

Jimenez-Sainz, M.C., Murga, C., Kavelaars, A., Jurado-Pueyo, M., Krakstad, B.F., Heijnen, C.J., Mayor, F., Jr., and Aragay, A.M. (2006). G protein-coupled receptor kinase 2 negatively regulates chemokine signaling at a level downstream from G protein subunits. Mol Biol Cell *17*, 25-31.

Katagiri, T., Takahashi, T., Sasaki, T., Nakamura, S., and Hattori, S. (2000). Protein-tyrosine kinase Pyk2 is involved in interleukin-2 production by Jurkat T cells via its tyrosine 402. J Biol Chem *275*, 19645-19652.

Kaye, J., Hsu, M.L., Sauron, M.E., Jameson, S.C., Gascoigne, N.R., and Hedrick, S.M. (1989). Selective development of CD4+ T cells in transgenic mice expressing a class II MHC-restricted antigen receptor. Nature *341*, 746-749.

Kaye, J., Porcelli, S., Tite, J., Jones, B., and Janeway, C.A., Jr. (1983). Both a monoclonal antibody and antisera specific for determinants unique to individual cloned helper T cell lines can substitute for antigen and antigen-presenting cells in the activation of T cells. J Exp Med *158*, 836-856.

Kaye, J., Vasquez, N.J., and Hedrick, S.M. (1992). Involvement of the same region of the T cell antigen receptor in thymic selection and foreign peptide recognition. J Immunol *148*, 3342-3353.
Kersh, E.N., Kaech, S.M., Onami, T.M., Moran, M., Wherry, E.J., Miceli, M.C., and Ahmed, R. (2003). TCR signal transduction in antigen-specific memory CD8 T cells. J Immunol *170*, 5455-5463.

Kersh, G.J., Kersh, E.N., Fremont, D.H., and Allen, P.M. (1998). High- and low-potency ligands with similar affinities for the TCR: the importance of kinetics in TCR signaling. Immunity *9*, 817-826.

Kimachi, K., Croft, M., and Grey, H.M. (1997). The minimal number of antigen-major histocompatibility complex class II complexes required for activation of naive and primed T cells. Eur J Immunol *27*, 3310-3317.

Kishimoto, H., Surh, C.D., and Sprent, J. (1995). Upregulation of surface markers on dying thymocytes. J Exp Med *181*, 649-655.

Kisielow, P., Bluthmann, H., Staerz, U.D., Steinmetz, M., and von Boehmer, H. (1988). Tolerance in T-cell-receptor transgenic mice involves deletion of nonmature CD4+8+ thymocytes. Nature *333*, 742-746.

Kistner, A., Gossen, M., Zimmermann, F., Jerecic, J., Ullmer, C., Lubbert, H., and Bujard, H. (1996). Doxycycline-mediated quantitative and tissue-specific control of gene expression in transgenic mice. Proc Natl Acad Sci U S A *93*, 10933-10938.

Klausner, R.D., Lippincott-Schwartz, J., and Bonifacino, J.S. (1990). The T cell antigen receptor: insights into organelle biology. Annu Rev Cell Biol *6*, 403-431.

Kleibeuker, W., Jurado-Pueyo, M., Murga, C., Eijkelkamp, N., Mayor, F., Jr., Heijnen, C.J., and Kavelaars, A. (2008). Physiological changes in GRK2 regulate CCL2-induced signaling to ERK1/2 and Akt but not to MEK1/2 and calcium. J Neurochem *104*, 979-992.

Koning, F., Maloy, W.L., and Coligan, J.E. (1990). The implications of subunit interactions for the structure of the T cell receptor-CD3 complex. Eur J Immunol *20*, 299-305.

Krasel, C., Dammeier, S., Winstel, R., Brockmann, J., Mischak, H., and Lohse, M.J. (2001). Phosphorylation of GRK2 by protein kinase C abolishes its inhibition by calmodulin. J Biol Chem *276*, 1911-1915.

Kreslavsky, T., Garbe, A.I., Krueger, A., and von Boehmer, H. (2008). T cell receptor-instructed alphabeta versus gammadelta lineage commitment revealed by single-cell analysis. J Exp Med *205*, 1173-1186.

Krogsgaard, M., Li, Q.J., Sumen, C., Huppa, J.B., Huse, M., and Davis, M.M. (2005). Agonist/endogenous peptide-MHC heterodimers drive T cell activation and sensitivity. Nature *434*, 238-243. Epub 2005 Feb 2020.

Kropshofer, H., Spindeldreher, S., Rohn, T.A., Platania, N., Grygar, C., Daniel, N., Wolpl, A., Langen, H., Horejsi, V., and Vogt, A.B. (2002). Tetraspan microdomains distinct from lipid rafts enrich select peptide-MHC class II complexes. Nat Immunol *3*, 61-68.

Kuhns, M.S., Girvin, A.T., Klein, L.O., Chen, R., Jensen, K.D., Newell, E.W., Huppa, J.B., Lillemeier, B.F., Huse, M., Chien, Y.H.,(2010). Evidence for a functional sidedness to the alphabetaTCR. Proc Natl Acad Sci U S A *107*, 5094-5099.

Kumar, A., Humphreys, T.D., Kremer, K.N., Bramati, P.S., Bradfield, L., Edgar, C.E., and Hedin, K.E. (2006). CXCR4 physically associates with the T cell receptor to signal in T cells. Immunity *25*, 213-224.

Kurobe, H., Liu, C., Ueno, T., Saito, F., Ohigashi, I., Seach, N., Arakaki, R., Hayashi, Y., Kitagawa, T., Lipp, M.*, et al.* (2006). CCR7-dependent cortex-to-medulla migration of positively selected thymocytes is essential for establishing central tolerance. Immunity *24*, 165-177.

Le Douarin NM, Jotereau FV. (1975) Tracing of cells of the avian thymus through embryonic life in interspecific chimeras. J Exp Med.,142(1):17-40.

Lee, W.T., and Vitetta, E.S. (1991). The differential expression of homing and adhesion molecules on virgin and memory T cells in the mouse. Cell Immunol *132*, 215-222.

Lin, J., and Weiss, A. (2003). The tyrosine phosphatase CD148 is excluded from the immunologic synapse and down-regulates prolonged T cell signaling. J Cell Biol *162*, 673-682.

Lind EF, P.S., Porritt HE, Petrie HT. (2001). Mapping precursor movement through the postnatal thymus reveals specific microenvironments supporting defined stages of early lymphoid development. J Exp Med *194*, 127-134.

Liu, S., Premont, R.T., Kontos, C.D., Zhu, S., and Rockey, D.C. (2005). A crucial role for GRK2 in regulation of endothelial cell nitric oxide synthase function in portal hypertension. Nat Med *11*, 952-958.

Lombardi, M.S., Kavelaars, A., Schedlowski, M., Bijlsma, J.W., Okihara, K.L., Van de Pol, M., Ochsmann, S., Pawlak, C., Schmidt, R.E., and Heijnen, C.J. (1999). Decreased expression and activity of G-protein-coupled receptor kinases in peripheral blood mononuclear cells of patients with rheumatoid arthritis. FASEB J *13*, 715-725.

London, C.A., Lodge, M.P., and Abbas, A.K. (2000). Functional responses and costimulator dependence of memory CD4+ T cells. J Immunol *164*, 265-272.

Love, P.E., Shores, E.W., Johnson, M.D., Tremblay, M.L., Lee, E.J., Grinberg, A., Huang, S.P., Singer, A., and Westphal, H. (1993). T cell development in mice that lack the zeta chain of the T cell antigen receptor complex. Science *261*, 918-921.

Malherbe, L., Hausl, C., Teyton, L., and McHeyzer-Williams, M.G. (2004). Clonal selection of helper T cells is determined by an affinity threshold with no further skewing of TCR binding properties. Immunity *21*, 669-679.

Malissen, B., and Schmitt-Verhulst, A.M. (1993). Transmembrane signaling through the T-cell-receptor-CD3 complex. Curr Opin Immunol *5*, 324-333.

Malissen, M., Gillet, A., Ardouin, L., Bouvier, G., Trucy, J., Ferrier, P., Vivier, E., and Malissen, B. (1995). Altered T cell development in mice with a targeted mutation of the CD3-epsilon gene. Embo J *14*, 4641-4653.

Mallabiabarrena, A., Fresno, M., and Alarcon, B. (1992). An endoplasmic reticulum retention signal in the CD3 epsilon chain of the T-cell receptor. Nature *357*, 593-596.

Mallaun, M., Naeher, D., Daniels, M.A., Yachi, P.P., Hausmann, B., Luescher, I.F., Gascoigne, N.R., and Palmer, E. (2008). The T cell receptor's alpha-chain connecting peptide motif promotes close approximation of the CD8 coreceptor allowing efficient signal initiation. J Immunol *180*, 8211-8221.

Manolios, N., Bonifacino, J.S., and Klausner, R.D. (1990). Transmembrane helical interactions and the assembly of the T cell receptor complex. Science *249*, 274-277.

Manolios, N., Letourneur, F., Bonifacino, J.S., and Klausner, R.D. (1991). Pairwise, cooperative and inhibitory interactions describe the assembly and probable structure of the T-cell antigen receptor. Embo J *10*, 1643-1651.

Mariggio, S., Garcia-Hoz, C., Sarnago, S., De Blasi, A., Mayor, F., Jr., and Ribas, C. (2006). Tyrosine phosphorylation of G-protein-coupled-receptor kinase 2 (GRK2) by c-Src modulates its interaction with Galphaq. Cell Signal *18*, 2004-2012.

Martin, S., and Bevan, M.J. (1998). Transient alteration of T cell fine specificity by a strong primary stimulus correlates with T cell receptor down-regulation. Eur J Immunol *28*, 2991-3002.

Martinez-Martin, N., Risueno, R.M., Morreale, A., Zaldivar, I., Fernandez-Arenas, E., Herranz, F., Ortiz, A.R., and Alarcon, B. (2009). Cooperativity between T cell receptor complexes revealed by conformational mutants of CD3epsilon. Sci Signal *2*, ra43.

Matloubian, M., Lo, C.G., Cinamon, G., Lesneski, M.J., Xu, Y., Brinkmann, V., Allende, M.L., Proia, R.L., and Cyster, J.G. (2004). Lymphocyte egress from thymus and peripheral lymphoid organs is dependent on S1P receptor 1. Nature *427*, 355-360.

McCarty, N., Paust, S., Ikizawa, K., Dan, I., Li, X., and Cantor, H. (2005). Signaling by the kinase MINK is essential in the negative selection of autoreactive thymocytes. Nat Immunol *6*, 65-72. Epub 2004 Dec 2019.

McNeil, L.K., Starr, T.K., and Hogquist, K.A. (2005). A requirement for sustained ERK signaling during thymocyte positive selection in vivo. Proc Natl Acad Sci U S A *102*, 13574-13579. Epub 12005 Sep 13578.

Minami, Y., Weissman, A.M., Samelson, L.E., and Klausner, R.D. (1987). Building a multichain receptor: synthesis, degradation, and assembly of the T-cell antigen receptor. Proc Natl Acad Sci U S A *84*, 2688-2692.

Minguet, S., Swamy, M., Alarcon, B., Luescher, I.F., and Schamel, W.W. (2007). Full activation of the T cell receptor requires both clustering and conformational changes at CD3. Immunity *26*, 43-54. Epub 2006 Dec 2021.

Misslitz A, B.G., Förster R. (2006). Trafficking on serpentines: molecular insight on how maturating T cells find their winding paths in the thymus.
. Immunol Rev *209*, 115-128.

Mombaerts, P., Iacomini, J., Johnson, R.S., Herrup, K., Tonegawa, S., and Papaioannou, V.E. (1992). RAG-1-deficient mice have no mature B and T lymphocytes. Cell *68*, 869-877.

Moran, M., and Miceli, M.C. (1998). Engagement of GPI-linked CD48 contributes to TCR signals and cytoskeletal reorganization: a role for lipid rafts in T cell activation. Immunity *9*, 787-796.

Naeher, D., Daniels, M.A., Hausmann, B., Guillaume, P., Luescher, I., and Palmer, E. (2007). A constant affinity threshold for T cell tolerance. J Exp Med *204*, 2553-2559.

Naga Prasad, S.V., Barak, L.S., Rapacciuolo, A., Caron, M.G., and Rockman, H.A. (2001). Agonist-dependent recruitment of phosphoinositide 3-kinase to the membrane by beta-adrenergic receptor kinase 1. A role in receptor sequestration. J Biol Chem *276*, 18953-18959.

Naga Prasad, S.V., Laporte, S.A., Chamberlain, D., Caron, M.G., Barak, L., and Rockman, H.A. (2002). Phosphoinositide 3-kinase regulates beta2-adrenergic receptor endocytosis by AP-2 recruitment to the receptor/beta-arrestin complex. J Cell Biol *158*, 563-575.

Nakano, N., Rooke, R., Benoist, C., and Mathis, D. (1997). Positive selection of T cells induced by viral delivery of neopeptides to the thymus. Science *275*, 678-683.

Nitta, T., Nitta, S., Lei, Y., Lipp, M., and Takahama, Y. (2009). CCR7-mediated migration of developing thymocytes to the medulla is essential for negative selection to tissue-restricted antigens. Proc Natl Acad Sci U S A *106*, 17129-17133.

Ostergaard, H.L., and Lysechko, T.L. (2005). Focal adhesion kinase-related protein tyrosine kinase Pyk2 in T-cell activation and function. Immunol Res *31*, 267-282.

Pages, G., Guerin, S., Grall, D., Bonino, F., Smith, A., Anjuere, F., Auberger, P., and Pouyssegur, J. (1999). Defective thymocyte maturation in p44 MAP kinase (Erk 1) knockout mice. Science *286*, 1374-1377.

Palmer, E. (2003). Negative selection--clearing out the bad apples from the T-cell repertoire. Nat Rev Immunol *3*, 383-391.

Pao, C.S., and Benovic, J.L. (2002). Phosphorylation-independent desensitization of G protein-coupled receptors? Sci STKE *2002*, pe42.

Peacock, J.W., and Jirik, F.R. (1999). TCR activation inhibits chemotaxis toward stromal cell-derived factor-1: evidence for reciprocal regulation between CXCR4 and the TCR. J Immunol *162*, 215-223.

Penela, P., Elorza, A., Sarnago, S., and Mayor, F., Jr. (2001). Beta-arrestin- and c-Src-dependent degradation of G-protein-coupled receptor kinase 2. EMBO J *20*, 5129-5138.

Penela, P., Murga, C., Ribas, C., Salcedo, A., Jurado-Pueyo, M., Rivas, V., Aymerich, I., and Mayor, F., Jr. (2008a). G protein-coupled receptor kinase 2 (GRK2) in migration and inflammation. Arch Physiol Biochem *114*, 195-200.

Penela, P., Ribas, C., Aymerich, I., Eijkelkamp, N., Barreiro, O., Heijnen, C.J., Kavelaars, A., Sanchez-Madrid, F., and Mayor, F., Jr. (2008b). G protein-coupled receptor kinase 2 positively regulates epithelial cell migration. EMBO J *27*, 1206-1218.

Peregrin, S., Jurado-Pueyo, M., Campos, P.M., Sanz-Moreno, V., Ruiz-Gomez, A., Crespo, P., Mayor, F., Jr., and Murga, C. (2006). Phosphorylation of p38 by GRK2 at the docking groove unveils a novel mechanism for inactivating p38MAPK. Curr Biol *16*, 2042-2047.

Perrino, C., Naga Prasad, S.V., Schroder, J.N., Hata, J.A., Milano, C., and Rockman, H.A. (2005). Restoration of beta-adrenergic receptor signaling and contractile function in heart failure by disruption of the betaARK1/phosphoinositide 3-kinase complex. Circulation *111*, 2579-2587.

Perez de Castro I, Bivona TG, Philips MR, Pellicer A.(2004). Ras activation in Jurkat T cells following low-grade stimulation of the T-cell receptor is specific to N-Ras and occurs only on the Golgi apparatus. Mol Cell Biol. 24(8):3485-96.

Petrie., H. (2003). Cell migration and the control of post-natal T-cell lymphopoiesis in the thymus. Nat Rev Immunol *3*, 859.

Pieters, J. (2000). MHC class II-restricted antigen processing and presentation. Adv Immunol *75*, 159-208.

Pihlgren, M., Dubois, P.M., Tomkowiak, M., Sjogren, T., and Marvel, J. (1996). Resting memory CD8+ T cells are hyperreactive to antigenic challenge in vitro. J Exp Med *184*, 2141-2151
.
Pinto da Silva, P., and Kan, F.W. (1984). Label-fracture: a method for high resolution labeling of cell surfaces. J Cell Biol *99*, 1156-1161.

Plotkin, J., Prockop, S.E., Lepique, A., and Petrie, H.T. (2003). Critical role for CXCR4 signaling in progenitor localization and T cell differentiation in the postnatal thymus. J Immunol *171*, 4521-4527.

Plotkin J, P.S., Lepique A, Petrie HT. (2003). Critical role for CXCR4 signaling in progenitor localization and T cell differentiation in the postnatal thymus.
. J Immunol *171*, 4521-4527.

Poznansky, M.C., Olszak, I.T., Evans, R.H., Wang, Z., Foxall, R.B., Olson, D.P., Weibrecht, K., Luster, A.D., and Scadden, D.T. (2002). Thymocyte emigration is mediated by active movement away from stroma-derived factors. J Clin Invest *109*, 1101-1110.

Premont, R.T., Claing, A., Vitale, N., Freeman, J.L., Pitcher, J.A., Patton, W.A., Moss, J., Vaughan, M., and Lefkowitz, R.J. (1998). beta2-Adrenergic receptor regulation by GIT1, a G protein-coupled receptor kinase-associated ADP ribosylation factor GTPase-activating protein. Proc Natl Acad Sci U S A *95*, 14082-14087.

Punt, J.A., Roberts, J.L., Kearse, K.P., and Singer, A. (1994). Stoichiometry of the T cell antigen receptor (TCR) complex: each TCR/CD3 complex contains one TCR alpha, one TCR beta, and two CD3 epsilon chains. J Exp Med *180*, 587-593.

Purbhoo, M.A., Irvine, D.J., Huppa, J.B., and Davis, M.M. (2004). T cell killing does not require the formation of a stable mature immunological synapse. Nat Immunol *5*, 524-530. Epub 2004 Mar 2028.
Rathmell, J.C., Lindsten, T., Zong, W.X., Cinalli, R.M., and Thompson, C.B. (2002). Deficiency in Bak and Bax perturbs thymic selection and lymphoid homeostasis. Nat Immunol *3*, 932-939.

Reth, M. (1989). Antigen receptor tail clue [letter]. Nature *338*, 383-384.

Ribas, C., Penela, P., Murga, C., Salcedo, A., Garcia-Hoz, C., Jurado-Pueyo, M., Aymerich, I., and Mayor, F., Jr. (2007). The G protein-coupled receptor kinase (GRK) interactome: role of GRKs in GPCR regulation and signaling. Biochim Biophys Acta *1768*, 913-922.

Risueno, R.M., Gil, D., Fernandez, E., Sanchez-Madrid, F., and Alarcon, B. (2005). Ligand-induced conformational change in the T-cell receptor associated with productive immune synapses. Blood *106*, 601-608. Epub 2005 Mar 2024.

Risueno, R.M., van Santen, H.M., and Alarcon, B. (2006). A conformational change senses the strength of T cell receptor-ligand interaction during thymic selection. Proc Natl Acad Sci U S A *103*, 9625-9630. Epub 2006 Jun 9629.

Rogers, P.R., Dubey, C., and Swain, S.L. (2000). Qualitative changes accompany memory T cell generation: faster, more effective responses at lower doses of antigen. J Immunol *164*, 2338-2346.

Ruiz-Gomez, A., Humrich, J., Murga, C., Quitterer, U., Lohse, M.J., and Mayor, F., Jr. (2000). Phosphorylation of phosducin and phosducin-like protein by G protein-coupled receptor kinase 2. J Biol Chem *275*, 29724-29730.

Sabapathy, K., Kallunki, T., David, J.P., Graef, I., Karin, M., and Wagner, E.F. (2001). c-Jun NH2-terminal kinase (JNK)1 and JNK2 have similar and stage-dependent roles in regulating T cell apoptosis and proliferation. J Exp Med *193*, 317-328.

Samelson, L.E. (2002). Signal transduction mediated by the T cell antigen receptor: the role of adapter proteins. Annu Rev Immunol *20*, 371-394.

Samelson, L.E., Germain, R.N., and Schwartz, R.H. (1983). Monoclonal antibodies against the antigen receptor on a cloned T-cell hybrid. Proc Natl Acad Sci U S A *80*, 6972-6976.

San Jose, E., Sahuquillo, A.G., Bragado, R., and Alarcon, B. (1998). Assembly of the TCR/CD3 complex: CD3 epsilon/delta and CD3 epsilon/gamma dimers associate indistinctly with both TCR alpha and TCR beta chains. Evidence for a double TCR heterodimer model. Eur J Immunol *28*, 12-21.

Sancho, J., Chatila, T., Wong, R.C., Hall, C., Blumberg, R., Alarcon, B., Geha, R.S., and Terhorst, C. (1989). T-cell antigen receptor (TCR)-alpha/beta heterodimer formation is a prerequisite for association of CD3-zeta 2 into functionally competent TCR.CD3 complexes. J Biol Chem *264*, 20760-20769.

Sancho D, Montoya MC, Monjas A, Gordón-Alonso M, Katagiri T, Gil D, Tejedor R, Alarcón B, Sánchez-Madrid F.(2002) TCR engagement induces proline-rich tyrosine kinase-2 (Pyk2) translocation to the T cell-APC interface independently of Pyk2 activity and in an immunoreceptor tyrosine-based activation motif-mediated fashion. J Immunol.;169(1):292-300.

Sarnago, S., Elorza, A., and Mayor, F., Jr. (1999). Agonist-dependent phosphorylation of the G protein-coupled receptor kinase 2 (GRK2) by Src tyrosine kinase. J Biol Chem *274*, 34411-34416.

Schagger, H., and von Jagow, G. (1991). Blue native electrophoresis for isolation of membrane protein complexes in enzymatically active form. Anal Biochem *199*, 223-231.

Schamel, W.W., Arechaga, I., Risueno, R.M., van Santen, H.M., Cabezas, P., Risco, C., Valpuesta, J.M., and Alarcon, B. (2005). Coexistence of multivalent and monovalent TCRs explains high sensitivity and wide range of response. J Exp Med *202*, 493-503. Epub 2005 Aug 2008.

Schamel, W.W., and Reth, M. (2000). Monomeric and oligomeric complexes of the B cell antigen receptor. Immunity *13*, 5-14.

Schamel, W.W., Risueno, R.M., Minguet, S., Ortiz, A.R., and Alarcon, B. (2006). A conformation- and avidity-based proofreading mechanism for the TCR-CD3 complex. Trends Immunol *27*, 176-182. Epub 2006 Mar 2009.

Schneider, O.D., Weiss, A.A., and Miller, W.E. (2009). Pertussis toxin signals through the TCR to initiate cross-desensitization of the chemokine receptor CXCR4. J Immunol *182*, 5730-5739.

Schwab, S.R., Pereira, J.P., Matloubian, M., Xu, Y., Huang, Y., and Cyster, J.G. (2005). Lymphocyte sequestration through S1P lyase inhibition and disruption of S1P gradients. Science *309*, 1735-1739.

Sebzda, E., Wallace, V.A., Mayer, J., Yeung, R.S., Mak, T.W., and Ohashi, P.S. (1994). Positive and negative thymocyte selection induced by different concentrations of a single peptide. Science *263*, 1615-1618.

Severs, N.J. (2007). Freeze-fracture electron microscopy. Nat Protoc *2*, 547-576.

Shen, T.L., and Guan, J.L. (2004). Grb7 in intracellular signaling and its role in cell regulation. Front Biosci *9*, 192-200.

Shinkai, Y., Koyasu, S., Nakayama, K., Murphy, K.M., Loh, D.Y., Reinherz, E.L., and Alt, F.W. (1993). Restoration of T cell development in RAG-2-deficient mice by functional TCR transgenes. Science *259*, 822-825.

Slifka, M.K., and Whitton, J.L. (2001). Functional avidity maturation of CD8(+) T cells without selection of higher affinity TCR. Nat Immunol *2*, 711-717.

Sohn, S.J., Rajpal, A., and Winoto, A. (2003). Apoptosis during lymphoid development. Curr Opin Immunol *15*, 209-216.

Sugawara, T., Moriguchi, T., Nishida, E., and Takahama, Y. (1998). Differential roles of ERK and p38 MAP kinase pathways in positive and negative selection of T lymphocytes. Immunity *9*, 565-574.

Sun, Z.Y., Kim, S.T., Kim, I.C., Fahmy, A., Reinherz, E.L., and Wagner, G. (2004). Solution structure of the CD3epsilondelta ectodomain and comparison with CD3epsilongamma as a basis for modeling T cell receptor topology and signaling. Proc Natl Acad Sci U S A *101*, 16867-16872. Epub 12004 Nov 16819.

Sussman, J.J., Bonifacino, J.S., Lippincott-Schwartz, J., Weissman, A.M., Saito, T., Klausner, R.D., and Ashwell, J.D. (1988). Failure to synthesize the T cell CD3-zeta chain: structure and function of a partial T cell receptor complex. Cell *52*, 85-95.

Suzuki, G., Nakata, Y., Dan, Y., Uzawa, A., Nakagawa, K., Saito, T., Mita, K., and Shirasawa, T. (1998). Loss of SDF-1 receptor expression during positive selection in the thymus. Int Immunol *10*, 1049-1056.

Suzuki A, Yamaguchi MT, Ohteki T, Sasaki T, Kaisho T, Kimura Y, Yoshida R, Wakeham A, Higuchi T, Fukumoto M, Tsubata T, Ohashi PS, Koyasu S, Penninger JM, Nakano T, Mak TW.(2001) T cell-specific loss of Pten leads to defects in central and peripheral tolerance. Immunity. 2001 14(5):523-34.

Swan, K.A., Alberola-Ila, J., Gross, J.A., Appleby, M.W., Forbush, K.A., Thomas, J.F., and Perlmutter, R.M. (1995). Involvement of p21ras distinguishes positive and negative selection in thymocytes. EMBO J *14*, 276-285.

Testi, R., D'Ambrosio, D., De Maria, R., and Santoni, A. (1994). The CD69 receptor: a multipurpose cell-surface trigger for hematopoietic cells. Immunol Today *15*, 479-483.

Torres, J., Briggs, J.A., and Arkin, I.T. (2002). Convergence of experimental, computational and evolutionary approaches predicts the presence of a tetrameric form for CD3-zeta. J Mol Biol *316*, 375-384.

Trampont, P.C., Tosello-Trampont, A.C., Shen, Y., Duley, A.K., Sutherland, A.E., Bender, T.P., Littman, D.R., and Ravichandran, K.S.(2010) CXCR4 acts as a costimulator during thymic beta-selection. Nat Immunol *11*, 162-170.

Ueno, T., Saito, F., Gray, D.H., Kuse, S., Hieshima, K., Nakano, H., Kakiuchi, T., Lipp, M., Boyd, R.L., and Takahama, Y. (2004). CCR7 signals are essential for cortex-medulla migration of developing thymocytes. J Exp Med *200*, 493-505.

Valitutti, S., Dessing, M., Aktories, K., Gallati, H., and Lanzavecchia, A. (1995). Sustained signaling leading to T cell activation results from prolonged T cell receptor occupancy. Role of T cell actin cytoskeleton. J Exp Med *181*, 577-584.

van Santen, H.M., Benoist, C., and Mathis, D. (2004). Number of T reg cells that differentiate does not increase upon encounter of agonist ligand on thymic epithelial cells. J Exp Med *200*, 1221-1230. Epub 2004 Nov 1228.

Varma, R., Campi, G., Yokosuka, T., Saito, T., and Dustin, M.L. (2006). T cell receptor-proximal signals are sustained in peripheral microclusters and terminated in the central supramolecular activation cluster. Immunity *25*, 117-127.

Veiga-Fernandes, H., Walter, U., Bourgeois, C., McLean, A., and Rocha, B. (2000). Response of naive and memory CD8+ T cells to antigen stimulation in vivo. Nat Immunol *1*, 47-53.

Veillette, A., Bookman, M.A., Horak, E.M., and Bolen, J.B. (1988). The CD4 and CD8 T cell surface antigens are associated with the internal membrane tyrosine-protein kinase p56lck. Cell *55*, 301-308.

Viola, A., Schroeder, S., Sakakibara, Y., and Lanzavecchia, A. (1999). T lymphocyte costimulation mediated by reorganization of membrane microdomains. Science *283*, 680-682.

Vogt, A.B., Spindeldreher, S., and Kropshofer, H. (2002). Clustering of MHC-peptide complexes prior to their engagement in the immunological synapse: lipid raft and tetraspan microdomains. Immunol Rev *189*, 136-151.

von Boehmer, H. (2000). T-cell lineage fate: instructed by receptor signals? Curr Biol *10*, R642-645.

von Boehmer, H., Teh, H.S., and Kisielow, P. (1989). The thymus selects the useful, neglects the useless and destroys the harmful. Immunol Today *10*, 57-61.

Vroon, A., Heijnen, C.J., Lombardi, M.S., Cobelens, P.M., Mayor, F., Jr., Caron, M.G., and Kavelaars, A. (2004). Reduced GRK2 level in T cells potentiates chemotaxis and signaling in response to CCL4. J Leukoc Biol *75*, 901-909.

Vroon, A., Kavelaars, A., Limmroth, V., Lombardi, M.S., Goebel, M.U., Van Dam, A.M., Caron, M.G., Schedlowski, M., and Heijnen, C.J. (2005). G protein-coupled receptor kinase 2 in multiple sclerosis and experimental autoimmune encephalomyelitis. J Immunol *174*, 4400-4406.

Wang, X., Gjorloff-Wingren, A., Saxena, M., Pathan, N., Reed, J.C., and Mustelin, T. (2000). The tumor suppressor PTEN regulates T cell survival and antigen receptor signaling by acting as a phosphatidylinositol 3-phosphatase. J Immunol *164*, 1934-1939.

Watanabe, N., Arase, H., Onodera, M., Ohashi, P.S., and Saito, T. (2000). The quantity of TCR signal determines positive selection and lineage commitment of T cells. J Immunol *165*, 6252-6261.

Watterson, K.R., Johnston, E., Chalmers, C., Pronin, A., Cook, S.J., Benovic, J.L., and Palmer, T.M. (2002). Dual regulation of EDG1/S1P(1) receptor phosphorylation and internalization by protein kinase C and G-protein-coupled receptor kinase 2. J Biol Chem *277*, 5767-5777.

Werlen, G., Hausmann, B., and Palmer, E. (2000). A motif in the alphabeta T-cell receptor controls positive selection by modulating ERK activity. Nature *406*, 422-426.

Willets, J.M., Challiss, R.A., and Nahorski, S.R. (2003). Non-visual GRKs: are we seeing the whole picture? Trends Pharmacol Sci *24*, 626-633

.

Winstel, R., Freund, S., Krasel, C., Hoppe, E., and Lohse, M.J. (1996). Protein kinase cross-talk: membrane targeting of the beta-adrenergic receptor kinase by protein kinase C. Proc Natl Acad Sci U S A *93*, 2105-2109.

Witherden, D., van Oers, N., Waltzinger, C., Weiss, A., Benoist, C., and Mathis, D. (2000). Tetracycline-controllable selection of CD4(+) T cells: half-life and survival signals in the absence of major histocompatibility complex class II molecules. J Exp Med *191*, 355-364.

Yasuda, T., and Kurosaki, T. (2008). Regulation of lymphocyte fate by Ras/ERK signals. Cell Cycle *7*, 3634-3640.

Yoshida, N., Haga, K., and Haga, T. (2003). Identification of sites of phosphorylation by G-protein-coupled receptor kinase 2 in beta-tubulin. Eur J Biochem *270*, 1154-1163.

Zapata, D.A., Schamel, W.W., Torres, P.S., Alarcon, B., Rossi, N.E., Navarro, M.N., Toribio, M.L., and Regueiro, J.R. (2004). Biochemical differences in the alphabeta T cell receptor.CD3 surface complex between CD8+ and CD4+ human mature T lymphocytes. J Biol Chem *279*, 24485-24492
.

Zehn, D., Lee, S.Y., and Bevan, M.J. (2009). Complete but curtailed T-cell response to very low-affinity antigen. Nature *458*, 211-214.

Zimmermann, C., Prevost-Blondel, A., Blaser, C., and Pircher, H. (1999). Kinetics of the response of naive and memory CD8 T cells to antigen: similarities and differences. Eur J Immunol *29*, 284-290.

APPENDIX I

APPENDIX I

Index of figures

Index of Tables

APPENDIX II

APPENDIX II

RESUMEN

Dos de los aspectos más fascinantes del complejo del TCR es su baja afinidad pero alta sensibilidad ante una estimulación por parte del antígeno, y su habilidad para activar diferentes rutas moleculares de señalización en función de la fuerza de la interacción con su ligando MHC-péptido (pMHC).

Durante el desarrollo de las células T, la discriminación entre un estímulo fuerte y débil con el ligando del MHC y la consecuente activación diferencial de rutas de señalización y programas genéticos, es la base principal de la selección positiva y negativa que tiene lugar en el timo, la cual asegura que los linfocitos que reaccionen frente a complejos propios sean eliminados y solo aquellos linfocitos T tolerantes maduren. Tras su completar con éxito la diferenciación en el timo, las células T entran en los órganos linfoides periféricos como células T vírgenes. Tras el encuentro con su antígeno específico estas células vírgenes se diferencian en células efectoras las cuales son capaces de coordinar respuestas inmunes. Parte de estas células efectoras se convierten en células de memoria y se mantienen latentes hasta un próximo encuentro con el antígeno. Estas células de memoria se caracterizan por responder más vigorosamente ante un reencuentro con el antígeno y por ser más sensibles a dosis bajas de antígeno que las células virgenes. Estas propiedades son la base de la inmunidad.

Los mecanismos que subyacen a esta habilidad del TCR de diferenciar entre ligandos de alta y baja afinidad y de transducir esta unión diferencial en cascadas de señalización diferentes, al igual que los mecanismos que otorgan a las células de memoria su alta sensibilidad, son aún desconocidos.

Previamente se ha descrito que en el caso de células en reposo, el TCR es expresado en su membrana como una combinación de oligómeros de diferentes tamaños, de los cuales los más grandes son activados preferecialmente en respuesta a bajas dosis de antígeno. Nosotros barajamos la hipótesis de que el enriquecimiento en un mayor número de oligómeros y un mayor tamaño de dichos complejos es lo que provee a las células de memoria con una alta sensibilidad al antígeno. En esta memoria, mostramos mediante un análisis cuantitativo por microscopia electrónica, que, tanto las células previamente activadas como las células de memoria tienen más y más grandes oligómeros del TCR en su superficie celular en comparación con las correspondientes células vírgenes. También mostramos que una mutación en la región transmembrana del la subunidad CD3ζ impide la formación de los complejos oligoméricos y que la pérdida de dichos complejos causa una reducción en la sensibilidad ante el antígeno de líneas celulares y de células previamente activadas. Estos hechos proporcionan una evidencia directa de que son los oligómeros del TCR y su incremento en número y tamaño, los responsables de la alta sensibilidad de las células T previamente activadas.

En la segunda parte de este trabajo se describe una búsqueda y un análisis inicial de los factores asociados de manera diferencial con al complejo del TCR en el proceso de selección negativa y positiva, barajando la hipótesis de que la asociación diferencial de determinados factores proporcionan a los timocitos la capacidad de activar rutas diferentes de señalización en función de la fuerza de unión entre el TCR y el pMHC. Hemos desarrollado un modelo murino de diferenciación de células T que nos permite la purificación de un gran número de timocitos que están sufriendo selección positiva o negativa en una manera sincronizada. Usando este modelo hemos realizado un análisis bioquímico para la búsqueda de proteínas fosforiladas que se unan de manera diferencial al TCR. Así encontramos que la quinasa de las receptores acoplados a proteínas G 2 (GRK2), se asocia con el TCR durante la selección positiva y se disocia tras la inducción de la selección negativa. Análisis de la diferenciación de células T en ratones que carecen de una copia del gen GRK2 indica que la eficiencia de la selección positiva está reducida. Además, la reducción en la expresión de GRK2 afecta a la sensibilidad de los timocitos DP hacia el antígeno, sugiriendo una función directa de GRK2 en la señalización dependiente del TCR. Además dicha ausencia afecta la migración de los timocitos DP y SP hacia la quimioquina SDF-1α. La observación de que esta migración está inhibida por la estimulación a través del TCR indica una unión funcional entre la migración mediada por SDF-1α y la señalización del TCR en estos timocitos.

INTRODUCCIÓN:

El sistema inmune adaptativo presenta tanto especificidad patogénica como memoria antigénica, y comprende dos tipos de respuestas: la respuesta humoral y la respuesta celular.

Los precursores hematopoyéticos de las células T se diferencian en el timo y migran a la periferia como células T vírgenes hasta que el encuentro con una antígena determinada las diferencia en células T efectoras, las cuales presentan un umbral de activación bajo pero una elevada capacidad de producir citoquinas. Tras la eliminación del foco de infección la mayoría de éstas células efectoras mueren, mientras que una pequeña fracción perduran como células T de memoria (Chandok and Farber, 2004). Por lo tanto, la memoria inmunológica permiteuna respuesta más rápida e intensa frente a un reencuentro con patógenos específicos.

El complejo αβ del receptor de la célula T y su organización en la superficie celular

El complejo TCR está formado por las subunidades α y β, que son las zonas de unión al antígeno, asociadas de forma no covalente a las subunidades CD3γ, CD3δ, CD3ε y CD3ζζ responsables de la transmisión de señales al interior celular (B Malissen, G Werlen). Las cadenas α y β están formadas por un dominio de inmunoglobulina variable y otro constante,y ambos estan unidos por un puente disulfuro. Estos dominios están seguidos de tallo region, un dominio transmembrana y una pequeña región intracelular.

Las subunidades CD3ε, γ y δ contienen un ectodominio de inmunoglobulina, un péptido conector, una región transmembrana y un dominio citoplasmático largo que presenta un motivo de activación de inmunoreceptor basado en tirosinas (ITAM) (Figura 1). El dominio citoplasmático de CD3ε presenta además una secuencia rica en prolinas (PRS) y otra rica en residuos básicos (BRS).

La subunidad CD3ζ forma un homodiméro unido por puentes disulfuros (Koning el al., 1990) y contiene una región extracelular muy pequeña, un dominio transmembrana, y una cola citoplasmática que contiene tres motivos ITAMs. Todas las subunidades TCR y CD3 se traslocan al retículo endoplasmático y mediante un estricto mecanismo de control se asegura que solo lleguen a la superfice de la célula los complejos TCR que estén totalmente ensamblados (Delgado y Alarcon, 2005; Mallabiabarrena et al., 1992,; Minami et al., 1987).

La estequiometría (el ratio de las distintas subunidades dentro de un complejo TCR) y la valencia (el número de heterodímeros TCR αβ por complejo) del complejo TCR en las células T, son puntos clave para entender el mecanismo de activación de estas células y especialmente para entender la necesidad de ligandos multivalentes de péptido-MHC (pMHC) necessarios para alcanzar dicha activación (Boniface et al., 1998; Cochran et al., 2000).

Inicialmente, el complejo TCR propuesto consiste en un solo dímero αβ asociado a los dímeros CD3γε, CD3δε y CD3ζζ. Los residuos de las regiones transmembrana de estos componentes presentan un desequilibrio de cargas. Posteriormente, se propuso otro modelo que consistía en dos subunidades αβ por cada subunidad de CD3 (αβ:γε:δε:ζζ en una estequiometría 2:1:1:1); este nuevo modelo resolvía el problema de desequilibrio de cargas mostrado a través de inmunoprecipitación y FRET de células de ratón que expresan dos complejos TCRαβ diferentes (Fernandez-Miguel et al., 1999). La determinación de la composición de los complejos TCR a través de electroforesis de geles nativos de poliacrilamida (BN-PAGE) ha mostrado que éstos complejos se presentan en forma monovalente y oligomérica.

La coexistencia de complejos TCR de diferentes tamaños está respaladada por los resultados obtenidos mediante microscopía electrónica (Figura 3). Se ha demostrado que los complejos oligoméricos se fosforilan a concentraciones de antígeno mucho más bajas que los monoméricos (Schamel et al., 2005). Esto ha llevado ha plantear la hipótesis de que los complejos TCR oligoméricos son responsables de la alta sensibilidad de las células T a pesar de la baja afinidad de los dímeros αβ por sus ligandos pMHC.

Diferenciación y activación de células T αβ:

Los distintos estadios de diferenciación de las células T en el timo coinciden con un patrón estereotipado de expresión de las moléculas CD4, CD8, CD25, CD44 y el propio TCR. En el estadio más temprano, los timocitos son negativos para CD4 y CD8 (DN) pero expresan las moléculas CD44 y CD25 en una secuencia parcialmente solapada. Durante el estadio DN3, CD44-

CD25+, reordenan el locus del T*crB*, dando lugar a la expresión de la cadena TCRβ. La heterodimerización de TCRβ con la cadena pre-Tα y la asociación con las subunidades CD3γε, CD3δε y CD3ζζ permite la progresión de los timocitos al estadio DP ó $CD4^+CD8^+$, donde se reordena el locus T*crA* y se empieza a expresar la cadena TCRα. A partir del momento en el que los timocitos expresan el complejo TCRαβ van a sufrir dos procesos selectivos, siendo ambos, dependientes de la señalización a través del complejo TCR-CD3. La selección positiva permite la maduración y supervivencia de aquellos timocitos que expresan un complejo TCR-CD3 con baja afinidad para los ligandos MHC-péptido (pMHC) (expresados por las células estromales del timo), dando lugar a las células T CD4 y CD8 simple-positivos (SP), que posteriormente migran hacia los organos linfáticos secundarios. La selección negativa promueve la apoptosis de los timocitos que expresen complejos TCR-CD3 con alta afinidad para los mismos ligandos. La correcta ejecución de ambos procesos selectivos es esencial para las generaciones de un repertorio de células T maduras, capaces de reconocer los antígenos presentados por las moléculas MHC de las células presentadoras de antígenos (APCs) siendo a su vez tolerantes al huésped.

Aunque se ha mostrado que las interacciones TCR-pMHC que inducen selección negativa o positiva activan de forma diferencial distintas vías de señalización, no se han aclarado los mecanismos moleculares que permiten al complejo TCR-CD3 conseguir esta activación diferencial. Vista la importancia de la correcta ejecución de la selección timica para el funcionamiento del sistema inmune es de suma relevancia estudiar los mecanismos que permiten esta activación diferencial.

Las distintas fases de la diferenciación tímica ocurren en distintas zonas del timo y los timocitos tienen que moverse activamente a estas zonas. Dichas zonas del timo están formadas por distintos tipos de células estromales que presentan un alto grado de especialización para los distintos procesos de desarrollo; y selección. Ademas la correcta migración es también un aspecto esencial de la diferenciación de las células T. La expresión celular de receptores de quimioquinas que confieren capacidad de movimiento hacia donde están los ligandos correspondientes juega por lo tanto un papel fundamental. Los receptores CXCR4 y CCR7 son los predominantes en los estadios DN y DP, mientras que el receptor CCR9 se expresa en las poblaciones maduras CD4SP y CD8SP.

Cuando las células T vírgenes reconocen en los organos linfáticos periféricos a su antígeno específico presentado por las APCs, se diferencian en células T efectora siendo capaces de coordinar tanto la respuesta inmune innata coma la respuesta inmune adaptativa frente al agente infeccioso. Cuando el patógeno ha sido eliminado con éxito, la mayoría de las células T efectoras mueren y sólo una pequeña fracción sobrevive como células T de memoria. En un futuro re-encuentro con el patógeno estas células T se re-activan con cantidades mas bajas de antígeno que las células T vírgenes, se expanden más rápidamente y producen moléculas efectoras mas rápidamente y en mayor cantidades. Todos estos eventos permite que la infección esté controlada de

manera mucho más rápido y forma la base de la inmunidad y por lo tanto de la eficacia de la vacunación.

En esta memoria hemos demostrado que los complejos TCR tanto en linfocitos humanos de sangre periférica no-estimulados, así como en líneas celulares de origen murino, existen como una combinación de TCRs monoméricos y oligoméricos de distintos tamaños. Los complejos TCR oligomericos, son activados preferentemente mediante una estimulación con bajas dosis de antígeno. Lo que sugiere que podrían conferir a las células T su alta sensibilidad. Por tanto, decidimos analizar si tanto las cellulas activas como las cellulas T memoria, de las que se sabe, poseen una mayor sensibilidad hacia su antígeno, que las células T virgenes, presentaban un enriquecimiento de TCRs oligoméricos en su superficie. Más aun, generamos un mutante en CD3ζ que impide la formación de TCRs oligomèricos, y lo usamos para demostrar tanto en una línea celular como en células primarias, que los complejos oligoméricos de TCRs proporcionan a las células T una mayor sensibilidad.

GRK2:

La familia de quinasas de receptores acoplados a proteína G (GRKs) está compuesta por siete proteínas distintas con actividad quinasa en serina y treonina. Todas las GRKs comparten una arquitectura estructural común: contienen un dominio catalítico, una secuencia de 185 aminoácidos de longitud en el extremo N-terminal importante para la unión del receptor a su ligando y de un domino C-terminal con alta variabilidad. El papel principal que le ha sido atribuido a las GRKs es el reconocimiento y fosforilación de los receptores acoplados a proteínas G (GPCRs), además de fosforilar otros sustratos independientes del receptor. Las GRKs tienen la capacidad de atenuar la traducción de la señal a través de los GPCRs independiente a la fosforilación, lo cual refuerza un papel alternativo a su actividad quinasa (Pao and Benovic, 2002), (Carman et al; 1999) además de sugerirse un papel adaptador a ésta familia de proteínas.

Muchas de las proteínas GRK2 se localizan en el citoplasma y son traslocadas a la membrana plasmática una vez que el GPCR es estimulado. Tanto la distribución como la actividad de GRK2 están finamente reguladas mediante la interacción con la subunidad Gβγ, lípidos, receptores agonistas activados, calmodulina o la fosforilación por parte de otras quinasas.

En diferentes trabajos ha sido mostrado que GRK2 tiene capacidad para interaccionar con una amplia variedad de proteínas y modular su actividad. Estas interacciones son tanto dependientes como independientes de fosforilación y muchas de estas proteínas tienen un papel importante en procesos biológicos de la célula T, lo que presupone un importante papel en el sistema inmune. Recientemente, ha sido demostrado que la MAPK 38p se asocia con el GRK2 endógeno y es fosforilada por éste (Peregrin et al, 2006). Otra de las proteínas con capacidad de interaccionar con GRK2 es PI3kinasa. La unión de GRK2 a PI3Kγ promueve su reclutamiento a la membrana plasmática una vez que ha sido estimulado por agonistas que inducen endocitosis del

receptor de quimioquinas en la línea celular HEK293T que expresa altos niveles de GRK2 (Naga Prasad et al, 2001). Recientemente se ha sugerido que la asociación de GRK2 con MEK y ERK controla la activación de MAPK a través del receptor de quimioquinas (Jimenez-Sainz et al, 2006). En este sentido, la interacción GRK2/MEK1/2 reduce la activación de ERK1/2 en células HEK293 que sobre-expresan GRK2 estimuladas con el ligando CCL2 de igual forma, una reducción de los niveles de GRK2 induce una intensa activación de ERK después de estimular mediante el uso de agonistas. Finalmente, se ha descrito que interacción directa entre el domino C-teminal de GRK2 y la serina treonina quinasa Akt produce la inhición de esta última a través de un mecanismo actualmente sin identificar.

La regulación dinámica de la expresión de altos niveles de GRK2 en las células del sistema inmune (Chuang et al, 1992; De Blasi et al, 1995) sugiere un importante papel de ésta proteína en la actividad inmunológica. Estudios en los que se utilizaron linfocitos T GRK2$^{+/-}$ mostraban un efecto en la movilidad celular. Se ha indicado que una reducción de alrededor el 50% de los niveles de GRK2 de las células aisladas de estos animales se correlaciona con un incremento significante de la respuesta "*In vitro*" a quimiotácticos, así como en la señalización celular.

OBJETIVOS DEL ESTUDIO:

Las células T previamente activadas y las células T de memoria tienen un bajo umbral de activación en comparación con las células vírgenes. Su activación es menos dependiente de señales co-estimuladoras y es iniciada con bajos niveles de antígeno. Sin embargo, aún es desconocido el mecanismo preciso que debe estar controlando este el aumento de sensibilidad de dichas células.

Recientemente ha sido descrito, mediante técnicas bioquímicas y de microscopia electrónica, que en la membrana de las células T vírgenes co-existen dos tipos de TCR, los TCR monoméricos y los oligoméricos. Además ha sido demostrado que los complejos oligoméricos se activan preferentemente a bajas dosis de antígeno, sugiriendo así la idea de que son estos complejos multivalentes los que dan la cualidad de alta sensibilidad a las células T.

Por lo tanto nosotros planteamos la hipótesis de qué la alta sensibilidad característica de las células T previamente activadas o de las células T de memoria es debida a un incremento en el número y tamaño de los complejos oligoméricos de TCR presentes en su membrana. Para abordar e intentar demostrar dicha hipótesis, los principales objetivos de la primera parte de esta memoria fueron:

1) Comparar el número y tamaño de los complejos oligoméricos de TCR presentes en células vírgenes y de memoria.

2) Diseño y obtención de formas mutantes del complejo del TCR que impiden

específicamente la oligomerización de los TCR en membrana.

3) Investigar la función de los complejos oligoméricos en el proceso de diferenciación y activación de las células T.

La segunda parte de esta memoria está focalizado en la búsqueda de nuevos mecanismos moleculares a través de los cuales el complejo TCR-CD3 es capaz de transmitir la señal apropiada para dar lugar a la selección positiva y negativa que sufren los timocitos DP en el proceso del desarrollo tímico. Actualmente, han sido descritas múltiples rutas de señalización controladas por el TCR, que están implicadas de manera cuantitativa y cualitativa en el proceso de selección que tiene lugar en el timo, pero es aún desconocido el mecanismo molecular a través del cual el TCR activa de forma diferencial las cascadas de señalización que van a dar lugar a la selección positiva o negativa.

Nosotros planteamos la hipótesis de que la señalización differencial que puede tener lugar en el proceso de selección tímica es dependiente de una asociación diferencial de factores intracelulares al complejo del TCR, dependiendo de la fuerza de la interacción del complejo del TCR con los ligandos del MHC expresados en las células del estroma del timo. Para comprobar la validez de nuestra hipótesis los objetivos principales de esta segunda parte de esta memoria fueron:

1) Estandarizar un modelo murino para obtener un gran número de timocitos doble positivos que estén sufriendo selección positiva y negativa *in-vivo.*

2) Realizar una criba bioquímica usando este modelo murino para la búsqueda de proteínas asociadas diferencialmente al complejo del TCR durante la selección positiva y negativa.

3) Investigar la función de dichas proteínas y de su asociación diferencial al TCR en el proceso de diferenciación tímica.

RESULTADOS:

Sección 1

En primer lugar, analizamos células previamente estimuladas, así como células T de memoria, de las que se sabe poseen una mayor sensibilidad hacia su antígeno que las células T vírgenes, y encontramos que estaban enriquecidas en TCRs oligoméricos en su superficie (Figuras 11 y 12), lo que indica que la estimulación de las células T conlleva un cambio en la distribución de los complejos de TCR. Con el objeto de establecer una relación causal entre los oligómeros de TCR y la sensibilidad hacia el antígeno diseñamos mutantes del TCR. Mutamos las leucinas en posiciones 9 y 19 de la región transmembrana de CD3ζ, de la cual se ha demostrado que muestra una gran energía de interacción en la forma tetramérica de la región transmembrana de CD3ζ (Torres et al., 2002), altamente conservados y en una posición favorable para establecer una interacción con otras moléculas (mutantes L9A y L19A, Figuras 13A y B). Las cadenas Wild Type (WT), L9A o L19A de CD3ζ fueron transfectadas en la línea celular MA 5.8, deficiente para CD3ζ. L19A CD3ζ reconstituyó la expresión del TCR a un nivel similar al de la forma WT, mientras que L9A, solo lo consiguió de forma parcial (Figura 14A). Por ello, continuamos el estudio únicamente con el mutante L19A. Experimentos de inmunoprecipitación e inmunoblot confirmaron la asociación correcta de L19A CD3ζ a los demás componentes del TCR (Figura 14B). Análisis mediante microscopia electrónica de una réplica de la superficie celular de la forma WT y el mutante L19A de CD3ζ muestran un descenso significativo en el número y tamaño de los complejos oligoméricos de TCR en comparación con la forma WT (Figura 15). Este impedimento en la formación de TCRs oligoméricos coincide con un descenso en la sensibilidad de L19A CD3ζ en respuesta a estímulos antigenicos, en comparación con la forma WT (Figura 16). Esto pone de manifiesto que los complejos oligoméricos de TCR proveen a las células T de una alta sensibilidad hacia el antígeno.

Con el propósito de determinar el papel de los complejos oligoméricos de TCR en la diferenciación y activación *in-vivo* de células T, decidimos transducir precursores de medula ósea OT-1 TCR-transgénico de un ratón deficiente en CD3ζ (Love et al., 1993) con las formas WT y L19A de CD3ζ. Para ello, generamos una construcción lentiviral en la que se hallan fusionados GFP y CD3ζ WT o L19A. Las proteínas de fusión resultantes fueron probadas en cuanto a su capacidad para restaurar la expresión en la superficie celular del TCR, y habilidad para asociarse a los demás componentes del TCR. (Figura 17). Células que expresaban CD3ζ L19A resultaron ser menos sensibles a la estimulación mediante antígeno y tenían menos y más pequeños complejos oligoméricos en la superficie que las células que expresaban CD3ζ WT (Figura 18). El análisis de los animales reconstituidos con L19A CD3ζ mostraron un perfil de diferenciación timico y periférico normales, en comparación con los WT (Figura 19), lo que sugiere que los complejos oligoméricos de TCR no juegan un papel importante en la diferenciación de células T OT-1 transgénicos, o que dichos complejos, no estaban presentes en los precursores de células T. Análisis

funcionales llevados a cabo en células T vírgenes periféricas, no mostraron diferencias en la estimulación entre CD3ζ WT y L19A (Figura 20), mientras que cuando células T activadas y expandidas *in-vitro*, fueron estimuladas frente a distintas concentraciones de su antígeno específico, se observó una diferencia sustancial entre ellos con respecto a la activación. Las células L19A CD3ζ fueron menos sensibles a la estimulación en relación a las WT (Figura 21) y esta inhibición en la actividad coincidió con un descenso del número de complejos oligoméricos de TCRs en la superficie celular (Figura 22).

Tomados en su conjunto, estos datos indican que el papel de los complejos de TCRs oligmericos *in-vivo* es más pronunciado en células que han recibido una estimulación antigénica previa, lo que está en concordancia con la observación de que estos complejos se encuentran enriquecidos en células estimuladas previamente así como en linfocitos T de memoria, de los que se conoce su mayor sensibilidad por el antígeno.

Sección 2

Anteriormente propusimos que la capacidad que tiene el complejo TCR de activar rutas de señalización en los timocitos en función de la fuerza de las interacciones con sus ligandos pMHC, depende de la asociación diferencial con otras proteínas involucradas en la producción de la señal. Teneido esto en cuenta, realizamos una búsqueda bioquímica para dichas proteínas, y desarrollamos un modelo de ratón de diferenciación de células T que nos permitiría obtener un gran número de timocitos DP que sufrirían selección positiva o negativa *in-vivo* (Figura 23, 24 y 25). Tras la estandarización de las condiciones para la selección de timocitos DP que experimentarán selección positiva y negativa, preparamos lisados de timo a partir de ambos grupos e hibridamos un array de anticuerpos, usando los controles apropiados (Figura 26 y 27). De entre las proteínas identificadas (Tabla 2) decidimos continuar con GRK2, confirmando mediante experimentos de inmunoprecipitación e inmunoblot independientes la asociación de GRK2 con el complejo TCR y por ultímo verifícado que esta asociación se producía en condiciones de selección positiva.

Para determinar si GRK2 juega un papel en la diferenciación de las células T, analizamos ratones que carecen de una copia funcional del gen GRK2 (ratones $GRK2^{+/-}$) y además transgenicos para los TCR OT-1 o/y AND^{tg} ya que los animales $GRK2^{-/-}$ no son viables. Analisis de los timocitos DP mostró una clara reducción en el porcentaje de timocitos GRK2+/- ANDtg que expresaban un alto nivel de TCR en la superficie celular (Figura 31 y 32C). Además se observó una disminución en la downmodulación de CD69 en la superficie celular de timocitos CD4 maduros simples positivos en $GRK2^{+/-}$ comparados con ratones $GRK2^{+/+}$. (Figura 31 y 32C). El aumento de la expresión del TCR en membrana en el estado de DP es una señal de una selección positiva con éxito y la downmodulación de CD69 en las SP es necesaria para la salida del timo de los timocitos. En conjunto estos datos indican que GRK2 realiza un papel limitante durante la selección positiva en el estado de DP y de igual manera durante la salida de los timocitos

maduros del timo tanto en células MHC de clase I cómo en MHC de clase II.

A continuación determinamos si la apoptosis celular causada por la carencia de un estímulo mediado por TCR o inducida por un estímulo fuerte de TCR se veía alterada en timocitos GRK2$^{+/-}$. Mientras que la apoptosis *in-vitro* causada por la carencia de un estímulo era ligeramente mayor en los timocitos DP GRK2$^{+/-}$, la apoptosis inducida por la estimulación del TCR no se veia afectada. Esto sugería que el fenotipo observado en los animales GRK2$^{+/-}$ era en su mayor parte debido a una alteracíon en la selección positiva y no a una selección negativa exacerbada.

Dado que la selección positiva es estrictamente dependiente de la señalización mediada por el complejo TCR, tratamos de determinar si una reducción en la cantidad de GRK2 afectaba directamente a eventos de activación dependientes de TCR-CD3. La estimulación *in-vitro* de timocitos AND^{tg} GRK2$^{+/+}$ y GRK2$^{+/-}$ muestra una reducción marcada de la downmodulación y un aumento en la expresión de CD69 en timocitos DP GRK2$^{+/-}$ comparados con timocitos DP GRK2$^{+/+}$ (Figura 34). Esta diferencia en la respuesta no fue observada en 4SP y ní en la periferia (Figura 35). Estos datos sugerían que GRK2 jugaba un papel directo en la vía de señalización del complejo TCR-CD3.

El estudio de la diferenciación de timocitos AND^{tg} GRK2$^{+/+}$ y GRK2$^{+/-}$ en fondo H2^{bb} mostró un fenotipo adicional. En el fondo H-2^{bb} las interacciones TCR-MHCp se producen de forma más débil, y por tanto la selección positiva es menor comparada con el fondo H-2^{kk}. Encontramos una población intermedia CD4^{lo}CD8^{lo} que era TCR^{lo}CD69^{lo} en ratones GRK2$^{+/-}$ (Figura 36); entonces sugirió que eran timocitos en transición del estadio DN a DP y no timocitos DP que habían downmodulado CD4 y CD8 tras recibir señales que inducen la selección negativa, ya que estos timocitos expresan CD69. La aparición de esta población intermedia en ratones AND^{tg} GRK2$^{+/-}$ era alelo-dependiente, lo que indicaba que jugaba un papel importante en la señalización mediada por el TCR en esta transición e implicaba un papel para GRK2 en este proceso de señalización. Finalmente, comparamos la capacidad de migración hacia SDF1α de ratones GRK2$^{+/+}$ con GRK2$^{+/-}$ en presencia o ausencia de estímulo mediado por TCR. La población de ratones GRK2$^{+/-}$ 4SP y DN migraban más en comparación con GRK2$^{+/+}$, lo que concuerda con los datos presentados anteriormente, aunque encontramos aquí un disminución en la capacidad migratoria de los timocitos DP (Figura 37). En conjunto estos datos muestran que la capacidad migratoria de los timocitos GRK2$^{+/-}$ estaba alterada y que la reducción en migración de los timocitos DP podría contribuir a la reducción en selección positiva observada en los ratones AND^{tg} GRK2$^{+/-}$.

DISCUSIÓN

Sección 1

El sistema inmune adquirido proporciona memoria antigénica, permitiendo una respuesta más rápida y más fuerte tras el encuentro con patógenos específicos, lo que proporciona inmunidad. Hemos demostrado en estudios anteriores que coexisten complejos del receptor de células T monoméricos y oligoméricos en la superficie de células T latentes, mediante ensayos bioquímicos y estudios de microscopía electrónica, y que además estos complejos oligomericos son más sensibles a dosis bajas de antígeno. De hecho, nosotros hipotetizamos que si estos complejos oligoméricos proporcionan a las células T una mayor sensibilidad al antígeno, la sensibilidad de respuesta a éste sería proporcional al número de complejos oligoméricos. Aquí se demuestra que tanto las células T activadas como las de memoria tienen un mayor número de complejos TCR, lo que les proporciona una mayor sensibilidad de respuesta al antígeno, en comparación con las células T vírgenes. Nuestros datos muestran una clara evidencia de los cambios que sufren los complejos TCR en su distribución tras su estimulación.

Ha sido demostrado previamente que la integridad de los complejos TCR oligoméricos dependen del contenido en colesterol de la membrana celular. Además ha observado que cambios en el contenido de colesterol tanto en células T previamente activadas como en células T memoria. podrían permitir la formación de mas complejos TCR oligomericos en estas células. Por otro lado, nuestros datos también son compatibles con un papel para los contactos proteína-proteína en la formación de complejos TCR oligoméricos. Teniendo en cuenta que el tamaño de las partículas de oro empleadas para la detección de agregados de TCR es casi idéntica al diámetro del complejo TCR-que CD3 y el espacio existente entre los partículas de oro observado en las técnicas de microscopia electrónica, esto índica que serían possible contactos proteína-proteína entre complejos TCR individuales. Puesto que se ha observado anteriormente que el dominio transmembrana de CD3ζ está implicado en la formación de un tetrámero, y que una mutación de una leucina a una alanina en la posición 19 (L19A), dentro de este transmembrana reduce la formación de complejos TCR oligoméricos, proponemos que CD3ζ puede formar interacciones heterotipicas o con otra cara, aun desconocida, del complejo TCR adyacente o una alteración de interacciones homotipicas de CD3ζ y de la otra cara (Figura 38A). Esta cara B podria estar formada principalmente por el dominio Cα, ya que recientemente se ha observado que las hebras C y F de Cα juegan un papel importante en la dimerización del complejo TCR. Finalmente una combinación de ambas caras (CD3ζ y Cα) podría estar implicada en la formación de los complejos TCR oligomericos (Figura 38b).

Los complejos TCR oligoméricos podrían también jugar un papel relevante en la selección tanto positiva como negativa de los timocitos debido a su propiedad de amplificar señales generadas por los ligandos. Sin embargo, al menos en el modelo de selección positiva que conocemos no hemos observado esta función de los complejos de TCR olgomericos. En cambio sí hemos observado

una clara reducción en la sensibilidad en linfoblastos primarios mutantes provenientes de estos ratones, sugiriendo que el papel principal de los complejos TCR oligomericos consiste en aumentar la sensibilidad tanto de las células T previamente activadas como de células T memoría por el antígeno.

Los mecanismos que proporcionan una mayor sensibilidad a las complejos TCR oligomericos probablemente tengan su base en la observación de que la estimulación de las células T depende estríctamente de complejos pMHC multivalentes. Un aumento en el valencia de los receptores y de los ligandos debería que aumentar la fuerza de interacción y por lo tanto la capacidad estimuladora. Por otra parte, se ha observado que dentro de los complejos TCR oligomerícos existen mecanismos de cooperación que podrían permitir una extensión la señal de activación de un TCR contactado por pMHC a los complejos TCR adyacentes no contactados.

Sección 2

Numerosos estudios han demostrado la relevancia de la señalización diferencial a través del TCR durante la selección positiva y negativa. En estos estudios, se pone de manifiesto la importancia de las vias pro y anti apoptóticas asi como de la vía de las MAPK. Sin embargo, todavía no se conocen los mecanismo de conexión de estas vías con el TCR (durante estos procesos). En este trabajo hemos realizado un análisis bioquímico en busca de nuevas proteínas asociadas con el TCR o de proteínas fosforiladas en tirosinas. Además desarrollado un modelo de ratón transgénico para el TCR que permite un enriquecimiento en timocitos DP en proceso de selección positiva y negativa. Las ventajas de este modelo son, por un lado, que la selección positiva ocurre en condiciones fisiológicas en presencia de MHC propios y por otro que al no ser necesaria la purificación de las células DP, la interacción entre los timocitos y las células estromales del timo se mantiene hasta el momento del procesamiento de las muestras para su análisis. Para la detección de proteínas q interaccionan con el TCR o que son fosforiladas durante la selección positiva se utilizaron arrays CHIPS? Utilizaron arrays de anticuerpos en lugar de arrays de RNA para poder identificar aquellas proteínas que sufrían modificaciones post-traduccionales o cambios de interaccíon durante la selección tímica aunque no se alterasen los niveles de su RNA mensajero correspondiente.

De entre todas las proteínas que se identificaron con esta aproximación, por ejemplo PTEN, PYK2, Grb7 y GRK2, escogimos GRK2 para continuar el estudio ya que su interacción con el TCR fue confirmada por varios métodos y porque está bien documentado tanto su papel regulador de la actividad de diferentes receptores de quimioquinas como su interacción con proteínas implicadas en la biología de las células T.

GRK2 se asocia al TCR durante el proceso de selección positiva y se disocia durante la selección negativa. Interacciona solamente con el TCR de timocitos DP y SP, y no de DN, a pesar de que todas estas células expresan tanto el TCR como GRK2. Esta asociación diferencial entre el TCR y GRK2 debe de ser consecuencia de la expresión de factores específicos en cada uno

de estos estadios de diferenciación de las células T. Otro grupo ha descrito recientemente la interacción TCR-GRK2 y, si bien no se menciona la asociación diferencial descrita en nuestro trabajo (DeFord-Watts et al, 2007). Muestran que GRK2 interacciona con la secuencia BRS de CD3ε. Puesto que la secuencia BRS es adyacente a la secuencia PRS un posible mecanismo para explicar la disociación de GRK2 del TCR durante la estimulación sería que el cambio conformacional que ocurre en la región PRS tras la unión de un agonista o un péptido que promueve la selección negativa, y que va su vez permite la unión de Nck a CD3e, induciría la disociación de GRK2 de BRS.bien por sí mismo o bien gracias a la unión de Nck

Puesto que GRK2 interacciona con el TCR durante la selección positiva, proponemos que el papel de GRK2 es más importante para la selección positiva que para la selección negativa. El análisis de animales $GRK2^{+/-}$ transgénicos para los TCRs OT-1 y/o AND muestra que GRK2 juega un papel relevante en la selección positiva mediante mecanismos dependientes e independientes del TCR. En ambos modelos animales, la población DP $GRK2^{+/-}$ muestra un aumento menos eficaz de la expresión del TCR, lo que sugiere un defecto en selección positiva. Otras respuesta mediadas a través del TCR como son la regulación negativa de la expresión del TCR en la membrana y el aumento de la expresión de CD69 en respuesta a estimulación antigénica *in-vitro*, también están alteradas en timocitos DP $GRK2^{+/-}$. Todo esto sugiere que GRK2 juega un papel en la señalización a través del TCR. El papel limitante de GRK2 en células en distintos estadios de diferenciación en el timo podría explicarse por la baja expresión del TCR en células DP en comparación con células 4SP y $CD4^{+,}$ lo que haría que la señalización a través del TCR en los timocitos DP fuera más sensible a pequeñas alteraciones en vías 'downstream'.

En ratones $GRK2^{+/-}$ AND^{tg} que expresan MHC del tipo $H2^{bb}$ (lo que se traduce en un ligando más débil del TCR AND) se observó una clara disminución en el número de timocitos DP y 4SP y la aparición de una población con baja expresión de los co-receptores CD4 y CD8, el TCR y CD69. Estas células parecen células transitorias entre los estadios DN y DP y el hecho de que su detección depende de una disminución del nivel de expresión de GRK2 indicaria que GRK2 esta implicado en esta transición. A favor de esta hipótesis, se ha observado que la región BRS de CDε, donde se une GRK2 , es esencial para la transición del estadio DN a DP.

La migración de los timocitos $GRK2^{+/-}$ DP en respuesta a SDF-1α está reducida. Ésta contrasta con el aumento de la capacidad migratoria de las células CD4 SP observado en nuestro estudio y en estudio de la migración de células T maduras. Aun a´si, en todas las poblaciones, una estimulación paralela del TCR reduce la capacidad migratoria hacia SDF-1α. Se ha demostrado que el receptor de quimioquinas CXCR4, receptor principal para SDF, necesita las vías de señalicaciòn dependientes del TCR para su propia señalización, y que el menos en timocitos DN la estimulación por CXCR4 es un componente esencial para la señalización a través del pre-TCR Proponemos que GRK2 sierve como un coordinador entr ambas rutas

de señalización en timocitos DP, y que ambas rutas de señalización dependen del otro para generar una señal suficientemente fuerte para permitir la migración y selección positiva. Es mas CXCR4 también está implicado en la transmisión de señales de supervivencia a través del pre-TCR. En nuestro trabajo, hemos observado un ligero aumento en la inducción de la apoptosis de células AND^{tg} GRK2$^{+/-}$ en comparación con timocitos AND^{tg} silvestre para GRK2, por lo tanto GRK2 podría promover la supervivencia de los timocitos DP. Finalmente, el hecho de que en los timocitos SP GRK2$^{+/-}$ la disminución de la expresión de CD69 en la membrana sea menor, sugiriendo un efecto en la salida de los timocitos maduros del timo, apunta hacia un papel de GRK2 independiente del TCR durante la selección positiva. Dado que no se ha descrito todavía la implicación de la señalización a través del TCR en este proceso.

CONCLUSIONES

1.-Las células T previamente activadas expresan en su membrana plasmática un mayor numero y tamaño de TCR oligoméricos que las células T vírgenes.

2.-La mutación de un residuo de Alanina a Leucina en la posición número 19 de la región transmembrana de la cadena de CD3ζ altera la formación de oligómeros de TCR en hibridomas de células T, sin afectar al ensamblaje del TCR ni a los niveles de expresión en la superficie celular.

3.-Esta alteración en la formación de TCRs oligoméricos en el hibridoma de células T que expresa la cadena mutante de CD3□ tiene como consecuencia una disminución de la sensibilidad en el reconocimiento de antígeno, lo que demuestra que la existencia de TCRs oligoméricos provoca un aumento en la sensibilidad a antígeno.

4.-La expresión de la cadena mutante de CD3ζ en precursores de un clon TCR-transgénico no afecta a su diferenciación tímica ni a la generación de células T virgenes, lo que sugiere que los TCRs oligómericos no están implicados en estos procesos.

5.-La respuesta primaria de células T vírgenes TCR-transgénicos que expresan la forma mutante de la cadena CD3ζ es normal. Sin embargo, estas células responden peor que aquellas que expresan la forma silvestre de CD3ζ a una segunda estimulación. Asimismo, estas células presentan un menor tamaño y número de TCRs oligoméricos, lo que indica que los TCRs oligoméricos son responsables del aumento en la sensibilidad a

antígeno de las células T primarias previamente activadas.

6.-Mediante el uso de un nuevo modelo animal de selección positiva y negativa sincronizada en el timo, se muestra que GRK2 se asocia con el TCR en timocitos DP durante la selección positiva.

7.-En timocitos de ratones transgénicos OT-1 y AND con niveles más bajos de expresión de GRK2, se detecta un menor aumento en la expresión del TCR en el estadio de DP. Esto sugiere que la selección positiva es menos eficiente en estas células e indica la implicación de GRK2 en este proceso.

8.-Los timocitos DP de animales transgénicos AND con menor expresión de GRK2 presentan una menor sensibilidad a antígeno en ensayos *in-vitro*, lo que sugiere que GRK2 está implicada en la señalización a través del TCR.

9.-Una población de timocitos con bajos niveles de CD4, CD8, TCR y CD69 surge en ratones AND transgénicos que expresan un nivel reducido de GRK2 y ligandos más debiles para la selección positiva. Esta sugiere que GRK2 tiene un papel en la transición del estadio DN a DP de las células AND-transgénicos.

10.-La reducción en expresión de GRK2 tiene efectos opuestos en la capacidad migratoria de las timocitos AND-transgenicos DP y 4SP hacia SDF-1α, indicando diferencias en la regulación GRK2-dependiente de estos procesos en ambas poblaciones. Estimulación paralela del TCR reduce la capacidad migratoria de ambas poblaciones, mostrando que las vías de señalización a través del TCR interaccionan funcionalmente con la vía de señalización inducida por SDF-1α.

APPENDIX III

Increased sensitivity of antigen-experienced T cells through the enrichment of oligomeric TCR complexes

Rashmi Kumar[1], María Ferez[1], Mahima Swamy[3,5], Ignacio Arechaga[4,6], María Teresa Rejas[2], Jose M. Valpuesta[4], Wolfgang W. A. Schamel[3], Balbino Alarcon[1,7] and Hisse M. van Santen[1,7]

[1]Departamento de Biología Celular e Inmunología, [2]Servicio de Microscopía Electrónica, Centro Biología Molecular Severo Ochoa, Consejo Superior de Investigaciones Científicas, Universidad Autónoma de Madrid, 28049 Madrid, Spain, [3]Centre for Biological Signalling Studies (bioss), Faculty of Biology, University Freiburg and Max Planck Institute for Immunobiology, 79108 Freiburg, Germany [4]Centro Nacional de Biotecnología, Consejo Superior de Investigaciones Científicas, 28049 Madrid, Spain

[5]: Current address: Peter Gorer Department of Immunobiology, King's College School of Medicine, Guy's Hopsital, London, UK

[6]: Current address: Departamento de Biología Molecular, Universidad de Cantabria (UC) and Instituto de Biomedicina y Biotecnología de Cantabria, IBBTEC (CSIC-UC-IDICAN), 39011 Santander, Spain.

[7]: To whom correspondence should be addressed: Balbino Alarcon at balarcon@cbm.uam.es and/or Hisse M. van Santen at hvansanten@cbm.uam.es

Running title: Avidity maturation in T cells

Summary

Although memory T cells respond more vigorously to stimulation and they are more sensitive to low doses of antigen than naive T cells, the molecular basis of this increased sensitivity remains unclear. We have shown that the TCR exists as different sized oligomers on the surface of resting T cells and that larger oligomers are preferentially activated in response to low antigen doses. Through biochemistry and electron microscopy we now show that previously stimulated and memory T cells have more and larger TCR oligomers at the cell surface than their naive counterparts. Reconstitution of cells and mice with a point mutant of the CD3ζ subunit which impairs TCR oligomer formation, demonstrates that the increased size of TCR oligomers is directly responsible for the increased sensitivity of antigen-experienced T cells. Thus, we propose that an "avidity maturation" mechanism underlies T cell antigenic memory.

Introduction

The acquired immune system provides its host with "antigenic memory", permitting a faster and stronger response when reencountering specific pathogens. At the population level, this antigenic memory is due to an increase in the size of T cell precursor population (Askonas et al., 1982) and preferential growth of higher affinity T cell clones that will form the memory T cell pool (Busch and Pamer, 1999; Malherbe et al., 2004; Zehn et al., 2009). At the cellular level, memory T cells convert more rapidly into effector T cells and produce larger amounts of effector molecules (Bachmann et al., 1999; Bruno et al., 1995; Cho et al., 1999; Veiga-Fernandes et al., 2000; Zimmermann et al., 1999). Moreover, previously stimulated and memory T cells ('antigen-experienced' T cells) are more sensitive to stimulation via their TCR than naive T cells. This is reflected in their relative independence of costimulatory signals (Croft et al., 1994; London et al., 2000) and it has been directly shown by the reduction in the amount of antigen needed to give rise to T cell activation (Ericsson et al., 1996; Kimachi et al., 1997; London et al., 2000; Pihlgren et al., 1996; Rogers et al., 2000; Slifka and Whitton, 2001). The increase in sensitivity of antigen-experienced T cells is unlikely to be due to an increase in the affinity of their TCR for the specific peptide-MHC (pMHC) ligands, as rearranged TCRs have not been found to undergo somatic hypermutation. Instead, other molecular changes must be at play.

Permanent changes in the TCR-associated signal transduction machinery of antigen-experienced T cells have been described and correlated with their increased sensitivity. For example, different isoforms of the tyrosine phosphatase CD45 are expressed by naive and antigen-experienced T cells (Beverley et al., 1992) and these isoforms differentially affect the sensitivity of TCR-mediated signaling (Novak et al., 1994). In addition, antigen-experienced T cells express higher levels of the tyrosine kinase Lck than naive T cells, which correlates with their increased sensitivity to antigen-specific stimulation (Kersh et al., 2003; Slifka and Whitton, 2001).

Lasting changes in the organization of the TCR complexes themselves may also be related to the behavior of antigen-experienced T cells. We have shown by biochemical and electron microscopy (EM) based approaches that the TCR on the surface of human and mouse T cell lines is expressed as a combination of oligomers of different sizes and monomeric TCR complexes (Schamel et al., 2005). The presence of these TCR oligomers is independent of antigenic stimulation and/or contact with an

antigen presenting cell (APC), making them distinct from the TCR microclusters and immunological synapses (Yokosuka and Saito, 2010). Importantly, we provided evidence that the larger TCR oligomers are preferentially phosphorylated during encounters with small amounts of antigen, suggesting that the large TCR oligomers are responsible for the exquisite sensitivity of T cells (Schamel et al., 2005).

Here, we show that primary antigen-experienced T cells have larger TCR oligomers on their cell surface than naive T cells, and that this is correlated with increased antigen sensitivity. Furthermore, we describe a mutation in the transmembrane domain of the CD3ζ chain that impairs the formation of TCR oligomers and that reduces sensitivity to antigen stimulation. This provides direct evidence of the importance of oligomeric TCR complexes in the sensitivity towards antigen. Finally, by reconstituting bone marrow precursors from CD3ζ-deficient mice with either wild type or mutant CD3ζ, we show that the presence of oligomeric TCR complexes on primary T cells is critical in the transition from naive to antigen-experienced T cells.

Results

Larger oligomeric TCR complexes on previously stimulated and memory T cells coincide with increased sensitivity to antigen stimulation.

TCR oligomers of different sizes coexist with isolated TCR complexes on the cell surface of resting human peripheral blood T cells and human and murine T cell lines (Schamel et al., 2005). We assessed whether the stimulation of primary T cells had a lasting effect on the size of the TCR complexes. Accordingly, fresh human peripheral blood T lymphocytes and peripheral blood lymphocytes stimulated for two days with PHA and then expanded for five more days in medium containing IL2 were fixed, labeled with the anti-CD3 antibody OKT3 and 10 nm gold-conjugated protein A. Subsequently cell surface replicas were prepared and the number and size of the gold clusters present on the replicas of individual cells was examined by EM. Single gold particles and clusters of gold particles coexisted on the surface of both freshly isolated and PHA-activated peripheral blood T lymphocytes (fig. 1a). However, quantitative analysis indicated that the previously stimulated cells had a higher percentage of the larger TCR oligomers than freshly isolated cells (fig. 1b), and that the clusters were bigger in these cells.

Since staining efficiency in these experiments only reached 10-20%, the frequency and size of oligomeric TCRs detected by immuno-gold EM might be underestimated. To overcome this limitation, we analyzed the size distribution of the TCR by Blue Native polyacrylamide gel electrophoresis (BN-PAGE). When extracted with the mild detergent Brij96, TCR oligomers are kept intact and can be separated according to their size (Alarcon et al., 2006; Schamel et al., 2005). Membranes from PHA-activated and IL2-expanded T cells or from fresh blood T cells were lysed in Brij96 and subjected to BN-PAGE and immunoblotting (fig. 1c). In both T cell populations, monomeric TCR complexes with a αβεδεγζζ stoichiometry (Schamel et al., 2005; Swamy et al., 2007) were seen just below the f1 marker, as well as oligomeric complexes. However, there was a clear increase in the ratio of oligomeric to monomeric TCRs in PHA-activated cells when compared to naive T cells. This was not due to a mobility shift in the BN-gel caused by PHA-bound TCRs, as addition of PHA to the purified TCR before separation by BN-PAGE did not change the size of the TCR (not shown). When we quantified the ratio of oligomeric to monomeric TCRs measured by BN-PAGE at different times after T cell stimulation (fig. 1d), it increased gradually

before reaching a maximum after day 9. This slow increase in the TCR oligomer content of T cells further excluded crosslinking effects caused by the lectin stimulus that would be expected to occur within minutes or hours. Together these experiments indicated that a lasting change in distribution of the TCR complexes towards large pre-formed TCR oligomers took place in antigen-experienced T cells several days after T cell stimulation.

To gain further evidence of the increase in oligomeric TCR complexes on antigen-experienced T cells, naive and memory $CD4^+$ T cells were isolated from the spleen and lymph nodes of C57BL/6 mice based on their reciprocal CD62L and CD44 expression (Budd et al., 1987; Lee and Vitetta, 1991). A depletion strategy was used in which only $CD4^+CD44^{lo}CD62L^{hi}$ (mostly naive) or $CD4^+CD44^{hi}CD62L^{lo}$ (mostly memory) T cells were spared (fig 2a). The size of the $CD4^+CD44^{hi}CD62L^{lo}$ T cells was similar to the size of the $CD4^+CD44^{lo}CD62L^{hi}$ T cells (fig. 2a, right panel), strongly suggesting that they were resting memory T cells and not recently activated $CD44^{hi}$ T cells. Both T cell populations were fixed and labeled with the anti-CD3 mAb 145-2C11, which was detected with gold-conjugated protein A. Analysis of cell surface replicas of these cells by electron microscopy showed an increase in the percentage of gold particles forming part of large oligomeric clusters on the memory T cell population (fig. 2b and c). Thus, enrichment for more and larger oligomeric TCR complexes also occurred *in vivo* in polyclonal $CD4^+$ memory T cells formed by encounter with their physiological antigens.

We then analyzed murine $CD8^+$, OT-1 TCR-transgenic ($OT\text{-}1^{tg}$) T cells, specific for an ovalbumin-derived peptide (OVAp) bound to the $H\text{-}2K^b$ molecule (Hogquist et al., 1994), which allowed us to compare naive and antigen-experienced T cells expressing identical TCRs. Naive $OT\text{-}1^{tg}$ T cells, purified from lymph nodes via depletion of $CD4^+$ T cells and B cells, expressed low to intermediate levels of CD44 (fig. 3a, left panel). *In vitro* stimulated and expanded $OT\text{-}1^{tg}$ T cells were obtained by stimulating splenic $OT\text{-}1^{tg}$ T cells with OVAp for 2 days and expanding them with IL2 for another 6 days, at which point all these T cells expressed a high level of CD44 (fig. 3a, right panel). Gold particles on cell surface replicas of naive $OT\text{-}1^{tg}$ T cells stained with anti-CD3 were mostly present as isolated particles with only a few, relatively small clusters. By contrast, replicas of previously stimulated $OT\text{-}1^{tg}$ cells were enriched in gold clusters that were also larger (fig. 3b and c).

We assessed whether the increase in size and number of the TCR oligomers in previously stimulated OT-1^{tg} T cells was correlated with greater sensitivity to antigen stimulation. Thus, OT-1^{tg} T cells from spleen were stimulated and expanded as above, with the sole exception that IL2 was withdrawn from the culture the day before the assay. Overnight stimulation with OVAp of these previously stimulated cells increased the expression of CD25 at a 10-fold lower concentration of OVAp while IFNγ production started at a 100-fold lower concentration of OVAp than in naive OT-1^{tg} T cells (fig. 3d). When we stimulated these cells with a soluble pentameric K^{b}-OVAp ligand, previously stimulated OT-1^{tg} cells were 100 to 3000-fold more sensitive to stimulation with this pentameric MHC ligand, as evident by up-regulation of CD69 and the production of IFNγ (fig. 3e). Hence, the increased sensitivity of previously stimulated T cells was independent of changes in expression of adhesion molecules.

Finally, we generated OT-1^{tg} memory T cells *in vivo*, in order to determine whether oligomeric TCR complex enrichment and increased sensitivity occurred in a physiologically relevant setting. Memory T cells were obtained by co-transferring naive OT-1^{tg} T cells and OVAp-loaded bone marrow-derived DCs into CD45.1 congenic recipients. Six weeks later a small population of CD8^{+} donor-derived T cells was evident in the spleen and lymph nodes isolated from the recipient animals (fig. 4a). When compared with freshly isolated naive OT-1^{tg} T cells, these cells were all CD44^{hi} and expressed more LFA-1. Both cell types were of equal size and expressed equal amounts of CD8, indicating that the CD44^{hi}LFA-1^{hi} T cells were resting memory cells. The memory OT-1^{tg} T cells were more sensitive to stimulation with K^{b}-OVAp tetramers than the naive OT-1^{tg} T cells, as measured by the expression of CD25 and by IFNγ production (fig. 4b). As both populations expressed equal amounts of the MHC class I binding co-receptor CD8, this showed that the increased sensitivity of the memory OT-1^{tg} T cells was directly related to stimulation via the TCR.

The small population of memory T cells in the recipient animals (fig. 4a) did not allow us to purify enough of these cells to perform EM analysis and directly establish that OT-1^{tg} memory T cells expressed more and larger oligomeric TCR complexes at the cell surface than naive OT-1^{tg} cells. Therefore, we stimulated spleen cells obtained from the recipient animals and from non-manipulated OT-1^{tg} mice with OVAp for two days *in vitro*, and then expanded them in the presence of IL-2 for six more days. Comparing the cell surface replicas of anti-CD3-labeled cells, *in vitro* activated cells derived from memory OT-1^{tg} cells expressed significantly more and larger TCR

oligomers than *in vitro* activated cells derived from naive OT-1^{tg} cells (fig. 4c). This suggested that the distribution of TCR complexes on the cell surface of memory T cells was different from that of naive T cells before *in vitro* activation, as otherwise no difference in distribution would be expected. This would also imply that repeated stimulation with antigen resulted in an additional increase in oligomeric TCR complexes.

Thus, in the three different types of T cells studied, antigen-experienced T cells have more and larger TCR oligomers when compared to their naive counterparts. Furthermore, in the antigen-specific settings the increased size of TCR oligomers coincided with an increased sensitivity to antigen stimulation.

A point mutation in the transmembrane region of CD3ζ disrupts TCR oligomers and reduces sensitivity to antigen

The data presented above highlighted the correlation between larger TCR oligomers and increased sensitivity to antigenic stimulation, in line with our previous observation that oligomeric TCR complexes are preferentially activated in the presence of small amounts of antigen (Schamel et al., 2005). To establish whether a causal relationship exists, we investigated the effect of mutations in TCR subunits that disrupt the formation of TCR oligomers without affecting TCR assembly and expression at the cell surface.

We focused our attention on CD3ζ, since earlier biophysical data showed that peptides representing the transmembrane domain of CD3ζ not only formed dimers, but also tetramers (Torres et al., 2002). Indeed, two leucine residues at positions 9 and 19 (L9 and L19) are thought to be critical for tetramer formation but not for dimer formation. In 2006, the structure of the transmembrane domain of the CD3ζ was solved (Call et al., 2006), which showed that it formed a symmetrical dimer (reproduced in fig. 5a). The L9 residue points towards the center of the dimer and it is implicated in interstrand hydrogen bonding between the two CD3ζ chains of the dimer. By contrast, L19 points outwards, in a position favorable to form potential contacts with a second dimer. Given the symmetry of the CD3ζ dimer and the finding that the transmembrane domains of CD3ζ could form tetramers (Torres et al., 2002), we tested whether mutation of L9 and L19 affected oligomeric TCR formation.

CD3ζ chains carrying a single L9A or L19A mutation were generated and expressed in the CD3ζ-deficient MA5.8 derivative of the murine T hybridoma 2B4,

specific for a moth cytochrome c (MCC)-derived peptide (Sussman et al., 1988). Pools of cells expressing the L9A or L19A CD3ζ chains were analyzed for their ability to express the TCR complex at the cell surface (fig. 5b). MA5.8 cells transfected with L19A CD3ζ expressed similar levels of the TCR at the cell surface as MA5.8 cells transfected with wild type CD3ζ or the 2B4 line. However, L9A CD3ζ only partially reconstituted the cell surface expression of the TCR complex, consistent with the previously described effect of this mutation on dimer formation (Call et al., 2006). As the amount of TCR expressed at the cell surface could influence the distribution of the TCR and the sensitivity of T cells, we focused our attention exclusively on the L19A mutant.

Immunoprecipitation and immunoblot experiments showed that L19A CD3ζ formed homodimers and was able to assemble with the other CD3 components to a similar extent as wild type CD3ζ (fig. 5c). However, L19A CD3ζ transfectants expressed significantly smaller oligomeric TCR complexes at the cell surface than wild type CD3ζ-expressing cells (fig. 5d). L19A CD3ζ transfectants could respond to high concentrations of antigen *in vitro*, indicating that the L19A mutation did not perturb TCR signaling *per se*, but they were less responsive than wild type transfectants, when measured in terms of CD69 induction and IFNγ production (fig. 5e). Hence, oligomeric TCR complexes endow T cells with greater sensitivity to antigen.

TCR oligomers increase the sensitivity of antigen-experienced primary T cells.

We wished to determine the relevance of oligomeric TCR complexes *in vivo*. We generated CD3ζ-GFP fusion proteins in order to facilitate detection of transduced cells. These fusion proteins recapitulated the properties of their counterparts without GFP when expressed in MA5.8 cells. Thus, wild type and L19A CD3ζ-GFP proteins were equally capable of rescuing the expression of the TCR complex at the cell surface and of associating with the other CD3 components. However the capacity of L19A CD3ζ-GFP expressing cells to form large TCR oligomers was significantly impaired and they were less sensitive to antigenic stimulation (fig. S1).

We transduced bone marrow cells isolated from OT-1^{tg}, CD3ζ-deficient mice (Love et al., 1993) with lentiviral vectors encoding the wild type or L19A CD3ζ-GFP fusion proteins, or GFP alone, and reconstituted sub-lethally irradiated C57BL/6 mice with the transduced bone marrow cells. Mice were sacrificed four to six weeks after reconstitution and the capacity of the CD3ζ-GFP-transduced bone marrow precursors to

give rise to thymic and peripheral T cells was assessed. Wild type and L19A CD3ζ-GFP expressing thymocytes differentiated similarly into CD8 SP thymocytes, while GFP expressing thymocytes did not differentiate beyond the DP stage (fig. 6a). Hence, the L19A CD3ζ-GFP protein permitted the TCR signaling necessary for positive selection. Consistent with normal thymic differentiation, both wild type and L19A CD3ζ-GFP expressing $CD8^+$ OT-1^{tg} T cells were found in peripheral lymphoid organs (fig. 6b). These cells had similar amounts of the TCR at the cell surface, and their expression of CD69, CD25, CD28, LFA-1, CD44 and CD62L was very similar to that observed on control OT-1^{tg} T cells, indicating that they were naive, resting T cells. Thus, the impairment of TCR oligomer formation by the L19A CD3ζ mutant did not appear to affect differentiation of T cell precursors into naive $CD8^+$ T cells.

However, the sensitivity to restimulation with antigen was strongly diminished when previously stimulated OT-1^{tg} T cells bearing the L19A mutation in CD3ζ were restimulated in vitro (fig. 6c). This loss of sensitivity coincided with a significant reduction in the number of oligomeric TCR complexes detected on these cells when compared to T cells reconstituted with the wild type CD3ζ chain (fig. 6d). These data indicated that the impairment of oligomeric TCR formation had a pronounced effect on the sensitivity of primary antigen-experienced T cells to antigen.

Discussion

We show here that antigen-experienced T cells, i.e. murine $CD4^+$ memory T cells and murine and human primed T cells have an increased proportion of TCR complexes organized into larger oligomeric TCR complexes, as compared to their naive counterparts. Unlike the TCR microclusters that form upon ligation with pMHC (Yokosuka and Saito, 2010), the TCR clusters studied here pre-exist, independent of TCR ligands, are of nanometer dimensions, and could therefore be named TCR nanoclusters. Using OVAp-specific OT-1^{tg} T cells, we show that the increase in TCR oligomer size is correlated with a greater sensitivity towards antigenic stimulation, suggesting that the reorganization of the TCR complexes is a mechanism by which effector and memory T cells acquire their increased antigen-sensitivity. Finally, using a mutant of CD3ζ that impairs oligomeric TCR formation, we provide direct evidence of the importance of oligomeric TCR complexes in the sensitivity of T cell lines and antigen-experienced primary T cells.

Our early studies on double TCR-transgenic mice, using FRET, co-modulation and co-precipitation techniques, showed that TCRs of different antigen specificity are physically associated (Fernandez-Miguel et al., 1999). BN-PAGE and immuno-gold EM analysis indicated that the TCR is expressed as a mixture of oligomers of different size in unstimulated resting T cells, ranging from single complexes to clusters of 20 or more TCR complexes arranged mainly in a linear manner (Schamel et al., 2005). By analysis of membrane sheets by EM, many membrane receptors have been seen to be non-randomly associated, forming “protein islands” supported by cholesterol and the underlying cytoskeleton (Lillemeier et al., 2006). The TCR is one such receptors, as demonstrated by two high-resolution confocal microscopy techniques (high-speed photoactivated localization microscopy and dual-color fluorescence cross-correlation spectroscopy), in combination with electron microscopy of membrane sheets (Lillemeier et al., 2009). It could be argued that the pre-existing TCR oligomers we detected by EM are artificially produced by the antibody used to detect the TCR clusters. However, a series of controls argues against this notion. First, T cells were fixed with an aldehyde before incubation with the anti-CD3 antibody and maintained at 0˚C throughout the whole procedure. Both these steps should block or limit the rearrangement of receptors in the membrane. Second, cholesterol extraction does not affect the density of the TCR in the membrane but it does disrupt the oligomeric TCRs (Schamel et al., 2005) arguing against an antibody-promoted effect. Third, the size of

the TCR oligomers differs for naive and antigen-experienced T cells, even if they are both analyzed with the same antibody. Fourth, the increase in size and number of oligomeric TCRs on antigen-experienced T cells can be detected with an independent method, namely BN-PAGE. Fifth, and more importantly, we demonstrate that oligomeric TCRs can be disrupted by genetically altering a single position in the transmembrane domain of the CD3ζ subunit, L19, having previously been predicted to participate in the formation of CD3ζ tetramers (Torres et al., 2002). Hence we believe our data does not simply reflect a technical artifact but rather, along with studies using a series of unrelated techniques (Lillemeier et al., 2009), this data shows that the TCR is expressed as pre-existing oligomers before the T cell is engaged by its pMHC ligand. Furthermore, the effect of the L19A mutation on sensitivity of antigen-experienced T cells suggests that the TCR is functionally multivalent in this population. However, TCRβ selection, positive selection and lineage commitment are not affected in OT-1^{tg} thymocytes expressing L19A CD3ζ, suggesting a minor or non-existent contribution of oligomeric TCRs in the thymus.

Soluble bivalent MHC ligands have been shown to bind better to previously activated mouse $2C^{tg}$ $CD8^+$ T cells than to their naive counterparts, suggesting that the distribution of the TCR changes after stimulation (Fahmy et al., 2001). We provide direct evidence here for such changes, and show that this leads to greater sensitivity for antigen. Interestingly, the bivalent MHC binding studies indicate the existence of uniform binding sites on naive $CD8^+$ $2C^{tg}$ T cells. This coincides remarkably with the observation that the overwhelming majority of gold clusters on naive mouse $CD4^+$ and $CD8^+$ T cells have a size of 1-3 particles. Due to the inefficiency of the gold labeling procedure, (only up to 10-20% of the total TCR is detected), we cannot be sure of whether the TCR is mainly expressed in naive T cells as monomers or as small oligomers. What is clear is that activation and differentiation into memory T cells is accompanied by an increase in the size of the oligomers and this could be the mechanism underlying the increased avidity of the TCR for bivalent pMHC ligands (Fahmy et al., 2001).

The increase in the size of oligomeric TCR complexes during their differentiation from naive to antigen-experienced T cells is a cell-inherent process that takes several days. This redistribution is maintained in the absence of antigen or continued contact with APCs, as the oligomeric TCR complexes can be detected on T cells that have been maintained in single cell suspensions. It is dependent on the

presence of cholesterol in the membrane, as both oligomeric TCR comlexes (Schamel et al., 2005) and strong MHC-binding (Drake and Braciale, 2001; Fahmy et al., 2001; Uhlin et al., 2003) are lost in cells exposed to methyl-β-cyclodextrin. An increase in membrane-associated cholesterol in antigen-experienced T cells could be important to permit the generation of larger TCR oligomers. Such lipid changes do occur upon stimulation of T cells with anti-TCR antibodies and are stably acquired by memory T cells *in vivo* (Brumeanu et al., 2007; Kersh et al., 2003). Changes in the lipid composition of the membrane would also explain why the increase in the size of TCR oligomers takes several days (see fig. 1d). In addition, protein-protein interactions may also play a role in the formation of TCR oligomers, as suggested by the effect of the L19A mutation. The outward position of the L19 residue in the transmembrane domain of CD3ζ (Call et al., 2006) and its role in the formation of CD3ζ tetramers *in vitro* (Torres et al., 2002), suggest that the L19A mutation disrupts the interaction between neighboring TCR complexes. Accordingly, the CD3ζ transmembrane domain would be part of the TCR-TCR interaction surfaces. In this regard, the effect of Cα mutants on the dimerization of TCRα/TCRβ chimeras containing the signaling cytoplasmic tail of the erythropoietin receptor described recently (Kuhns et al., 2010) indicates that the C and F strands of Cα could constitute part of the same interaction site, together with the transmembrane domain of CD3ζ, or constitute opposing interaction sites (Fig. 7).

How might oligomeric TCRs increase the sensitivity of T cells? T cell activation is dependent on the interaction with multivalent pMHC ligands (Boniface et al., 1998; Cochran et al., 2000), which induces a structural rearrangement in the TCR complex required for signaling (Minguet et al., 2007). Indeed, the MHC molecules on the cell surface of APCs can form clusters that may even be enriched for particular antigenic peptides (Anderson et al., 2000; Kropshofer et al., 2002). However, stimulation by adjacent MHC molecules presenting identical antigenic peptides does not appear to be absolutely required for T cell activation, as soluble bivalent MHC complexes presenting one antigenic peptide in combination with another unrelated peptide can stimulate T cells (Krogsgaard et al., 2005). Thus, a pMHC cluster in which at least one of the bound peptides is an agonist for the TCR of the interacting T cell could trigger activation of this T cell. TCR oligomers would enhance the avidity to such multimeric pMHC, which would be especially critical if an agonist peptide is presented next to low affinity self-peptides. In addition, TCR oligomers could allow spreading of TCR activation from the agonistic pMHC-engaged TCR to the adjacent ones. For example, this lateral spreading

could be mediated via lateral ITAM phosphorylation within the TCR oligomer by agonist pMHC-dependent Lck recruitment. Alternatively, the TCR itself could cause this lateral spreading. Conformational changes can serve as a means to transmit information on ligand binding to the cytoplasmic tails of the CD3 signaling subunits (Gil et al., 2002) Hence, TCR oligomers could facilitate signal spreading by permitting the transmission of the active conformation from agonist pMHC-contacted TCRs to others within the same oligomer (Schamel et al., 2006). Such a cooperative effect was recently demonstrated by expressing a conformational inactive mutant of CD3ε in T cells that carry an excess of endogenous wild type CD3ε (Martinez-Martin et al., 2009). Expression of the conformational inactive mutant prevents the active conformation from being adopted by the TCRs containing wild type CD3ε. Therefore, in addition to higher avidity for antigen derived from the multivalency of the TCR oligomers, the organization of the TCR into oligomeric structures would facilitate extensive cooperativity between agonist pMHC-engaged TCRs and TCRs engaged by self-peptide/MHC complexes. Accordingly, it would be plausible that previously activated and memory T cells would have greater antigen sensitivity than naive T cells because more and larger TCR oligomers would increase the chance of a multivalent TCR-MHC interaction and permit more extensive signal spreading.

In summary, our data provide evidence that the extent of antigen-independent oligomerization of the TCR increases in the transition from naive to antigen-experienced T cells and that this oligomerization of the TCR provides these antigen-experienced T cells with greater sensitivity. Future studies should focus on the molecular mechanisms that enable the formation and enrichment of oligomeric complexes, thereby providing a potential tool to strengthen or weaken T cell responses at will.

Materials and methods

Mice. C57BL/6 mice, CD3ζ-deficient mice (Love et al., 1993), (acquired from the Jackson Laboratories), OT-1^{tg} mice (Hogquist et al., 1994) and CD45.1-congenic C57BL/6 mice (kindly provided by Dr C. Ardavin, Centro Nacional de Biotecnología, Madrid) were maintained under SPF conditions at the animal facility of the 'Centro de Biología Molecular Severo Ochoa' in accordance with current national and European guidelines. All animal procedures were approved by the ethical committee of the 'Consejo Superior de Investigaciones Científicas'.

T cell purification and culture. Human PBLs were obtained via density centrifugation of whole blood and grown in RPMI with 10% FCS in the presence of PHA (2 μg/ml). After two days, cultures were washed in PBS and expanded for three more days in medium containing IL2. At this point >90% of the culture was positive for staining with the anti-CD3ε mAb OKT3. Unstimulated human peripheral blood T cells were enriched from whole blood by density centrifugation, followed by panning of macrophages and monocytes on tissue culture plates, and the removal of B cells through nylon wool columns. The remaining population contained over 80% of T cells. Murine CD4^{+} CD44^{hi}CD62L^{lo} and CD62L^{hi}CD44^{lo} T cells were enriched from the spleen and superficial lymph nodes of C57BL/6 mice using mouse CD4 memory and naive T cell enrichment kits (R&D Systems). Naive OT-1^{tg} T cells were purified by depleting lymph nodes from OT-1^{tg} mice of CD4^{+} and CD24^{+} cells using magnetic beads (Dynal Biotech). Previously stimulated OT-1^{tg} T cells were generated by stimulating spleen cells of OT-1^{tg} mice with 10 pM of OVAp (SIINFEKL, synthesized in our proteomic facility via f-moc chemistry) and anti-CD28 (0.5 μg/ml, clone 37.51, BD Pharmingen) in RPMI-10% FCS, supplemented with 2 mM glutamine, 1 mM sodium pyruvate and 1x10^{-5} M β-mercaptoethanol (R10 medium). After two days, the cells were washed and cultured for six more days in fresh medium supplemented with saturating amounts of recombinant IL2.

Immunogold labeling, replica preparation and EM analysis. Immunogold labeled cell surface replicas were obtained as described previously (Pinto da Silva and Kan, 1984; Schamel et al., 2005). T cell preparations were washed in PBS and fixed in 1% paraformaldehyde, before they were labeled on ice with the anti-human CD3 mAb

OKT3 or the anti-murine CD3 mAb 145-2C11 and 10 nm gold-conjugated protein A (Sigma-Aldrich; Cell Microscopy Center, University Medical Center Utrecht). Labeled cells were adhered to poly-L-lysine-coated mica strips and post-fixed with 0.1% glutaraldehyde. Samples were covered with another mica sheet and plunge frozen in liquid propane. Frozen sandwiches were split under liquid nitrogen and mounted on the sample table of a Balzers400T freeze fracture (FF) apparatus. Samples were placed in the FF unit cooled at -150 ºC and etched for 12 min to remove excess of ice, after switching the stage temperature from -150 ºC to -90 ºC. The samples were shaded with platinum (2 nm at 45º angle) and coated with carbon (20 nm at 90º angle) before they were floated overnight on a domestic bleach solution to remove the organic material. The replicas were extensively washed in distilled water, mounted on 400 mesh copper grids and examined on a JEM1010 electron microscope (Jeol, Japan) operating at 80 kV. Images were taken with a slow scan CCD camera (Bioscan, Gatan, Pleasanton, CA).

BN-PAGE, IP, SDS-PAGE and Western blotting. Membrane fractions for BN PAGE were prepared by disrupting T cells with a Dounce homogenizer in hypotonic buffer (10 mM HEPES pH 7.4, 42 mM KCl, 5 mM MgCl2, and protease inhibitors) and pelleting the membranes by ultracentrifugation at 150,000 g. The membranes were lysed in 250 µl BN lysis buffer (500 mM 6-aminohexanoic acid, 20 mM NaCl, 10% glycerol, 2 mM EDTA, 1% Brij96, 20 mM BisTris pH7.0, 10 µg/ml leupeptin, 10 µg/ml aprotinin, 1 mM PMSF), and BN-PAGE gradient gels (4%–9%) were prepared and run as described (Schagger and von Jagow, 1991; Swamy et al., 2006). Ferritin was used as the marker protein in its 24-mer and 48-mer forms (f1, 440 kDa; f2, 880 kDa). MA5.8 cells were lysed in Brij lysis buffer (0.33% Brij96, 150 mM NaCl, 20 mM Tris-HCl pH 7.8), and protease inhibitors), followed by immunoprecipiation with anti-CD3ζ serum (448) (San Jose et al., 1998) or anti-CD3 mAb (145-2C11) and protein G sepharose beads. SDS-PAGE and Western blotting were performed according to standard protocols, and the membranes were probed with the anti-CD3ζ serum and the anti-CD3ε mAb M-20 (Santa Cruz) and visualized by ECL detection. Quantification was performed on ECL autoradiography films using ImageJ software.

Generation of mutated CD3ζ chains. The L9A and L19A mutations of CD3ζ were introduced by PCR-based site-specific mutation protocols using the pGEM3z-CD3ζ

plasmid as template in combination with the QuickChange-XL kit (Stratagene). L9A and L19A mutant and wildtype CD3ζ-coding sequences were re-amplified with flanking oligos containing XhoI restriction sites and inserted into the XhoI site of pSRα. The CD3ζ-GFP fusion constructs were generated by introducing a BglII site directly upstream of the stop codon of wild type and L19A mutant CD3ζ by PCR, cloning of the XhoI-BglII fragment directly upstream of EGFP of the XhoI-BamHI-digested pLEGFP-N1 retroviral vector (Clontech). CD3ζ-GFP fusion constructs were finally cloned into the lentiviral expression vector pHRSIN-CSGW-dlNotI (kindly provided by Dr J.A. Pintor, CABIMER-CSIC, Sevilla) by introducing a NotI site directly downstream of the stop codon of the CD3ζ-GFP fusion constructs in pLEGFP-N1, and cloning the BglII-NotI fragment into BamHI-NotI-digested pHRSIN-CSGW-dlNotI. All constructs generated by PCR were verified by DNA sequencing.

MA5.8 reconstitution. MA5.8 cells were transfected with the pSRα-CD3ζ constructs by electroporation and stably expressing pools of cells were obtained through selection with geneticin (G418) for 3 weeks. CD3ζ-GFP fusion protein expressing MA5.8 cells were obtained by transducing these cells with lentiviral particles (see below). For biochemical and EM analysis of these cells, populations were sorted for GFP^+ cells on a FACSVantage cell sorter (Becton-Dickinson).

Bone marrow reconstitution. Lentiviral particles were produced by cotransfecting HEK 293T cells with the pHRSIN CSGW-dlNotI-CD3ζ vectors and the pCMVΔR8.2 and pMDG plasmids (Zufferey et al., 1997) with JetPEI reagent (PolyPlus Transfection). Culture supernatants obtained after 48 hours in culture were used to transduce target cells. For transduction of bone marrow cells, 8-10 week old $CD3\zeta^{o/o}OT\text{-}1^{tg}$ mice were inoculated i.p. with 5-fluorouracil (150 mg/kg) and were sacrificed two days later. Bone marrow cells were collected from the femurs and cultured for 12 hours at 37°C in Iscove's medium supplemented with 10% FBS, 25 ng/ml IL-7, 25 ng/ml IL-6, 50 ng/ml SCF, and 50 ng/ml Flt3-ligand (all cytokines from Peprotech). Bone marrow cells were then transduced by addition of filtered 293T cell supernatants, followed by centrifugation for 90 min at 975g and 32 °C in 24-well culture plates in presence of 8 μg/ml polybrene. The cells were harvested 24 hours later, washed and i.v. injected in sub-lethally irradiated (6 Gy) C57BL/6 or C57BL/6 CD45.1-congenic recipient mice (3-

$5x10^6$ cells/mouse). Recipient mice were kept on drinking water supplemented with tetracycline (200 μg/ml, Sigma) for 6-8 weeks before sacrifice and analysis.

T cell stimulation assays. Thioglycolate-induced primary macrophages from C57BL/6 mice were grown in R10 medium at $7x10^4$ cells per well in flat bottom 96 well plates the day before the stimulation assay. The macrophages were loaded with OVAp for 7 to 10 hours and they were then washed with PBS before adding $0.5\text{-}2x10^5$ cells per well in R10 medium. Biotinylated K^bOVAp pentamers (ProImmune) and K^bOVAp tetramers (Daniels and Jameson, 2000), generated by incubation of pre-folded c-terminally biotinylated soluble K^bOVAp complexes (kindly provided by Dr E. Palmer, University of Basel) with unlabeled streptavidin, were added to $2\text{-}5x10^5$ lymph node cells at the start of culture in R10 medium in round bottom 96 well plates. MA5.8 cells were stimulated at $1x10^5$ cells per well in flat bottom 96 well plates containing a monolayer of $5x10^4$ I-E^k- and CD80-transfected DCEK fibroblasts (a gift of Dr R. Germain, NIH, Bethesda, MD) loaded with MCCp (ANERADLIAYLKQATK, synthesized in our center by f-moc chemistry). T cells were cultured for the times indicated before assessing the expression of CD25 and CD69 and IFNγ production. To measure intracellular IFNγ, cells were treated for the last 4 hours of culture with Brefeldin A (BFA, 2.5 μg/ml).

Flow cytometry. Cells were pre-incubated with the anti CD16/32-specific mAb 2.4G2 in PBS, 1% BSA, 0.02% sodium azide before they were labeled with saturating amounts of the indicated fluorochrome-labeled or biotinylated mAbs and, where applicable, fluorochrome-labeled streptavidin (reagents purchased from BD Pharmingen, eBioscience, Immunotools and Miltenyi). To detect intracellular IFNγ, BFA-treated cells were surface-stained before fixation and permeabilization using a commercial kit (BD Pharmingen), and they were then stained with an anti-murine IFNγ mAb. Labeled cells were acquired on a FACSCalibur or FACSCanto II flow cytometer (Becton-Dickinson) and the data analyzed with FlowJo software (TreeStar).

Acknowledgments

We thank E. Palmer for the generous supply of the K^b-OVA tetramers, C. Prieto and T. Gomez for excellent maintenance of the animal colony, and M. Nieto and M. Sefton for critical reading of the manuscript. This work was supported by grants SAF2006-01391 from the CICYT, and FP7/2007-2013 (Sybilla) from the EU to BA and BFU2006-04031 from the Ministerio de Ciencia e Innovación to HMvS. WWAS was supported by the Deutsche Forschungsgemeinschaft through the Emmy Noether program, the excellence cluster bioss and the SFB620. MF is a recipient of a FPI pre-doctoral fellowship (ref BES-2007-15570) from the Ministerio de Ciencia e Innovación. HMvS was supported by a Ramón y Cajal fellowship from the Ministerio de Educación y Ciencia during the initial stages of this project.

References

Alarcon, B., Swamy, M., van Santen, H. M., and Schamel, W. W. (2006). T-cell antigen-receptor stoichiometry: pre-clustering for sensitivity. EMBO Rep *7*, 490-495.
Anderson, H. A., Hiltbold, E. M., and Roche, P. A. (2000). Concentration of MHC class II molecules in lipid rafts facilitates antigen presentation. Nat Immunol *1*, 156-162.
Askonas, B. A., Mullbacher, A., and Ashman, R. B. (1982). Cytotoxic T-memory cells in virus infection and the specificity of helper T cells. Immunology *45*, 79-84.
Bachmann, M. F., Barner, M., Viola, A., and Kopf, M. (1999). Distinct kinetics of cytokine production and cytolysis in effector and memory T cells after viral infection. Eur J Immunol *29*, 291-299.
Beverley, P. C., Daser, A., Michie, C. A., and Wallace, D. L. (1992). Functional subsets of T cells defined by isoforms of CD45. Biochem Soc Trans *20*, 184-187.
Boniface, J. J., Rabinowitz, J. D., Wulfing, C., Hampl, J., Reich, Z., Altman, J. D., Kantor, R. M., Beeson, C., McConnell, H. M., and Davis, M. M. (1998). Initiation of signal transduction through the T cell receptor requires the multivalent engagement of peptide/MHC ligands [corrected]. Immunity *9*, 459-466.
Brumeanu, T. D., Preda-Pais, A., Stoica, C., Bona, C., and Casares, S. (2007). Differential partitioning and trafficking of GM gangliosides and cholesterol-rich lipid rafts in thymic and splenic CD4 T cells. Mol Immunol *44*, 530-540.
Bruno, L., Kirberg, J., and von Boehmer, H. (1995). On the cellular basis of immunological T cell memory. Immunity *2*, 37-43.
Budd, R. C., Cerottini, J. C., Horvath, C., Bron, C., Pedrazzini, T., Howe, R. C., and MacDonald, H. R. (1987). Distinction of virgin and memory T lymphocytes. Stable acquisition of the Pgp-1 glycoprotein concomitant with antigenic stimulation. J Immunol *138*, 3120-3129.
Busch, D. H., and Pamer, E. G. (1999). T cell affinity maturation by selective expansion during infection. J Exp Med *189*, 701-710.
Call, M. E., Pyrdol, J., Wiedmann, M., and Wucherpfennig, K. W. (2002). The organizing principle in the formation of the T cell receptor-CD3 complex. Cell *111*, 967-979.
Call, M. E., Schnell, J. R., Xu, C., Lutz, R. A., Chou, J. J., and Wucherpfennig, K. W. (2006). The structure of the zetazeta transmembrane dimer reveals features essential for its assembly with the T cell receptor. Cell *127*, 355-368.
Cochran, J. R., Cameron, T. O., and Stern, L. J. (2000). The relationship of MHC-peptide binding and T cell activation probed using chemically defined MHC class II oligomers. Immunity *12*, 241-250.
Croft, M., Bradley, L. M., and Swain, S. L. (1994). Naive versus memory CD4 T cell response to antigen. Memory cells are less dependent on accessory cell costimulation and can respond to many antigen-presenting cell types including resting B cells. J Immunol *152*, 2675-2685.
Cho, B. K., Wang, C., Sugawa, S., Eisen, H. N., and Chen, J. (1999). Functional differences between memory and naive CD8 T cells. Proc Natl Acad Sci U S A *96*, 2976-2981.
Daniels, M. A., and Jameson, S. C. (2000). Critical role for CD8 in T cell receptor binding and activation by peptide/major histocompatibility complex multimers. J Exp Med *191*, 335-346.
Drake, D. R., 3rd, and Braciale, T. J. (2001). Cutting edge: lipid raft integrity affects the efficiency of MHC class I tetramer binding and cell surface TCR arrangement on CD8+ T cells. J Immunol *166*, 7009-7013.

Ericsson, P. O., Orchansky, P. L., Carlow, D. A., and Teh, H. S. (1996). Differential activation of phospholipase C-gamma 1 and mitogen-activated protein kinase in naive and antigen-primed CD4 T cells by the peptide/MHC ligand. J Immunol *156*, 2045-2053.
Fahmy, T. M., Bieler, J. G., Edidin, M., and Schneck, J. P. (2001). Increased TCR avidity after T cell activation: a mechanism for sensing low-density antigen. Immunity *14*, 135-143.
Fernandez-Miguel, G., Alarcon, B., Iglesias, A., Bluethmann, H., Alvarez-Mon, M., Sanz, E., and de la Hera, A. (1999). Multivalent structure of an alphabetaT cell receptor. Proc Natl Acad Sci U S A *96*, 1547-1552.
Gil, D., Schamel, W. W., Montoya, M., Sanchez-Madrid, F., and Alarcon, B. (2002). Recruitment of Nck by CD3 epsilon reveals a ligand-induced conformational change essential for T cell receptor signaling and synapse formation. Cell *109*, 901-912.
Hogquist, K. A., Jameson, S. C., Heath, W. R., Howard, J. L., Bevan, M. J., and Carbone, F. R. (1994). T cell receptor antagonist peptides induce positive selection. Cell *76*, 17-27.
Kersh, E. N., Kaech, S. M., Onami, T. M., Moran, M., Wherry, E. J., Miceli, M. C., and Ahmed, R. (2003). TCR signal transduction in antigen-specific memory CD8 T cells. J Immunol *170*, 5455-5463.
Kimachi, K., Croft, M., and Grey, H. M. (1997). The minimal number of antigen-major histocompatibility complex class II complexes required for activation of naive and primed T cells. Eur J Immunol *27*, 3310-3317.
Krogsgaard, M., Li, Q. J., Sumen, C., Huppa, J. B., Huse, M., and Davis, M. M. (2005). Agonist/endogenous peptide-MHC heterodimers drive T cell activation and sensitivity. Nature *434*, 238-243. Epub 2005 Feb 2020.
Kropshofer, H., Spindeldreher, S., Rohn, T. A., Platania, N., Grygar, C., Daniel, N., Wolpl, A., Langen, H., Horejsi, V., and Vogt, A. B. (2002). Tetraspan microdomains distinct from lipid rafts enrich select peptide-MHC class II complexes. Nat Immunol *3*, 61-68.
Kuhns, M. S., Girvin, A. T., Klein, L. O., Chen, R., Jensen, K. D., Newell, E. W., Huppa, J. B., Lillemeier, B. F., Huse, M., Chien, Y. H.*, et al.* (2010). Evidence for a functional sidedness to the {alpha}{beta}TCR. Proc Natl Acad Sci U S A *107*, 5094-5099.
Lee, W. T., and Vitetta, E. S. (1991). The differential expression of homing and adhesion molecules on virgin and memory T cells in the mouse. Cell Immunol *132*, 215-222.
Lillemeier, B. F., Mortelmaier, M. A., Forstner, M. B., Huppa, J. B., Groves, J. T., and Davis, M. M. (2009). TCR and Lat are expressed on separate protein islands on T cell = concatenate during activation. Nat Immunol *11*, 90-96.
Lillemeier, B. F., Pfeiffer, J. R., Surviladze, Z., Wilson, B. S., and Davis, M. M. (2006). Plasma membrane-associated proteins are clustered into islands attached to the cytoskeleton. Proc Natl Acad Sci U S A *103*, 18992-18997.
London, C. A., Lodge, M. P., and Abbas, A. K. (2000). Functional responses and costimulator dependence of memory CD4+ T cells. J Immunol *164*, 265-272.
Love, P. E., Shores, E. W., Johnson, M. D., Tremblay, M. L., Lee, E. J., Grinberg, A., Huang, S. P., Singer, A., and Westphal, H. (1993). T cell development in mice that lack the zeta chain of the T cell antigen receptor complex. Science *261*, 918-921.
Malherbe, L., Hausl, C., Teyton, L., and McHeyzer-Williams, M. G. (2004). Clonal selection of helper T cells is determined by an affinity threshold with no further skewing of TCR binding properties. Immunity *21*, 669-679.

Martinez-Martin, N., Risueno, R. M., Morreale, A., Zaldivar, I., Fernandez-Arenas, E., Herranz, F., Ortiz, A. R., and Alarcon, B. (2009). Cooperativity between T cell receptor complexes revealed by conformational mutants of CD3epsilon. Sci Signal *2*, ra43.
Minguet, S., Swamy, M., Alarcon, B., Luescher, I. F., and Schamel, W. W. (2007). Full activation of the T cell receptor requires both clustering and conformational changes at CD3. Immunity *26*, 43-54. Epub 2006 Dec 2021.
Novak, T. J., Farber, D., Leitenberg, D., Hong, S. C., Johnson, P., and Bottomly, K. (1994). Isoforms of the transmembrane tyrosine phosphatase CD45 differentially affect T cell recognition. Immunity *1*, 109-119.
Pihlgren, M., Dubois, P. M., Tomkowiak, M., Sjogren, T., and Marvel, J. (1996). Resting memory CD8+ T cells are hyperreactive to antigenic challenge in vitro. J Exp Med *184*, 2141-2151.
Pinto da Silva, P., and Kan, F. W. (1984). Label-fracture: a method for high resolution labeling of cell surfaces. J Cell Biol *99*, 1156-1161.
Rogers, P. R., Dubey, C., and Swain, S. L. (2000). Qualitative changes accompany memory T cell generation: faster, more effective responses at lower doses of antigen. J Immunol *164*, 2338-2346.
San Jose, E., Sahuquillo, A. G., Bragado, R., and Alarcon, B. (1998). Assembly of the TCR/CD3 complex: CD3 epsilon/delta and CD3 epsilon/gamma dimers associate indistinctly with both TCR alpha and TCR beta chains. Evidence for a double TCR heterodimer model. Eur J Immunol *28*, 12-21.
Schagger, H., and von Jagow, G. (1991). Blue native electrophoresis for isolation of membrane protein complexes in enzymatically active form. Anal Biochem *199*, 223-231.
Schamel, W. W., Arechaga, I., Risueno, R. M., van Santen, H. M., Cabezas, P., Risco, C., Valpuesta, J. M., and Alarcon, B. (2005). Coexistence of multivalent and monovalent TCRs explains high sensitivity and wide range of response. J Exp Med *202*, 493-503. Epub 2005 Aug 2008.
Schamel, W. W., Risueno, R. M., Minguet, S., Ortiz, A. R., and Alarcon, B. (2006). A conformation- and avidity-based proofreading mechanism for the TCR-CD3 complex. Trends Immunol *27*, 176-182. Epub 2006 Mar 2009.
Slifka, M. K., and Whitton, J. L. (2001). Functional avidity maturation of CD8(+) T cells without selection of higher affinity TCR. Nat Immunol *2*, 711-717.
Sussman, J. J., Bonifacino, J. S., Lippincott-Schwartz, J., Weissman, A. M., Saito, T., Klausner, R. D., and Ashwell, J. D. (1988). Failure to synthesize the T cell CD3-zeta chain: structure and function of a partial T cell receptor complex. Cell *52*, 85-95.
Swamy, M., Minguet, S., Siegers, G. M., Alarcon, B., and Schamel, W. W. (2007). A native antibody-based mobility-shift technique (NAMOS-assay) to determine the stoichiometry of multiprotein complexes. J Immunol Methods *324*, 74-83.
Swamy, M., Siegers, G. M., Minguet, S., Wollscheid, B., and Schamel, W. W. (2006). Blue native polyacrylamide gel electrophoresis (BN-PAGE) for the identification and analysis of multiprotein complexes. Sci STKE *2006*, pl4.
Torres, J., Briggs, J. A., and Arkin, I. T. (2002). Convergence of experimental, computational and evolutionary approaches predicts the presence of a tetrameric form for CD3-zeta. J Mol Biol *316*, 375-384.
Uhlin, M., Masucci, M. G., and Levitsky, V. (2003). Pharmacological disintegration of lipid rafts decreases specific tetramer binding and disrupts the CD3 complex and CD8 heterodimer in human cytotoxic T lymphocytes. Scand J Immunol *57*, 99-106.

Veiga-Fernandes, H., Walter, U., Bourgeois, C., McLean, A., and Rocha, B. (2000). Response of naive and memory CD8+ T cells to antigen stimulation in vivo. Nat Immunol *1*, 47-53.
Yokosuka, T., and Saito, T. (2010). The Immunological Synapse, TCR Microclusters, and T Cell Activation. Curr Top Microbiol Immunol *340*, 81-107.
Zehn, D., Lee, S. Y., and Bevan, M. J. (2009). Complete but curtailed T-cell response to very low-affinity antigen. Nature *458*, 211-214.
Zimmermann, C., Prevost-Blondel, A., Blaser, C., and Pircher, H. (1999). Kinetics of the response of naive and memory CD8 T cells to antigen: similarities and differences. Eur J Immunol *29*, 284-290.
Zufferey, R., Nagy, D., Mandel, R. J., Naldini, L., and Trono, D. (1997). Multiply attenuated lentiviral vector achieves efficient gene delivery in vivo. Nat Biotechnol *15*, 871-875.

Figure legends

Figure 1 - Distribution of TCRs on previously stimulated and freshly isolated human peripheral blood T cells. **(A)**. High magnification images (100,000x) showing the distribution of gold particles on the cell surface replicas (scale bar: 50 nm). **(B)**. Quantification (mean +/- sem) of gold particles in clusters of the indicated sizes for freshly isolated (grey bars) and previously stimulated (black bars) human T cells. The inset shows the distribution of gold between clusters of 1, 2, 3, 4 or more particles and the statistical analysis (1-tailed Student's T test: * $p<0.05$; ** $p<0.01$; *** $p<0.001$). Replicas of 19 PHA-activated T cells (9414 particles) and 9 freshly isolated T cells (2707 particles) were counted. **(C)**. T cells were purified from blood of a healthy human donor, and an aliquot of the freshly isolated cells was frozen. The rest of the cells were stimulated for 2 days with PHA and subsequently with IL2 for a further 7 days. The cells were harvested, frozen and membrane fractions were prepared from stimulated and non-stimulated cells. The sizes of the Brij96-solublized TCRs were analyzed by BN-PAGE and anti-CD3ζ immunoblotting. The marker protein is ferritin (f1, 440 and f2, 880 kDa forms). **(D)**. The same experiment as in C was performed, but aliquots of the stimulated cells were taken at various time points during their expansion. The ratio of the oligomeric and monomeric TCRs was quantified and plotted as a function of time (h, hour; d, day).

Figure 2 - Incidence of oligomeric TCR complexes on murine $CD62L^{hi}CD44^{lo}$ and $CD44^{hi}CD62L^{lo}$ $CD4^+$ T cells. **(A)**. Enrichment of $CD62L^{hi}$ and $CD44^{hi}$ $CD4^+$ T cell populations. The overlay plot shows the FSC profiles of the $CD62L^{hi}$ and $CD44^{hi}$ $CD4^+$ T cells. **(B)**. High magnification images (100,000x) of cell surface replicas of CD62Lhi and CD44hi CD4+ T cells (scale bar: 100 nm). **(C)**. Quantitative analysis (mean +/- sem) of distribution of gold particles between clusters of the indicated sizes for CD62Lhi (grey bars) and CD44hi (black bars) CD4+ T cells. The inset shows the distribution between clusters of 1, 2, 3, 4 or more particles and statistical analysis (* $p<0.05$; ** $p<0.01$; *** $p<0.001$). Quantification of 5 replicas of $CD62L^{hi}$ cells (2718 particles) and 5 $CD44^{hi}$ cells (3198 particles).

Figure 3 - Analysis of naive and previously stimulated OT-1^{tg} T cells. **(A)**. Phenotype and purity of naive and previously stimulated OT-1^{tg} T cell populations. **(B)**. High

magnification images (100,000x) of cell surface replicas of naive and previously stimulated OT-1 T^{tg} cells (scale bar: 100 nm). **(C)**. Quantification (mean +/- sem) of the gold particles on naive (grey bars) and previously stimulated (black bars) OT-1^{tg} T cells. The inset shows the distribution of gold particles between clusters of 1, 2, 3, 4 or more particles, and the statistical analysis (* $p<0.05$; ** $p<0.01$; *** $p<0.001$). Quantification of 10 naive cells (3733 particles) and 9 previously stimulated cells (2928 particles) is shown. **(D)**. Expression of CD25 (upper panel) and IFNγ production (lower panel) by naive and previously stimulated OT-1^{tg} T cells (open and black circles, respectively) after overnight stimulation with OVAp presented by macrophages. **(E)**. Expression of CD69 (upper panel) and IFNγ production (lower panel) by naive and previously stimulated OT-1^{tg} T cells (open and black circles, respectively) upon stimulation with an H-$2K^b$-OVA pentamer for 3 and 24 hours, respectively. Data are representative of at least 2 experiments.

Figure 4 - Further skewing towards larger oligomeric TCR complexes in re-activated OT-1^{tg} memory T cells. **(A)**. Phenotypic comparison of OT-1^{tg} memory T cells generated *in vivo*. The dot plot shows the proportion of $CD45.2^+CD8^+$ OT-1^{tg} T cells in the superficial lymph nodes of a $CD45.1^+$ recipient 6 weeks after adoptive transfer of naïve $CD45.2^+$ OT-1^{tg} T cells and OVAp-loaded DCs. Overlay plots compare the cell size and expression level of the molecules indicated on $CD45.2^+CD8^+$ lymph node cells from the CD45.1 recipient (black lines) and a non-manipulated $CD45.2^+$ OT-1^{tg} mouse (grey lines). **(B)**. Expression of CD25 and IFNγ production by memory and naive OT-1^{tg} T cells (black and open circles, respectively) after a 2 days of stimulation with H-$2K^b$OVAp tetramer. Data are representative of 3 experiments **(C)**. Quantification (mean +/- sem) of gold particles on cell surface replicas of naive and memory OT-1^{tg} T cell-derived cells, stimulated and grown *in vitro* for seven days (grey and black bars, respectively). The inset shows the distribution of gold particles between clusters of 1, 2, 3, 4 or more particles, and the statistical analysis (* $p<0.05$; ** $p<0.01$; *** $p<0.001$). Quantification of replicas of 7 naive cells (4284 particles) and 7 memory cells (5491 particles).

Figure 5 - A mutation in the transmembrane region of CD3ζ impairs oligomeric TCR formation. **(A).** Representation of the transmembrane region of the CD3ζ dimer, as determined by NMR (Call et al., 2006). The α-helix forming backbone is shown as a

ribbon diagram with all amino acids implicated in tetramer formation represented in blue and with side chain residues as lines. The L9 and L19 residues are indicated and their side chains represented as sticks. The amino acid sequences of wild type and L9A and L19A CD3ζ are shown below. **(B)**. Flow cytometric measurement of CD3ε expression by MA5.8 cells (filled grey histogram), 2B4 cells (dashed black line), and MA5.8 cells transfected with wild type CD3ζ (grey line), L9A CD3ζ (dashed grey line) and L19A CD3ζ (black line). **(C)**. Assembly of wild type or L19A CD3ζ chains within the TCR complex. Whole lysates or immunoprecipates with the indicated antibodies were run on non-reducing SDS gels, and immunoblots were probed with the antibodies indicated. **(D)**. Quantification (mean +/- sem) of the TCR complex in oligomeric clusters on MA5.8 cells reconstituted with wild type (black bars) or L19A CD3ζ (grey bars). The inset shows the distribution of gold particles between clusters of 1, 2, 3, 4 or more particles and the statistical analysis (* $p<0.05$; ** $p<0.01$; *** $p<0.001$). Quantification of replicas of 15 WT CD3ζ-reconstituted cells (12041 particles) and 21 L19A CD3ζ-reconstituted cells (8348 particles) is shown. **(E)**. Cell surface expression of CD69 (upper panel) and IFNγ production (lower panel) by wild type (black circles) or L19A CD3ζ (open circles) reconstituted MA5.8 cells after overnight stimulation with MCCp. Data are representative of 2 experiments.

Figure 6 - The role of oligomeric TCR complexes *in vivo*. **(A)**. Differentiation capacity of thymocytes from CD3ζ-deficient, OT-1^{tg} bone marrow precursors transduced with the indicated constructs. **(B)**. Expression of the L19A CD3ζ-GFP chain permits the generation of naive OT-1^{tg} $CD8^+$ T cells. Overlay plots show expression of the molecules indicated on $V\alpha2^+$ cells of OT-1^{tg} mice (shaded histogram) and $V\alpha2^+GFP^+$ cells from wild type (dashed black line) and L19A (grey line) CD3ζ-GFP reconstituted animals. **(C)**. Functional analysis of WT (black circles) or L19A (open circles) CD3ζ-expressing T cells obtained by previous stimulation and expansion in presence of IL2. Cells were re-stimulated overnight with OVAp-loaded macrophages or with K^b-OVA tetramers and CD69 (top panel) and IFNγ production (bottom panel) were measured by flow cytometry. IFNγ production index is the product of the percentage of $IFN\gamma^+$ cells and the MFI of the IFNγ signal. **(D)**. Quantification (mean +/- sem) of TCR complex oligomer distribution on the cell surface of T lymphoblasts expressing WT (black bars) or L19A (grey bars) CD3ζ-GFP chains. The inset shows the distribution of gold particles between clusters of 1, 2, 3, 4 or more particles and statistical analysis (*

$p<0.05$; ** $p<0.01$; *** $p<0.001$). Quantification of 7 WT CD3ζ-GFP reconstituted cells (3137 particles) and 7 L19A CD3ζ-GFP reconstituted cells (4257 particles) is shown. Data are representative of 4 independent reconstitutions and a total of 6 WT and 6 L19A reconstituted animals.

Figure 7 - Models of CD3ζ-dependent TCR oligomerization. **(A).** Oligomerization via interactions between individual TCR complexes (boxes) dependent on a heterotypic, L19-dependent interaction between CD3ζ dimers (A-face) and another, as yet undefined TCR component (B-face) (top line) or on the alternation of homotypic, L19-dependent interactions between CD3ζ dimers and homotypic interactions between the other TCR components (bottom line). The B-face could be formed primarily by the Cα domain, according to recent findings that the C and F strands of Cα play an important role in the dimerization of TCRαβ heterodimers (Kuhns et al., 2010). **(B)**. TCR oligomerization mediated by concatenation of homotypic L19-dependent interactions between CD3ζ dimers. This model assumes that due to its symmetry, the CD3ζ dimer can interact on both sides with adjacent CD3ζ dimers. This model is compatible with that of Davis and colleagues (Kuhns et al., 2010), since the A-face could consist of both the Cα ectodomain and the transmembrane domain of CD3ζ. The lower part of the figure provides a hypothetical ordering of the transmembrane regions (circles) of the TCR components indicated, taking into account the proposed orientation of these segments in digitonin-solubilized ER microsomes (Call et al., 2002) and making it compatible with the data of Davis and colleagues (Kuhns et al., 2010). The red squares indicate the interaction between the CD3ζ dimers and the dashed lines the interaction face between the ectodomais of Cα.

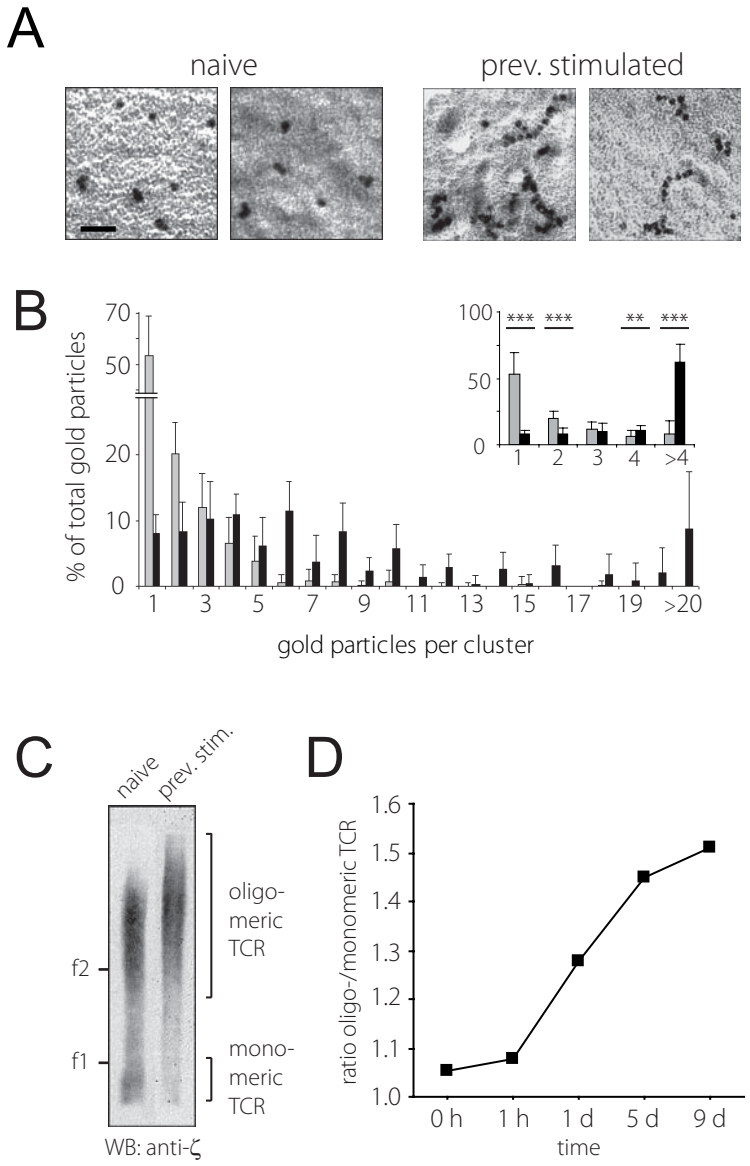
A
naive
prev. stimulated
B
% of total gold particles
gold particles per cluster
***
***
**
***
C
naive
prev. stim.
oligo-
meric
TCR
mono-
meric
TCR
f2
f1
WB: anti-ζ
D
ratio oligo-/monomeric TCR
time
0 h
1 h
1 d
5 d
9 d

Figure 1

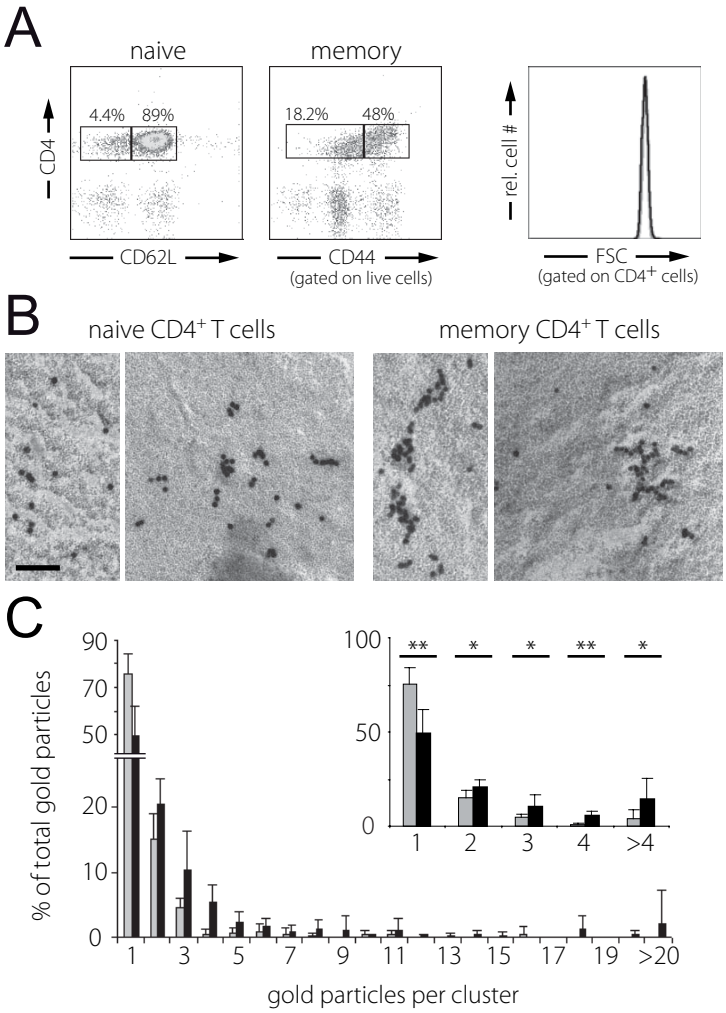
A
naive
memory
4.4%
89%
18.2%
48%
CD4
CD62L
CD44
(gated on live cells)
rel. cell #
FSC
(gated on CD4+ cells)
B
naive CD4+ T cells
memory CD4+ T cells
C
% of total gold particles
gold particles per cluster
**
*
*
**
*
1
2
3
4
>4

Figure 2

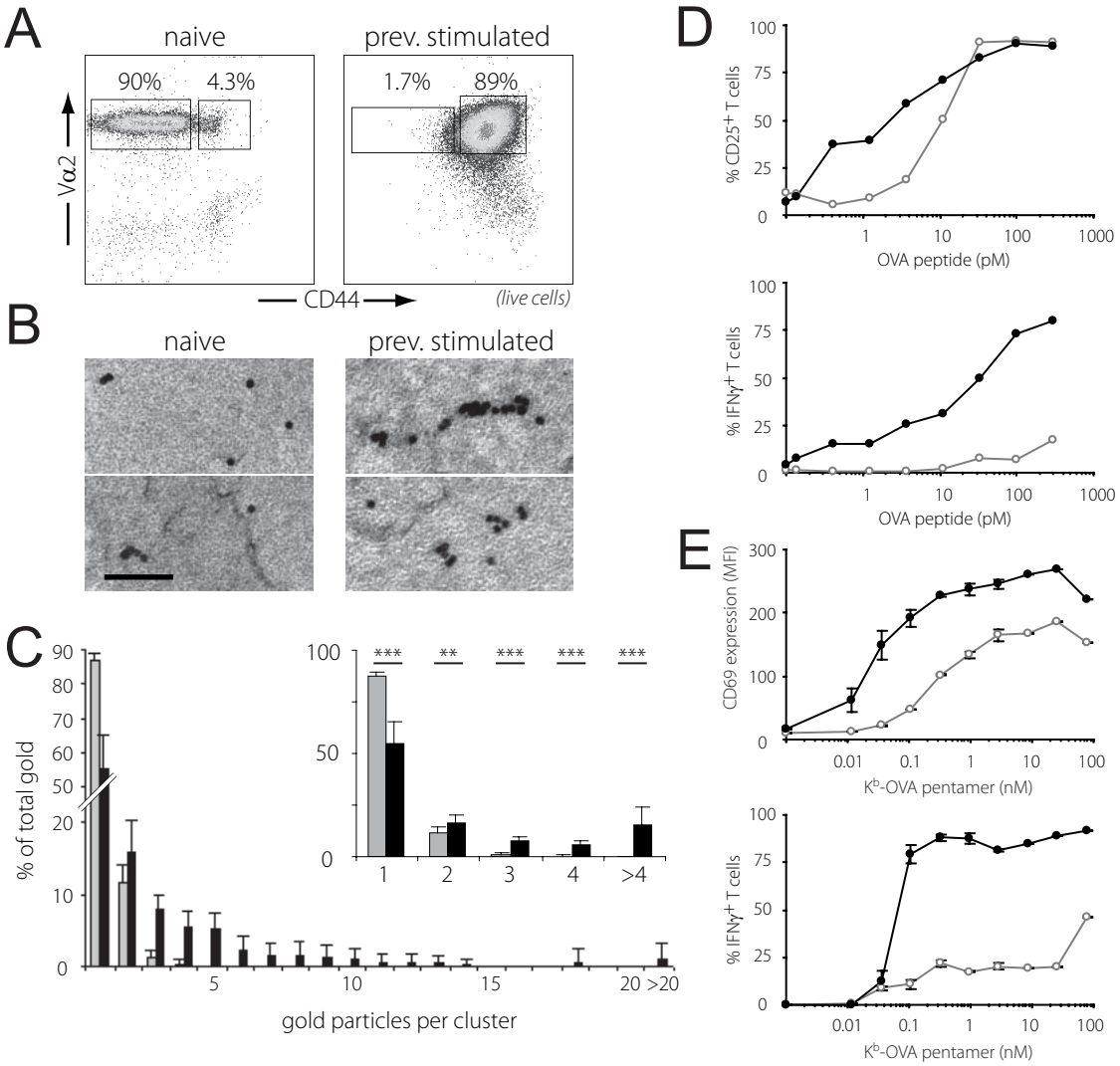
A
naive
prev. stimulated
90%
4.3%
1.7%
89%
Vα2
CD44
(live cells)
B
naive
prev. stimulated
C
% of total gold
gold particles per cluster
***
**
***
***
***
1
2
3
4
>4
D
% CD25+ T cells
OVA peptide (pM)
% IFNγ+ T cells
OVA peptide (pM)
E
CD69 expression (MFI)
Kb-OVA pentamer (nM)
% IFNγ+ T cells
Kb-OVA pentamer (nM)

Figure 3

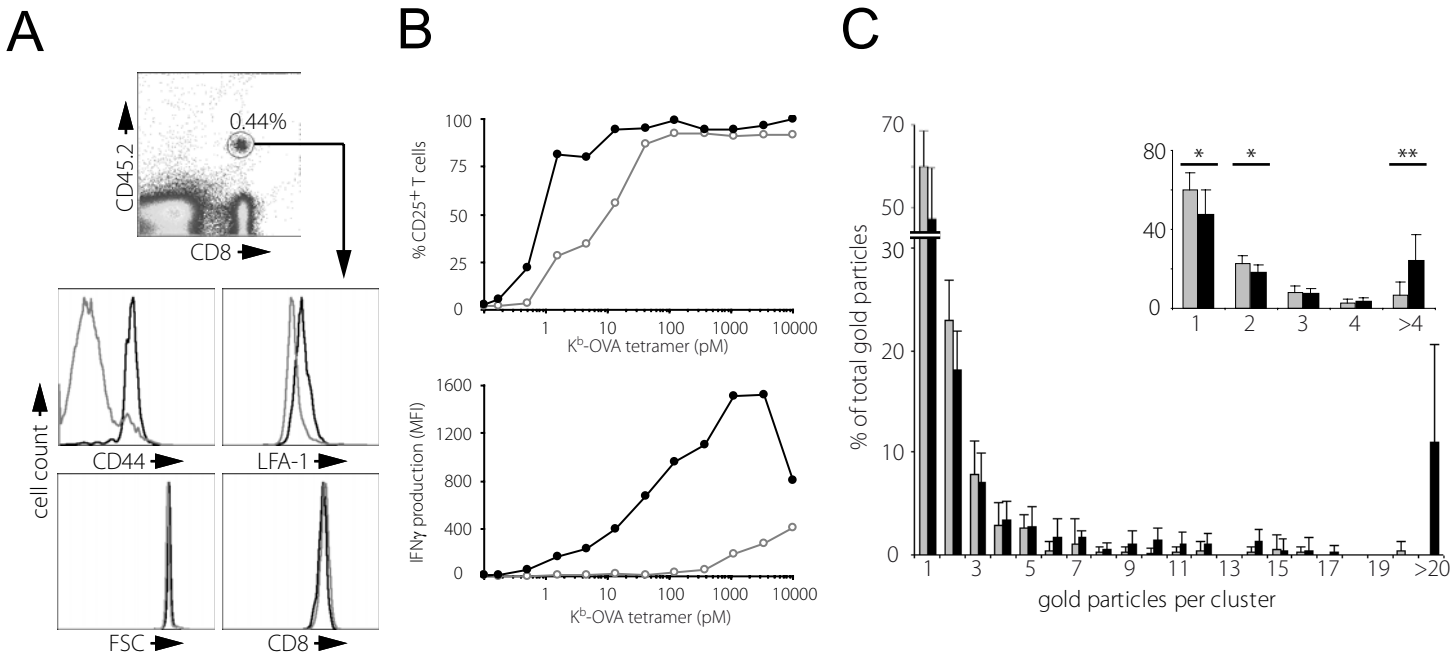
A
B
C
0.44%
CD45.2
CD8
cell count
CD44
LFA-1
FSC
CD8
% CD25+ T cells
Kb-OVA tetramer (pM)
IFNγ production (MFI)
Kb-OVA tetramer (pM)
% of total gold particles
gold particles per cluster
*
*
**

Figure 4

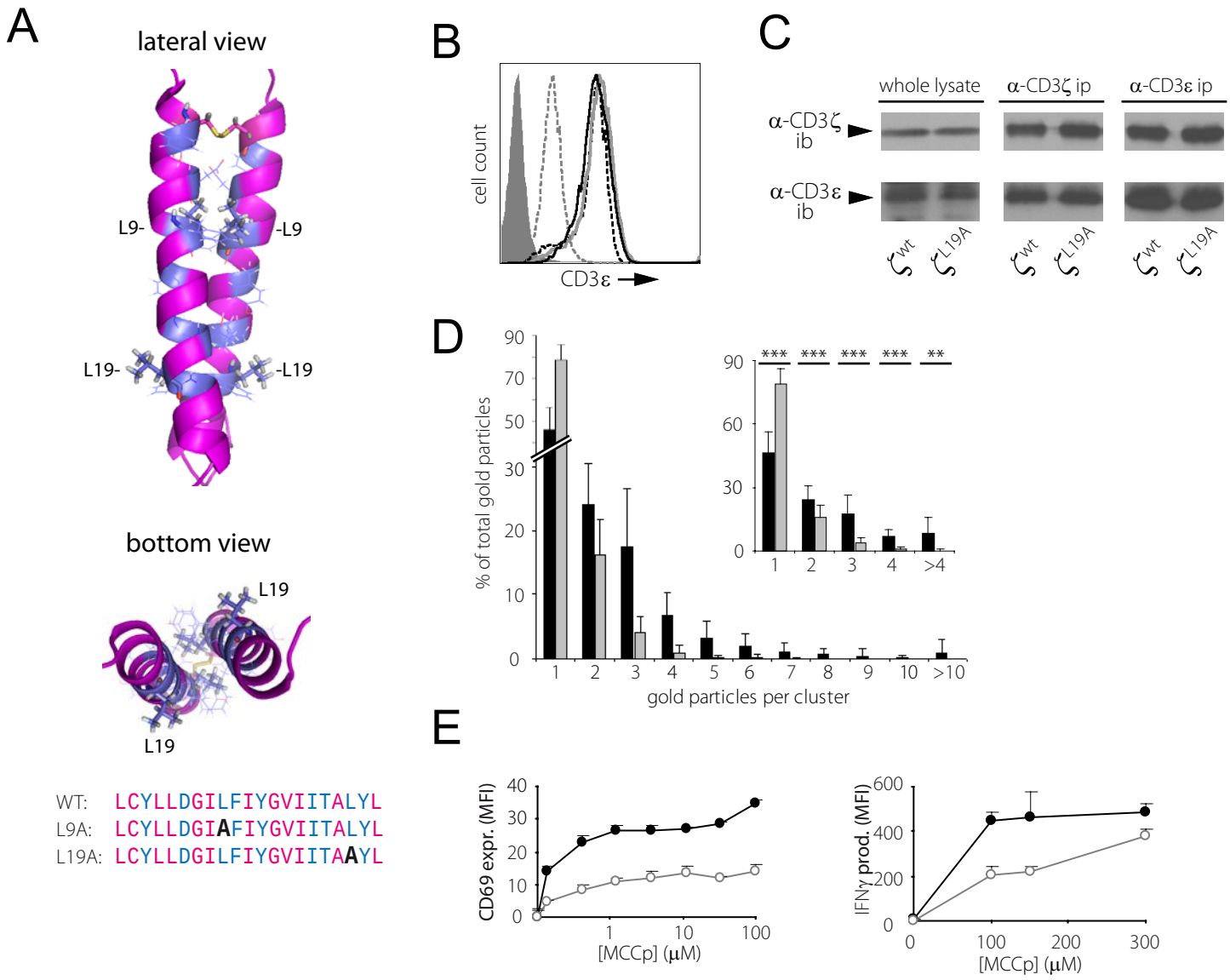
A
lateral view
L9-
-L9
L19-
-L19
bottom view
L19
L19
WT: LCYLLDGILFIYGVIITALYL
L9A: LCYLLDGIAFIYGVIITALYL
L19A: LCYLLDGILFIYGVIITAAYL
B
cell count
CD3ε
C
whole lysate
α-CD3ζ ip
α-CD3ε ip
α-CD3ζ ib
α-CD3ε ib
ζwt
ζL19A
D
% of total gold particles
gold particles per cluster
***
**
E
CD69 expr. (MFI)
[MCCp] (μM)
IFNγ prod. (MFI)
[MCCp] (μM)

Figure 5

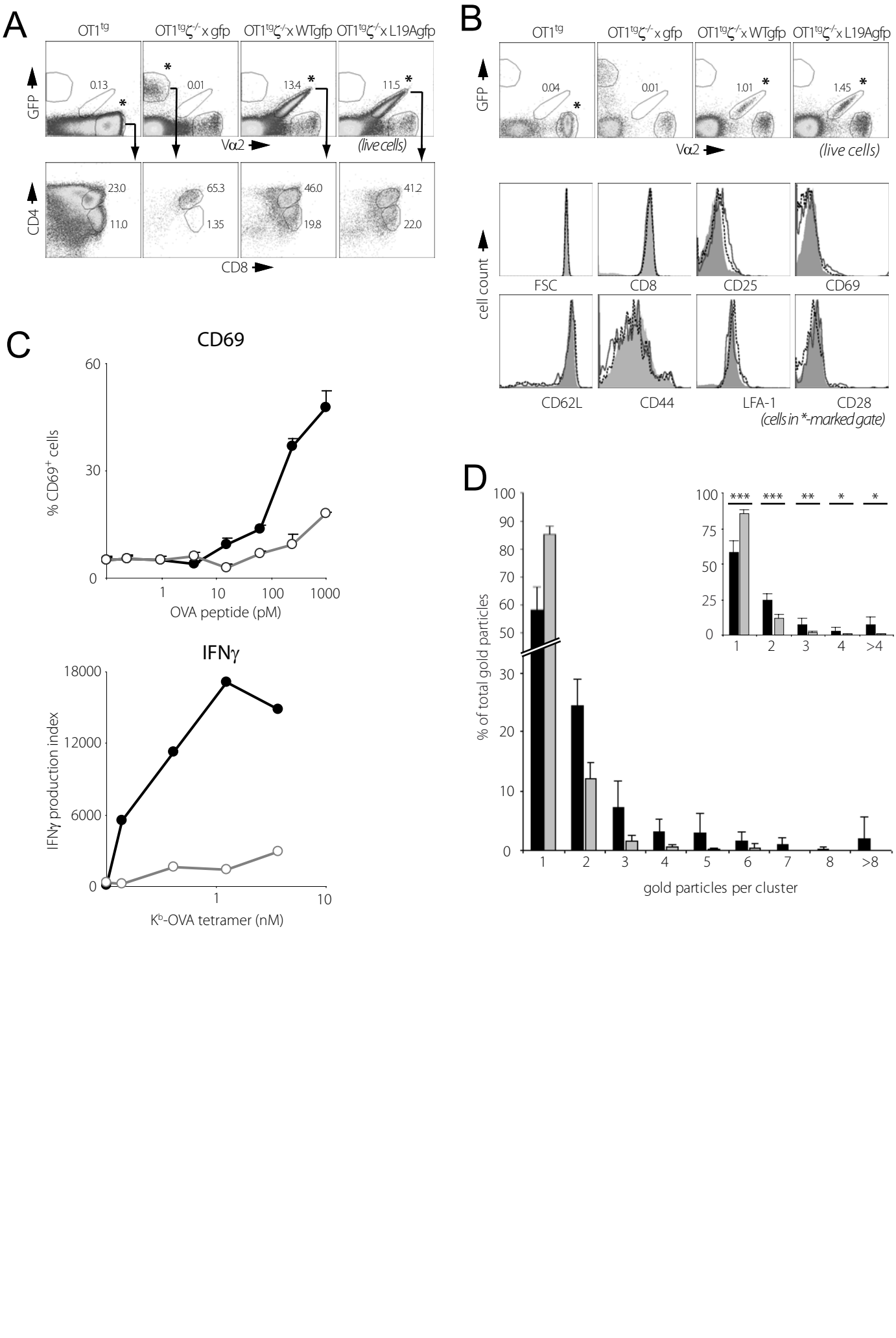
A
OT1tg
OT1tgζ-/- x gfp
OT1tgζ-/- x WTgfp
OT1tgζ-/- x L19Agfp
GFP
0.13
0.01
13.4
11.5
Vα2
(live cells)
CD4
23.0
11.0
65.3
1.35
46.0
19.8
41.2
22.0
CD8
B
OT1tg
OT1tgζ-/- x gfp
OT1tgζ-/- x WTgfp
OT1tgζ-/- x L19Agfp
GFP
0.04
0.01
1.01
1.45
Vα2
(live cells)
cell count
FSC
CD8
CD25
CD69
CD62L
CD44
LFA-1
CD28
(cells in *-marked gate)
C
CD69
% CD69+ cells
60
30
0
1
10
100
1000
OVA peptide (pM)
IFNγ
IFNγ production index
18000
12000
6000
0
1
10
Kb-OVA tetramer (nM)
D
% of total gold particles
100
90
80
70
60
50
30
20
10
0
1
2
3
4
5
6
7
8
>8
gold particles per cluster
***
***
**
*
*
100
75
50
25
0
1
2
3
4
>4

Figure 6

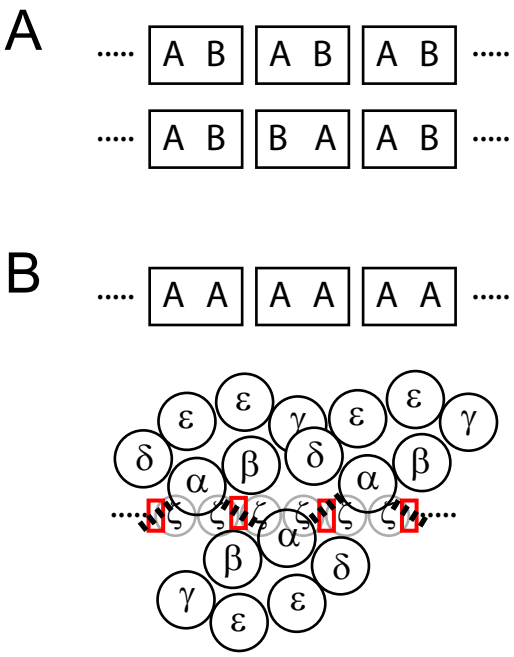

Figure 7

Kumar et al., Figure S1 related to Figure 6

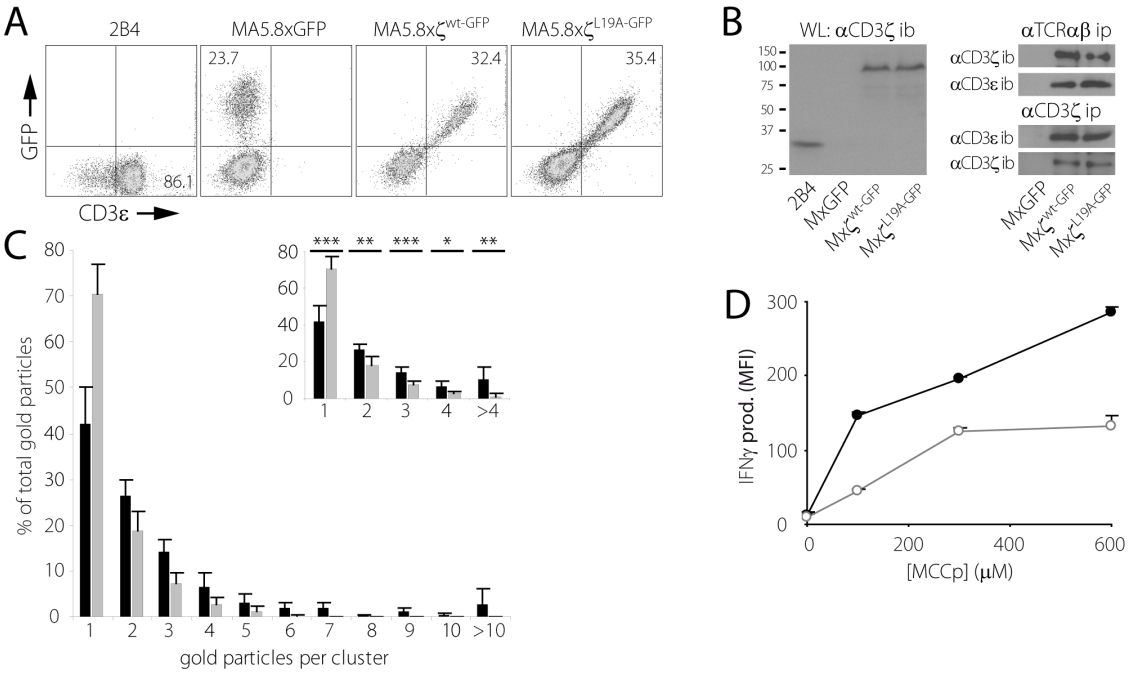

Supplementary Figure 1 - Reconstitution of MA5.8 cells with GFP-linked wild type and L19A CD3ζ. **(A)**. Cell surface expression of the TCR complex in MA5.8 cells transduced with wild type and L19A CD3ζ-GFP chains. 2B4 cells and MA5.8 cells reconstituted with GFP alone are included as controls. Cells were surface-stained with a mAb against CD3ε and signals for both this staining and GFP were measured by flow cytometry. Note that both constructs can rescue TCR cell surface expression to a similar extent and that they quantitatively associate with CD3ε. **(B)**. Biochemical analysis of homodimer formation by wild type and L19A GFP-linked CD3ζ, and their capacity to interact with TCRαβ and CD3ε. Whole cell lysates (WL) and immunoprecipitates of the anti-TCRβ mAb H57.597 or the anti-CD3ζ serum of Brij96-solubilized cells were separated by non-reducing SDS-PAGE and immunoblots were probed with the indicated antibodies. **(C)**. Quantification (mean +/- sem) of the distribution of the TCR complex on the surface of MA5.8 T cells reconstituted with wild type or L19A GFP-linked CD3ζ chains. The inset shows the distribution of gold particles between clusters of 1, 2, 3, 4 or more particles and the statistical analysis (* $p<0.05$; ** $p<0.01$; *** $p<0.001$). Quantification of 6 WT CD3ζ-GFP reconstituted cells (5375 particles) and 6 L19A CD3ζ-GFP reconstituted cells (6462 particles) is shown. **(D)**. IFNγ production by reconstituted MA5.8 cells upon stimulation by DCEK cells loaded with MCCp (black circles: wild type GFP-linked CD3ζ; open circles L19A GFP-linked CD3ζ).